Resegmenting *Halimeda*

Molecular and morphometric studies of species boundaries within a green algal genus

Heroen Verbruggen

Universiteit Gent
Faculteit Wetenschappen
Vakgroep Biologie
Onderzoeksgroep Algologie
Krijgslaan 281 (S8)
9000 Gent, België
http://allserv.ugent.be/phycology

Ghent University
Faculty of Sciences
Biology Department
Phycology Research Group
Krijgslaan 281 (S8)
9000 Ghent, Belgium
http://allserv.ugent.be/phycology

Resegmenting *Halimeda*

Molecular and morphometric studies of species boundaries within a green algal genus

Heroen Verbruggen

Proefschrift ingediend tot het behalen van de graad van Doctor in de Wetenschappen (Biologie)

Promotoren:
Prof. Dr. Eric Coppejans
Dr. Olivier De Clerck

April 22nd, 2005

Dissertation submitted for the degree of Doctor of Sciences (Biology)

Supervisors:
Prof. Dr. Eric Coppejans
Dr. Olivier De Clerck

22 april 2005

Supervisors

Prof. Dr. Eric Coppejans
Dr. Olivier De Clerck

Members of the reading committee:

Prof. Dr. Eric Coppejans
Prof. Dr. Wytze Stam
Dr. Olivier De Clerck
Dr. Wiebe Kooistra

Members of the examination committee:

Prof. Dr. Wim Vyverman (chairman)
Prof. Dr. Dominique Adriaens
Prof. Dr. Eric Coppejans
Prof. Dr. Koen Sabbe
Prof. Dr. Erik Smets
Prof. Dr. Wytze Stam
Dr. Olivier De Clerck
Dr. Wiebe Kooistra

Notes:

1. This dissertation is not to be considered as printed matter in the sense of International Code of Botanical Nomenclature[1] article 29.
2. The author and the supervisors give authorization to consult and copy parts of this work for personal use. Any other use is limited by laws of copyright. Permission to reproduce any material contained in this work should be obtained from the author.

[1] Greuter, W., McNeill J., Barbie F.R., Burdet H.M., Demoulin V., Filgueiras T.S., Nicolson D.H., Silva P.C., Skog J.E., Trehane P., Turland N.J. & Hawksworth D.L. (eds.): International Code of Botanical Nomenclature (Saint Louis Code) adopted by the Sixteenth International Botanical Congress St. Louis, Missouri, July – August 1999. Published in 2000. *Regnum Vegetabile* 138. Koeltz Scientific Books, Königstein.

Table of contents

Dankwoord – Acknowledgements

Verschillende mensen zeggen mij dat het toch wel sterk is dat ik er in slaag mijn doctoraatsproefschrift af te hebben op slechts drie en een half jaar. Ik kan dat alleen bevestigen, maar moet er dadelijk aan toevoegen dat dit meer te maken heeft met de ondersteuning die ik van alle kanten heb gekregen dan wel met mijn ijver. Ik zou dan ook iedereen die heeft bijgedragen aan dit proefschrift uitgebreid willen danken.

Eric, het is mede door jouw publicaties dat gedurende mijn studententijd mijn interesse voor zeewieren is gegroeid. Jij hebt me aangespoord om een doctoraat te maken over *Halimeda*, en het is mede dankzij jou dat ik over de fondsen en faciliteiten kon beschikken die dit alles hebben mogelijk gemaakt. Jij hebt me bijgestaan met oneindig veel kleine administratieve en praktische dingetjes, waarvan ik waarschijnlijk al de helft vergeten ben, maar zonder dewelke het lang niet zo gemakkelijk zou zijn geweest. Bovendien is jouw uitgebreide wiercollectie, al kon ik ze niet gebruiken voor mijn moleculair en morfometrisch werk, een bron van inspiratie en informatie geweest. Ten slotte wil ik je danken voor het nauwlettend nalezen van mijn vaak nonchalante teksten.

Oli, alleen een overtreffende trap van dank kan uitdrukken hoeveel jij hebt betekend voor dit doctoraat. Jij hebt me begeleid door de alledaagse beslommeringen, me geïnspireerd door jouw bewondering voor de wieren en me richting gegeven door eenvoudige suggesties en vragen. Jouw inzichten, praktische hulp bij de uitvoering van het onderzoek en het schrijven van de teksten, en inzet voor het centrum voor moleculaire fylogenie en evolutie hebben er voor gezorgd dat dit werk is wat het is. Ik sta er telkens weer van versteld hoe je erin slaagt je geduld te bewaren wanneer ik voor de 523ste keer op één dag je lokaal kom binnengestormd met een vraag of een tekst om na te lezen. Bedankt ook voor de casual praatjes en activiteiten buiten het werk, en om me bij momenten met beide voeten op de grond te houden. Bedankt voor alles. Zonder jou had ik dit niet gekund.

Wiebe, dankzij jou heeft mijn doctoraat een vliegende start gehad. Nog voor ik er goed en wel aan begon heb jij me voorzien van een collectie specimens, een set DNA sequenties en een berg ideeën, zonder dewelke dit doctoraat er helemaal anders had uitgezien. Door jouw inzichten en door mij te betrekken in twee van jouw publicaties ben ik dadelijk op het goede spoor terecht gekomen. Verder was jij er altijd om de zwakke punten van mijn publicaties aan te wijzen en voor te stellen hoe het beter kon. Ook veel dank voor de gastvrijheid tijdens mijn twee bezoeken in Napels en om gids-ad-interim te spelen die me de stad toonde.

Ellen, al kom jij minder op de voorgrond in mijn publicaties, zonder jou had ik dit nooit klaargespeeld. Jij was verantwoordelijk voor het grootste deel van het praktisch moleculair werk zodat ik me heb kunnen concentreren op microscopie, gegevensanalyse en schrijven. Respect! Ik wens je heel veel succes met je nieuwe project en hoop dat we nog verder zullen kunnen samenwerken aan allerlei groenwier-histories. Tom, jij hebt me gedurende de volledige rit vergezeld als bureaugenoot van de bovenste plank. Ik heb jou mogen terroriseren met de meest uiteenlopende muzikale uitspattingen en de laatste remixes van god-weet-wat, zonder daarvoor agressie te moeten incasseren. Verder kon ik bij jou altijd terecht voor een praatje over het duiken, de onderwaterfotografie, de wetenschap, of het leven zoals het is. Hopelijk kunnen we in de nabije toekomst samen nog meer inzichten opdoen over de wieren van de Arabieren. In sha' Allah! Frederik, de andere man die er bijna de hele tijd bij was, heel erg bedankt voor de gesprekken over allerlei wetenschappelijke en andere onderwerpen. Je bent een fantastische kerel die veel kleur geeft aan de onderzoeksgroep. Veel plezier met je nieuwe project! Enrico, il mio amico dall'Africa del Sud, many thanks for your company during various excursions in Ghent and for your total insight in many aspects of life, not in the least 007 movies. It was a pleasure hanging out with you. Henry, jij bent de man waarmee over zo ongeveer alles kan gebabbeld worden. Grandioze verteller! Geweldig bedankt daarvoor en spijtig dat je er niet meer bij bent. Klaas, de

nieuwe man op het lab die met enkele klikken, een paar kaarten en een satellietbeeld of twee een computer kan doen kreunen, je bent een fantastische nieuwe bureaugenoot. Veel succes met je onderzoek! Caroline, onze nieuwe aanwinst op de Ledeganck die met gemak centrifuges en thermocyclers de baas blijft, ik wens je veel plezier in je werk bij ons. Christelle, jij slaagt er telkens in mij te verbazen met hoe simpel SAP kan zijn. Ongelooflijk bedankt om mij tal van administratieve taken uit de handen te nemen. Het is dankzij zulke dingetjes dat ik veel gemakkelijker kon werken aan dit proefschrift. Verder nog een dikke merci om altijd voor de vrolijke noot te zorgen op de gang. Cathy, de vrouw die bijtijds de hongerigen spijst en de dorstigen laaft, heel erg bedankt voor de dagelijkse koffietafel, om de herbariumspecimens te monteren, de databases zorgvuldig bij te houden, en voor zoveel andere kleine dingen.

Ook de protistologen en aquatische ecologen hebben bijgedragen tot de goede sfeer op de werkvloer. Jullie zijn met te veel om op te noemen, maar toch stevig bedankt allemaal! Een speciaal woordje van dank en respect aan Mieke, die gedurende de laatste weken een uitstekende stresscopiloot is geweest. Griet, bedankt om de Astrid-gesprekken altijd van de nodige spice te voorzien en voor de praatjes over ITS en meer down-to-earth dingen. Hara, bedankt om me gedurende de laatste maanden regelmatig eens een hart onder de riem te steken. Ook de mariene biologen van het centrum voor moleculaire fylogenie en evolutie wil ik bedanken voor de leuke werksfeer. Danny, Sofie, Thomas, het wordt geapprecieerd! Verder nog een stevige merci aan Renata en Andy, twee andere werkpaarden op het centrum voor moleculaire fylogenie en evolutie. Renaat, bedankt om me te helpen met de SEM.

Dit werk werd mogelijk gemaakt door de medewerking van tal van fondsen, waaronder het Bijzonder onderzoeksfonds van de Universiteit Gent, het Fonds voor Wetenschappelijk Onderzoek–Vlaanderen en het Leopold III–Fonds voor Natuuronderzoek en Natuurbehoud. Je remercie Paino Vanai de faciliter mes travaux sur le terrain sur l'île de Wallis. I thank Claude Payri, Antoine N'Yeurt, André Pham, and Francesca Benzoni for their friendship and help during my fieldwork in the South Pacific. Courtney and Tom, my two dive buddies in Jamaica, many thanks for all the help during my two stays at HUML. I had a great time with you guys and hope to see you again soon! Cristine, Dinky, Lawrence, Roxie and Filip, many thanks for your help and company during my phycological exploration of the Philippines. Another word of thanks goes out to Else, Yves, Bruno, Kerry, John and Rob for their company and help during an expedition to Kwazulu-Natal. The following people are acknowledged for sending herbarium specimens and/or pictures hereof: Willem Prud'homme van Reine and Pieter Baas (L), Mike Wynne and Stuart Lyndsey (MICH), Edith Bury and Bruno de Reviers (PC), and Jenny Bryant (BM). I thank Antoine N'Yeurt, Peter Vroom, Heather Spalding, Kimberly Page, Peter Wirtz, Manfred Kaufmann and Oliver Gussmann, and all the other people who have sent me specimens. I would like to thank all the reviewers of the individual papers and of my thesis for the constructive remarks and discussions.

Los amigos, te veel om allemaal bij naam te noemen, maar zeker niet minder belangrijk en daarom allemaal heel hard bedankt. Een speciaal woordje van dank aan Kurt, Katrien, Debbie en Liesbeth, die er in slagen mijn verstand op bijna wekelijkse basis te resetten met de nodige Flatergesprekken en bijhorende humor. Een dikke merci ook aan alle mensen van Poseidon Leuven.

En last but not least, mijn familie... Er zijn geen woorden om uit te drukken hoe dankbaar ik jullie ben. Zonder jullie steun van morele en andere aard had ik dit nooit gekund. Moeder, vader, Lu en Caroline, en alle grootouders, bedankt voor alle zorgen! Het is aan jullie dat ik dit werk opdraag.

Heroen Verbruggen

Gent, 7 april 2005

Part 1

Introduction and objectives

Taxonomic difficulties and objectives

The genus *Halimeda* Lamouroux (1812) belongs to the chlorophyte algae and is characterized by thalli composed of calcified green segments. Like all members of the bryopsidalean algae, *Halimeda* thalli consist of a single, multinucleate, tubular cell. The branches of this cell are called siphons and are spatially organized to form the segments and string them together. Chapter 2 provides an elaborate treatise of the external morphological and anatomical features of *Halimeda*. Appendix 1 lists the 36 species recognized at present, the current sectional subdivision, and the taxonomy of the most recent monograph (Hillis-Colinvaux 1980).

Owing to its importance in tropical ecosystems, *Halimeda* has received a great deal of taxonomic attention. The monographs of Barton (1901), Hillis (1959) and Hillis-Colinvaux (1980) are three milestones of *Halimeda* taxonomy. In the course of time research methods and focal characters evolved, resulting in considerable differences between the abovementioned taxonomic treatises. Chapter 3 provides an historical account of *Halimeda* taxonomy, stressing the characters used by different authors and outlining how this affected classification.

The application of molecular phylogenetic techniques to the genus has perturbed previous taxonomic insights (Kooistra et al. 2002). Firstly, the molecular phylogenetic subdivision of the genus disaccords with the classic sectional subdivision. Secondly, several species comprise two unrelated, cognate taxa. These molecular phylogenetic findings are elaborated in Chapter 4. In conclusion, the work of Kooistra et al. (2002) pinpoints a number of shortcomings of the antecedent morphological studies, providing rationale for new taxonomic attention.

The present study has three principal goals:

1. to elaborate the molecular phylogenetic and phylogeographic structure within the species-rich sections *Rhipsalis* and *Halimeda* of the genus *Halimeda*
2. to delineate species boundaries within problematic morpho-complexes on the basis of DNA sequences
3. to reconcile morphological and molecular insights in species- and section-level taxonomy using a series of morphometric tools

To address these broadly defined goals, a number of narrower goals, which form the basis of the research chapters of the thesis, can be delineated.

1. A first aim is to search for congruence between morphology and the molecular phylogeny of Kooistra et al. (2002) at a sectional level. Kooistra et al. (2002) demonstrated that the sections of Hillis-Colinvaux (1980) did not correspond with molecular phylogenies. The aim is to delineate sections on the basis of groups recognized in the phylogram of Kooistra et al. (2002) and to reinvestigate morphologically the samples of the phylogenetic analysis as well as additional samples to yield morphological definitions of the sections. This goal will be addressed in Chapter 5.
2. A second specific aim of this study is to reassess species boundaries in a group of species resembling *H. distorta*, *H. hederacea*, and *H. opuntia* using molecular and morphological data and to investigate the phylogeography and inter-oceanic dispersal of *H. opuntia* using molecular data. This goal will be addressed in Chapter 6.
3. The disjunct distribution of *H. cuneata* in the subtropical regions of the Indian Ocean (Hillis-Colinvaux 1980) entices speculation about the patterns of relatedness of these disjunct populations. A third aim of this study is to assess the phylogeographic study of this species in

a framework of related species using molecular phylogenetic tools. A first subgoal within this research topic is to investigate species boundaries between *H. cuneata* and the related species *H. discoidea* and *H. tuna* on the basis of plastid and nuclear DNA sequence data. A second subgoal within this research topic is to compare the possible phylogeographic pattern within *H. cuneata* with the scenarios that Hommersand (1986) put forward to explain the affinities between subtropical floras in the Indian Ocean. These goals will be addressed in Chapter 7.

4. Another aim of this study is to develop a set of morphometric techniques that can help reconcile morphological and molecular insights in species-level taxonomy. A first subgoal within this research topic is to assess the taxonomic utility of a number of morphometric methods and morphological characters. This subgoal will be addressed in Chapter 8. A second subgoal is to investigate whether morphological data gathered from segments with aberrant properties (e.g. not calcified, in the basal thallus zone) have an impact on the taxonomic power of the data. This subgoal will be addressed in Chapter 9.

5. The last aim is to apply the developed morphometric methods to a comprehensive set of specimens of section *Rhipsalis*, which is known to comprise several ill-defined species and a species within which cryptic diversity is apparent (Noble et al. 1987, Kooistra et al. 2002). More specifically, a first subgoal is to delineate species on the basis of concordant genotypic clusters in a set of plastid and nuclear DNA sequences. A second subgoal is to pinpoint morphological species boundaries by applying discriminant analysis to a set of morphometric data gathered from the same specimens used for genotypic species delineation, using the genotypic clusters as a priori groups. A third subgoal is to adapt the taxonomy of section *Rhipsalis* to conform to the new insights. The first and second subgoals will be addressed in Chapter 10, the third in Chapter 11.

References

Barton E.S. (1901) The genus *Halimeda*. *Monographs of the Siboga Expedition* **60**. Brill, Leiden. 32pp.

Hillis L. (1959) A revision of the genus *Halimeda* (order Siphonales). *Publications of the Institute of Marine Science* **6**: 321–403.

Hillis-Colinvaux L. (1980) Ecology and taxonomy of *Halimeda*: primary producer of coral reefs. *Advances in Marine Biology* **17**: 1–327.

Hommersand M.H. (1986) The biogeography of the South African marine red algae: a model. *Botanica Marina* 24: 257–270.

Kooistra W.H.C.F., Coppejans E.G.G. & Payri C. (2002) Molecular systematics, historical ecology, and phylogeography of *Halimeda* (Bryopsidales). *Molecular Phylogenetics and Evolution* **24**: 121–138.

Lamouroux J.V.F. (1812) Extrait d'une mémoire sur la classification des polypiers coralligères non entièrement pierreux. *Nouveau Bulletin des Sciences par la Societe Philomatique de Paris* **3**: 181–188.

Noble J.M. (1987) A taxonomic study of the genus *Halimeda* Lamouroux (Chlorophyta, Caulerpales) from the Heron Island region of the southern Great Barrier Reef, Australia. Masters degree thesis, University of Melbourne, Melbourne, Australia.

Appendix 1: **Taxonomy of the genus *Halimeda* and species authorities. The first column represents contemporary insights (including results from this work), the second those of Hillis-Colinvaux (1980). Species whose taxonomic position has changed are in boldface; changes are specified with colors. Species published since Hillis-Colinvaux (1980) are underlined.**

contemporary insights	Hillis-Colinvaux (1980)
section *Rhipsalis* J. Agardh ex De Toni	section *Rhipsalis* J. Agardh ex De Toni
H. borneensis Taylor	*H. borneensis* Taylor
H. cylindracea Decaisne	*H. cylindracea* Decaisne
H. favulosa Howe	*H. favulosa* Howe
H. incrassata (Ellis) Lamouroux	*H. incrassata* (Ellis) Lamouroux
H. heteromorpha N'Yeurt	*H. macroloba* Decaisne
H. kanaloana Vroom	*H. monile* (Ellis & Solander) Lamouroux
H. macroloba Decaisne	*H. simulans* Howe
***H. melanesica* Valet**	*H. stuposa* Taylor
H. monile (Ellis & Solander) Lamouroux	
H. simulans Howe	section *Crypticae* Hillis-Colinvaux
H. stuposa Taylor	*H. cryptica* Colinvaux & Graham
section *Micronesicae* Hillis-Colinvaux	section *Micronesicae* Hillis-Colinvaux
***H. cryptica* Colinvaux & Graham**	*H. fragilis* Taylor
H. fragilis Taylor	*H. melanesica* Valet
H. micronesica Yamada	*H. micronesica* Yamada
section *Halimeda*	section *Halimeda* J. Agardh ex De Toni
H. cuneata Hering	*H. bikinensis* Taylor
H. discoidea Decaisne	*H. cuneata* Hering
H. gigas Taylor	*H. discoidea* Decaisne
H. hummii Ballantine	*H. gigas* Taylor
H. lacunalis Taylor	*H. gracilis* Harvey ex J. Agardh
H. macrophysa Askenasy	*H. lacrimosa* Howe
H. magnidisca Noble	*H. lacunalis* Taylor
H. scabra Howe	*H. macrophysa* Askenasy
H. taenicola Taylor	*H. scabra* Howe
H. tuna (Ellis & Solander) Lamouroux	*H. taenicola* Taylor
H. xishaensis Tseng & Dong	*H. tuna* (Ellis & Solander) Lamouroux
section *Pseudo-opuntia* J. Agardh ex De Toni	
***H. gracilis* Harvey ex J. Agardh**	
***H. lacrimosa* Howe**	
section *Opuntia* J. Agardh ex De Toni	section *Opuntia* J. Agardh ex De Toni
H. copiosa Goreau & Graham	*H. copiosa* Goreau & Graham
H. distorta (Yamada) Colinvaux	*H. distorta* (Yamada) Colinvaux
H. goreauii Taylor	*H. goreauii* Taylor
H. howensis Kraft & Noble	*H. minima* (Taylor) Colinvaux
H. minima (Taylor) Colinvaux	*H. opuntia* (Linnaeus) Lamouroux
H. opuntia (Linnaeus) Lamouroux	*H. renschii* Hauck
H. renschii Hauck	*H. velasquezii* Taylor
H. velasquezii Taylor	
species of uncertain affinity	
***H. bikinensis* Taylor**	
species of unconfirmed status	species of unconfirmed status
H. irregularis Lamouroux	*H. irregularis* Lamouroux
H. nervata Zanardini	*H. nervata* Zanardini
H. papyracea Zanardini	*H. papyracea* Zanardini
H. rectangularis J. Agardh	*H. rectangularis* J. Agardh

Morphology of the green algal genus *Halimeda* [1]

Heroen Verbruggen

The aim of this chapter is to give an overview of the morphology of the segmented, calcified green algal genus *Halimeda*. Generalities and particularities of the appearance of mature thalli, segment morphology and anatomical features are described and illustrated. Sexual reproduction and calcification are also shortly mentioned.

General appearance

Thalli of the green algal genus *Halimeda* are characterized by a segmented habit (Figs 1–6; Lamouroux 1812). From its holdfast, the alga grows in pulses, at each time giving rise to a new, flat, green segment (Colinvaux et al. 1965, Hillis-Colinvaux 1980; Hay et al. 1988). New segments grow from certain points on the distal edge of the mother segment (Verbruggen & Kooistra 2004). This progressive growth of one segment on top of the former gives rise to a catenate appearance (Hillis-Colinvaux 1980).

In essence, thalli consist of rows of segments. At certain points along the thallus these rows branch. This happens when two or more daughter segments sprout from the distal edge of a segment and subsequently each give rise to a branch. Substantial variation in the number and location of ramifications exists among and within species (Figs 1–6; Barton 1901, Gilmartin 1960, Hillis-Colinvaux 1980).

Halimeda occupies many habitats of the tropical and subtropical marine environment (Goreau & Graham 1967, Hillis-Colinvaux 1974, 1977, 1980, Noble 1987, Littler & Littler 2000, 2003). Their habitat reflects in their morphology in a variety of ways (Gilmartin 1960, Colinvaux et al. 1965, Hillis-Colinvaux 1980, Kooistra et al. 2002, Verbruggen et al. submitted). The most apparent adaptation to environmental factors is the holdfast of the algal body (Hillis-Colinvaux 1980, Verbruggen & Kooistra 2004). In essence, *Halimeda* holdfasts are composed of a more or less organized mass of branching rhizoids (Hillis 1959, Hillis-Colinvaux 1980).

Species growing on hard substrate are attached by means of a felt-like holdfast (Fig. 7; Verbruggen & Kooistra 2004). In a felt-like holdfast, rhizoids are compacted into a dense mass (Hillis-Colinvaux 1980). Near the substrate, the rhizoid mass spreads outwards to some extent, resulting in a relatively large contact area between holdfast and substrate (Fig. 7).

The second type of holdfast is present in sand-dwelling species, where a mass of rhizoids penetrates into the sand. Rhizoids adhere to adjacent sand grains. As such, a bulbous structure of sand and interwoven rhizoids is formed (Fig. 8; Barton 1901, Hillis 1959, Hillis-Colinvaux 1980). This bulbous holdfast provides stability in the sandy substratum much like the root of a land plant does.

A third holdfast type occurs in species sprawling over rubble. In these species, the holdfast consists of a few branched, loose rhizoids attaching to morsels of rock and sand (Fig. 9; Hillis-Colinvaux 1980, Verbruggen & Kooistra 2004). In contrast to the other two holdfast types, where a single holdfast attaches the thallus at its base, this type of holdfast occurs at multiple points along the sprawling

[1] This chapter was adapted from a manuscript of an invited review article in preparation. As a consequence, it anticipates a few results presented in the research chapters of this thesis.

thallus, usually at the nodes between segments (Hillis-Colinvaux 1980). The occurrence of multiple holdfasts strongly improves the strength of attachment to a substrate that is relatively unstable by nature.

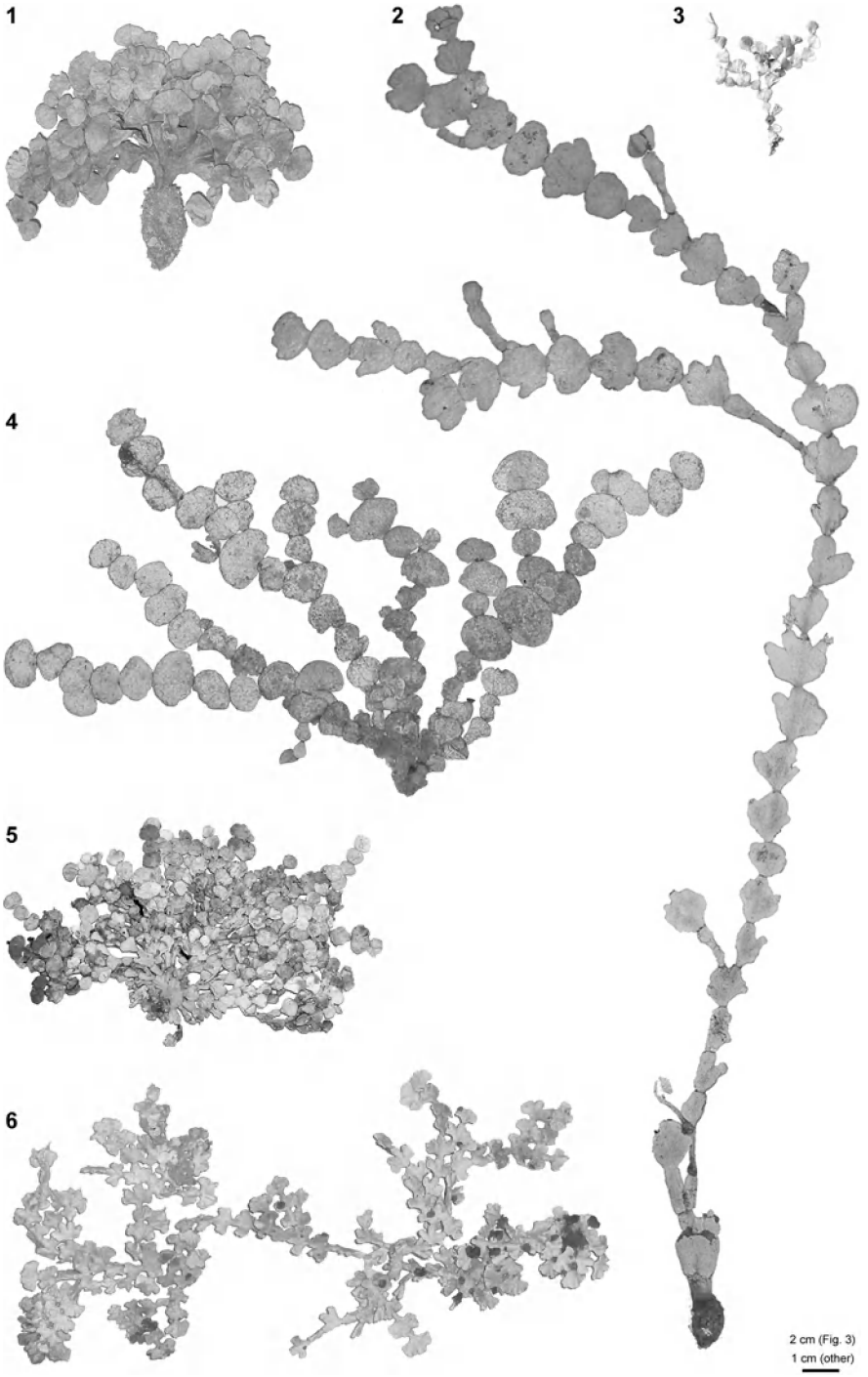

Figs 1–6. General appearance of *Halimeda* thalli. **Fig. 1.** *H. simulans*, specimen H.0030. **Fig. 2.** *H. macroloba*, specimen HV47c. **Fig. 3.** *H. hummii*, specimen H.0233. **Fig. 4.** *H. tuna*, specimen HV55. **Fig. 5.** *H. micronesica*, specimen HV295. **Fig. 6.** *H. opuntia*, specimen HV940. All specimens deposited in the Ghent University Herbarium (GENT).

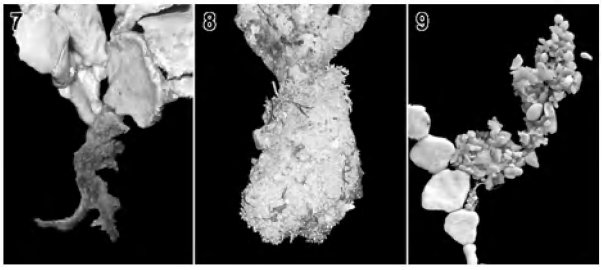

Figs 7–9. Holdfast types. **Fig. 7.** Felt-like holdfast consisting of a dense mat of rhizoids; *H. cuneata* f. *undulata*, specimen HV742. **Fig. 8.** Bulbous holdfast consisting of rhizoids attaching to sand particles; *H. cylindracea*, specimen HV558. **Fig. 9.** Secondary holdfast of a few branched, loose rhizoids attached to sand; *H. gracilis*, specimen KZNb2243. All specimens deposited in GENT.

External features of segments and nodes

Segments range in size from 0.2 mm in *H. hummii* (Ballantine 1982) to over five centimeters in *H. magnidisca* (Noble 1986 – measurements of segment width; species authorities listed in Appendix 1). Segment shape also varies considerably. Among the most common shapes are reniform, ovate, elliptical, obovate and cuneate (Figs 10–14; Hillis-Colinvaux 1980, Verbruggen et al. 2005a). Within most of these categories, the relative width (e.g. measured as width over length ratio) can change considerably. Although many species have segments with entire margins, shallow to deep lobes along the margin of the segment are present in a variety of species (Figs 15–18; Hillis-Colinvaux 1980, Noble 1987, Verbruggen et al. submitted). The shape of the segment base varies from auriculate to acute and features a small stalk in some species (e.g. Fig. 10).

Although there is definitely a genetic component to segment size and shape (Verbruggen & Kooistra 2004, Verbruggen et al. 2005b), environmental conditions are also important (Hillis-Colinvaux 1980, Vroom et al. 2003, Smith et al. 2004, Verbruggen et al. submitted). The best known and most striking example is the segment form variability of *H. opuntia* (Barton 1901, Kooistra & Verbruggen 2005). This sprawling species occurs in a relatively broad range of environmental conditions (Taylor 1950, 1960, Hillis-Colinvaux 1980) and its segments range from broad and reniform in exposed habitats to elongate and trilobed in sheltered habitats. Not only do such differences exist between segments of specimens from different habitats; they can also be situated within individual specimens. Cushions of *H. opuntia* occurring in lagoonal and back-reef habitats throughout the tropics (Taylor 1950, 1960, Hillis-Colinvaux 1980, Coppejans et al. 1992, Silva et al. 1996, Littler & Littler 2000, Payri et al. 2000, Littler & Littler 2003) feature horizontal runner branches ramifying infrequently and consisting of long, trilobed segments on the one hand and densely branching clumps with segments that are usually broad and reniform (pers. obs.). Culture experiments have confirmed that segment shape varia-

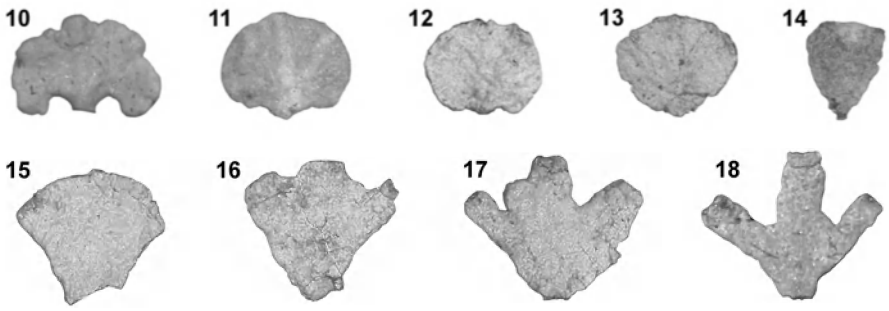

Figs 10–18. Segment shape. **Fig. 10.** Reniform segment; *H. opuntia*, specimen HV61. **Fig. 11.** Broad ovate segment; *H. distorta*, specimen HV767. **Fig. 12.** Elliptical–discoid segment; *H. heteromorpha*, specimen HV629. **Fig. 13.** Broad obovate segment; *H. heteromorpha*, specimen HV629. **Fig. 14.** Cuneate segment; *H. discoidea*, specimen HV605. **Fig 15.** Segment with entire distal margin; *H. heteromorpha*, specimen HV763. **Fig 16.** Shallowly lobed segment; *H. heteromorpha*, specimen HV763. **Fig 17.** Medium deeply lobed segment; *H. heteromorpha*, specimen HV763. **Fig 18.** Deeply lobed segment; *H. heteromorpha*, specimen HV763. All specimens deposited in GENT.

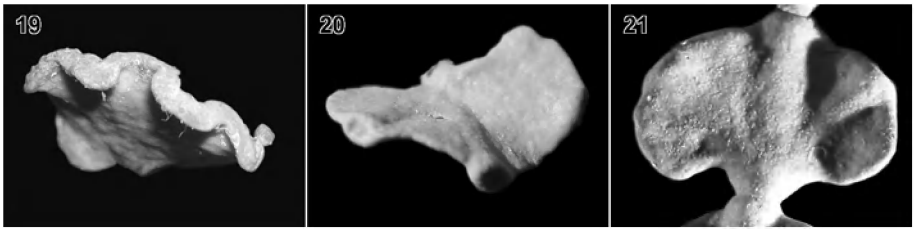

Figs 19–21. Three-dimensional segment properties. **Fig. 19.** Undulate segment; *H. cuneata* f. *undulata*, specimen HV742. **Fig. 20.** Keeled segment; *H. distorta*, specimen HV82. **Fig. 21.** Ribbed segment; *H. distorta*, specimen HV767. All specimens deposited in GENT.

bility of *Halimeda* species can be caused by environmental factors such as light intensity (Colinvaux et al. 1965, Hillis-Colinvaux 1980).

So far, attention has been paid only to size and shape of segments, in other words two-dimensional characters. Inclusion of the third dimension adds another couple of characters of potential taxonomic significance. Segment thickness varies considerably within and among species, ranging from 0.4 mm in *H. hummii* to almost 10 mm in basal segments of *H. cylindracea*. Further three-dimensional characters include the planarity and ribbedness of segments. While in most species segments are flat, in certain species (or forms) they are not. In *H. cuneata* f. *undulata*, for example, segments are markedly undulated (Fig. 19; Barton 1901, Littler & Littler 2003), and in *H. distorta*, segments are often keeled or distorted (Fig. 20; Hillis-Colinvaux 1980, Kooistra & Verbruggen 2005). In a few species, ribbed segments occur (Fig. 21; Barton 1901, Hillis-Colinvaux 1980). These ribs are longitudinal zones of the segment that are thicker than the surrounding segment. Ribs start at the segment base and run longitudinally across the segment towards the daughter segments.

The segment surface can have different appearances. In some species, it is rugged as a consequence of the presence of pits or projections (e.g. *H. favulosa*; Hillis-Colinvaux 1980, Verbruggen et al. submitted). At the other extreme, segments can be smooth and glossy (e.g. *H. hederacea*; Hillis 1959, Hillis-Colinvaux 1980, Kooistra & Verbruggen 2005). Most species are situated in between.

As mentioned above, new segments sprout from the distal margin of their parent segment. Due to anatomical constraints (see below), daughter segments can only grow from certain zones along the margin of the parent segment. The extent of these zones varies strongly. In certain species, daughter segments can grow from the entire distal margin of the segment. On the other edge of the spectrum, there are species in which segments can only grow from a single or a limited number of pits situated along the distal margin.

The contact zone between *Halimeda* segments is usually called node. The appearance and flexibility of nodes vary considerably (Kooistra et al. 2002, Verbruggen & Kooistra 2004). While in most species daughter segments are sessile at the margin of the mother segment, in *H. cuneata* the daughter segments are separated from the mother segment by a stalk zone (Hillis 1959, Hillis-Colinvaux 1980). The extent of development of these stalk zones varies (Hillis 1959). In essence, two types can be distinguished. In the first type, the stalks consist of a naked bundle of siphons (Fig. 22). In the second type, the stalk zone is developed into a so-called cushion segment, which is basically a mini-segment intercalated between the mother- and daughter segments (Fig. 23).

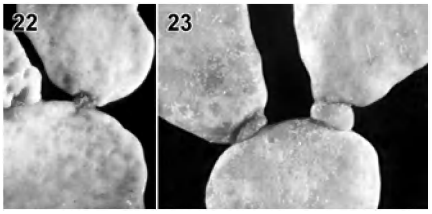

Figs 22, 23. Stalked *H. cuneata* nodes. **Fig. 22.** Stalk consisting of decorticate filaments; specimen KZNb2249. **Fig. 23.** Stalk consisting of corticated filaments (cushion segment); specimen KZNb2352. All specimens deposited in GENT.

Anatomical structures

Like all Caulerpalean algae, *Halimeda* consists of a single, multinucleate cell (van den Hoek et al. 1995, Vroom et al. 1998, Vroom & Smith 2001). The tubular cell branches and anastomoses to form the thallus. Within each segment, two zones of differently organized siphons (branches of the tubular cell) can be discerned: a central medulla and its surrounding cortex (Fig. 24). In order to observe the different anatomical features, segments have to be appropriately dissected and sectioned. Procedures for doing so have been described in Barton (1901), Hillis-Colinvaux (1980) and Verbruggen et al. (2005a).

Features of the medulla

In the medulla, siphons are arranged parallel to the thallus axis (Fig. 24). The bundle of filaments comprising the medulla forms the organic skeleton of the thallus, proceeding through the nodes and stringing segments together (Fig. 24). Siphons branch at more or less regular intervals (Fig. 25). At ramifications, the main branch proceeds towards the distal edge of the segment while the majority of side branches gives rise to the cortex (Fig. 26). The size of medullar siphon segments between ramifications varies considerably between species, within species and even within individual segments (Verbruggen et al. 2005a). The shape of medullar siphon segments shows some variability as well. In *H. gracilis*, for example, medullar siphons are markedly more slender than in other species (Verbruggen & Kooistra 2004). Ramifications in themselves show some features too. In most species, they are trichotomous (Fig. 27), with the central branch continuing upwards and the two side branches proceeding into the cortex. However, dichotomous and quadrichotomous ramifications occur (Figs 28, 29) and even dominate in certain species (unpublished results). Above the ramifications, the main and

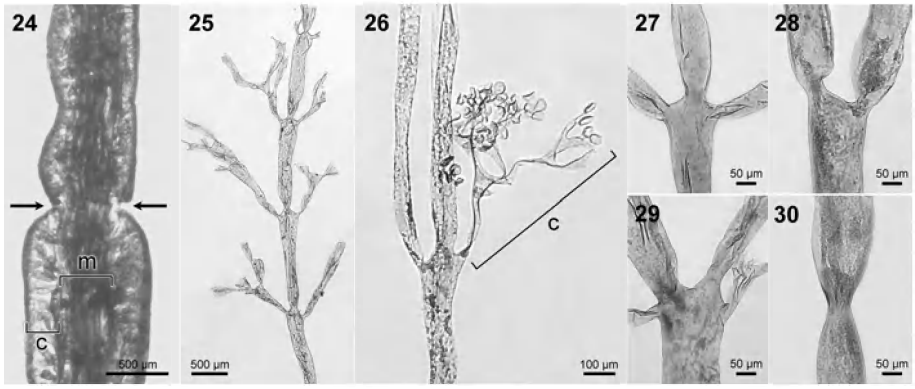

Figs 24–30. Segment anatomy – medulla. **Fig. 24.** Cross section through two subsequent segments showing medulla (m) and cortex (c); arrows indicate the position of the node; *H. incrassata*, specimen H.0667. **Fig. 25.** Medullar siphon ramifying at more or less constant distance, with smaller side branches; *H. incrassata*, specimen H.0668. **Fig. 26.** Side branch of medullar siphon branching into the cortex (c); *H. micronesica*, specimen H.0014. **Fig. 27.** Trichotomous ramification of medullar siphon; *H. monile*, specimen HV344. **Fig. 28.** Dichotomous ramification of medullar siphon; *H. tuna*, specimen HV319. **Fig. 29.** Quadrichotomous ramification of medullar siphon; *H. lacunalis*, specimen HV306-1. **Fig. 30.** Medullar siphon showing constriction but no ramification; *H. taenicola*, specimen HV285-1. All specimens deposited in GENT.

side branches are constricted (Figs 27–29). In a few species, some siphons are constricted at relatively constant intervals without branching (Fig. 30, pers. obs.) and the intervals between subsequent constrictions correspond to the length of medullar siphon segments of the more common, trichotomously branching siphons in the same species.

In ribbed segments, medullar siphons are unevenly distributed within the segment. Anatomically, the ribs consist of thick bundles of medullar siphons surrounded by a cortex (Kooistra & Verbruggen 2005). The remainder of the segment consists of a much thinner layer of medullar siphons enveloped with a cortex.

Features of the nodal zone

In most species, medullar siphons fuse at the nodes. The presence or absence and the type of anastomosis have been treated before in Barton (1901), Hillis (1959) and Hillis-Colinvaux (1980). In a first fusion type, all siphons anastomose into a single unit. Siphons keep their normal appearance below the node, and, at the node, fuse sidewise with their adjacent neighbors. This results in a pattern of large pores visible in properly prepared slides (Figs 31, 32). Above the node, all siphons reappear in line with their subnodal counterparts. In other words, for each siphon arriving at the node, there is one that departs into the subsequent segment. Two adaptations of this fusion pattern occur (Hillis 1959, Hillis-Colinvaux 1980). The first adaptation involves the number of siphons participating in the fusion. In the species where this type of adaptation occurs, siphons fuse into a small number of groups (with numerous siphons each). A second type of adaptation is observed in *H. melanesica* and *H. heteromorpha*, where the large pores have been reduced to small ones or are absent altogether (Figs 33, 34, Verbruggen et al. submitted).

A second common pattern of nodal siphon anatomy is present in many rock-growing species of wave-affected habitats. Here, the siphons get narrower and start branching irregularly shortly below the node. At the node, pairs or triplets of these narrow siphons anastomose. Unlike the former and subsequent fusion patterns, a lower number of siphons reappears above the node. For all siphons that anastomose into a unit, only a single siphon re-emerges above the node (Figs 35, 36). Owing to the irregular branching just below the node and the anastomosis of the resulting branches in different fusion units, this type of anastomosis leads to strong entanglement of siphons below the node (Fig. 35). Anastomosis of several siphons into a single unit that continues in the subsequent segment as a single siphon is called complete fusion.

A third and similar fusion pattern, which is much less common than the former, was described by Verbruggen & Kooistra (2004). The difference with the former pattern is that the appearance of the subnodal siphons is similar to that of the medullar siphons throughout the segments. In other words, siphons do not get narrower below the node, and there is neither dense branching nor siphon entanglement just below the node (Figs 37, 38).

A fourth pattern is one of incomplete fusion of a small number of siphons (usually 2–4). At the node, siphons fuse with one or two neighbors over a short distance (Fig. 39, 40). To put it differently, the node is composed of many pairs or small groups of siphons that are connected sideways with large pores. In this group species too, reduction of the pattern of anastomosis (in the sense of smaller pores) occurs in a few species.

Alternatively to all patterns described above, in a few species, siphons proceed through the node without any form of fusion (Fig. 41). In most species in which this type of nodal siphon behavior occurs, several parallel siphons pass through the node. However, in the species *H. cryptica*, the number of siphons going through the node is reduced to one (Colinvaux & Graham 1964, Verbruggen & Kooistra 2004).

The former patterns are fairly constant within species. Nevertheless, a few exceptions have been noted. For example, in *H. hummii* some siphons go through the node without fusing, but most show complete or incomplete fusion in pairs or triplets (Ballantine 1982, Wysor & Kooistra 2003). A second example is *H. lacrimosa*, in which complete and incomplete fusion can occur in combination (Hillis-Colinvaux 1980). The nodes of *H. cuneata* are a class on their own (see above). In this species, siphon fusion is of the second type. As in other species, fusion occurs at the distal edge of the parent segment (Fig. 42). In the stalk zone, siphons feature thick cell walls and irregular constrictions (Fig. 42; Bandeira-Pedrosa et al. 2004). From the base of the daughter segment onwards, siphons return to their normal, medullar form (Fig. 42). In case a cushion segment is present (Fig. 23), the central strand of siphons is surrounded by a cortex, much as in regular segments (see below).

As mentioned above, new segments can originate along the entire distal margin of the parent segment or at a limited number of pits along the distal segment edge. Medullar siphons fuse just below the pits in question and the fused medullar siphons reach the segment surface at the height of the pit. It seems that new segments can only grow from such fused medullar siphons. As mentioned above, pits can become more elongated and cover the entire distal segment margin.

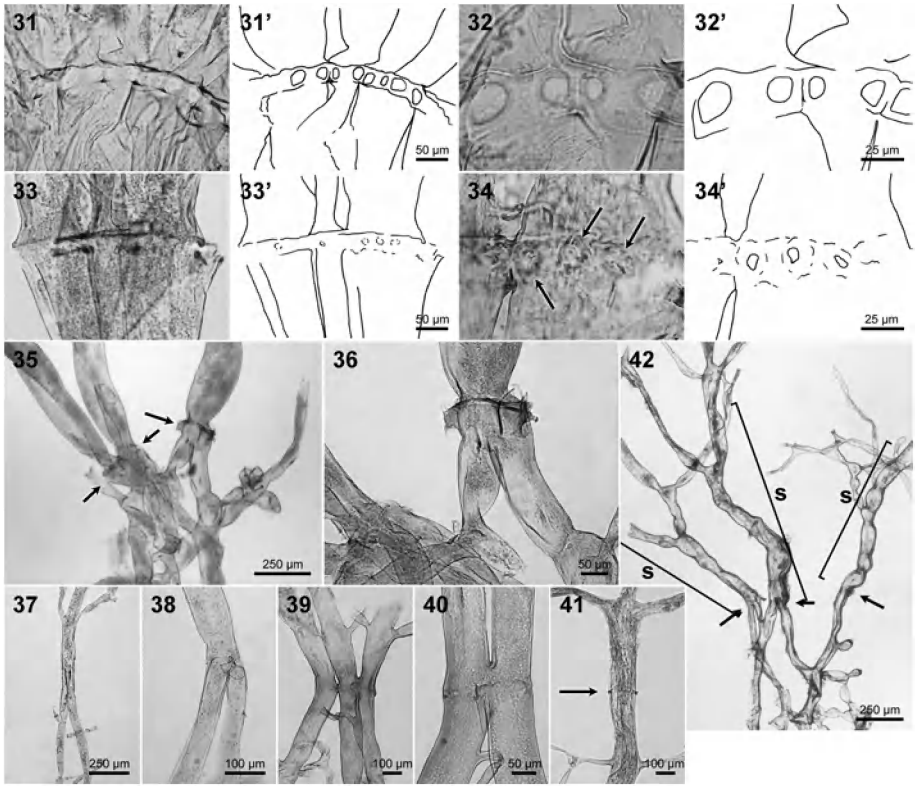

Figs 31–42. Segment anatomy – node. **Figs 31, 32.** Fusion into a single unit with obvious pores connecting adjacent siphons; *H. incrassata*, specimen HV448. **Figs 33, 34.** Fusion into a single unit with diminutive pores connecting some adjacent siphons; *H. heteromorpha*, specimen HV629. **Figs 35, 36.** Complete fusion of siphons in pairs or triplets, with chaotic branching of siphons beneath the node; arrows in Fig. 35 pinpoint fusions; *H. tuna*, specimen HV319. **Figs 37, 38.** Complete fusion of a siphon pair, without chaotic branching of siphons beneath the node; *H. lacrimosa*, specimen H.0308. **Figs 39, 40.** Incomplete fusion of siphons in triplets or pairs; *H. copiosa*, specimen H.0265. **Fig. 41.** Siphon going through the node without any kind of fusion; arrow indicates position of node; *H. micronesica*, specimen H.0014. **Fig. 42.** Nodal anatomy of *H. cuneata*, showing complete siphon fusion in pairs at the distal margin of the parent segment (indicated with arrows), irregularly constricted siphons going through the stalk zone (s) and resumption of regular medullar branching above the stalk zone; specimen KZNb2263. All specimens deposited in GENT.

Features of the cortex

The cortex originates from side branches of the medullar siphons (Fig. 26). In most cases, side branches of medullar siphons have a similar shape, but are somewhat smaller (Fig. 25); and the closer to the segment periphery, the shorter the siphon segments get (Fig. 43, Barton 1901). The segments between closely spaced siphon ramifications are called utricles.

The pattern described above is not fixed. In certain species, especially those with thin segments, the gradual change from medullar siphon to utricle is replaced by a more sudden change, in which side branches of medullar siphons take the form of utricles (Fig. 44). In heavily calcified segments, there is usually only one layer of siphons connecting the medullar siphons and the utricles. In this case, the

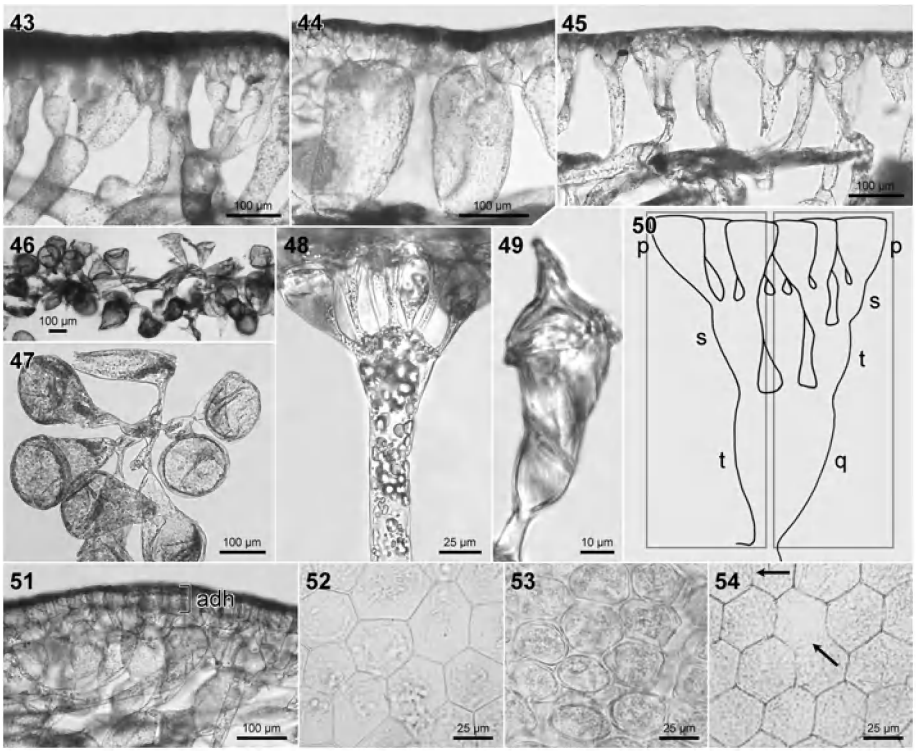

Figs 43–54. Segment anatomy – cortex. **Fig. 43.** Cortical utricles gradually decreasing in size from the medulla (below) to the periphery (above) of the segment; *H. monile*, specimen HV333. **Fig. 44.** Giant subperipheral utricles arising directly from medullar siphons; *H. taenicola*, specimen H.0037. **Fig. 45.** Single layer of cylindrical utricles spanning most of the distance between the medulla and the periphery of the segment; *H. distorta*, specimen HV572. **Fig. 46.** Cross-section through a *H. macrophysa* segment showing the medullar strand of siphons and large, detached, peripheral utricles; specimen HV8. **Fig 47.** Detail of large, detached, peripheral utricles and minute subperipheral utricles of *H. macrophysa*, specimen HV8. **Fig. 48.** Cylindrical secondary utricle suddenly widening at its distal end and giving rise to seven peripheral utricles; *H. gracilis*, specimen HV312. **Fig. 49.** Spined peripheral utricle; *H. scabra*, specimen L.0351084. **Fig. 50.** Schematic diagram of differential branching rates; p – peripheral utricle, s – secondary utricle, t – tertiary utricle, q – quaternary utricle. **Fig. 51.** Lateral adhesion of peripheral utricles (adh); *H. discoidea*, specimen OMII118. **Fig. 52.** Firmly attached peripheral utricles in an irregular polygonal pattern (surface view); *H. melanesica*, specimen HV818. **Fig. 53.** Detached peripheral utricles in surface view; *H. macroloba*, specimen HV206. **Fig. 54.** Surface view showing fusion between adjacent peripheral utricles (arrows); *H. discoidea*, specimen H.0204. All specimens deposited in GENT except L.0351084 (*H. scabra*) from the National Herbarium of the Netherlands, Leiden University Branch (L).

side branches of medullar siphons are elongate and pass through the most heavily calcified segment zone towards the periphery of the segments where they branch several times over a short distance to form the cortical utricles (Fig. 45).

Utricles often occur in more or less definable layers, which are sometimes numbered from the segment surface inwards (Hillis 1959; Hillis-Colinvaux 1980). Utricles from the peripheral layer are referred to as primary utricles, those from the layer inwards as secondary utricles, and so on. Numbering layers is sometimes problematic due to differential branching rates. A situation that often occurs is that tertiary utricles have different numbers of subsequent utricle generations. Imagine a tertiary utricle with three daughter utricles of which the first one bears three peripheral utricles (Fig. 50, left box). Imagine another one of the daughter utricles of the tertiary utricle bearing daughter utricles which, in turn, each bear peripheral daughter utricles (Fig. 50, right box). In this situation, the original tertiary utricle becomes a quaternary utricle. This situation suggests that the developmental process of utricle formation is not a definite one but can adapt to circumstances at a very small scale.

Considerable size and shape variation can be observed in utricles. In certain species, utricles are strongly inflated (Figs 44, 51). Opposite to that, utricles can be non-inflated, cylindrical tubes (Fig. 45). The whole spectrum of intermediates occurs. Utricle shape is diagnostic for a few species and sections. For example, peripheral utricles of *H. scabra* bear a terminal spine (Fig. 49, Howe 1905), peripheral utricles of *H. macrophysa* are markedly inflated (Figs 46, 47, Askenasy 1888), peripheral utricles of Brazilian *H. cuneata* are characterized by lenticular thickenings on the inside of their distal cell wall (Bandeira-Pedrosa et al. 2004), and secondary utricles of section *Pseudo-opuntia* widen suddenly at their distal end (Fig. 48; Verbruggen & Kooistra 2004). Most species, however, have highly similar cortex features and are usually diagnosed on the basis of size characteristics of the utricles.

Peripheral utricles usually attach to one another laterally due to the presence of a common cuticle-like structure (Bandeira-Pedrosa et al. 2003). The degree of attachment varies from attachment at the very distal girdle of the utricles, in which case only the cuticle-like layer provides adhesion, to attachment along two-thirds of the utricle length, in which case the lateral cell walls fuse (e.g. *H. discoidea*, Fig. 51). In some species, utricles are unattached (e.g. *H. macrophysa*, Fig. 47). In surface view, the appearance of peripheral utricles depends mostly on their degree of attachment. When they are fully attached, the surface view is one of polygons (mostly hexagons) closely fitted together (Fig. 52). When the attachment is less strict, polygons become rounded in the corners (Fig. 53) or get reduced to loose circles when the utricles are not attached at all. In a few species with fully attached peripheral utricles, some adjacent primary utricles fuse with one another (Fig. 54, Howe 1907).

Reproductive structures

Halimeda gametes are formed in stalked gametangial clusters. Such clusters vary strongly in size, shape, structural origin and position on the segment, both among and within species (Hillis-Colinvaux 1980, Vroom & Smith 2003). Gametangial clusters are situated mostly along the outer rim of segments (Fig. 55). Nonetheless, several species also have gametangial clusters arising from the segment surface (Fig. 56). In *H. cryptica*, all gametangial clusters are situated on one side of the segment (Graham 1975). Gametophores, the stalks that carry gametangial clusters, have been observed to originate in three ways (Hillis 1959, Hillis-Colinvaux 1980). First, they can arise at the distal segment rim or pits, as continuations of the main medullary filaments subsequent to nodal fusion (Fig. 57). Second, they can originate as lateral outgrowths from medullary filaments without fusion (i.e. not at pores or distal segment rim – not depicted here). Third, they can originate as extensions from peripheral or secondary utricles (Figs 58, 59). In general, the gametophore is a long, unbranched siphon, whereas branches within the gametangial cluster are short (Figs 57, 58). However, in several species, the gametophore ramifies once or twice along its length, giving rise to multiple gametangial clusters (Fig.

60). Each gametangial group comprises a number of spherical to pyriform gametangia and a more elongate, club-shaped discharge papilla (Figs 57, 58; Drew & Abel 1988, Vroom & Smith 2003).

Reproduction in *Halimeda* is holocarpic: after the cell content of the whole thallus has been transformed into and released as gametes, the thallus dies (Meinesz 1980 and references therein). Reproductive events show seasonal and lunar periodicity (Beth 1962, Drew & Abel 1988, Clifton 1997, Clifton & Clifton 1999), but certain species are found reproductive in different seasons at different localities (Drew & Abel 1988) and low fractions of populations of certain species are reproductive throughout the year (Verbruggen et al. submitted). Where observed in detail, gametangial clusters are formed during the night, grow darker during the first day and second night, and discharge around dawn of the second day (Hillis-Colinvaux 1980, Drew & Abel 1988, Clifton 1997, Clifton & Clifton 1999). *Halimeda* is dioecious and thalli carrying macrogametangia can be discerned from thalli carrying microgametangia because macrogametangia are large and brown to dark green while microgametangia are smaller and yellow to light green (Feldmann 1951, Meinesz 1980). Broadcast spawning (simultaneous release of gametes in the water column) generally occurs around dawn, in species-specific time-frames (Clifton 1997). Just prior to release, the gametes from all gametangia in a gametangial cluster migrate downwards through the gametangial stalks to be released through the cluster's discharge papilla (Hillis-Colinvaux 1980, Drew & Abel 1988).

Halimeda gametes are biflagellate, pyriform cells that vary in size from about 2 to about 20 µm in size (Meinesz 1980, Hillis-Colinvaux 1980, Clifton & Clifton 1999 and references in these). Macrogametes, characterized by an eyespot, are generally larger than the microgametes lacking eyespots. Development of the *H. tuna* zygote into a filamentous life-stage, similar to *Pseudochlorodesmis* thalli, is described in Meinesz (1972, 1980). It is has not been ascertained how the filamentous form is linked to the segmented thallus.

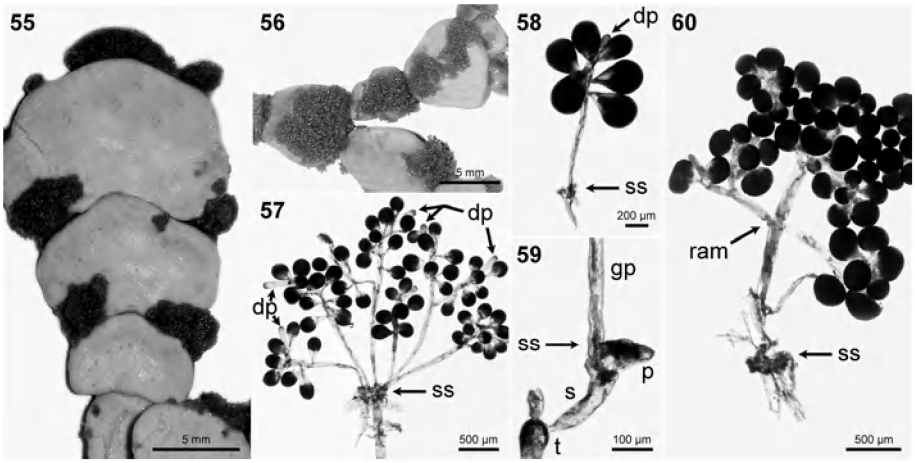

Figs 55–60. Reproductive structures. **Fig 55.** Gametangial clusters originating from distal edges of segments; *H. macroloba*, specimen HV206. **Fig. 56.** Gametangial clusters originating from the segment surface; *H. cuneata*, specimen KZNb2263. **Fig. 57.** Gametophores originating from the main medullary filaments subsequent to nodal fusion at the distal segment edge; dp – discharge pores, ss – segment surface; *H. macroloba*, specimen HV206. **Fig. 58.** Gametophore originating from secondary utricle; *H. incrassata*, specimen H.0143. **Fig. 59.** Gametophore originating from secondary utricle; gp – gametophore, p – peripheral utricle, s – secondary utricle, t – tertiary utricle; *H. incrassata*, specimen H.0143. **Fig. 60.** Gametophore originating from the main medullary filaments subsequent to nodal fusion at the distal segment edge and separating into three clusters by a central ramification (ram); *H. cylindracea*, specimen HV590. All specimens deposited in GENT.

Calcification

Several bryopsidalean algae are characterized by intra- and/or extracellular calcium carbonate deposition (Böhm et al. 1978). The mechanisms of calcification have been reviewed by Borowitzka (1982). In *Halimeda*, calcium carbonate is deposited extracellularly, in between cortical and (to a lesser extent) medullar siphons (Figs 61, 62; Askenasy 1888, Wilbur et al. 1969, Borowitzka & Larkum 1977, Böhm et al. 1978). The needle-shaped crystals are orthorhombic (aragonite; Fig. 63; McConnell & Colinvaux 1967). The degree of calcification is an important determinant of color, flexibility and brittleness of *Halimeda* segments. Segment color varies from dark green in barely calcified segments to greenish white in segments of strongly calcified species. In addition, segments can become brownish by cell wall thickening, in particular near the thallus base. Flexible thalli allow specimens to grow in habitats characterized by high water movement by aligning the thallus with the current, thus reducing drag. There are two major components to thallus flexibility. First, flexibility of nodes plays a role. Second, segment pliability is of importance, especially in species with rigid nodes. Several species feature highly swollen secondary utricles (Figs 44, 51), leaving little space for calcification and rendering segments flexible (Verbruggen & Kooistra 2004). An important drawback of reduced calcification in tropical reef ecosystems characterized by high grazing pressure is increased palatability (Duffy & Hay 1990, Hay et al. 1994, Schupp & Paul 1994, Paul 1997). Initial segment growth occurs at night (Hay et al. 1988) and calcification, which is dependent upon photosynthesis, starts on the second day of segment development (Wilbur et al. 1969). Segments are fully calcified after about 2–3 days. When calcified segments are shed from the thallus after reproduction, they form an important fraction of the sediment and are responsible for much of the sand formation in tropical lagoons (e.g. Chapman & Mawson 1906; Drew 1983; Freile et al. 1995).

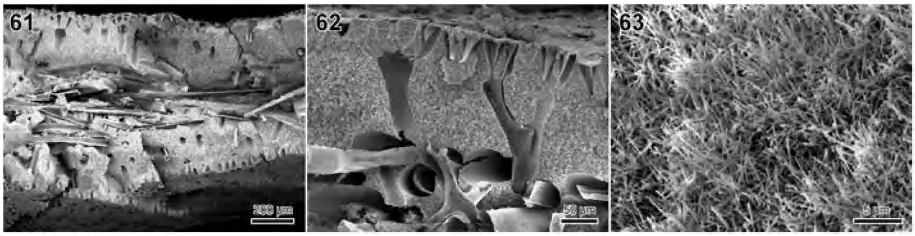

Figs 61–63. Calcification. **Fig. 61.** SEM micrograph of fractured segment showing a central zone of medullary filaments and relatively little carbonate and a heavily calcified cortical zone on either side; *H. gracilis*, specimen HV824. **Fig. 62.** SEM micrograph of cortical zone of fractured segment showing the calcium carbonate depositions in between cortical siphons; *H. gracilis*, specimen HV824. **Fig. 63.** SEM micrograph of needle-shaped aragonite crystals; *H. gracilis*, specimen HV824. All specimens deposited in GENT.

References

Askenasy E. (1888) Algen. In: *Die Forschungsreise S.M.S. Gazelle* Th. 4, Bot., Berlin.

Ballantine D.L. (1982) *Halimeda hummii* sp. nov., *Halimeda cryptica* v. *acerifolia* var. nov. (Caulerpales, Chlorophyta), and additional records of *Halimeda* species from Puerto Rico. *Journal of Phycology* **18**: 86–91.

Bandeira-Pedrosa M.E., Bouzon Z.L., Pereira S.M. & Oliveira E.C. (2003) Ultrastructure of some species of *Halimeda* (Bryopsidales, Chlorophyta) from Brazil. *Cryptogamie Algologie* **24**: 219–231.

Bandeira-Pedrosa M.E., Pereira S.M.B., Bouzon Z.L. & Oliveira E.C. (2004) *Halimeda cuneata* (Bryopsidales, Chlorophyta), a new record for the Atlantic Ocean. *Phycologia* **43**: 50–57.

Barton E.S. (1901) The genus *Halimeda*. *Monographs of the Siboga Expedition* **60**. Brill, Leiden. 32pp.

Beth K. (1962). Reproductive phases in populations of *Halimeda tuna* in the Bay of Naples. *Publicazione della Stazione Zoologica di Napoli* **32**: 515–534.

Böhm L., Fütterer D., Kaminski E. (1978) Algal calcification in some Codiaceae (Chlorophyta): ultrastructure and location of skeletal deposits. *Journal of Phycology* **14**: 486–493.

Borowitzka M.A. (1982) Mechanisms in algal calcification. In: Round F.E. & Chapman D.J. (eds.) *Progress in Phycological Research*. Vol. 1. Elsevier, Amsterdam, The Netherlands. pp. 137–178.

Borowitzka M.A. & Larkum A.D.W. (1977) Calcification in the green alga *Halimeda*. I. An ultrastructure study of the thallus development. *Journal of Phycology* 13: 6–16.

Chapman F. & Mawson D. (1906) On the importance of *Halimeda* as a reef-forming organism: with a description of the *Halimeda*-limestones of the New Hebrides. *Journal of the Geological Society of London* **62**: 702–711.

Clifton K.E. (1997) Mass spawning by green algae on coral reefs. *Science* **275**: 1116–1118.

Clifton K.E. & Clifton L.M. 1999. The phenology of sexual reproduction by green algae (Bryopsidales) on Caribbean coral reefs. *Journal of Phycology* **35**: 24–34.

Colinvaux L.H. & Graham E.A. (1964) A new species of *Halimeda*. *Nova Hedwigia* 7: 5–10.

Colinvaux L.H., Wilbur K.M. & Watabe N. (1965) Tropical marine algae: growth in laboratory culture. *Journal of Phycology* **1**: 69–78.

Coppejans E., Beeckman H. & De Wit M. (1992) The seagrass and associated macroalgal vegetation of Gazi Bay (Kenya). *Hydrobiologia* **247**: 59–75.

Drew E.A. (1983) *Halimeda* biomass, growth rates and sediment generation on reefs in the central Great Barrier Reef province. *Coral Reefs* **2**: 101–110.

Drew E.A. & Abel K.M. (1988) Studies on *Halimeda* I. The distribution and species composition of *Halimeda* meadows throughout the Great Barrier Reef Province. *Coral Reefs* **6**: 195–205.

Duffy J.E. & Hay M.E. (1990) Seaweed adaptations to herbivory. *Bioscience* **40**: 368–375.

Feldmann J. (1951) Sur la reproduction sexuée de l'*Halimeda tuna* (Ell. et Sol.) Lamour. f. *platydisca* (Decaisne) Barton. *Comptes Rendus Hebdomadaires des Séances de l'Académie des Sciences, Série D* **233**: 1309–1310.

Freile D., Milliman J.D. & Hillis L. (1995) Leeward bank margin *Halimeda* meadows and draperies and their sedimentary importance on the western Great Bahama bank slope. *Coral Reefs* **14**: 27–33.

Gilmartin M. (1960) The ecological distribution of the deep water algae of Eniwetok. *Ecology* **41**: 210–221.

Goreau T.F. & Graham E.A. (1967) A new species of *Halimeda* from Jamaica. *Bulletin of Marine Science* **17**: 432–441.

Graham E.A. (1975) Fruiting in *Halimeda* (order Siphonales) 1. *Halimeda cryptica* Colinvaux and Graham. *Bulletin of Marine Science* **25**: 130–133.

Hay M.E., Kappel Q.E. & Fenical W. (1994) Synergisms in plant defenses against herbivores: interactions of chemistry, calcification, and plant quality. *Ecology* **75**: 1714–1726.

Hay M.E., Paul V.J., Lewis S.M., Gustafson K., Tucker J. & Trindell R.N. (1988) Can tropical seaweeds reduce herbivory by growing at night? Diel patterns of growth, nitrogen content, herbivory, and chemical versus morphological defenses. *Oecologia* **75**: 233–245.

Hillis L. (1959) A revision of the genus *Halimeda* (order Siphonales). *Publications of the Institute of Marine Science* **6**: 321–403.

Hillis-Colinvaux L. (1974) Productivity of the coral reef alga *Halimeda* (Siphonales). *Proceedings of the 2nd International Coral Reef Symposium* **1**: 35–42.

Hillis-Colinvaux L. (1977) *Halimeda* and *Tydemania*: distribution, diversity and productivity at Enewetak. *Proceedings of the 3rd International Coral Reef Symposium* **1**: 365–370.

Hillis-Colinvaux L. (1980) Ecology and taxonomy of *Halimeda*: primary producer of coral reefs. *Advances in Marine Biology* **17**: 1–327.

Howe M.A. (1905) Phycological studies. II. New Chlorophyceae from Florida and the Bahamas. *Bulletin of the Torrey Botanical Club* **32**: 241–252.

Howe M.A. (1907) Phycological studies. III. Further notes on *Halimeda* and *Avrainvillea*. *Bulletin of the Torrey Botanical Club* **34**: 491–515.

Kooistra W.H.C.F., Coppejans E.G.G. & Payri C. (2002). Molecular systematics, historical ecology and phylogeography of *Halimeda* (Bryopsidales). *Molecular Phylogenetics and Evolution* **24**: 121–138.

Kooistra W.H.C.F. & Verbruggen H. (2005) Genetic patterns in the calcified tropical seaweeds *Halimeda opuntia*, *H. distorta*, *H. hederacea* and *H. minima* (Bryopsidales, Chlorophyta) provide insights in species boundaries and inter-oceanic dispersal. *Journal of Phycology* **41**: 177–187.

Lamouroux J.V.F. (1812) Extrait d'une mémoire sur la classification des polypiers coralligères non entièrement pierreux. *Nouveau Bulletin des Sciences par la Societe Philomatique de Paris* **3**: 181–188.

Littler D.S. & Littler M.M. (2000) *Caribbean reef plants. An identification guide to the reef plants of the Caribbean, Bahamas, Florida and Gulf of Mexico.* OffShore Graphics, Washington. 542 pp.

Littler D.S. & Littler M.M. (2003) *South Pacific Reef Plants. A diver's guide to the plant life of South Pacific coral reefs.* OffShore Graphics, Washington. 331 pp.

McConnell D. & Colinvaux L.H. (1967) Aragonite in *Halimeda* and *Tydemania* (order Siphonales). *Journal of Phycology* **3**: 198–200.

Meinesz M.A. (1972) Sur le cycle de l'*Halimeda tuna* (Ellis et Solander) Lamouroux (Udoteaceae, Caulerpale). *Comptes Rendus Hebdomadaires des Séances de l'Académie des Sciences, Série D* **275**: 1363–1365.

Meinesz A. (1980) Connaissances actuelles et contribution a l'etude de la reproduction et du cycle des Udoteacees (Caulerpales, Chlorophytes). *Phycologia* **19**: 110–138.

Noble J.M. (1986) *Halimeda magnidisca* (Caulerpales, Chlorophyta), a new species from the Great Barrier Reef, Australia. *Phycologia* **25**: 331–339.

Noble J.M. (1987) A taxonomic study of the genus *Halimeda* Lamouroux (Chlorophyta, Caulerpales) from the Heron Island region of the southern Great Barrier Reef, Australia. MSc thesis, University of Melbourne, Melbourne, Australia. 200pp.

Paul V.J. (1997) Secondary metabolites and calcium carbonate as defenses of calcareous algae on coral reefs. *Proceedings of the 8th International Coral Reef Symposium*: 707–712.

Payri C., N'Yeurt A.D.R. & Orempuller J. (2000) *Algae of French Polynesia*. Au Vent des Iles, Tahiti, French Polynesia. 320 pp.

Schupp P.J. & Paul V.J. (1994) Calcium carbonate and secondary metabolites in tropical seaweeds: variable effects on herbivorous fish. *Ecology* **75**: 1172–1185.

Silva P.C., Basson P.W. & Moe R.L. (1996) *Catalogue of Indian Ocean Algae.* University of California Publications in Botany (vol. 79), Berkeley, CA.

Smith J.E., Smith C.M., Vroom P.S., Beach K.L. & Miller S. (2004) Nutrient and growth dynamics of *Halimeda tuna* on Conch Reef, Florida Keys: Possible influence of internal tides on nutrient status and physiology. *Limnology and Oceanography* **49**: 1923–1936.

Taylor W.R. (1950) *Plants of Bikini and other northern Marshall Islands. Algae: Chlorophyceae.* University of Michigan Press, Ann Arbor, Michigan. 218 pp.

Taylor W. R. (1960) *Marine algae of the Eastern tropical and sub-tropical coasts of the Americas.* University of Michigan Press, Ann Arbor, Michigan. 870 pp.

van den Hoek C., Mann D.G. & Jahns H.M. (1995) Algae: an introduction to phycology. Press Syndicate, University of Cambridge, Cambridge, England.

Verbruggen H., De Clerck O., Cocquyt E., Kooistra W.H.C.F. & Coppejans E. (2005) Morphometric taxonomy of siphonous green algae: a methodological study within the genus *Halimeda* (Bryopsidales). *Journal of Phycology* **41**: 126–139.

Verbruggen H., De Clerck O., Kooistra W.H.C.F. & Coppejans E. (2005b) Molecular and morphometric data pinpoint species boundaries in *Halimeda* section *Rhipsalis* (Bryopsidales, Chlorophyta). *Journal of Phycology*: accepted.

Verbruggen H. & Kooistra W.H.C.F. (2004) Morphological characterization of lineages within the calcified tropical seaweed genus *Halimeda* (Bryopsidales, Chlorophyta). *European Journal of Phycology* **39**: 213–228.

Verbruggen H., N'Yeurt A.D.R., Spalding H.I. & Vroom P.S. (submitted) Phylogeny and taxonomy of *Halimeda incrassata*, including the description of *H. kanaloana* and *H. heteromorpha* spp. nov. (Bryopsidales, Chlorophyta). Submitted to *European Journal of Phycology*.

Vroom P.S. & Smith C.M. (2001) The challenge of siphonous green algae. *American Scientist* **89**: 524–531.

Vroom P.S. & Smith C.M. (2003) Reproductive features of Hawaiian *Halimeda velasquezii* (Bryopsidales, Chlorophyta), and an evolutionary assessment of reproductive characters in *Halimeda*. *Cryptogamie Algologie* **24**: 355–370.

Vroom P.S., Smith C.M., Coyer J.A., Walters L.J., Hunter C.L., Beach K.S. & Smith J.E. (2003) Field biology of *Halimeda tuna* (Bryopsidales, Chlorophyta) across a depth gradient: comparative growth, survivorship, recruitment, and reproduction. *Hydrobiologia* **501**: 149–166.

Vroom P.S., Smith C.M. & Keeley S.C. (1998) Cladistics of the Bryopsidales: a preliminary analysis. *Journal of Phycology* **34**: 351–360.

Wilbur K.M., Colinvaux L.H., Watabe N. (1969) Electron microscope study of calcification in the alga *Halimeda* (order Siphonales). *Phycologia* **8**: 27–35.

Wysor B. & Kooistra W.H.C.F. (2003) An annotated list of marine Chlorophyta from the Caribbean coast of the Republic of Panama. *Nova Hedwigia* **77**: 487–523.

A synopsis of *Halimeda* morpho-taxonomic history

Heroen Verbruggen

The aim of this chapter is to give an overview of *Halimeda* taxonomic history, focusing on trends of character use. Throughout the history of *Halimeda* systematics, taxonomists have stressed different characters, resulting in significantly different species delineations and classifications. The general trend is towards expansion of the arsenal of characters. After an initial period in which segment morphology and thallus habit were the main diagnostic features, an increasing number of anatomical characters were examined and stressed in species descriptions. Recently, electron microscopy and statistical analysis of morphological data have been added to the miscellany of techniques used.

Foundations

The foundations of *Halimeda* taxonomy were reviewed in great detail in the monograph of Hillis-Colinvaux (1980). Therefore, only a selection of interesting topics and the characters used for species delineation are discussed here. The earliest historical record of *Halimeda tuna* (as *Sertolara*; authorities of *Halimeda* species and sections in Appendix 1 of Chapter 1), the type species of the genus, dates back to 1599 (Hillis-Colinvaux 1980), and it was not until the 18th century that additional species were described. The first taxonomic studies of the genus were by John Ellis, who diagnosed several species of the genus (Ellis & Solander 1786). Even though Ellis studied the anatomy of *H. incrassata* (as *Corallina incrassata*; Ellis 1767, cited after Hillis-Colinvaux 1980), no anatomical characters were used to distinguish between the species described in Ellis & Solander (1786). Ellis' anatomical observations enticed him to consider *Halimeda* (as *Corallina*) as an animal (Hillis-Colinvaux 1980). The genus *Halimeda* was separated from *Corallina* only in 1812 by Jean Vincent Felix Lamouroux[1].

The description of *Halimeda* species solely based on segment morphological differences persisted throughout most of the 19th century (Lamouroux 1816, Decaisne 1842, Zanardini 1851, Kützing 1858, Agardh 1887), bringing the total number of species to 26 in 1887. Jacob Georg Agardh (1887) partitioned the genus into four species groups (*Tunae*, *Pseudo-opuntiae*, *Opuntiae*, and *Rhipsales*) of implicit rank on the basis of differences in segment morphology and thallus appearance. Giovanni Batista De Toni (1889) cited Agardh's descriptions as diagnoses for sections.

Eugen Askenasy (1888) studied a collection of Pacific specimens of *Halimeda* from the S.M.S. Gazelle expedition. He pioneered the use of anatomical features for taxonomic purposes. He found significant differences in peripheral utricle size and, from these differences, described a new species (*H. macrophysa*) and a new variety (*H. opuntia* var. *macropus* Askenasy). Furthermore, Askenasy discovered that adjacent medullar siphons of *H. incrassata* and *H. macroloba* were interconnected at nodes by means of lateral pores.

[1] *Halimeda* is a conserved name (Silva 1952). The name *Sertularia* was proposed for this genus in 1760 (Ludwig 1760, cited after Silva 1952), 52 years before the establishment of the *Halimeda* denomination by Lamouroux (1812).

Barton monograph

Ethel Sarel Barton was the first to provide a comprehensive monograph of the genus (Barton 1901). She studied large collections from the coral-boring expedition to Funafuti (Barton 1900) and the Siboga expedition to Indonesia (Barton 1901). Additionally, she had the collections of the British Museum and Kew Herbarium at hands.

Barton meticulously studied a variety of anatomical characters and asserted that such characters were taxonomically more informative than thallus habit and segment shape. She stated about segment morphology that "the connecting links [between species] were so complete that it would have been necessary, using these characters alone, to reduce the number of species to two" (Barton 1901, p. 9). A first anatomical character studied in a taxonomic context was the pattern of nodal siphon fusion. Barton recognized three fusion types, namely fusion into a single unit by pores, complete fusion into pairs or triplets, and incomplete fusion into pairs or triplets, and she used these types to discern between groups of species and some individual species. Following Askenasy's example, Barton also carefully noted the size of peripheral utricles, and introduced the degree of lateral adhesion between adjacent peripheral utricles as a character. Size and adhesion of peripheral utricles were exclusively used for distinguishing *H. cuneata*, *H. macrophysa* and *H. tuna* (as interpreted by her). Three-dimensional segment structure (ribbedness, undulateness) was another character introduced by her.

Barton's taxonomy was characterized by extensive lumping of existing species into only a few morpho-types that did not show overlap in the characters used. The number of species was reduced from 27 to seven[2]. Within most species, several (often distinct) forms were described.

With hindsight, the monograph of Barton has been a significant advancement of *Halimeda* taxonomy. First, it reported on the systematic variability in nodal fusions, which could be used for delineating species groups. Second, through the study of the majority of type specimens, Barton tidied up the taxonomic confusion created by many species descriptions based on segment morphology alone. Third, she carefully described intraspecific plasticity of external morphological and anatomical characters. Lastly, the illustrations of Barton were of exceptional quality, and, together with her clear descriptions, pinpoint differences between entities that are informative to this day.

Post-Barton taxonomy

In the period after Barton's monograph, many new collections from the Caribbean region became available. These were studied mainly by Marshall Avery Howe (1905a, b, 1907, 1909) and Frederik Børgesen (1911, 1913). These authors used the whole gamut of external morphological and anatomical characters used by Barton (1901) and added a few of their own. Howe used utricular spines to distinguish the new species *H. scabra* from *H. tuna* (Howe 1905a) and thoroughly examined the utility of secondary utricle size and shape for distinguishing *H. tuna* from *H. discoidea* (Howe 1907) as well as for the description of *H. lacrimosa* (Howe 1909). Furthermore, he used primary utricle size and the absence of utricle adherence to recognize a new species *H. favulosa* (Howe 1905b). The presence of lateral fusions between adjacent peripheral utricles and the number of peripheral utricles borne on secondary utricles were also introduced as taxonomic characters (Howe 1907, 1909). Some of the broad species described by Barton (1901) were split up. Børgesen (1911, 1913) more closely hung onto Barton's taxonomy, not recognizing *H. monile* and *H. simulans* as separate taxa from *H. incrassata*. However, Børgesen did agree with Howe on the distinctness of *H. tuna* and *H. discoidea*. Børgesen's taxonomy is characterized by a few broad species with many well-described and illustrated forms and varieties recognized within each of them.

[2] With hindsight, several of the species of Barton (1901) were poly- and paraphyletic.

The first major collections from the Pacific Ocean were made in the framework of the Bikini bombing project. These collections contained many new species described by William Randolph Taylor (1950), using the broad range of external and anatomical characters used by Barton, Howe and Børgesen. Another species from the Pacific Ocean (*H. micronesica*) was described by Yukio Yamada (1941, 1944). Both Yamada and Taylor recognized a nodal siphon pattern not discussed by any of the former authors, namely the proceeding of medullar siphons from one segment into the next without any kind of fusion.

Hillis monographs

Llewellya Hillis monographed the genus twice (Hillis 1959, Hillis-Colinvaux 1980) and, together with colleagues, published numerous papers on the taxonomy, ecology, culturing, calcification and sedimentology of *Halimeda*. In her first monograph, all known species were described and illustrated. She followed Howe (1907) in the recognition of *H. simulans* and *H. monile* at the specific rank. The height of nodal fusions appeared in some of the descriptions and was considered useful for identification of *H. simulans*. Although initially introduced by Howe (1907, 1909), Hillis (1959) provided the first comprehensive overview of the number of peripheral utricles borne by secondary utricles. She did not recognize many subspecific entities, even though she elaborated intraspecific morphological variability within *H. tuna*, *H. discoidea*, *H. opuntia*, and a few other species. The monograph by Hillis (1959) contained illustrations of the thallus habit and cortex of all species. In sharp contrast to Barton's (1901) monograph, intraspecific plasticity in external morphological features was barely illustrated. The scarce information on reproductive structures available at that time was summarized and illustrated, but not used in the taxonomic treatise.

During the two decennia following Hillis' (1959) monograph, several new *Halimeda* species were described (Taylor 1962, Colinvaux & Graham 1964, Valet 1966, Goreau & Graham 1967, Colinvaux 1968, Taylor 1975, Hillis-Colinvaux 1975). The most explosive expansion of species was in section *Opuntia*, which was enlarged from one to seven species by description of new species (Taylor 1962, Goreau & Graham 1967) and recognition of entities formerly described as forms within other species at the specific rank (Colinvaux 1968, Hillis-Colinvaux 1975). With these studies a new type of nodal siphon pattern was revealed: in *H. cryptica* only a single siphon passes through the node (Colinvaux & Graham 1964). Apart from this, no new characters were revealed and the recognition of new species was based on combinations of external morphological and anatomical characters.

Hillis' second monograph (Hillis-Colinvaux 1980) was a comprehensive review of the knowledge on *Halimeda*, including chapters on morphology, taxonomic history, contemporary taxonomy, culture, growth and calcification, reproduction, biogeography, productivity and ecology. Hillis-Colinvaux paid a lot of attention to the historical account, in particular to the earliest taxonomic works. The taxonomy presented in this monograph was very close to that of Hillis (1959), with incorporation of the new species or changes in rank established in the meanwhile. No new taxonomically informative characters were added and, as in her 1959 monograph, intraspecific morphological variability was barely illustrated. For the majority of species a photograph of a single specimen, representing the morphology of the type, was presented. Hillis-Colinvaux (1980) brought the sectional subdivision of the genus back into prominence. This subdivision, which had remained unchanged and unused since De Toni (1889), had lost credibility because it was based only on segment shape and thallus habit, which were regarded as exceedingly variable characters. Hillis-Colinvaux (1980) based her sectional division on the anatomical character that had dominated the division of the genus into species groups since Barton (1901), namely the nodal siphon pattern. She recognized five patterns, among which the three of Barton (1901), continuation of several siphons without any form of fusion, and the node consisting of a single siphon.

Recent developments

In the period since Hillis-Colinvaux' (1980) monograph, four additional species have been described (*H. xishaensis*: Dong & Tseng 1980, *H. hummii*: Ballantine 1982, Wysor & Kooistra 2003; *H. magnidisca*: Noble 1986; *H. howensis*: Kraft 2000). All these descriptions were based on thorough examinations of external and anatomical characters used in the monographs of Hillis. Except Noble (1986), who introduced the use of cortical anatomy of basal segments to support the identity of *H. magnidisca*, none of these authors added new taxonomic characters.

Joanne Margaret Noble monographed the *Halimeda* species from Heron Island in the southern Great Barrier Reef in an unpublished MSc thesis (Noble 1987). She used the same species concept as Hillis-Colinvaux (1980) and provided excellent descriptions and illustrations of the Great Barrier Reef specimens and several type collections. She thoroughly discussed morphological differences between species and the vagueness of certain species boundaries. No new characters were introduced in Noble's thesis.

Dragastan et al. (2002) investigated the morphology of recent collections of extant species and of segments in limestone drilling cores from the western Pacific. They gathered a dataset of measurements of segments and several anatomical structures. Segments from near the base, center, and apex of thalli of extant species were examined. The obtained dataset was used to identify Pleistocene–Pliocene segments from the cores. Many extant species were identified from the deposits and were photographed with remarkable detail. Additionally, Dragastan et al. (2002) synonymized a number of fossil species with extant species because the fossil species, which were often described only on the basis of anatomical structures as observed in thin sections, conformed to basal segments of extant species.

Vroom & Smith (2003) assessed the putative taxonomic information contained in reproductive structures. They gathered morphometric information on gametophores, gametangia and gametes from the literature and carried out statistical analysis of these data in a taxonomic context. Although it must be taken into account that their study was based on low numbers of observations, Vroom & Smith's (2003) analyses indicated that certain reproductive features, in particular gametophore length, are taxonomically informative. However, the absence of reproductive structures from the majority of collections limits the taxonomic utility of such structures.

Very recently, Bandeira-Pedrosa et al. (2003, 2004) studied the ultrastructure of six *Halimeda* species from Brazil in search for new taxonomic characters. However, they found great ultrastructural uniformity among species. Nonetheless, they did reveal lenticular thickenings on the inside of cell walls of peripheral utricles of Brazilian *H. cuneata*. This character could, however, be easily observed using regular light microscopy after toluidine blue staining (Bandeira-Pedrosa 2004). Its presence in other species remains to be determined.

In conclusion, the *Halimeda* studies published since the monograph of Hillis-Colinvaux (1980) have added a few new characters, some of which could be widely applicable (e.g. basal segment anatomy, reproductive features). Additionally, morphometric data are more often compiled and analyzed statistically.

References

Agardh J.G. (1887). Till algernes systematik. Nya bidrag. (Femte afdelningen). *Acta Universitatis Lundensis* **23** (2): 1-174.

Askenasy E. (1888) Algen. In: *Die Forschungsreise S.M.S. Gazelle* Th. 4, Bot., Berlin.

Ballantine D.L. (1982) *Halimeda hummii* sp. nov., *Halimeda cryptica* v. *acerifolia* var. nov. (Caulerpales, Chlorophyta), and additional records of *Halimeda* species from Puerto Rico. *Journal of Phycology* **18**: 86–91.

Bandeira-Pedrosa M.E., Bouzon Z.L., Pereira S.M. & Oliveira E.C. (2003) Ultrastructure of some species of *Halimeda* (Bryopsidales, Chlorophyta) from Brazil. *Cryptogamie Algologie* **24**: 219–231.

Bandeira-Pedrosa M.E., Pereira S.M.B., Bouzon Z.L. & Oliveira E.C. (2004) *Halimeda cuneata* (Bryopsidales, Chlorophyta), a new record for the Atlantic Ocean. *Phycologia* **43**: 50–57.

Barton E.S. (1900) On the forms, with a new species, of *Halimeda* from Funafuti. *Bot. J. Linnean Soc. London* **34**: 479–482.

Barton E.S. (1901) The genus *Halimeda*. *Monographs of the Siboga Expedition* **60**. Brill, Leiden. 32pp.

Børgesen F. (1911) Some Chlorophyceae from the Danish West Indies. *Botanisk Tidsskrift* **31**: 127–152.

Børgesen F. (1913) The marine algae of the Danish West Indies. Part 1. Chlorophyceae. *Dansk Botanisk Arkiv* **1** (4): 1–160. Reprinted in 1985 by Koeltz, Koenigstein, Germany.

Colinvaux L.H. (1968) New species of *Halimeda*: A taxonomic reappraisal. *Journal of Phycology* **4**: 30–35.

Colinvaux L.H. & Graham E.A. (1964) A new species of *Halimeda*. *Nova Hedwigia* **7**: 5–10.

Decaisne J. (1842) Mémoires sur les corallines ou polypiers calcifères. *Annales des Sciences Naturelles, Botanique Ser. 2*, vol **16**: 85–120.

De Toni G.B. (1889) *Sylloge algarum omnium hucusque cognitarum*. Vol. I. Chlorophyceae. Patavii, privately published.

Dong M.L. & Tseng C.K. (1980) Studies on some marine green algae from the Xisha Islands, Guangdong Province, China. II. *Studia Marina Sinica* **17**: 1–10.

Dragastan O.N., Littler D.S. & Littler M.M. (2002) Recent vs. fossil *Halimeda* species of Angaur Island, Palau and adjacent western Pacific areas. *Acta Palaeontologica Romaniae Special Publication No. 1.* Cartea Universitara, University of Bucharest. Bucharest, Romania.

Ellis J. (1767) Extract of a letter from John Ellis, Esq. F.R.S. to Dr. Linnaeus, of Upsal F.R.S., on the animal nature of the genus of zoophytes called *Corallina*. *Philosophical Transactions* **57**: 404–427.

Ellis J. & Solander D. (1786) The natural history of many curious and uncommon zoophytes, collected from various parts of the globe by the late John Ellis ... Systematically arranged and described by the late Daniel Solander. B. White & son, London.

Goreau T.F. & Graham E.A. (1967) A new species of *Halimeda* from Jamaica. *Bulletin of Marine Science* **17**: 432–441.

Hillis L. (1959) A revision of the genus *Halimeda* (order Siphonales). *Publications of the Institute of Marine Science* **6**: 321–403.

Hillis-Colinvaux L. (1975) *Halimeda renschii* revived, and *Halimeda batanensisi* (Chlorophyta, Siphonales). *Phycologia* **14**: 93–96.

Hillis-Colinvaux L. (1980) Ecology and taxonomy of *Halimeda*: primary producer of coral reefs. *Advances in Marine Biology* **17**: 1–327.

Howe M.A. (1905a) Phycological studies. I. New Chlorophyceae from Florida and the Bahamas. *Bulletin of the Torrey Botanical Club* **32**: 241–252.

Howe M.A. (1905b) Phycological studies. II. New Chlorophyceae, new Rhodophyceae and miscellaneous notes. *Bulletin of the Torrey Botanical Club* **32**: 563–586.

Howe M.A. (1907) Phycological studies. III. Further notes on *Halimeda* and *Avrainvillea*. *Bulletin of the Torrey Botanical Club* **34**: 491–515.

Howe M.A. (1909) Phycological studies. IV. The genus *Neomeris* and notes on other Siphonales. *Bulletin of the Torrey Botanical Club* **36**: 75–104.

Kraft G.T. (2000) Marine and estuarine benthic algae (Chlorophyta) of Lord Howe Island, Southwestern Pacific. *Australian Systematic Botany* **13**: 509–648.

Kützing F.T. (1858) *Tabulae phycologicae*. Vol. 8. Nordhausen, Germany.

Lamouroux J.V.F. (1812) Extrait d'un memoire sur la classification de polypes coralligenes non entierement pierreux. *Nouveau Bulletin Scientifique de la Societe Philomatique* **3**: 181–188.

Lamouroux J.V.F. (1816) *Histoire des polypiers coralligenes flexibles, vulgairement nommés geophytes.* Poisson, Caen, France.

Ludwig C.G. (1760) D. Christiano Gottlieb Ludwig ... Definitiones generum plantarum ... nucn auctas et emendatas edidit D. Georgius Rudolphus Boehmer ... Leipzig.

Noble J.M. (1986) *Halimeda magnidisca* (Caulerpales, Chlorophyta), a new species from the Great Barrier Reef, Australia. *Phycologia* **25**: 331–339.

Noble J.M. (1987) *A taxonomic study of the genus* Halimeda *Lamouroux (Chlorophyta, Caulerpales) from the Heron Island region of the southern Great Barrier Reef, Australia.* Masters degree thesis, University of Melbourne. Melbourne, Australia.

Silva P.C. (1952) A review of nomenclatural conservation in the algae from the point of view of the type method. *University of California Publications in Botany* **25** (4): 241–324.

Taylor W.R. (1950) *Plants of Bikini and other northern Marshall Islands.* University of Michigan Press, Ann Arbor, MI.

Taylor W.R. (1962) Two undescribed species of *Halimeda*. *Bulletin of the Torrey Botanical Club* **89**: 172–177.

Taylor W.R. (1975) A new species of *Halimeda* from Malaysia. *Contributions from the University of Michigan Herbarium* **11**: 81-83.

Valet G. (1966) Sur une espèce rare et une nouvelle espèce d'*Halimeda* de Mélanésie. *Revue Générale de Botanique* **73**: 680–685.

Vroom P.S. & Smith C.M. (2003) Reproductive features of Hawaiian *Halimeda velasquezii* (Bryopsidales, Chlorophyta), and an evolutionary assessment of reproductive characters in *Halimeda*. *Cryptogamie Algologie* **24**: 355–370.

Yamada Y. (1941) [On the species of *Halimeda* from Micronesia]. *Kagaku Nanyõ* **4**: 108–121.

Yamada Y. (1944) New *Caulerpas* and *Halimedas* from Micronesia. *Scientific Paper of the Institute of Algological Research of Hokhaido University* **3**: 27–29.

Wysor B. & Kooistra W.H.C.F. (2003) An annotated list of marine Chlorophyta from the Caribbean coast of the Republic of Panama. *Nova Hedwigia* **77**: 487–523.

Zanardini G. (1851) Algae novae vel minus cognitae in mari Rubro a Portiero collectae. *Flora* **34**: 33–38.

The molecular revolution in *Halimeda* systematics

Heroen Verbruggen

The aim of this chapter is to describe the molecular phylogenetic studies that had been carried out on *Halimeda* before the onset of my PhD research. Before that, however, the employed molecular markers are introduced. This section is not limited to the markers used before my research; it also introduces the DNA regions used in my own work. After a short introduction to some preliminary studies, the most comprehensive study by Kooistra et al. (2002) is expanded on. Their phylogenetic tree is interpreted in terms of ecological divergence and further diversification of the genus. Furthermore, the historical biogeography and taxonomic consequences of this study are stressed.

Molecular markers

Nuclear ribosomal DNA

Molecular phylogenetic studies of *Halimeda* have been mainly based on nuclear ribosomal DNA sequences. Nuclear ribosomal DNA is organized into arrays at one or more chromosomal locations (Rogers & Bendich 1987, Wendel et al. 1995). Each array contains hundreds to thousands repeats of a basic element (Figure 1). This basic element, the rDNA cistron, is composed of the 18S ribosomal subunit, the internal transcribed spacer 1, the 5.8S ribosomal subunit, the internal transcribed spacer 2, the 28S ribosomal subunit, and the intergenic spacer (IGS) (Figure 1). The intergenic spacer comprises a nontranscribed part at the 5' end and a transcribed part at the 3' end (Figure 1). In most circumstances, all subsequent elements in the repeat are identical as a result of concerted evolution. Concerted evolution is the molecular process of DNA sequence homogenization among different loci within multigene families and thus also affects the nrDNA (Arnheim et al. 1980). Sequence homogenization via concerted evolution is driven by the molecular processes of gene conversion and unequal crossing over (Liao 1999). Nuclear ribosomal DNA is inherited biparentally and crossing over between maternal and paternal copies is known to occur.

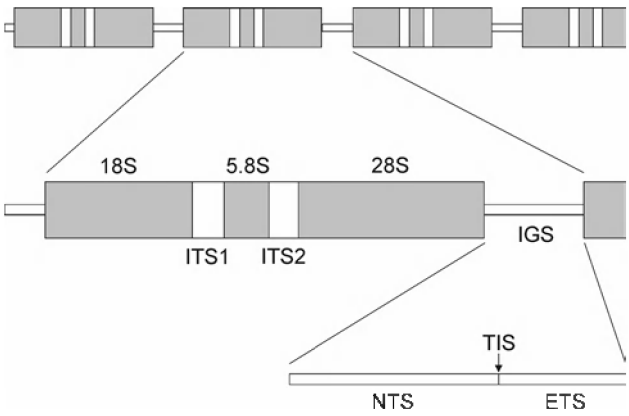

Figure 1. Nuclear ribosomal genes are organized in arrays (above). Each repeat unit contains DNA coding for the 18S (small) rRNA subunit, a first internal transcribed spacer (ITS1), the 5.8S rRNA subunit, a second internal transcribed spacer (ITS2), and the 28S (large) rRNA subunit. The intergenic spacer (IGS) separates such gene clusters from one another in the array. It consists of a nontranscribed spacer (NTS), at the end of which the transcription initiation sequence (TIS) is situated, and an external transcribed spacer (ETS). Individual arrays, of which several can be present in a single genome, contain hundreds to thousands of repeat units. After Wendel et al. (1995) and Linder et al. (2000).

Both small (18S) and large (28S) ribosomal subunit sequences are commonly used in plant phylogenetic studies at higher taxonomic levels (Small et al. 2004). In general, their rate of evolution is too slow to provide resolution at lower taxonomic levels. For phylogenetic inference at these

levels, the more variable ITS region is routinely employed (Small et al. 2004). ETS, which is also more variable than the rRNA coding sequences, has also been employed for low-level phylogenetics (Baldwin & Markos 1998, Linder et al. 2000). ITS and ETS sequences are excised from the precursor RNA resulting from transcription of the ribosomal RNA cistron. Highly conserved secondary and higher order structural features play a vital role in the excision process (van Nues et al. 1995). Between the conserved regions, more variable regions are present (van Nues et al. 1995).

Plastid DNA

Each plastid contains several nucleoids, which each contain multiple plastid genomes (Armbrust 1998). Individual plastid DNA molecules come in various structures, among which circular, linear and branched (Oldenburg & Bendich 2004). Individual DNA molecules generally comprise several genome copies (Oldenburg & Bendich 2004). Normally, plastid DNA inheritance is uniparental and non-recombinational, which is beneficial for phylogenetic inference. Yet these generalizations are not without exceptions (Peters et al. 2004, briefly reviewed in Small et al. 2004).

Two types of plastid markers have been used for phylogenetic inference in *Halimeda*. The first is *tuf*A, which codes one part of the peptide chain elongation factor Tu (van der Meide et al. 1982). This gene of prokaryotic origin (Delwiche et al. 1995) is present in chlorophytes plastids, and was transferred from the chloroplast to the nucleus during streptophyte evolution (Baldauf & Palmer 1990). The use of *tuf*A in chlorophyte phylogenetics has been limited. Results from Delwiche et al. (1995) suggest that it does not provide much resolution among chlorophyte lineages. On the other hand, *tuf*A has proven a useful marker for phylogenetic inference within the genus *Caulerpa* (Famà et al. 2002, de Senerpont-Domis et al. 2003).

Provan et al. (2004) developed eight universal primer pairs for amplification of green algal plastid DNA. They studied the plastid genome of four chlorophytes and found that the region between *rps*11 and *rpl*2 contains mostly ribosomal proteins in a constant order. Primers were designed from conservative regions within genes, each primer pair spanning an intergenic spacer (Figure 2).

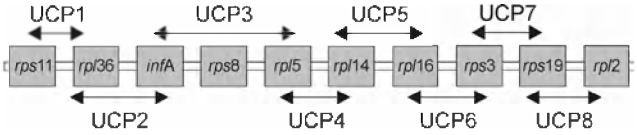

Figure 2. Graphical representation of the syntenic region between the genes for ribosomal protein s11 (*rps*11) and *rpl*2. These genes occur in a constant sequence in the four chlorophyte plastid genomes studied by Provan et al. (2004). The UCP stretches indicated above and below indicate regions amplified by the universal chlorophyte primers of Provan et al. (2004). Not shown to scale. After Provan et al. (2004)

Molecular phylogenetics

Preliminary assays

Hillis et al. (1998) conducted the first phylogenetic study of *Halimeda*. They analyzed sequences of the latter half of the nuclear 18S ribosomal DNA (723 bp), including an insert of approximately 102 bp. This preliminary study included only 10 species out of 33 recognized at that time, but allowed prudent confirmation of four out of the five sections defined by Hillis-Colinvaux (1980). Furthermore, Hillis et al. (1998) demonstrated that phylogenetic analysis of molecular and qualititative morpho-anatomical data yielded the same basic generic subdivision.

A first expansion of the sequence set appeared in Kooistra et al. (1999). Their phylogeny was based on partial 18S sequences of 48 specimens belonging to 15 species. The traditional sectional subdivision, which was based on nodal fusion patterns (Hillis-Colinvaux 1980), was further confirmed with the inclusion of *H. cryptica*. Nonetheless, the sections *Halimeda* and *Opuntia* appeared non-monophyletic. Next to this finding, Kooistra et al. (1999) stressed the historical biogeographic patterns in the phylogeny. The *H. discoidea* and section *Rhipsalis* clades split up into distinct Indo-Pacific and Caribbean

clusters. The distinctness of entities from Atlantic and Indo-Pacific ocean basins was linked to the interruption of the marine tropical belt by the land bridges of Suez and Panama.

Hillis (1999, 2001) put the phylogenetic results of Hillis et al. (1998) and Kooistra et al. (1999) in a paleontological perspective. These papers provied no new data and very few new insights.

A comprehensive phylogenetic study

The most comprehensive study on *Halimeda* evolution is Kooistra et al. (2002). This study expanded the dataset to include 28 species and sequences of ITS1, 5.8S, and ITS2. Inclusion of these more variable markers yielded a well-resolved phylogeny (Figure 3).

Basic subdivision of the genus

Kooistra et al. (2002) recognized five clear-cut clades within the genus (Figure 3), of which only one (lineage 5) corresponded to a traditional section (*Opuntia*). The other four lineages were subsets of previously described sections or included species from different sections. Morphological character evolution was inferred by plotting morphological data over the phylogeny. This allowed morphological characterization of certain lineages and identification of morphological convergence (Kooistra et al. 2002). Relationships between lineages were fairly well resolved, but a tree featuring swapped lineages 2 and 3 was not significantly worse according to the Kishino-Hasegawa test.

Historical ecology

Kooistra et al. (2002) plotted species' ecological characteristics, such as attachment to unconsolidated substrate and growth in sheltered localities, onto their nrDNA tree. The ecological features were clearly linked to major clades in the phylogeny. Nonetheless, in all lineages featuring a certain ecological character, there were one or a few species which didn't feature the character in question. It was hypothesized that ecological niche shifts were at the base of the intial radiation of the genus into its major lineages and that, within these principal lineages, similar niche shifts were responsible for the incomplete corellation between ecology and topology. Kooistra et al. (2002) also showed that certain morphological characters corellated with ecological features, suggesting that these traits have an adaptive value. For example, large, bulbous holdfasts can anchor *Halimeda* in unconsolidated substrata, and strong calcification keeps herbivores away. Pliable, barely calcified

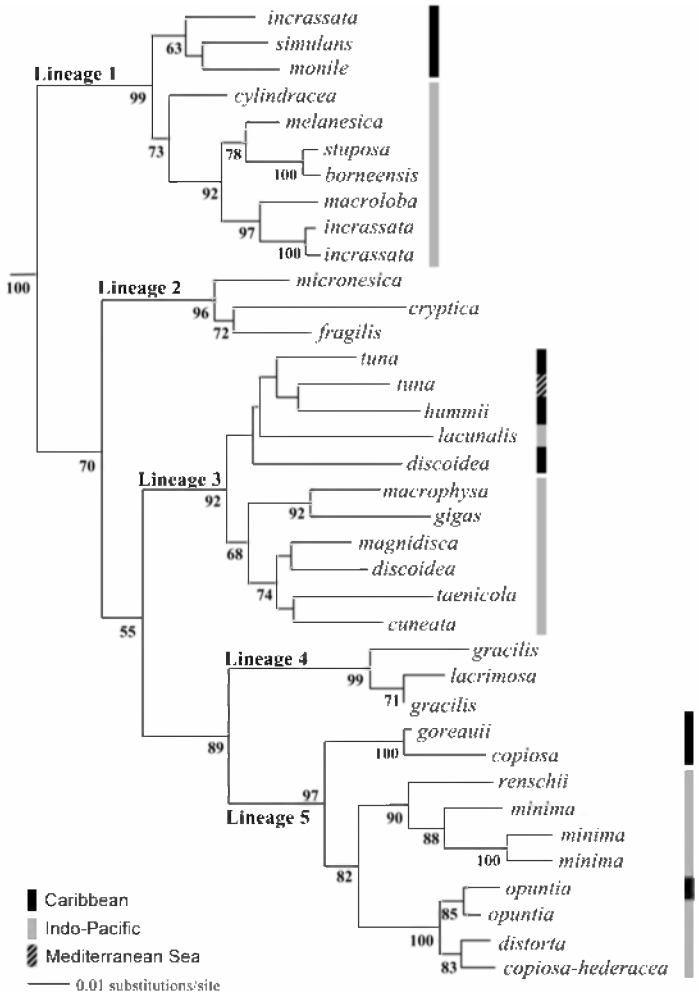

Figure 3. Phylogenetic tree of 28 *Halimeda* species inferred by maximum likelihood from nuclear ribsomal partial SSU, ITS1, 5.8S, ITS2 and partial LSU sequences. Maximum parsimony bootstrapping proportions are indicated at nodes. Adapted from Kooistra et al. (2002). Note: The species *H. hederacea*, which was not included in Appendix 1 of Chapter 1, has recently been synonymized with *H. distorta* (Kooistra & Verbruggen 2005)

segments probably evolved as an adaptation to drag reduction in herbivore-poor habitats.

Historical biogeography

The three most species-rich lineages show a basal partitioning of the species into Atlantic and Indo-Pacific clusters (Figure 3), although some exceptions are present (e.g. *H. lacunalis*). Near-perfect separation of lineages into Atlantic and Indo-Pacific sister clades suggests allopatric divergence following a vicariance event. Kooistra et al. (2002) listed the closure of the Tethys Seaway in the Middle East (ca. 13 Ma), the shoaling of the Central American Isthmus (ca. 3.5 Ma), and the intensification of the Benguela upwelling (ca. 2 Ma) as possible events causing vicariance between the Atlantic and Indo-Pacific ocean basins. Of these alternatives, vicariance caused by the rise of the Panamanian Isthmus was considered most probable.

Cryptic species diversity

One of the most significant results from Kooistra et al. (2002) was the discovery of cryptic diversity within species. All but one amphitropical species of the genus were shown to consist of two, only distantly related, genetic entities (Figure 3). Given the distant relatedness of the genetic entities within presumed morpho-species, and the fact that they occur in highly similar habitats, morphological convergence triggered by comparable selective pressures was put forward as the presumed cause of the observed cryptic diversity.

References

Armbrust E.V. (1998) Uniparental inheritance of chloroplast genomes. In Merchant S. (ed.) *The Molecular Biology of Chloroplasts and Mitochondria in* Chlamydomonas. Kluwer, Amsterdam, The Netherlands. pp. 93–113.

Arnheim N., Krystal M., Schmickel R., Wilson G., Ryder O. & Zimmer E. (1980) Molecular evidence for genetic exchanges among ribosomal genes on nonhomologous chromosomes in man and apes. *Proceedings of the National Academy of Sciences of the USA* **77**: 7323–7327.

Baldauf S.L. & Palmer J.D. (1990) Evolutionary transfer of the chloroplast *tuf*A gene to the nucleus. *Nature* **344**: 262–265.

Baldwin B.G. & Markos S. (1998) Phylogenetic utility of the external transcribed spacer (ETS) of 18S-26S rDNA: congruence of ETS and ITS trees of *Calycadenia* (Compositae). *Molecular Phylogenetics and Evolution* **10**: 449–463.

Delwiche C.F., Kuhsel M. & Palmer J.D. (1995) Phylogenetic analysis of *tuf*A sequences indicates a cyanobacterial origin of all plastids. *Molecular Phylogenetics and Evolution* **4**: 110–128.

de Senerpont-Domis L.N., Fama P., Bartlett A.J., Prud'homme van Reine W.F., Espinosa C.A. & Trono G.C. (2003) Defining taxon boundaries in members of the morphologically and genetically plastic genus *Caulerpa* (Caulerpales, Chlorophyta). *Journal of Phycology* **39**: 1019–1037.

Famà P., Wysor B., Kooistra W.H.C.F. & Zuccarello G.C. (2002) Molecular phylogeny of the genus *Caulerpa* (Caulerpales, Chlorophyta) inferred from chloroplast *tuf*A gene. *Journal of Phycology* **38**: 1040–1050.

Hillis L.W. (1999) Phylogeny of *Halimeda* (Bryopsidales): linking paleontological, morphological and molecular data. *Acta Palaeontologica Romaniae* **2**: 183–189.

Hillis L.W. (2001) The calcareous reef alga *Halimeda* (Chlorophyta, Bryopsidales): a Cretaceous genus that diversified in the Cenozoic. *Palaeogeography, Palaeoclimatology, Palaeoecology* **166**: 89–100.

Hillis L.W., Engman J.A. & Kooistra W.H.C.F. (1998) Morphological and molecular phylogenies of *Halimeda* (Chlorophyta, Bryopsidales) identify three evolutionary lineages. *Journal of Phycology* **34**: 669–681.

Hillis-Colinvaux L. (1980) Ecology and taxonomy of *Halimeda*: primary producer of coral reefs. *Advances in Marine Biology* **17**: 1–327.

Kooistra W.H.C.F., Caldéron M. & Hillis L.W. (1999) Development of the extant diversity in *Halimeda* is linked to vicariant events. *Hydrobiologia* **398**: 39–45.

Kooistra W.H.C.F., Coppejans E.G.G. & Payri C. (2002) Molecular systematics, historical ecology, and phylogeography of *Halimeda* (Bryopsidales). *Molecular Phylogenetics and Evolution* **24**: 121–138.

Kooistra W.H.C.F. & Verbruggen H. (2005) Genetic patterns in the calcified tropical seaweeds *Halimeda opuntia*, *H. distorta*, *H. hederacea* and *H. minima* (Bryopsidales, Chlorophyta) provide insights in species boundaries and inter-oceanic dispersal. *Journal of Phycology* **41**: 177–187.

Liao D.Q. (1999) Concerted evolution: Molecular mechanism and biological implications. *American Journal of Human Genetics* **64**: 24–30.

Linder C.R., Goertzen L.R., Heuvel B.V., Francisco-Ortega J. & Jansen R.K. (2000) The complete external transcribed spacer of 18S-26S rDNA: Amplification and phylogenetic utility at low taxonomic levels in Asteraceae and closely allied families. *Molecular Phylogenetics and Evolution* **14**: 285–303.

Oldenburg D.J. & Bendich A.J. (2004) Most chloroplast DNA of maize seedlings in linear molecules with defined ends and branched forms. *Journal of Molecular Biology* **335**: 953–970.

Peters A.F., Scornet D., Müller D.G., Kloareg B. & Cock J.M. (2004) Inheritance of organelles in artificial hybrids of the isogamous multicellular chromist alga *Ectocarpus siliculosus* (Phaeophyceae). *European Journal of Phycology* **39**: 235–242.

Provan J., Murphy S. & Maggs C.A. (2004) Universal plastid primers for Chlorophyta and Rhodophyta. *European Journal of Phycology* **39**: 43–50.

Rogers S.O. & Bendich A.J. (1987) Ribosomal RNA genes in plants: variability in copy number and in the intergenic spacer. *Plant Molecular Biology* **9**: 509–520.

Small R.L., Cronn R.C. & Wendel J.F. (2004) Use of nuclear genes for phylogeny reconstruction in plants. *Australian Systematic Botany* **17**: 145–170.

van der Meide P.H., Vijgenboom E., Dicke M. & Bosch L. (1982) Regulation of the expression of *tuf*A and *tuf*B, the two genes coding for the elongation factor EF-Tu in *Escherichia coli*. *FEBS letters* **139**: 325–330.

van Nues R.W., Rientjes J.M., Morre S.A., Mollee E., Planta R.J., Venema J. & Raue H.A. (1995) Evolutionarily conserved structural elements are critical for processing of Internal Transcribed Spacer 2 from *Saccharomyces cerevisiae* precursor ribosomal RNA. *Journal of Molecular Biology* **250**: 24–36.

Wendel J.F., Schnabel A. & Seelanan T. (1995) Bidirectional interlocus concerted evolution following allopolyploid speciation in cotton (*Gossypium*). *Proceedings of the National Academy of Sciences of the USA* **92**: 280–284.

Part 2

Basic subdivision of the genus

Morphological characterization of lineages within the calcified tropical seaweed genus *Halimeda*

Heroen Verbruggen & Wiebe H.C.F. Kooistra

European Journal of Phycology 39: 213–228 (2004)

Abstract

Halimeda Lamouroux constitutes a genus of calcified and segmented green seaweeds within the Bryopsidales. Molecular phylogenetic assessments have uncovered five principal monophyletic lineages within the genus. In the present study we define these lineages morphologically. We gathered morphological data from specimens used in the molecular analyses as well as from collections having a similar morphology and originating from the same geographical region. Starting from the lineages and their morphological synapomorphies, we define and illustrate five natural sections within *Halimeda*. All or most medullary siphons traversing the nodes between segments fuse into a single unit in specimens of lineage 1 (section *Rhipsalis*), and segments at the thallus base fuse with one another. Medullary siphons of specimens in lineage 2 (section *Micronesicae*) traverse the node without fusing. Medullary siphons of specimens in lineage 3 (section *Halimeda*) divide frequently below the nodes and become entangled among one another. The segments of specimens in this lineage possess a continuous uncorticated band along the distal perimeter instead of three or more pits as encountered in segments of specimens in all other lineages. Members of lineage 4 (section *Pseudo-opuntia*) possess club-shaped subperipheral utricles in their cortical region. Medullary siphons of specimens in lineage 5 (section *Opuntia*) fuse over only a short distance at the nodes and retain their identity. Apart from these synapomorphies, the lineages can be delimited further by a characteristic combination of symplesiomorphies and homoplasies. In addition we examined the morphology of *H. bikinensis* Taylor, a species not included in the molecular analyses, and discuss its ambiguous position in our sectional system.

Introduction

The green calcified seaweed genus *Halimeda* Lamouroux (1812) (Bryopsidales, Chlorophyta) occurs in reefs and lagoons across the tropics and subtropics (Barton 1901, Taylor 1950, Tsuda & Wray 1977, Dong & Tseng 1980, Hillis-Colinvaux 1980, 1988, Drew & Abel 1988, Tsuda & Kamura 1991, Drew 1995, Littler & Littler 2000, Bandeira-Pedrosa *et al.* 2001). The characteristically segmented thalli are composed of ramifying siphons forming a medulla and a surrounding cortex (Barton 1901; Hillis-Colinvaux 1980). The siphons in the medulla string segments together and ramify into the cortex. There they rebranch frequently and terminate in a layer of inflated peripheral utricles. The latter adhere to one another and so enclose the segment's intersiphonal spaces (Barton 1901, Hillis-Colinvaux 1980). There, calcium carbonate precipitates as aragonite (Borowitzka & Larkum 1977). Some medullary siphons surface in weakly calcified regions along the segment's distal perimeter where they adhere and may fuse. New segments (Hay *et al.* 1988), secondary holdfasts (Hillis-Colinvaux 1980, Walters & Smith 1994) or gametophores bearing bladder-like gametangia (Gepp 1904, Kamura 1966, Graham 1975, Drew & Abel 1988) develop from their tips. Thalli propagate clonally by means of

'runner' rhizoids (Hillis-Colinvaux 1980) or fragmentation (Walters & Smith 1994, Walters *et al.* 2002). Sexual reproduction occurs periodically; the gametes are released in concert in species-specific short intervals (Meinesz 1980, Drew & Abel 1988, Clifton 1997, Clifton & Clifton 1999).

The genus currently comprises 34 described extant species and several fossil taxa (Braga *et al.* 1996, Schlagintweit & Ebli 1998, Hillis 2000). All extant species[1] and their taxonomic authorities are listed in Table 1. Hillis-Colinvaux (1980) proposed five sections within the extant diversity based predominantly on patterns of medullary siphon anatomy at nodes between segments (Askenasy 1888, Barton 1901). These patterns often conflict with distributions of character states associated with utricle morphology and branching modes as well as with thallus habit across the taxa (Kooistra *et al.* 2002). Results of molecular phylogenetic studies in Kooistra *et al.* (2002) indicate that most sections sensu Hillis-Colinvaux are not monophyletic.

Table 1. List of currently[1] recognized *Halimeda* species and their taxonomic authorities. Species indicated with an asterisk were not examined in this study.

Species	authority
H. bikinensis	Taylor
H. borneensis	Taylor
H. copiosa	Goreau & Graham
H. cryptica	Colinvaux & Graham
H. cuneata	Hering
H. cylindracea	Decaisne
H. discoidea	Decaisne
H. distorta	(Yamada) Colinvaux
H. favulosa	Howe
H. fragilis	Taylor
H. gigas	Taylor
H. goreauii	Taylor
H. gracilis	Harvey *ex* J. Agardh
H. howensis	Kraft & Noble*
H. hummii	Ballantine
H. incrassata	(Ellis) Lamouroux
H. lacrimosa	Howe
H. lacunalis	Taylor
H. macroloba	Decaisne
H. macrophysa	Askenasy
H. magnidisca	Noble
H. melanesica	Valet
H. micronesica	Yamada
H. minima	(Taylor) Colinvaux
H. monile	(Ellis & Solander) Lamouroux
H. opuntia	(Linnaeus) Lamouroux
H. renschii	Hauck
H. scabra	Howe
H. simulans	Howe
H. stuposa	Taylor
H. taenicola	Taylor
H. tuna	(Ellis & Solander) Lamouroux
H. velasquezii	Taylor
H. xishaensis	Dong & Tseng*

The principal goals of this study are to demarcate monophyletic sections within *Halimeda* and to uncover their defining morphological traits. A morphological definition of these natural groups not only provides a helpful tool towards accurate identification of species but also allows, at least tentatively, placement of relatively recent fossil specimens in these sections. To achieve our goals, we inferred a maximum likelihood phylogeny from nuclear rDNA sequences of specimens across the taxonomic diversity and demarcated principal lineages therein. We then examined morphology and anatomy of the specimens included in the phylogeny in search of those traits whose states define one or more of these lineages. In addition, we included specimens in the morphological analyses for which no sequences were available but we used the latter specimens only to ascertain their fit into sections, not to redefine the sections.

Materials and methods

A list of specimens, together with their taxonomic identifications, herbarium codes and the GenBank accession numbers for their partial nuclear rDNA sequences is presented in Appendix 1. Details of preservation, taxonomic identification, DNA extraction, PCR and sequencing protocols can be found in Kooistra *et al.* (2002). The 155 specimens of *Halimeda* used in this study were attributable to 32 of 34 currently recognized species (Table 1). All 49 specimens used for molecular analyses in this study

[1] This refers to all extant species recognized at the time this paper was published (i.e. May 2004).

as well as those used in previous publications on *Halimeda* by Kooistra and co-workers (Kooistra *et al.* 2002) are deposited in the GENT herbarium.

Phylogenetic analyses of the alignment were carried out using PAUP* version 4.0.b10 (Swofford 2002). In all analyses, ambiguities were treated as uncertainties and gaps as missing data. Sequences of *Udotea flabellum* (Ellis & Solander) Howe and *Penicillus capitatus* Lamarck were used as the outgroup (Kooistra 2002, Kooistra *et al.* 2002). Hierarchical likelihood ratio tests (hLRT's) were performed using Modeltest v3.06 (Posada & Crandall 1998). Resulting optimal parameters were then used to constrain maximum likelihood (ML) analysis. The ML analysis was carried out under the heuristic search option and tree bisection/reconnection branch swapping and was constrained using optimal hLRT parameter settings. Weighted (K=2; Goloboff 1993) maximum parsimony (MP) analysis was carried out under the heuristic search option and tree bisection/reconnection branch swapping. Bootstrap analyses (1000 replicates) were performed in weighted MP under the same settings.

Morphological analysis was also carried out on specimens used in the molecular analysis unless, in a few cases, not enough material was available. In that case, specimens unambiguously belonging to the same species and coming from the same geographical region were used. Additional specimens, for which no sequences were available, have also been examined (Appendix 1). Thallus and segment characteristics were noted. Anatomical details were gathered by dissection of segments as described in Hillis-Colinvaux (1980) with the following modifications. The cortex was sectioned following decalcification. The medullary and nodal regions therein were examined after decalcification and removal of the surrounding cortical parts. In those cases where all nodal siphons fused into a single aggregate, nodal structures were also sectioned lengthwise. Scraped-off cortex fragments were used to examine segment surface. Observations on cortical structures were done using a slide with a cavity, allowing a better 3D impression. Camera lucida drawings were made using an Olympus BX51 microscope (Olympus, Tokyo, Japan).

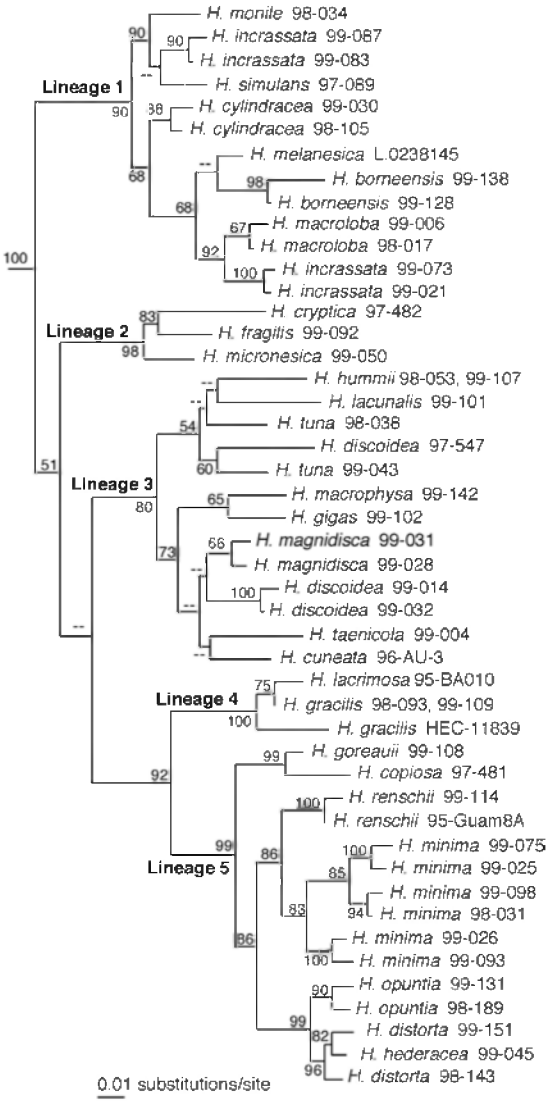

Figure 1. Maximum likelihood phylogram inferred from partial SSU nrDNA, ITS1, 5.8S rDNA and ITS2 of 47 specimens of *Halimeda* species and two outgroup species (see Appendix 1). – Ln likelihood = 9895.44751, tree-length = 1390 steps. The phylogram presented here has been redrawn with the outgroup taxa pruned away. MP bootstrap values >50% are indicated below internodes. Lineages 1–5 are explained in text.

Results

Hierarchical likelihood ratio tests performed on the sequence data set favored a general-time-reversible base substitution model with estimated values for the following parameters: base frequencies: A = 0.206, C = 0.271, G = 0.305, T = 0.218; substitution rates: A ↔ C = 1.211, A ↔ G = 1.890, A ↔ T = 1.524, C ↔ G = 0.653, C ↔ T = 3.525 relative to G ↔ T = 1.000; proportion of invariable sites = 0.550; gamma shape parameter = 0.455. The tree resulting from our ML analysis constrained with these pa-

rameters is presented in Figure 1. The topology is highly similar to those in Kooistra *et al.* (2002). The tree-topology resulting from weighted MP analysis (not shown) differed only in a single aspect from that in Figure 1: *H. hummii* and *H. lacunalis* did not form a clade. Five principal lineages marked in Figure 1 obtained high bootstrap support as did the clade containing lineages 4 and 5. Yet, the basal clades grouping these lineages obtained poor or insufficient support as in Kooistra *et al.* (2002). All sequence pairs belonging to the same morphologically defined species obtained high bootstrap support. Figures 2 to 42 illustrate the general morphology and anatomical characters of specimens in each of the five lineages.

Lineage 1, Figures 2–10.

Western Atlantic (Caribbean region):
H. favulosa, *H. incrassata*, *H. monile*, *H. simulans*
Indo-Pacific basin: *H. borneensis*, *H. cylindracea*, *H. incrassata*, *H. macroloba*, *H. melanesica*

Most specimens were anchored in sandy substrata by means of a bulbous holdfast (Figures 2, 3). Lower segments were large and barrel-shaped and the walls of their cortical siphons were strongly thickened thus giving rise to a stiff, stipe-like structure. In many species, segments on top of this so-called pseudo-stipe were moderately calcified, enlarged and partially fused in a fan- or squat-pillar-like structure (Figure 2). *Halimeda melanesica* was also recovered in lineage 1, yet it lacked a bulbous holdfast and a pseudo-stipe. Nonetheless, the lowermost segments were also considerably larger than those in the upper region of the thallus. This species was encountered on wave-affected rock and rubble.

Nodes connecting segments in the middle thallus region possessed relatively thick-walled medullary siphons connecting with all their immediate neighbors by means of pores (Figures 4, 5, 6) thus giving rise to a single pack of interconnected medullary siphons. Notably, siphons did not fuse at the nodes in partially fused (basal) segments of *H. borneensis* and *H. macroloba*.

The cortex was dense and, depending on the species and the location of the examined segment in the thallus, consisted of three to many layers of moderately inflated utricles (Figures 9, 10). In general, peripheral utricles were irregularly polygonal in surface view (Figures 7, 8).

Lineage 2, Figures 11–17.

Western Atlantic (Caribbean region): *H. cryptica*
Indo-Pacific basin: *H. fragilis*, *H. micronesica*

The specimens of Indo-Pacific species were found in wave-affected biotopes (mostly *H. micronesica*), on shallow reef slopes and in channels with strong tidal currents (both *H. fragilis* and *H. micronesica*). Our specimens of *H. cryptica* originated from deep (> 25m) cliffs facing the open sea. Segments of lineage 2 specimens appeared strongly calcified and brittle with flexible nodes. The specimens belonging to *H. fragilis* and *H. micronesica* were dull grayish green whereas those of *H. cryptica* were grass green on the segment side facing the light and white on the opposite side.

Specimens from this lineage possessed a single huge nodal siphon (*H. cryptica*) or several smaller ones passing through the nodes without fusion (*H. fragilis* and *H. micronesica*, Figures 13, 14).

Figures 2–17 (facing page). Morphology of *Halimeda* sections. Figs 2–10. Section *Rhipsalis*, Lineage 1. Figs 2, 3. General morphology. Fig. 2. *H. simulans*, H.0032. Fig. 3. *H. cylindracea*, HEC7612. Figs 4, 5. Medullary and nodal fusion. Fig. 4. *H. cylindracea*, H.0018. Fig. 5. *H. simulans*, H.0071. Fig. 6. Detail of nodal fusion. *H. simulans*, H.0071. Figs 7, 8. Surface view. Fig. 7. *H. simulans*, H.0071. Fig. 8. *H. cylindracea*, H.0018. Figs 9, 10. Cortical structures. Fig. 9. *H. simulans*, H.0071. Fig. 10. *H. cylindracea*, H.0018. Arrows indicate the location of the node. Figs 11–17. Section *Micronesicae*, Lineage 2. Figs 11, 12. General morphology. Fig. 11. *H. fragilis*, HEC14230. Fig. 12. *H. micronesica*, WLS184-02. Fig. 13. Medulla going through the nodal region. *H. micronesica*, H.0014. Fig. 14. Detail of a siphon at the node. *H. fragilis*, HV53.

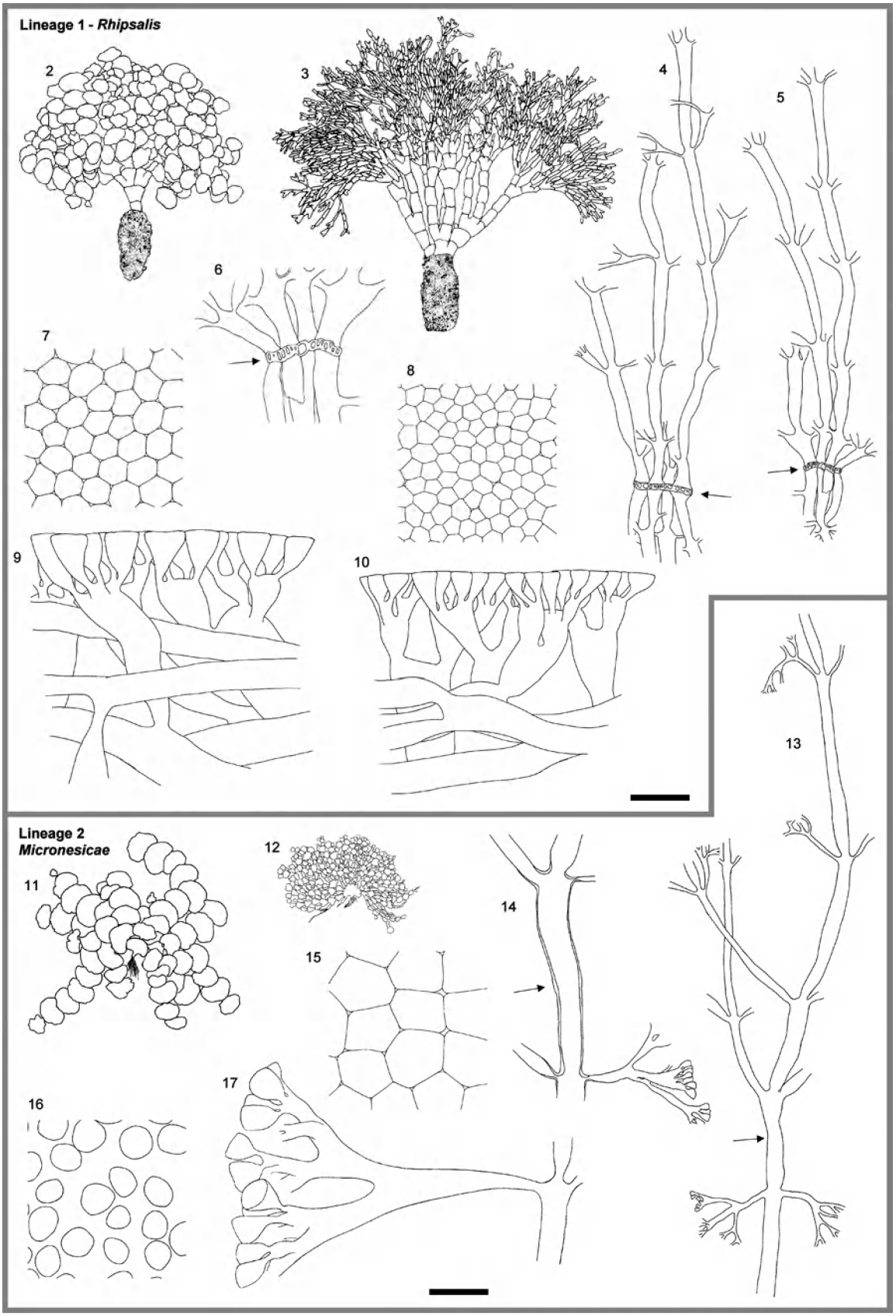

Figs 15, 16. Surface view. Fig. 15. *H. cryptica*, H.0237. Fig. 16. *H. micronesica*, WLS184-02. Fig. 17. Cortical structures. *H. micronesica*, WLS184-02. The cortical structures of *H. micronesica* are drawn from a slide prepared differently from those of all other species, because of the total lack of adhesion between utricles. Arrows indicate the location of the node. Scale bars represent: 25 mm for thalli, 500 mm for medulla, 250 mm for details of nodal structure, 60 mm for cortical structures and surface view.

The cortex was relatively thin and consisted of a series of cylindrical utricles gradually becoming longer and broader from the periphery inwards (Figure 17). Both Indo-Pacific species possessed primary utricles separating completely on decalcification of the segment and being round in surface view (Figure 16). In contrast, the peripheral utricles of *H. cryptica* adhered to each other and were irregularly polygonal in surface view (Figure 15).

Lineage 3, Figures 18–27.

Atlantic: *H. discoidea*, *H. hummii*, *H. scabra*, Mediterranean *H. tuna*, Western Atlantic *H. tuna*
Indo-Pacific basin: *H. discoidea*, *H. gigas*, *H. lacunalis*, *H. macrophysa*, *H. magnidisca*, *H. taenicola*
Indo-Pacific and possibly Brazil: *H. cuneata* (Bandeira-Pedrosa *et al.* 2001)

Specimens of this lineage were found in semi-sheltered to exposed biotopes. In general, the thallus attached to hard substrata by means of a felt-like, discoid holdfast. Two major thallus morphologies were encountered: *Halimeda lacunalis*, *H. hummii* and *H. cuneata* possessed smooth, small and moderately calcified segments with flexible nodes whereas others such as *H. discoidea*, *H. gigas* and *H. macrophysa* had pliable, weakly calcified and large segments with broad but rather inflexible nodes. Yet, the division is not strict because *H. magnidisca* possessed large, pliable and weakly calcified segments with narrow and flexible nodes and thalli of *H. taenicola* were composed of small, moderately calcified segments with broad, inflexible nodes. These distinct thallus morphologies did not cluster in the phylogenetic tree. Our specimens of *H. magnidisca* deviated from the type material in that their holdfasts, though sand-encrusted, were not perfectly bulbous; the thalli grew on hard substrata covered with a thin layer of sand. On the other hand, we occasionally observed specimens of other lineage 3 species anchoring in unconsolidated substrata by a minute bulbous holdfast.

Medullary siphons branched frequently and entangled strongly below the distal perimeter of the segment to fuse in a single band in the segment's upper rim (Figures 20–23). New segments emerged from anywhere along this band (Figures 18, 19). The nodal fusions were complete: the fused units continued into the subsequent segment as single, broad siphons (Figures 20–23) until they ramified. In species with large pliable segments, the cortex consisted of a single or double layer of large and swollen sub-peripheral utricles leaving little space for calcification (*H. discoidea*, *H. gigas*, *H. macrophysa*, *H. magnidisca*) whereas in species with small segments and flexible nodes, the cortex contained one to several layers of variously formed subperipheral utricles (*H. cuneata*, *H. lacunalis*, see Hillis-Colinvaux 1980, Figure 20; see also *H. hummii* in Ballantine 1982). In all but one species (*H. macrophysa*), peripheral utricles adhered firmly, did not separate after we decalcified the segment, and showed an irregularly polygonal surface pattern (Figures 24, 25).

Lineage 4, Figures 28–33.

Atlantic (Caribbean region): *H. gracilis*, *H. lacrimosa*
Indo-Pacific basin: *H. gracilis*

The specimens of this lineage were collected from relatively deep sites; they sprawled over rocky or partially unconsolidated substrata on reef slopes. Their fairly small segments were strongly calcified. In *H. gracilis*, three to several uncorticated pits were distributed along the segment's apical rim. In *H. lacrimosa* these pits appeared reduced and scattered over the upper part of the segment.

Medullary siphons fused completely at the nodes (Figures 30, 31) though Hillis-Colinvaux (1980) reported occasional occurrence of incomplete fusions in *H. lacrimosa*. The distance between subsequent ramifications in the subnodal region was larger than in other lineages and the siphons did not entangle among one another.

Secondary cortical utricles expanded only at their apex, the expanded areas forming a distinct layer. Numerous peripheral utricles sprouted from the broadened distal end of each secondary utricle (Figure

33). Similarly, peripheral utricles broadened only slightly at their base and more strongly towards their distal end (Figure 33). Peripheral utricles were round in cross-section. Around their tips, they formed lateral cell wall extensions that adhered to those of adjacent utricles in a hexagonal pattern. In the resulting surface view, the utricles appeared rounded as well as hexagonal, the prominence of each depending on the focal plane (Figure 32). The peripheral utricles adhered to each other, although not strongly.

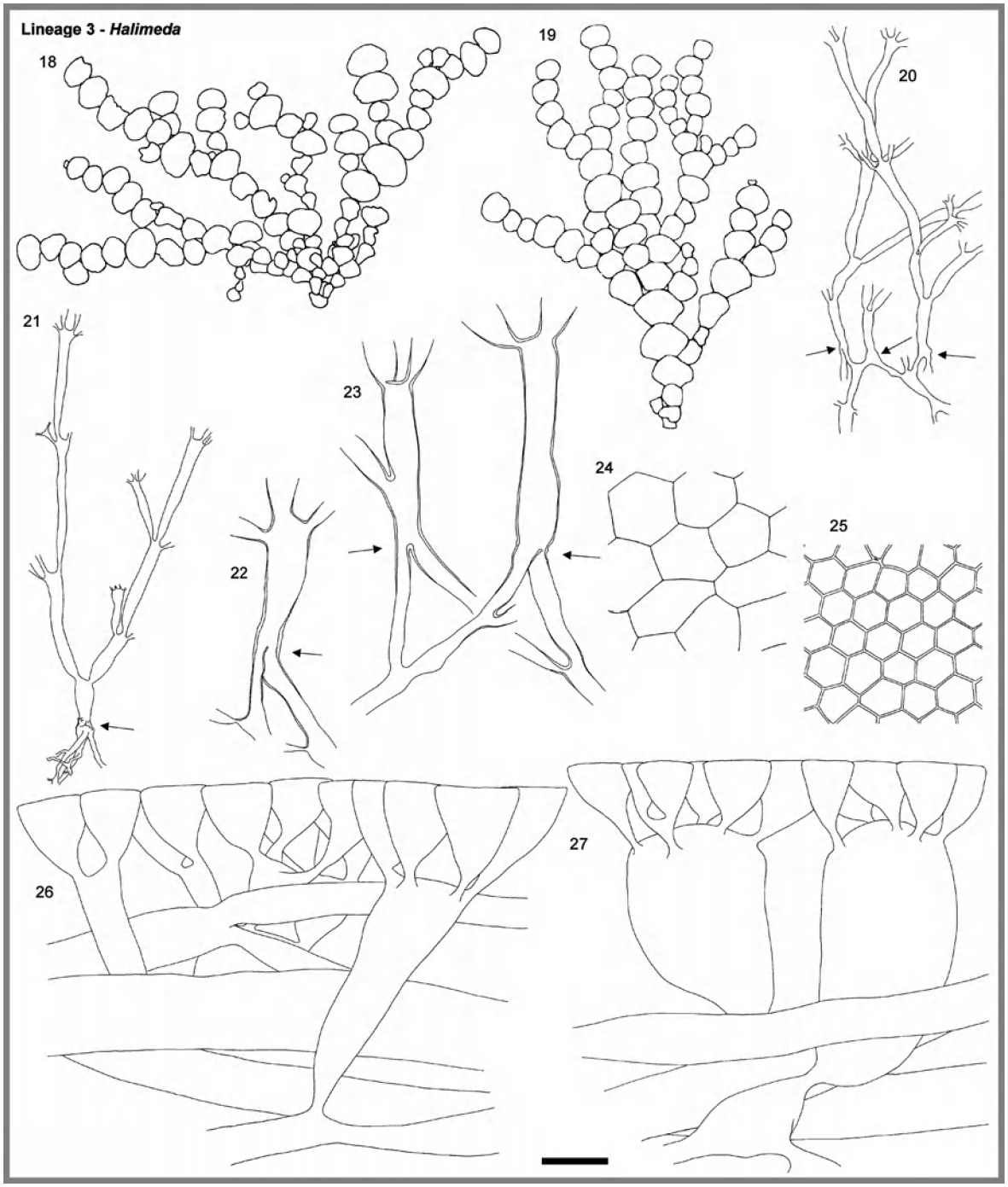

Figures 18–27. Section *Halimeda*, Lineage 3. Figs. 18, 19. General morphology. Fig. 18. *H. tuna*, HV55. Fig. 19. *H. lacunalis*, HV306. Figs. 20, 21. Medullary and nodal fusion. Fig. 20. *H. tuna*, HV54. 21. *H. lacunalis*, HV306. Figs. 22, 23. Detail of nodal fusion. Fig. 22. *H. lacunalis*, H.0118. Fig. 23. *H. tuna*, H.0113. Figs. 24, 25. Surface view. Fig. 24. *H. tuna*, HV54. Fig. 25. *H. lacunalis*, HV306. Figs. 26, 27. Cortical structures. Fig. 26. *H. tuna*, H.0113. Fig. 27. *H. taenicola*, H.0037. The cortical structures of *H. taenicola* are highly variable between specimens and can be quite different from what is drawn in Fig. 27. Arrows indicate the location of the node. Scale bar represents: 25 mm for thalli, 500 mm for medullary, 250 mm for details of nodal structure, 60 mm for cortical structures and surface view.

Lineage 5, Figures 34–42.

Atlantic (Caribbean region): *H. copiosa*, *H. goreauii*
Indo-Pacific basin: *H. distorta-hederacea* species complex, *H. minima*, *H. renschii*, *H. velasquezii*
Pan-tropical: *H. opuntia*

The specimens of this lineage were collected from various reef habitats. Most species showed a preference for a single habitat type: our specimens of *H. renschii* were found in moderately wave-exposed localities whereas those of *H. copiosa*, *H. goreauii*, *H. minima* and *H. distorta* always came from sheltered localities. *Halimeda opuntia* was ecologically plastic, abounding in a range of habitats from shaded sheltered lagoons and deep fore reefs to moderately exposed reef crests. Thallus shape was also strongly linked with habitat type: *H. renschii* thalli were erect, whereas those of specimens found in more sheltered habitats were pendant or sprawling (Figures 34, 35). The segments of specimens belonging to this lineage were relatively small and heavily calcified.

Nodal medullary siphons fused briefly (in pairs and threes) without losing their identity (Figures 36–38).

The cortex appeared thin: the few siphons emerging from the medulla usually did not ramify until close to the segment's periphery (Figures 41, 42).

Opuntioid lineages

The clade with lineages 4 and 5 possessed morphological synapomorphies as well. Specimens abounded in habitats under moderate to high grazing pressure and often revealed a sprawling mode of growth. The primary holdfast of full-grown thalli was often difficult to locate or was altogether absent. In the latter case, numerous secondary holdfasts attached the thallus to the substratum. Specimens of the sister species *H. goreauii* and (Atlantic) *H. copiosa* lacked such holdfasts.

The medullary siphons were generally narrower and smaller than those in the three other lineages.

The cortical siphons emerging from the medulla usually did not ramify until close to the segment's periphery. The large intersiphonal space was filled with aragonite, rendering the segments rigid and generally brittle. As in lineage 2, subperipheral utricles were cylindrical or widened only slightly towards their distal end.

Morphological observations on the type specimen of *H. bikinensis*

We have re-examined the type material of *H. bikinensis* (WRT46-156, MICH). The cortex was thin, the utricles were club-shaped, and the peripheral utricles possessed lateral cell wall extensions at their tips. In the subnodal medullary, siphon ramifications were widely spaced and trichotomous and did not become entangled with one another. Complete and incomplete fusions occurred together at the node. These character states were all typical for lineage 4 taxa. Furthermore, the segments were heavily calcified and brittle and possessed rhizoid tufts emerging from the uncorticated rim adjacent to the

Figures 28–42 (facing page). Morphology of *Halimeda* lineages. Figs. 28–33. Section *Pseudo-opuntia*, Lineage 4. Fig. 28. General morphology. *H. gracilis*, C&PvR13865B. Fig. 29. General morphology. *H. lacrimosa*, redrawn from Hillis-Colinvaux (1980). Fig. 30. Medullary and nodal fusion. *H. gracilis*, HV317. Fig. 31. Detail of nodal fusion. *H. gracilis*, H.0259. Fig. 32. Surface view. *H. gracilis*, HV317. Fig. 33. Cortical structures. *H. gracilis*, HV317. Figs. 34–42. Section *Opuntia*, Lineage 5. Fig. 34. General morphology. *H. hederacea*, HV1 Fig. 35. General morphology. *H. distorta*, HV199. Figs. 36, 37. Medullary and nodal fusion. Fig. 36. *H. opuntia*, HV19. Fig. 37. *H. hederacea*, HV9. Fig. 38. Detail of nodal fusion. *H. copiosa*, H.0265. Figs. 39, 40. Surface view. Fig. 39. *H. distorta*, HV199. Fig. 40. *H. hederacea*, HV9. Figs. 41, 42. Cortical structures. Fig. 41. *H. distorta*, HV199. Fig. 42. *H. hederacea*, HV9. Arrows indicate the location of the node. Scale bars represent: 25 mm for thalli, 500 mm for medullary, 250 mm for details of nodal structure, 60 mm for cortical structures and surface view.

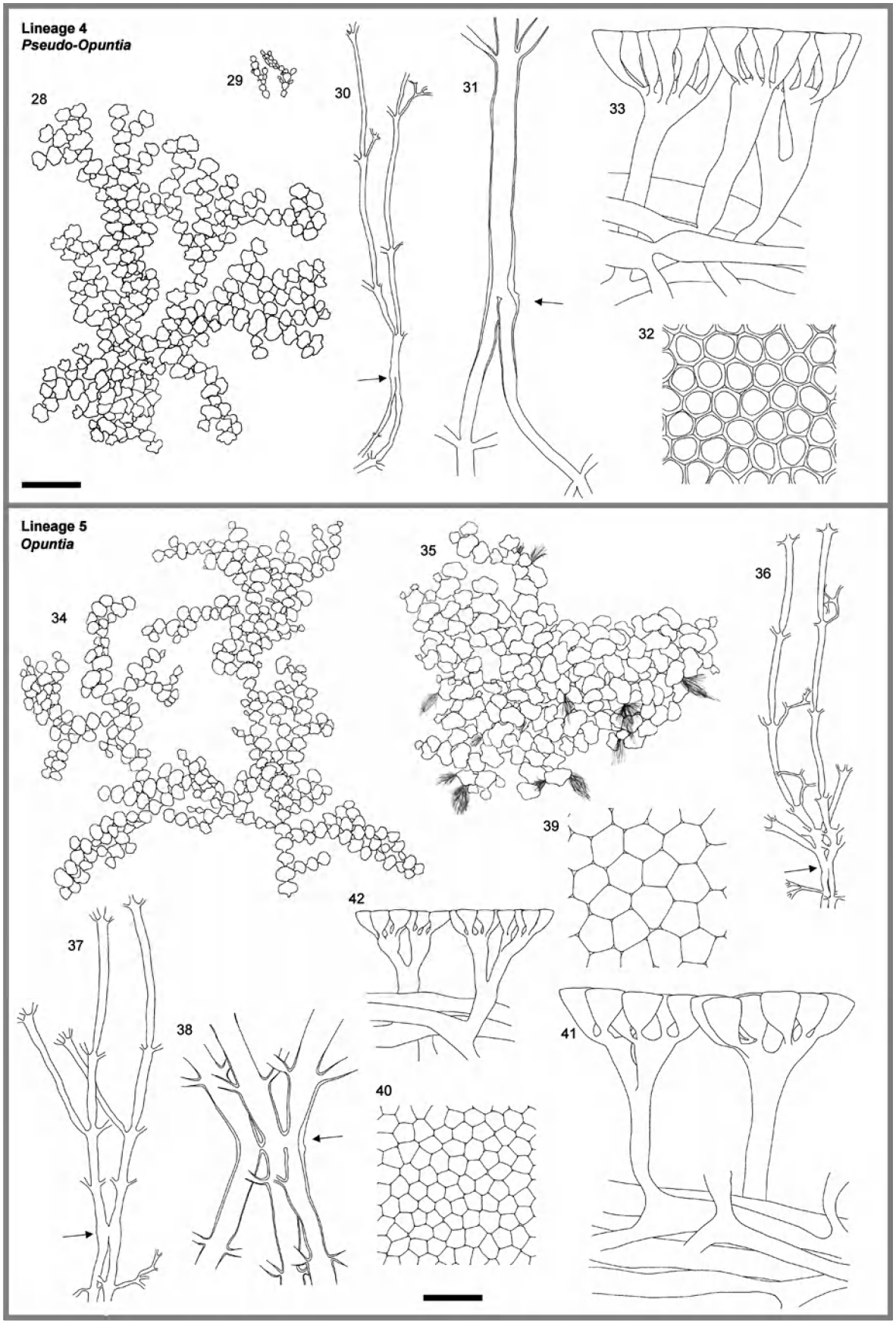
Lineage 4
Pseudo-Opuntia
28
29
30
31
33
32
Lineage 5
Opuntia
34
35
36
39
42
37
38
41
40

attachment region of daughter segments. These character states are also encountered in *H. gracilis* (lineage 4). What was peculiar, however, is that the type specimen of *H. bikinensis* also possessed an uncorticated rim along the distal segment perimeter, a character state typical for species in lineage 3. We attempted a molecular examination of the type specimen but unfortunately, its DNA was totally degraded.

Discussion

This study reveals that the five natural lineages from phylogenies based on partial nuclear rDNA sequences (Kooistra *et al.* 2002) possess readily recognizable morphological characters. Using the groups' morphological character states, we redefine sections established by Hillis-Colinvaux (1980). Her sections based solely on medullary siphon patterns at the nodes between segments are already surprisingly close to the ones we establish here indicating that Barton (1901) and Hillis-Colinvaux (1980) were right in their notion that these patterns delimited natural groups. We define our sections only through synapomorphies, though we note the symplesiomorphies since each section is defined by a particular combination. Although we provide some ecological information with the sections, we refer to Kooistra *et al.* (2002) for detailed historic ecological patterns in the evolution of the lineages and for habitat descriptions of species to Hillis-Colinvaux (1980) and references therein.

History of subdivisions in *Halimeda*

De Toni (1889) introduced sections in *Halimeda* taxonomy. He cited the descriptions of Agardh's (1887) subgeneric groupings of implicit hierarchy as diagnoses for his sections *Tunae*, *Pseudo-opuntiae*, *Opuntia* and *Rhipsales*. His division is based mainly on thallus appearance, a notoriously unreliable feature (Hillis-Colinvaux 1980, Kooistra *et al.* 2002). Moreover, several species in his sections are of uncertain status (Hillis-Colinvaux 1980). Almost a century later, Hillis-Colinvaux (1980) revised the generic subdivision. She redescribed three out of De Toni's four sections (*Tunae*, *Opuntiae*, *Rhipsales*) and diagnosed two novel sections (*Micronesicae* and *Crypticae*). She further altered the spelling of De Toni's section names to conform to the ICBN. Section *Tunae* was renamed *Halimeda* because it contains *H. tuna*, the type species of the genus. She based her sectional descriptions solely on nodal fusion patterns, although she noted that other characters accompanied these patterns.

A new sectional division

Section *Rhipsalis* J. Agardh ex De Toni, Lineage 1

Type species: Caribbean *H. incrassata*

The defining characters of this lineage are the interconnecting pores of the nodal siphons and the segment agglutination in the basal thallus region in *H. melanesica* and in the thallus region above the pseudo-stipe in all other species. The bulbous holdfast and the pseudo-stipe are not diagnostic for this section because *H. melanesica* (lineage 1) lacks these traits whereas *H. magnidisca*, which is a member of lineage 3, does possess a bulbous holdfast and a stipe-like basal zone when growing on sand (Noble 1986). Both the bulbous holdfast and the pseudo-stipe are adaptations to growth in unconsolidated substrata (Hillis-Colinvaux 1980; Kooistra *et al.* 2002).

Hillis-Colinvaux (1980) assigned *H. melanesica* to her section Micronesicae (our lineage 2) because the description (Valet 1966) mentions only sparse siphon fusion if any at all. Yet placement in lineage 1 corroborates its morphology because minute pores connect the nodal medullary siphons (Kooistra *et al.* 2002).

Section *Micronesicae* Hillis-Colinvaux, Lineage 2

Type species: *H. micronesica*

A single character defines this lineage: broadened siphons pass unfused through the nodes. Unfused nodal siphons appear to render nodes flexible minimizing drag in wave-affected environments (*H. micronesica*), and habitats with strong tidal currents (*H. fragilis* and *H. micronesica*). The single nodal medullary siphon observed in *H. cryptica* may result from secondary reduction related to the species' adaptation to deep sites. Yet such environments are not necessarily sheltered. There, thalli are exposed to current, swell from long surface waves and high-amplitude internal waves (Pinkel 1983, personal observations).

The single siphon traversing the node between segments of *H. cryptica* enticed Hillis-Colinvaux (1980) to propose a monotypic section *Crypticae* because it sets the species apart from all other *Halimeda* species. However, recovery of *H. cryptica* in lineage 2 indicates that section *Crypticae* Hillis-Colinvaux is obsolete.

Section *Halimeda* Lineage 3

The defining traits of this lineage are the subnodal entanglement of medullary siphons and the presence of an uncorticated band along the distal part of the segment perimeter. New segments emerge from anywhere along this band. De Toni (1889) validly described this section as *Tunae* based on the description of a grouping of implicit hierarchy by Agardh (1887). Hillis-Colinvaux (1980) renamed the section *Halimeda* because a section containing the type species of the genus must have the same name as the genus (ICBN). However, she retained the original authorities, meaning that the full name of the section was *Halimeda* J. Agardh ex De Toni. The Saint Louis ICBN states that the name of a section containing the type species of the genus should not be followed by an author citation. This is here corrected.

Noble (1986) did not allocate *H. magnidisca* to any of Hillis-Colinvaux' sections because the specimens examined by her possess segments and siphon fusion patterns typical for section *Halimeda* but bulbous holdfasts and stipitate lower segments typical of section *Rhipsalis* sensu Hillis-Colinvaux (1980). Kooistra *et al.* (2002) showed that this species is a member of lineage 3 (section *Halimeda*). Apparently, bulbous holdfasts have been acquired multiple times independently as an adaptation to growth on soft substrata.

Halimeda hummii was placed in section *Opuntia* sensu Hillis-Colinvaux (1980) by Hillis *et al.* (1998), but according to the molecular phylogeny in Kooistra *et al.* (2002) this species belongs within lineage 3 (section *Halimeda*). Apparently, many characters have evolved in this species to states similar to those in lineage 5 (section *Opuntia*). Incidentally, some medullary siphons may fuse incompletely, but if present, they are always accompanied by completely fused siphons. The non-entangling behavior of siphons in the subnodal region, too, is reminiscent of lineages 4 or 5 rather than of lineage 3. The difference from lineages 4 and 5 lies in the way new segments arise. In *H. hummii*, as in all other members of the *Halimeda* section, segments can emerge anywhere along the uncorticated band in the distal part of the segment perimeter whereas in lineages 4 and 5, new segments emerge only from uncorticated pits.

Section *Pseudo-opuntia* J. Agardh ex De Toni, Lineage 4

Type species: Indo-Pacific *H. gracilis*

The defining character of this lineage is encountered in the cortical structure: secondary cortical utricles expand only at their apex and have a large and fairly constant number of peripheral utricles arranged around their distal end (Kooistra *et al.* 2002). The section was first validly described by De Toni (1889) but later rendered obsolete by Hillis-Colinvaux (1980). She moved *H. gracilis*, the only

unambiguous species in it, to her section *Halimeda*. Complete nodal siphon fusion is the defining trait of Hillis-Colinvaux' (1980) section *Halimeda*. Yet, her section is paraphyletic and the trait is a symplesiomorphy shared between specimens in lineages 3 and 4. Therefore we propose to re-establish De Toni's (1889) section *Pseudo-opuntia*, with *H. lacrimosa* and *H. gracilis* as its members. This treatment renders both sections *Halimeda* and *Pseudo-opuntia* natural units.

The *Pseudo-opuntia* lineage shares its main nodal fusion pattern with the *Halimeda* lineage. The distinction lies in the behavior of medullary siphons just below the nodes and in the way new segments arise. In members of section *Halimeda*, the medullary siphons ramify frequently below the nodes and consequently, become entangled with one another. In members of *Pseudo-opuntia*, the medullary siphons show no sign of entanglement in the subnodal zone because the distance between subsequent ramifications is relatively large. Moreover, in members of section *Halimeda*, segments arise from anywhere in the uncorticated band that spans the distal part of the segment perimeter. In section *Pseudo-opuntia*, segments arise from round to slightly elongated pits.

Section *Opuntia* J. Agardh ex De Toni, Lineage 5

Type species: *H. opuntia*

This section has only a single defining character: the nodal medullary siphons fuse briefly in pairs or threes (and rarely in small groups) without losing their identity. Yet, *H. lacrimosa* (Hillis-Colinvaux 1980), *H. hummii* (Ballantine 1982) and *H. borneensis* can occasionally show similar patterns in the nodes, alongside the typical patterns in these species. Section *Opuntia* was erected by De Toni (1889), and drastically expanded by Hillis-Colinvaux (1980). The species composition of this section as in Hillis-Colinvaux (1980) is maintained unaltered.

Opuntioid lineages

Lineages 4 and 5 could also be merged into a single section. The defining traits would then be a thin subperipheral cortex and heavily calcified segments. All but two species (*H. lacrimosa*, *H. renschii*) show a sprawling, or pendant, habit and live in sheltered to semi-exposed habitats. Nonetheless, we believe that the dominant patterns of nodal fusion and the shape of the peripheral and secondary utricles differ sufficiently between the two lineages to maintain them as different sections.

Morphological symplesiomorphies and homoplasies

Many characters are present in two or more lineages that are not sister clades. For example, the presence of uncorticated pits from which daughter segments can emerge is an ancestral trait. This character only changed state in the common ancestry of lineage 3. The central uncorticated pit appears to have stretched out laterally to occupy most of the upper segment rim (Kooistra *et al.* 2002). Unlike in all other lineages where new segments emerge exclusively from the uncorticated pits in the segment rim, new segments emerge from anywhere along this band.

Lineages 3 and 4 share patterns of nodal siphon fusion while all other lineages possess their own nodal pattern of siphon behavior. In *Figure* 1, complete fusion is a symplesiomorphy of these lineages.

Lineage 2 and the opuntioid clade (lineages 4 and 5) share generally well-calcified and often brittle segments. In addition, the utricles in the subperipheral cortex are generally not notably swollen. Yet, it should be noted that calcification and utricle shape are related because the more swollen the utricles, the less intersiphonal space remains to be filled with aragonite. Morphologically, it would be more parsimonious to let lineages 2 and 3 switch positions. Such a switch is not improbable because bootstrap support for the clade uniting lineages 3, 4 and 5 is below 50% and Kooistra *et al.* (2002) showed that this alternative topology is not significantly worse using the Kishino-Hasegawa test option in

PAUP*. It should be noted however, that even in this alternative topology strong calcification does not become a synapomorphy because several species in lineage 3 also possess strongly calcified segments.

Species not included in the phylogeny

Although we did not have access to specimens of the following taxa for molecular analyses, we expect that *H. favulosa* will be recovered in lineage 1 (section *Rhipsalis*), *H. scabra* and *H. xishaensis* will fall within lineage 3 (section *Halimeda*), and *H. howensis* will be recovered in lineage 5 (section *Opuntia*) because according to their descriptions in Hillis-Colinvaux (1980), Dong & Tseng (1980) and Kraft (2001) these taxa share all synapomorphies and the proper combination of symplesiomorphies with these lineages. However, whether these species constitute genetically and biologically valid taxa or just plastic extremes within other species remains to be resolved.

Placement of *H. bikinensis* in our system remains puzzling. Its original description (Taylor 1950) and those in Hillis (1959) and Hillis-Colinvaux (1980) as well as the anatomical characteristics we observed in the type permit placement in either lineage 3 or 4. The anatomy and general morphology of the type specimen indicate that it belongs to section *Pseudo-opuntia* rather than section *Halimeda*. The thin cortex, the club-shaped secondary utricles and the lateral cell wall extensions at the tips of peripheral utricles as well as the widely spaced, trichotomous ramifications of the subnodal medullary and the complete and incomplete nodal fusions occurring side by side are all typical for species in our section *Pseudo-opuntia* (lineage 4). However, the presence of the uncorticated rim along the distal segment perimeter of *H. bikinensis* is a synapomorphy of section *Halimeda* (lineage 3) in our molecular phylogeny. In section *Pseudo-opuntia*, the uncorticated region is limited to a series of round to slightly elongate pits along the perimeter (*H. gracilis*) or a number of reduced pits scattered over the upper part of the segment (*H. lacrimosa*).

If *H. bikinensis* groups within lineage 4 then the uncorticated rim is not a synapomorphy of lineage 3 whereas if it goes with lineage 3 then the apically inflated secondary utricles in the cortex do not define section *Pseudo-opuntia*. If the species forms a lineage on its own behalf, then only the entangling siphons below the nodes remain a synapomorphy of lineages 3, and taxa in lineage 4 do not possess a single synapomorphy.

Given the problems *H. bikinensis* creates in our sectional division, it is understandable that Hillis-Colinvaux (1980) grouped species in lineages 3 and 4 in a single section *Halimeda* defined by complete fusion of medullary siphon in pairs and triplets at the nodes. According to the molecular phylogenies, however, her section is paraphyletic. It should be stressed also that Hillis-Colinvaux' (1980) concept of *H. bikinensis* differs from that of Taylor (1950). The rhizoidal tufts emerging from the uncorticated rim suggest a sprawling habit of the type specimen Taylor collected. This sprawling behaviour goes unnoticed in Hillis-Colinvaux (1980). Instead, she states that thalli are erect. The general morphology of the specimen depicted by her corresponds very well to that of some Indo-Pacific *Halimeda discoidea*. Also, re-examination of specimens from the National History Museum (London) identified by her as *H. bikinensis* revealed only thoroughly swollen, albeit smallish, secondary utricles as encountered in some Indo-Pacific *H. discoidea*.

Key to the sections

In order to facilitate assignment of specimens to our sections, we present a key based on morphological characters. The two most problematic cases of morphological convergence (*H. hummii* and *H. melanesica*) key out even if a misstep occurs. *Halimeda bikinensis* also keys out separately.

1 a Siphons not fusing at the nodes between segments 2
1 b Siphons fusing at the nodes between segments, either over a short or a long distance.....3

2 a Subperipheral cortex dense, consisting of moderately swollen utricles with a constriction at their base. Nodal siphons adhering in groups and usually communicating with each other through minute pores. Thalli erect ..... *H. melanesica* of section *Rhipsalis*

2 b Subperipheral cortex thin, consisting of cylindrical utricles (neither swollen, nor constricted). Diameter and length of subperipheral utricles increasing towards the medulla. Adherence of nodal siphons absent or weak. No pores connecting the neighbouring nodal siphons. Thalli erect or pending ..... section *Micronesicae*

3 a Complete fusion of siphons at the node: fused siphons continue into the subsequent segment as a single, thicker siphon 4

3 b Nodal siphon fusion over a short distance (once to twice the siphon diameter) 8

4 a Siphons below the node relatively narrow and frequently branching. Subnodal branches numerous, entangling and fusing towards the node, resulting in difficult observation of the fusion pattern. Segments weakly to moderately calcified. Uncorticated rim present along the distal perimeter of the segment. Daughter segments arising from any point along this rim. Thalli erect ..... section *Halimeda*

4 b Siphons not branching more frequently below the node than elsewhere in the medulla. Entanglement of subnodal siphons absent or weak, resulting in easy observation of the fusion pattern 5

5 a Uncorticated belt extending along the distal part of the segment perimeter. Daughter segments emerging anywhere along this belt. Thalli erect or partially sprawling ..... *H. bikinensis*

5 b No uncorticated belt along the distal part of the segment perimeter. Daughter segments emerging from isolated pits or from small, slightly elongate uncorticated regions along the segment perimeter. Thalli erect, sprawling or pending 6

6 a Segments flattened, paper-thin, moderately calcified. Segments emerging from anywhere along the distal part of the perimeter of the parent segment ..... *H. hummii* of section *Halimeda*

6 b Segments thicker than 0.6 mm, either flattened or globose to tear-shaped, and strongly calcified 7

7 a Segments flattened or globose to tear-shaped. Daughter segments of flattened segments emerging from large pits along the distal segment perimeter; daughter segments of globose to tear-shaped segments arising from (generally three) reduced pits spread over the top region of the segment ..... section *Pseudo-opuntia*

7 b Segments flattened. Daughter segments emerging anywhere along the uncorticated belt along the distal part of the segment perimeter ..... *H. bikinensis*

8 a Nodal siphons generally fusing into a single unit. Nodal siphons adhering to all their neighbours and communicating with them by means of large pores. Occasionally, siphons fusing in large groups (more than five siphons) rather than into a single unit. Thallus erect and often possessing a bulbous holdfast. Segments in the basal zone of the thallus usually agglutinating into stipe- and/or fan-like structures. Segments moderately to strongly calcified. Pores occasionally minute rather than large; in this case nodal siphons adhering in groups and thallus holdfast felt-like ..... section *Rhipsalis*

8 b Siphons fusing in twos, threes, or occasionally in small groups (less than five siphons). Thalli erect, pending or sprawling. Attachment to the substrate by means of rhizoid tufts or a non-bulbous, felty holdfast. Segments in the basal thallus region not agglutinating to a stipe- and/or fan-like structure 9

9 a Incomplete (short) fusions and complete fusions co-occur. Mature thalli smaller than 5 cm ..... *H. hummii* of section *Halimeda*

9 b All fusions incomplete. Mature thalli larger than 5 cm ..... section *Opuntia*

Perspectives

A revision of *Halimeda* species is needed, given the existence of paraphyletic species[2], of cryptic diversity hidden within a single perceived species (e.g. *H. minima*) and of cognate pairs, genetically distant species that have converged morphologically (Kooistra *et al.* 2002). Hillis-Colinvaux (1980) had access only to morphological character states; she had no analysis of independent data to determine which morphological features were homologous. For instance, she could not identify all the cognates reported by Kooistra *et al.* (2002). Although she noticed slight morphological differences between what she perceived as the same species in different geographical regions [see Colinvaux (1969) on *H. copiosa – H. hederacea* and Hillis-Colinvaux (1980) on Mediterranean and western Atlantic *H. tuna*], she could not evaluate the meaning of these differences because the characters also varied within geographical regions. Many species in her most recent monograph (Hillis-Colinvaux 1980) are thus biphyletic entities. They may, in fact, differ between one another morphologically, either in as yet unexplored characters or in characters that are now considered variable. A new monograph ought, apart from proper illustrations of anatomical details, to incorporate a thorough evaluation of measurable features associated with medullary, cortical and gametangial siphon anatomy and segment morphology. Such an approach may uncover currently overlooked differences among species and sections; differences that will not only facilitate distinction of cognates and other look-alikes but will also permit more sound comparison with the morphology of fossil *Halimeda*.

Acknowledgements

We thank M. Coffroth, P. Colinvaux, E. Coppejans, O. Dargent, O. De Clerck, G. De Smedt, R. Haroun, I. Hendriks, L. Hillis, L. Kirkendale, F. Leliaert, L. Liao, J. Maté , A. N'Yeurt, C. Payri, G. Procaccini, W.F. Prud'homme van Reine, T. Schils and B. Wysor for sample collection, E. Coppejans, P. Baas, W.F. Prud'homme van Reine and M.G. Wynne for facilitating access to herbarium specimens from the GENT, L and MICH herbaria, P. Vanai (Environmental Service of Wallis and Futuna) for facilitating fieldwork on Uvea Island, and P. Goetghebeur for his help on nomenclature. We thank E. Coppejans for his valuable comments on the manuscript. H.V. is indebted to the Bijzonder Onderzoeksfonds (Ghent University) for grant 011D9101 and to the Fund for Scientific Research Flanders for research project grant 3G002496.

References

Agardh, J.G. (1887). *Till Algernes Systematik*, nya bidrag, femte afdelningen. Lunds Universitets års-Skrift, Afdeln. Mathem. Naturvet.

Askenasy, E. (1888). Algen. In: *Die Forschungsreise S.M.S. Gazelle* Th. 4, Bot., Berlin.

Ballantine, D.L. (1982). *Halimeda hummii* sp. nov., *Halimeda cryptica* v. *acerifolia* var. nov. (Caulerpales, Chlorophyta), and additional records of *Halimeda* species from Puerto Rico. *J. Phycol.*, **18**: 86–91.

Bandeira-Pedrosa, M.E., Pereira, S.M.B. & Oliveira, E.C. (2001). Taxonomy and distribution of the genus *Halimeda* Lamouroux (Bryopsidales, Chlorophyta) in the Brazilian coast. In *Supplemental abstracts in Programme 7th Int. Phycol Congress*, 72. Aristotle Univ. of Thessaloniki, Greece.

Barton, E.S. (1901). The genus *Halimeda*. *Monographs of the Siboga Expedition* **60**. Leiden.

Borowitzka, M.A. & Larkum, A.D.W. (1977). Calcification in the green alga *Halimeda*. V. An ultrastructure study of the thallus development. *J. Phycol.*, **13**: 6–16.

Braga, J.C., Martin, J.M. & Riding, R. (1996). Internal structure of segment reefs: *Halimeda* algal mounds in the Mediterranean Miocene. *Geology*, **24**: 35–38.

Clifton, K.E. (1997). Mass spawning by green algae on coral reefs. *Science*, **275**: 1116–1118.

[2] Clarification: morphologically defined species that are paraphyletic on the basis of molecular data

Clifton, K.E. & Clifton, L.M. (1999). The phenology of sexual reproduction by green algae (Bryopsidales) on Caribbean coral reefs. *J Phycol.*, **35**: 24–34.

Colinvaux, L. Hillis. (1969). *Halimeda copiosa* and *Halimeda hederacea*. *J. Phycol.*, **5**: 88.

De Toni, J.B. (1889). Sylloge Algarum. Vol. I. Sect. I. Chlorophyceae.

Dong, M. & Tseng, C.K. (1980). Studies on some marine green algae from the Xisha Islands, Guandong Province, China. II. *Stud. Mar. Sinica*, **17**: 1–10.

Drew, E.A. (1995). Diversity of the green algal genus *Halimeda* in the Chagos Archipelago, central Indian Ocean. *Aquat. Bot.*, **52**: 143–150.

Drew, E.A. & Abel, K.M. (1988). Studies on *Halimeda*. II: reproduction, particularly the seasonality of gametangia formation, in a number of species from the Great Barrier Reef Province. *Coral Reefs*, **6**: 207–218.

Gepp, E.S. (1904). The sporangia of *Halimeda*. *J. Bot., Lond.*, **42**: 193–197.

Goloboff, P.A. (1993). Estimating character weights during tree search. *Cladistics,* **9:** 83-91.

Graham, E.A. (1975). Fruiting in *Halimeda* (order Siphonales) 1. *Halimeda cryptica* Colinvaux and Graham. *Bull. Mar. Sci.*, **25**: 130–133.

Hay, M.E., Paul, V.J., Lewis, S.M., Gustafson, K., Tucker, J. & Trindell, R.N. (1988). Can tropical seaweeds reduce herbivory by growing at night? Diel patterns of growth, nitrogen content, herbivory, and chemical versus morphological defenses. *Oecologia*, **75**: 233–245

Hillis, L.W. (1959). A revision of the genus *Halimeda* (order Siphonales). *Publications of the Institute of Marine Science* **6**: 321–403

Hillis, L.W. (2000). Phylogeny of *Halimeda* (Bryopsidales): linking paleontological, morphological and molecular data. *Acta Palaeontologica Romaniae, Cluj-Napoca*, **2**: 183–189.

Hillis, L.W., Engman, J.A. & Kooistra, W.H.C.F. (1998). Morphological and molecular phylogenies of *Halimeda* (Chlorophyta, Bryopsidales) identify three evolutionary lineages. *J Phycol.*, **34**: 669–681.

Hillis-Colinvaux, L. (1980). Ecology and taxonomy of *Halimeda*: primary producer of coral reefs. *Adv. Mar. Biol.*, **17**: 1–327.

Hillis-Colinvaux, L. (1988). Calcareous green algae in the reefs of the Indian Ocean. *Biol. Soc. Wash. Bull.*, **8**: 14–18.

Kamura, S. (1966). On the sexual reproduction of two species of *Halimeda* (Chlorophyta) *Bulletin of Arts and Science, University of the Ryukyus, Mathematics and Natural Sciences*, **9**: 302–313.

Kooistra, W.H.C.F. (2002). Molecular phylogenies of Udoteaceae (Bryopsidales, Chlorophyta) reveal non-monophyly for *Udotea, Penicillus* and *Chlorodesmis*. *Phycologia*, **41**: 453–462.

Kooistra, W.H.C.F., Coppejans, E.G.G. & Payri, C. (2002). Molecular systematics, historical ecology and phylogeography of *Halimeda* (Bryopsidales). *Mol. Phylogen. Evol.*, **24**: 121–138.

Kraft, G.T. (2001). Marine and estuarine benthic algae (Chlorophyta) of Lord Howe Island, Southwestern Pacific. *Aust. Syst. Bot.*, **13**: 509–648.

Lamouroux, J.V.F. (1812). Extrait d'un mémoire sur la classification des polypes coralligènes non entièrement pierreux. *Nouveau Bulletin Scientifique de la Société Philomatique*, **3**: 181–188.

Littler, D.S. & Littler, M.M. (2000). *Caribbean reef plants: an identification guide to the reef plants of the Caribbean, Bahamas, Florida and Gulf of Mexico*. Offshore graphics Inc., Washington D.C.

Meinesz, A. (1980). Connaissances actuelles et contribution à l'étude de la reproduction et du cycle des Udotéacées (Caulerpales, Chlorophytes). *Phycologia*, **19**: 110–138.

Noble, J.N. (1986). *Halimeda magnidisca* (Caulerpales, Chlorophyta), a new species from the Great Barrier Reef, Australia. *Phycologia*, **25**: 331–339.

Pinkel, R. (1983). Doppler sonar observations of internal waves: wave-field structure. *J. Phys. Oceanogr.*, **13**: 804–815.

Posada, D. & Crandall, K.A. (1998). Modeltest: testing the model of DNA substitution. *Bioinformatics*, **14**: 817–818.

Schlagintweit, F. & Ebli, O. (1998). *Halimeda paucimedullaris* n. sp. and *Oroseina pletzachensis* n. sp., two new calcareous algae from the Upper Cretaceous of the Northern Calcareous Alps (Gosau Group, Austria), followed by remarks on *Dissocladella ? pyriformis* Schlagintweit, 1991. *Revue Paléobiol.*, Genève, **17**: 361–371.

Swofford, D.L. (2002). "*PAUP* Phylogenetic Analysis Using Parsimony (* and other methods)* Version 4.0b10," Sinauer Associates Inc., Sunderland, Massachusetts.

Taylor, W.R. (1950). *Plants of Bikini and other northern Marshall Islands*. Univ. of Michigan Press, Ann Arbor, Michigan.

Tsuda, R.T. & Kamura, S. (1991). Floristics and geographic distribution of *Halimeda* (Chlorophyta) in the Ryukyu Islands. *Jpn. J. Phycol.*, **39**: 57–76.

Tsuda, R.T. & Wray, R.O. (1977). Bibliography of marine benthic algae in Micronesia. *Micronesica*, **13**: 85–120.

Valet, G. (1966). Sur une espèce rare et une nouvelle espèce d'*Halimeda* de Mélanésie. *Rev. Gén. Bot.*, **73**: 680–685.

Walters, L.J. & Smith, C.M. (1994). Rapid rhizoid production in *Halimeda discoidea* Decaisne (Chlorophyta, Caulerpales) fragments: a mechanism for survival after separation from adult thalli. *J. Exp. Mar. Biol. Ecol.*, **175**: 105–120.

Walters, L.J., Smith, C.M., Coyer, J.A., Hunter, C.L., Beach, K.S. & Vroom, P.S. (2002). Asexual propagation in the coral reef macroalga *Halimeda* (Chlorophyta, Bryopsidales): production, dispersal and attachment of small fragments. *J. Exp. Mar. Biol. Ecol.*, **278**: 47–65

Appendix 1. List of specimens used in this study.

The second column lists the accession number of the specimens as they are lodged in the GENT herbarium. Codes in brackets after the specimen number indicate specimen from other herbaria; L denotes Leiden, MICH denotes Michigan. The third column lists the specimen numbers as used in Fig. 1 and in Kooistra *et al.* (2002). Geographical location: CAR: Caribbean Sea; MED: Mediterranean Sea; RS: Red Sea; C: central; E: eastern; W: western; A: Atlantic Ocean; I: Indian Ocean; P: Pacific Ocean.

Species	Specimen number	Voucher	Geographical location	GenBank
H. borneensis	HV18		Zanzibar, Tanzania (WI)	
	HEC12603a		Zanzibar, Tanzania (WI)	
	HEC12603b	99-128	Zanzibar, Tanzania (WI)	AF525559
	Snellius-II 10101		Maisel Islands, Indonesia (WP)	
	PH534		Mindanao, Philippines (WP)	
	H.0267	99-138	New Caledonia (WP)	AF525550
H. stuposa	L0238148 (L)		Marshall Islands (CP)	
	L0238149 (L)		Marshall Islands (CP)	
	WRT46-591 (MICH)		Marshall Islands (CP)	
H. melanesica	HV22		Zanzibar, Tanzania (WI)	
	L0238145 (L)	L0238145	Taka Garlarang, Indonesia (WP)	AF407237
H. incrassata IP	PH194		Cebu, Philippines (WP)	
	PH197	99-073	Cebu, Philippines (WP)	AF407241
	HV146		Moorea, French Polynesia (CP)	
	H.0019	98-117	Great Barrier Reef, Australia (WP)	
	H.0035	99-001	Tahiti, French Polynesia (CP)	
	H.0040	99-009	Rangiroa, French Polynesia (CP)	
	H.0045	99-021	Rangiroa, French Polynesia (CP)	AF525573
H. macroloba	HV5		Zanzibar, Tanzania (WI)	
	HEC12583		Zanzibar, Tanzania (WI)	
	H.0157	98-017	Pangasinan, Philippines (WP)	AF525560
	H.0228	97-486	Exmouth, W Australia (EI)	
	H.0038	99-006	Tahiti, French Polynesia (CP)	AF525563
	HV183		Tahiti, French Polynesia (CP)	
	HV206		Tahiti, French Polynesia (CP)	
H. cylindracea	HV323		East Sinai, Egypt (RS)	
	SOC364	99-030	Socotra, Yemen (WI)	AF525546
	HEC7612		Madang, Papua New Guinea (WP)	
	H.0018	98-105	Great Barrier Reef, Australia (WP)	AF525548
H. simulans	H.0032		Galeta, Panama (CAR)	
	H.0071	97-071	Bocas del Toro, Panama (CAR)	
	H.0367	97-089	Panama (CAR)	AF407235
H. incrassata CAR	H.0179	99-087	Bahamas (CAR)	AF407233
	H.0180	99-084	Florida, U.S.A. (CAR)	
	H.0181	99-083	Florida, U.S.A. (CAR)	AF525537
H. favulosa	L0351088 (L)		Bahamas (CAR)	
H. monile	H.0145	98-100	Florida, U.S.A. (CAR)	
	HOD-RD2.02-65		Dominican Republic (CAR)	
	HOD-RD2.02-50		Dominican Republic (CAR)	
	H.0228	98-034	Yucatan, Mexico (CAR)	AF407234
H. cryptica	H.0237	97-482	Discovery Bay, Jamaica (CAR)	AF407244
	HV401		St. Ann's Bay, Jamaica (CAR)	
	HV483		Priory Bay, Jamaica (CAR)	
H. micronesica	HV4		Zanzibar, Tanzania (WI)	
	SEY484		Poivre Atoll, Seychelles (CI)	
	no voucher	99-050	Great Barrier Reef, Australia (WP)	AF407243
	H.0014	98-110	Great Barrier Reef, Australia (WP)	
	WLS184-02		Wallis Island (CP)	

	WLS420-02		Wallis Island (CP)	
H. fragilis	HEC14230		Mnazi Bay, Tanzania (WI)	
	HV53		Mnazi Bay, Tanzania (WI)	
	PH316		Luzon, Philippines (WP)	
	HEC10230		Motupore, Papua New Guinea (WP)	
	H.0125	99-092	Bile Bay, Guam (WP)	AF407245
	WRT46-394 (MICH)		Marshall Islands (CP)	
H. hummii	H.0002		Galeta, Panama (CAR)	
	H.0232	99-052	Portobelo, Panama (CAR)	
	H.0235	99-107	Isla Mamey, Panama (CAR)	AF525582
	H.0251	98-164	Portobelo, Panama (CAR)	
	H.0253	98-053	San Blas, Panama (CAR)	AF525581
H. discoidea ATL	H.0138	99-187	Isla Grande, Panama (CAR)	
	H.0144	99-105	Florida, U.S.A. (CAR)	
	H.0207	97-547	Gran Canaria, Canary Islands (EA)	AF407249
	H.0209	98-052	Sao Vicente, Cape Verde (CA)	
H. tuna MED	H.0113	99-043	Naples, Italy (MED)	AF407250
	HV55		Ischia Island, Italy (MED)	
	HV319		Rosas, Spain (MED)	
H. tuna ATL	H.0074	97-069	Panama (CAR)	AF525589
	H.0140	99-189	Panama (CAR)	
	H.0231	98-038	Puerto Morelos, Mexico (CAR)	AF407248
H. scabra	L0351081 (L)		Florida, U.S.A. (CAR)	
	L0351084 (L)		Florida, U.S.A. (CAR)	
H. lacunalis	H.0118	99-095	Bile Bay, Guam (WP)	
	H.0121	99-101	Agat Bay, Guam (WP)	AF525579
	WRT46-21 (MICH)		Marshall Islands (CP)	
	WRT46-424 (MICH)		Marshall Islands (CP)	
H. magnidisca	SOC252	99-031	Socotra, Yemen (WI)	AF525595
	SOC348	99-028	Socotra, Yemen (WI)	AF525596
	SOC385		Socotra, Yemen (WI)	
H. discoidea IP	HV3		Zanzibar, Tanzania (WI)	
	SOC299	99-032	Socotra, Yemen (WI)	AF407254
	H.0041	99-014	Moorea, French Polynesia (CP)	AF525604
	H.0203	98-068	Huatulco, Mexico (EP)	
	H.0204	98-161	Bahia Banderas, Mexico (EP)	
	HV215		Tahiti, French Polynesia (CP)	
	HV216		Tahiti, French Polynesia (CP)	
H. taenicola	WRT46-551 (MICH)		Marshall Islands (CP)	
	H.0037	99-004	Tahiti, French Polynesia (CP)	AF407255
	HV285		Rangiroa, French Polynesia (CP)	
	HV306-1		Rangiroa, French Polynesia (CP)	
H. cuneata	no voucher	96-AU-3	W Australia (EI)	AF525606
	WA102		Rottnest Island, W Australia (EI)	
	WA182		Rottnest Island, W Australia (EI)	
	WA206		Carnac Island, W Australia (EI)	
	KZN352		KwaZulu Natal, South Africa (WI)	
	KZN703		KwaZulu Natal, South Africa (WI)	
	KZN2048		KwaZulu Natal, South Africa (WI)	
	HEC15194		Fort Dauphin, Madagascar (WI)	
H. macrophysa	HV8		Zanzibar, Tanzania (WI)	
	HEC15023		Tuléar, Madagascar (WI)	
	H.0024	98-125	Great Barrier Reef, Australia (WP)	
	H.0271	99-142	New Caledonia (WP)	AF525590
H. gigas	HV48		Mnazi Bay, Tanzania (WI)	
	H.0122	99-102	Cocos Island, Guam (WP)	
	WRT46-419 (MICH)		Marshall Islands (CP)	
	L0238136 (L)		Marshall Islands (CP)	

H. gracilis IP	HEC11839	HEC-11839	Beruwala, Sri Lanka (CI)	
	HEC12045		Zanzibar, Tanzania (WI)	AF407257
	C&PvR13087B		Madang, Papua New Guinea (WP)	
	C&PvR13255B		Madang, Papua New Guinea (WP)	
	C&PvR13346B		Madang, Papua New Guinea (WP)	
	HV317		Rangiroa, French Polynesia (CP)	
H. lacrimosa	H.0308	95-BA-010	Bahamas (CAR)	AF407258
	L0351077 (L)		Mariguana, Bahamas (CAR)	
H. gracilis CAR	H.0259	99-109	Galeta, Panama (CAR)	AF407259
	H.0266	99-112	Galeta, Panama (CAR)	
	H.0405	98-093	Isla Grande, Panama (CAR)	AF525609
H. minima	SOC251	99-025	Socotra, Yemen (WI)	AF407264
	SOC384	99-026	Socotra, Yemen (WI)	AF407263
	Snellius-II 10184		Tukang Besi, Indonesia (WP)	
	Snellius-II 10229		Tukang Besi, Indonesia (WP)	
	no voucher	98-031	Tukang Besi, Indonesia (WP)	AF525621
	PH526	99-075	Mindanao, Philippines (WP)	AF525618
	HOD-PH99-46		Mindanao, Philippines (WP)	
	H.0380	99-093	Bile Bay, Guam (WP)	AF525622
	H.0382	99-098	Apra Harbor, Guam (WP)	AF407265
	WRT46-108 (MICH)		Marshall Islands (CP)	
	HV67		Moorea, French Polynesia (CP)	
H. renschii	HV7		Zanzibar, Tanzania (WI)	
	HEC15079		Tuléar, Madagascar (WI)	
	SOC384		Socotra, Yemen (WI)	
	Snellius-II 10943		Komodo Island, Indonesia (EI)	
	C&PvR13855B	99-114	Madang, Papua New Guinea (WP)	AF407262
	no voucher	95-Guam8A	Double Reef, Guam (WP)	AF525614
H. opuntia ATL	HOD-RD2.02-1		Dominican Republic (CAR)	
	HOD-RD2.02-41		Dominican Republic (CAR)	
	H.0263	97-083	Bocas del Toro, Panama (CAR)	
	H.0262	98-189	Tamandare, Brazil (EA)	AF525639
H. opuntia IP	HV19		Zanzibar, Tanzania (WI)	
	HV5		Zanzibar, Tanzania (WI)	
	HEC12584	99-131	Zanzibar, Tanzania (WI)	AF525629
	HV162		Tahiti, French Polynesia (CP)	
H. distorta	no voucher	98-143	Cebu, Philippines (WP)	AF525652
	H.0280	99-151	New Caledonia (WP)	AF525641
	H.0475	99-045	Great Barrier Reef, Australia (WP)	AF407269
	HV199		Tahiti, French Polynesia (CP)	
H. hederacea IP	HV1		Kunduchi, Tanzania (WI)	
	HV9		Zanzibar, Tanzania (WI)	
H. copiosa ATL	H.0264	97-085	Bocas del Toro, Panama (CAR)	
	H.0265	97-095	Bocas del Toro, Panama (CAR)	
	H.0330	97-481	Discovery Bay, Jamaica (CAR)	AF525612
H. goreauii	A.3336 (MICH)		Jamaica (CAR)	
	A.3337 (MICH)		Jamaica (CAR)	
	H.0258	99-108	Isla Galeta, Panama (CAR)	AF525610
H. velasquezii	HV28		Zanzibar, Tanzania (WI)	
	GV2379 (MICH)		Luzon, Philippines (WP)	
H. bikinensis	WRT46-156 (MICH)		Marshall Islands (CP)	
Penicillus capitatus	H.0349	98-181	San Blas, Panama (CAR)	AF407271
Udotea flabellum	H.0415	98-196	Portobelo, Panama (CAR)	AF407270

Part 3

Phylogenetics and biogeography

Genetic patterns in the calcified tropical seaweeds *Halimeda opuntia*, *H. distorta*, *H. hederacea* and *H. minima* provide insights in species boundaries and inter-oceanic dispersal

Wiebe H.C.F. Kooistra & Heroen Verbruggen

Journal of Phycology 41: 177–187 (2005)

Abstract

The section *Opuntia* within the green seaweed genus *Halimeda* includes sprawling and pendant thalli composed of strongly calcified segments. Within this section, identification of Atlantic material is straightforward, but Indo-Pacific material is often difficult to key out. This is particularly true for specimens resembling *H. opuntia*, *H. distorta*, and *H. hederacea*; many specimens do not fit any type or are morphologically intermediate. The goals of the present study are to define morphologically and genetically distinct groups among such specimens and to assess phylogeographic patterns within these groups. Specimens were collected throughout the geographical and morphological range. Sequences of *H. minima* and *H. gracilis* were included as outgroups. Two morphological groups were discerned within the ingroup; the first fit *H. opuntia*, whereas most specimens in the second group, referred to as the *distorta–hederacea* complex, did not fit any species description unambiguously. The latter were subdivided into two subgroups corresponding more or less to *H. hederacea* and *H. distorta*, yet intermediates between these morphs existed. A phylogeny inferred from partial nuclear rDNA sequences showed one lineage with *H. opuntia* and a second one containing the *distorta–hederacea* complex, thus corroborating the two major morphological groups. The *distorta–hederacea* complex contained two clades that show only partial correspondence with the morphological subgroups. Therefore, *H. hederacea* is synonymized with *H. distorta*. Phylogeographic structure within *H. opuntia* indicated that this species dispersed from the Indo-Pacific into the Atlantic. Fossil records of the species also show occurrence at Pacific sites throughout the last 10^5 years and a sudden appearance in the Caribbean and Bahamas during the last millennium.

Introduction

The seaweed genus *Halimeda* (Bryopsidales, Chlorophyta) is easily recognized by its calcified and segmented habit (Hillis-Colinvaux 1980). Yet identification at the species level is, at times, more demanding (Hillis-Colinvaux 1980), especially within section *Opuntia* (Verbruggen and Kooistra 2004). This section currently includes nine described species: western Atlantic *H. copiosa* Goreau & Graham and *H. goreauii* Taylor; Indo-western Pacific *H. distorta* (Yamada) Colinvaux, *H. hederacea* Colinvaux, *H. howensis* Noble & Kraft, *H. minima* (Taylor) Colinvaux, *H. renschii* Hauck, and *H. velasquezii* Taylor; and pantropical *H. opuntia* (Linnaeus) Lamouroux (Hillis-Colinvaux 1980, Kraft 2000, Bandeira-Pedrosa et al. 2003).

Our first goal is defining species boundaries within a particularly problematic group of specimens within the section *Opuntia*, namely, specimens resembling *H. opuntia*, *H. distorta*, and *H. hederacea* (Barton 1901, Yamada 1941, 1944, Colinvaux 1968, 1969, Hillis-Colinvaux 1980). The group is monophyletic according to phylogenies in Kooistra et al. (2002) and Verbruggen and Kooistra (2004),

but it is unclear whether the species are monophyletic. Type specimens and species descriptions in this group often poorly reflect the morphological diversity encountered and many intermediate morphologies occur.

Morphological plasticity could present one reason for identification problems. *Halimeda opuntia*, for example, forms brittle networks composed of almost tripartite segments in shaded sheltered lagoons and compact cushions of reniform segments on wave-exposed rocky surfaces (Littler and Littler 2000, p. 406, personal observations). Plasticity can obscure species boundaries, resulting in description of oddities on the fringes of the plasticity range as new species. Unjust lumping is also possible because discrimination between species may fail if shared morphological trends along environmental gradients obscure species-specific differences. Moreover, genetic, biological, and morphological boundaries between some species may become fuzzy through hybridization. Recent work in the related genus *Caulerpa* (Famà et al. 2000, Durand et al. 2002, de Senerpont Domis et al. 2003) and in several coral genera (Veron 1995, Van Oppen 2001) also shows considerable intraspecific genetic diversity and ill-defined species boundaries.

Our second goal is to address phylogeographic patterns and in particular dispersal directionality within the aforementioned group. Kooistra et al. (2002) revealed phylogeographic structure within the genus *Halimeda*, but their sample coverage did not permit addressing intraspecific patterns. Their data suggest interoceanic dispersal within *H. opuntia*, but more specimens are needed to confirm directionality and to assess whether it has been a unique event or happened multiple times independently.

To address these issues, we collected specimens across the morphological diversity and distribution range of the group and sorted them based on shared morphological traits. A phylogeny was inferred from a region of their nuclear rDNA sequence also used in Kooistra et al. (2002). Obtained morphological groups were then compared with clades in the phylogeny to define monophyletic taxa and identify their boundaries. Collection sites of the specimens were used to construct an area phylogram to identify dispersal events and to determine their directionality. Morphological information from specimens belonging to *H. minima* was included to ascertain morphological distinctness of this species from the group in the focus of this study. Sequences of *H. minima* and *H. gracilis* Harvey ex J. Agardh were included as nearby and more distant outgroups, respectively. The latter species belongs to section *Pseudo-opuntia*, the sister of section *Opuntia* (Verbruggen and Kooistra 2004).

Materials and methods

Collections of specimens and their preservation were carried out as described in Kooistra et al. (2002). The specimens in Table 1, which are lodged in the Ghent University Herbarium, were assigned to groups on the basis of their gross morphology. When possible, these groups were given species names by comparison with descriptions and illustrations in Barton (1901), Taylor (1950, 1960), Colinvaux (1968, 1969), and Hillis-Colinvaux (1980).

The DNA purification, PCR amplification, and sequencing of the target region were as described in Kooistra et al. (2002). The region comprised the small subunit (SSU, from approximately position 500 onward), an insert in the SSU (Hillis et al. 1998, Durand et al. 2002), the internal transcribed spacer regions (ITS1, ITS2), and the 5.8S rDNA. Alignment was done by eye using Sequence Alignment Editor Se-Al, version 2.0a11 (http://evolve.zoo.ox.ac.uk/). The alignment is available at the TreeBASE server (http://www.treebase.org) under study accession number S1208, matrix accession number M2087.

Phylogenetic analyses of the alignment were carried out using PAUP*, version 4.0.b10 (Swofford 2002). Hierarchical likelihood ratio tests (alpha = 0.01) were performed on a sequence data set including all *Halimeda* rDNA sequences available to us on 1 January 2004 using Modeltest v3.06 (Posada and Crandall 1998) to find the most appropriate model and settings for maximum likelihood

(ML) analyses. The ML analysis was carried out under the heuristic search option and tree bisection/reconnection-branch swapping and was constrained using aforementioned Modeltest parameter settings. The ML-bootstrap analysis (1000 replicates) was carried out using the fast stepwise addition option and other settings as with the heuristic search in ML analysis.

The ML-bootstrap analyses were carried out first among the sequences within the *H. opuntia* clade only and among those within the *distorta–hederacea* complex only. Then, two sequences were selected from the *H. opuntia* clade and two from the *distorta–hederacea* clade, each on both sides of the

Table 1. Taxa used in analyses with voucher number of specimen, collection site, and the GenBank accession code of the obtained sequences. An "A" behind the voucher code indicates that the sample contained several specimens from which more than one has been sequenced. Sequences indicated in bold have been included in the global ML analysis. Vouchers with an L number are located in the Leiden herbarium. All other specimens have been lodged in the Ghent University Herbarium, Belgium (GENT). CP, central Pacific; EA, eastern Atlantic; EP, eastern Pacific; I, island; IO, Indian Ocean; MED, Mediterranean Sea; WA, western Atlantic; WP, western Pacific. [a]Also used in Kooistra et al. (2002). [b]ITS2 of this specimen could not be amplified.

Taxon	Specimen number	GENT accession	Region	Geographical location	GenBank
Halimeda hederacea	**99–045**[a]	H.0475	WP	Townsville, Queensland, Australia	**AF407269**
H. cf. hederacea	97–059	H.0008	CP	Honounou, Hawaii	AF525647
	98–143	H.0509	WP	Lapu Lapu, Mactan I., Cebu, Philippines	**AF525652**
	99–005	H.0287	CP	Tahiti, Fr. Polynesia	AF525653
	L0238135	Not applicable	WP	E. of Melolo, Sumba, 09°54'S 120°42.5'E, Indonesia	AF525648
H. distorta	WLS060-02	WLS060-02	CP	Wallis Island (France)	AY649375
H. cf. distorta	98–111	H.0023	WP	Lizard Island, Queensland, Australia	AF525642
	98–121[a]	H.0522	WP	Lizard Island, Queensland, Australia	AF407268
	98-152	H.0507	WP	Lapu Lapu, Mactan I., Cebu, Philippines	AF525651
	99–007	H.0288	CP	Tuamotu, Rangiroa Atoll, Fr. Polynesia	AF525643
	99–011	H.0291	CP	Tuamotu, Rangiroa Atoll, Fr. Polynesia	AF525646
	99–012	H.0292	CP	Tuamotu, Rangiroa Atoll, Fr. Polynesia	AF525644
	99-013	H.0293	CP	Tuamotu, Rangiroa Atoll, Fr. Polynesia (*minima*-like)	AF525645
	99–147	H.0276	WP	New Caledonia	AF525640
	99–151	H.0280	WP	New Caledonia	**AF525641**
	HV275	HV275	CP	Tuamotu, Rangiroa Atoll, Fr. Polynesia	AY649374
	WLS422-02	WLS422-02	CP	Wallis Island (France)	AY649377
H. distorta–hederacea	98–135	H.0526	WP	Lapu Lapu, Mactan I., Cebu, Philippines	AF525649
	98–142	H.0483	WP	Lapu Lapu, Mactan I., Cebu, Philippines	AF525650
H. gracilis	97–076	No voucher	WA	Cayo Zapatilla, Panama	AF525608
	97–089	H.0367	WA	I. Escudo de Veraguas, Panama	AF525607
	98–093	H.0405	WA	I. Grande, Panama	**AF525609**
	99–109[a]	H.0259	WA	Galeta I., Panama	AF407259
	HEC-11839[a]	HEC11839	IO	Beruwala, Sri Lanka	**AF407257**
H. minima	98–128A	H.0336	WP	Lizard I., Queensland, Australia	AF525619
	99–025[a]	SOC251	IO	Rhiy di-Quatanhin, SW-tip, Socotra, Jemen	**AF407264**
	99–026[a]	SOC384	IO	Bidolih, Nogid, S-coast, Socotra, Jemen	**AF407263**
	99–075	PH526	WP	Santa Cruz I., Zamboanga City, Mindanao, Philippines	**AF525618**
	99–089	H.0381	WP	Bile Bay, Guam	AF525620
	99–093	H.0380	WP	Apra Harbor (–25 m), Guam	**AF525622**
	99–098[a]	H.0382	WP	Apra Harbor (–25 m), Guam (fragil, lax specimen)	**AF407265**
	WLS169-02	WLS169-02	CP	Wallis Island (France)	AY649379
	WLS193-02	WLS193-02	CP	Wallis Island (France)	AY649378
H. opuntia	95–Guam1	H.0618	WP	Agat Bay, Guam	AF525630
	95–hon-07	H.0616	WA	I. Roatan, Honduras	AF525628
	95–sa-2	H.0566	WA	I. San Andres, Colombia	AF525623
	96-io-002	H.0534	IO	Chagos Islands	AF525627
	98-096	H.0485	WA	I. Grande, Panama	AF525624
	98–106	H.0519	WP	Lizard I., Queensland, Australia	AF525632
	98–114[b]	H.0332	WP	Lizard I., Queensland, Australia	AF525615
	98–119	H.0481	WP	Lizard I., Queensland, Australia	AF525636
	98–126	H.0525	WP	Lizard I., Queensland, Australia	AF525635
	98–144	H.0523	WP	Lapu Lapu, Mactan I., Cebu, Philippines	AF525637
	98–189	H.0262	WA	Tamardane, Brazil	**AF525639**
	98–192	H.0527	WA	Key Largo, Florida	AF525626
	99–017	H.0289	CP	Tuamotu lagoon, Rangiroa, Fr. Polynesia	AF525631
	99–044[a]	H.0484	WP	One Tree I. Near Townsville, Australia	AF407267
	99–047	H.0489	WP	Townsville, Queensland, Australia	AF525634
	99–096	H.0482	WP	Apra Harbor, Guam	AF525638
	99–131	HEC12583	IO	Zanzibar, Tanzania	**AF525629**
	99–185	H.0506	WA	Cayo Nancy, Bocas del Toro, Panama (brittle mesh)	AF525625
	HV450	HV450	WA	Discovery Bay, Jamaica	AY649373
	HV61	HV61	CP	Moorea, Fr. Polynesia	AY649380
	WLS090-02	WLS090-02	CP	Wallis Island (France)	AY649376

basal dichotomies of these clades in the ML tree. All other sequences in the *H. opuntia* clade and the *distorta–hederacea* clade were then deleted before a global bootstrap analysis.

Maximum parsimony (MP) trees were generated under the heuristic search procedure with the tree bisection/reconnection-branch swapping algorithm. Ambiguities were treated as polymorphisms and gaps as missing data. Branches were collapsed if their minimum length was zero. The resulting trees were filtered to retain only the shortest ones. MP-bootstrap values were obtained using 1000 replicates under the same settings as with MP analysis but with maximum number of trees retained per cycle (set MaxTrees) limited to 200.

Results

Morphological observations

The specimens in Table 1 could be divided into three major morphological groups. In the first group, thalli consisted of small segments; the basal ones were thick and tripartite and the upper segments were thin and flat, most often broad ellipsoidal to ovate (Fig. 1a) but sometimes broad trilobed (Fig. 1b). Segments were often markedly ribbed; the ribs resulted from bundles of medullary siphons connecting the segment's basal node with the nodes along the segments upper rim. Thalli attached at their basal segment only (Fig. 1, a and b), pending from the side of rocks. This morphology conforms to the descriptions of *H. minima* in Taylor (1950), Colinvaux (1968), and Hillis-Colinvaux (1980).

Specimens in the second group possessed thalli of which the upper segments have a reniform outline and a clearly lobed outer edge (Fig. 1d). In most cases, segments were markedly ribbed. The three to five ribs ran from the segments' base to the nodes along the distal perimeter. The nodes were clearly visible and often protruded above the segment perimeter. The segment surface appeared dull and felt rough. Considerable plasticity was observed in segment shape. Segments from cushion-shaped specimens encountered on wave-affected reef crests were reniform (Fig. 1, d and e), whereas those in the brittle networks found in shaded lagoonal environments possessed an almost tripartite outline (Fig. 1c). This morphology conforms to the descriptions of *H. opuntia* in the literature (Barton 1901, Taylor 1950, 1960, Hillis-Colinvaux 1980).

Specimens in the third group possessed segments of different morphology at the base and the apex of the thallus (Fig. 2, a–j). Near the base, segments were often tripartite (Fig. 2, g–j). These segments consisted basically of three bundles of medullary siphons and their surrounding cortex, each proceeding from the segment base to the daughter segments or uncorticated pits. Segments higher up the thallus were flat to contorted, often in one and the same thallus. They usually showed a clear ribbing, and their nodes were not elevated markedly above the segment perimeter. The outline of the upper segments was highly variable and led us to define morphological subgroups with "varieties" in each. These different morphologies were quite distinct, but a few intermediates were observed. Thalli were sprawling (Fig. 2, a, f, and i), and rhizoid tufts for secondary attachment were usually present throughout the thallus (Fig. 2e). As a reference, the third group is cited as the *distorta–hederacea* complex.

The first subgroup (Fig. 2, a–e) included stiff sprawling thalli forming mats about 10–15 cm across. In all specimens, segments of the middle and distal regions were relatively large; those near the base were smaller, thick, and tripartite. The segment surface appeared shiny and felt smooth in some dried specimens. This subgroup is referred to as *H. hederacea*. Two varieties were present within this subgroup.

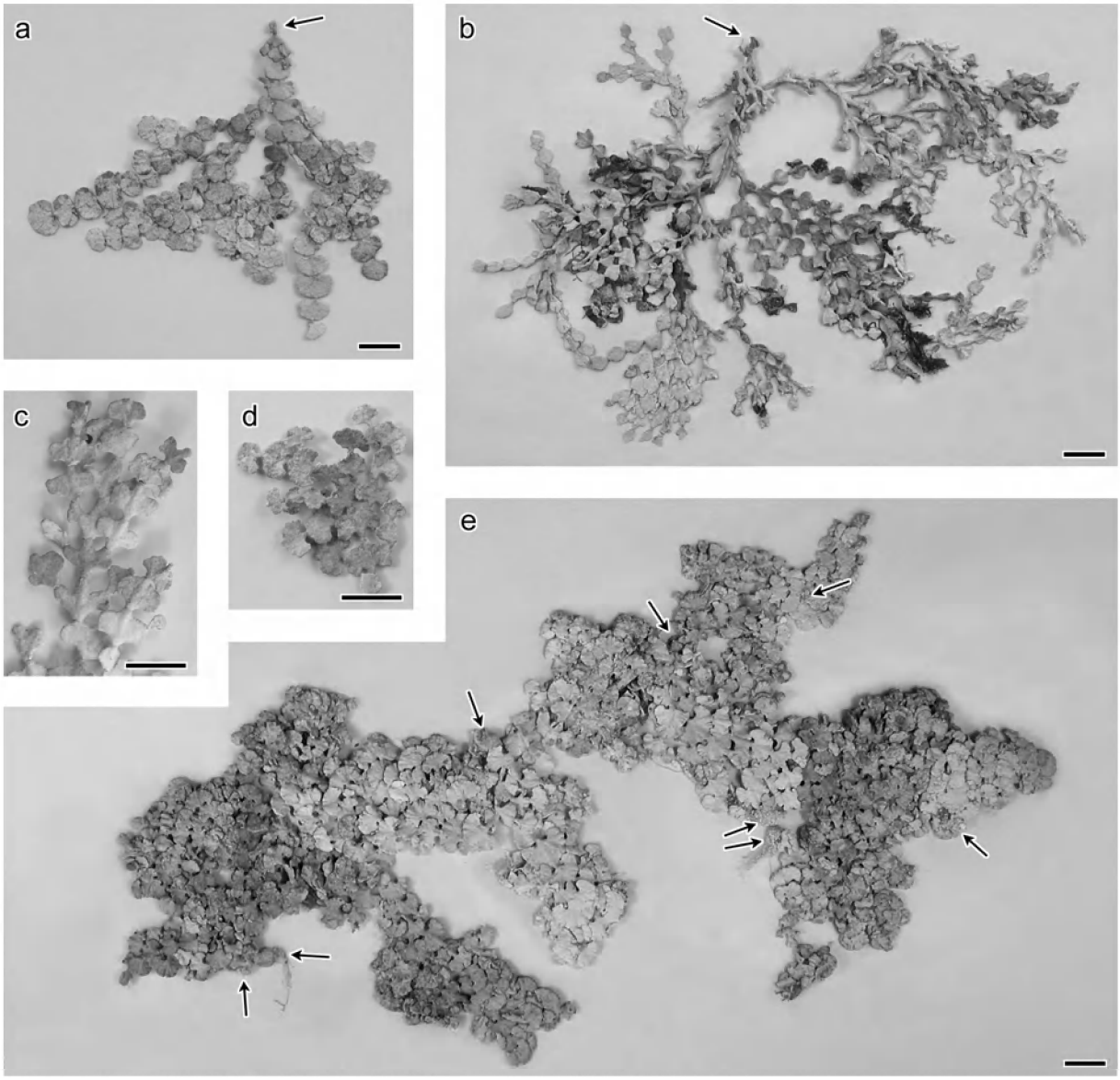

Fig. 1. *Halimeda minima* and *Halimeda opuntia*. Arrows indicate holdfasts. Scale bars, 1 cm. (a–b) *Halimeda minima*. (a) Habit of a plant with broad ovate segments, HV746. (b) Habit of a plant with relatively narrow segments, HV765. (c–e) *Halimeda opuntia*. (c) Tripartite segments of a plant growing in the shade, SEY735. (d) Reniform segments of a plant growing in sunny conditions, PH163. (e) Habit of a plant growing in sunny conditions, HV6.

(1a) Distal segments large, hederifoliate, broader than high, relatively thick, usually ribbed, and, at times, keeled (Fig. 2, ac). These thalli are conform *H. opuntia* forma *hederacea* as described in Barton (1901).

(1b) Distal segments large, reniform, broader than high, relatively thin, flat (not keeled), and usually not ribbed (Fig. 2d). This morph is not described in the *Halimeda* monographs.

The second subgroup included lax sprawling thalli with relatively small upper segments. Segments near the base were thick and tripartite. The segment surface was dull and coarse in dried specimens. This subgroup is referred to as *H. distorta* and contained three varieties.

(2a) Distal segments small, about as broad as high, relatively thin, distorted. This morph is depicted in Hillis-Colinvaux' (1980) description of *H. distorta*. It is not depicted here.

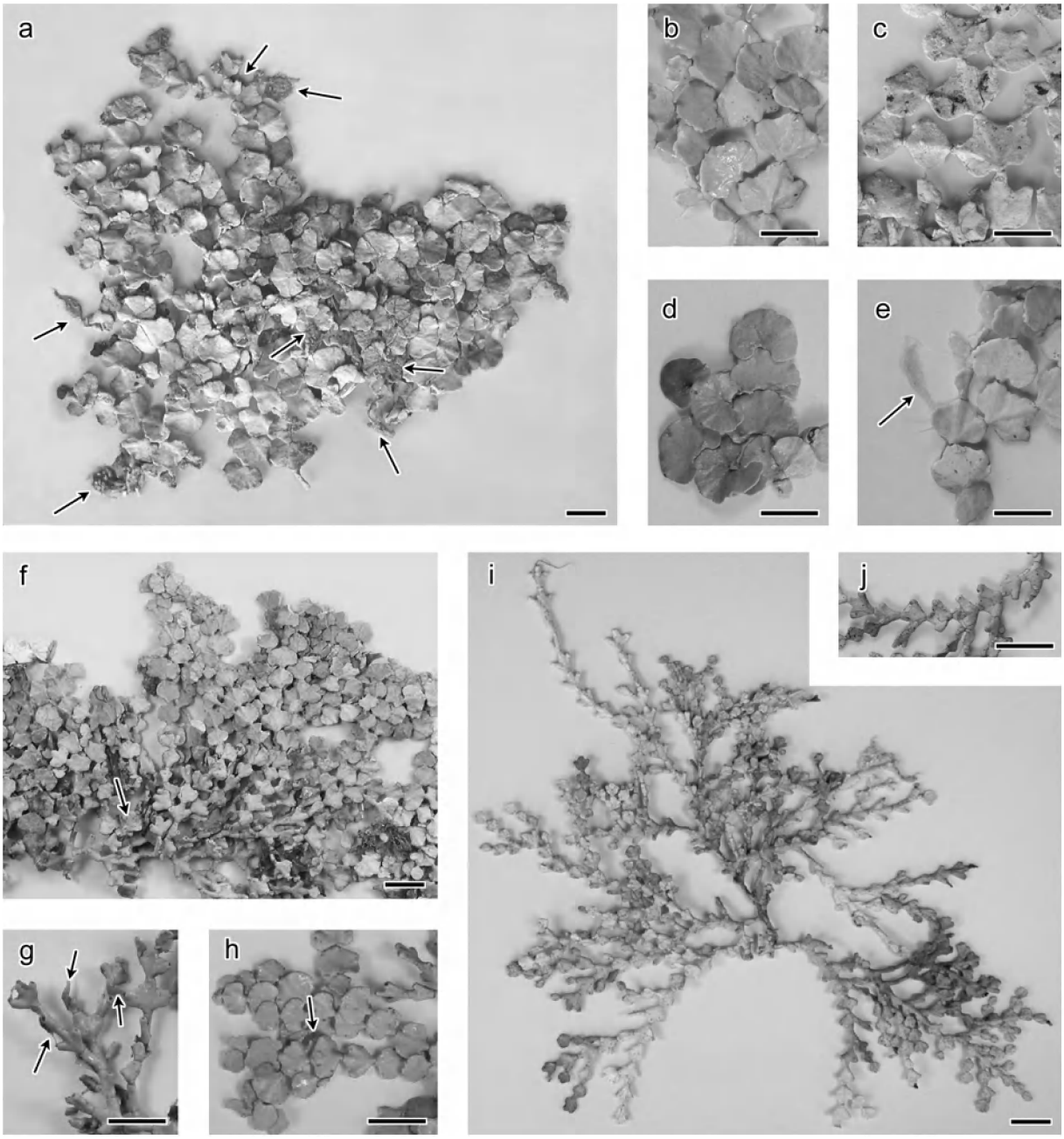

Fig. 2. *Halimeda distorta–hederacea* complex. Arrows indicate holdfasts. Scale bars, 1 cm. (a–e) *Halimeda* cf. *hederacea* (morphs 1a and 1b). (a) Thallus habit (morph 1a), HV199. (b) Segment morphology (morph 1a), HV600. (c) Segment morphology (morph 1a), HV572. (d) Segment morphology (morph 1b), HV127. (e) Detail of a tuft of holdfast rhizoids, HV600. (f–j) *Halimeda* cf. *distorta* (morphs 2b and 2c). (f) Part of a chimerical thallus (morph 2b), HV767. (g) Segment morphology of proximal segments (morph 2b), HV767. (h) Segment morphology of distal segments (morph 2b), HV767. (i) Thallus habit (morph 2c), HV275b. (j) Segment morphology (morph 2c), HV275b.

(2b) Distal segments relatively small, broad ovate to reniform, broader than high, flat, usually ribbed (Fig. 2, f and h). This morph is not depicted in the *Halimeda* monographs unless maybe in figure 20 in Barton (1901, as *H. opuntia* forma *triloba*).

(2c) Distal segments generally as those of the basal region: tripartite over trilobed to rhomboidal, relatively small, flat to slightly distorted (Fig. 2, i and j). This morph is depicted in Taylor (1950) as *H. opuntia* forma *elongata* (plate 41).

The specimens used for molecular phylogenetic analyses have been assigned to the above-mentioned subgroups and varieties (Fig. 3a). Note that the specimens depicted in Figures 1 and 2 do not always correspond to sequenced specimens (Table 1). This is because the latter were often clippings, too small to give a complete image of the thallus morphology as seen in Figures 1 and 2.

Sequence analyses and phylogenies

The alignment of the 53 sequences was straightforward; only 24 of 1758 positions needed introduction of gaps in some of the sequences, and no ambiguous alignment possibilities were encountered. One hundred forty-nine positions were parsimony informative and were located predominantly in the ITS regions. Virtually none of the sequences obtained from conspecific specimens were identical, not even if the specimens originated from proximal sites. The least rejected sequence evolution model resulting from the hierarchical likelihood ratio test was a general time reversible one with estimated values for the following parameters: base frequencies: A = 0.206, C = 0.271, G = 0.305, T = 0.218; substitution rates: A ↔ C = 1.211, A ↔ G = 1.890, A ↔ T = 1.524, C ↔ G = 0.653, CT = 3.525 relative to G ↔ T = 1.000; proportion of invariable sites = 0.550; gamma shape parameter = 0.455. An ML tree inferred from all 54 sequences is shown in Figure 3a. The tree is 619 steps long (rescaled consistency index = 0.689, homoplasy index = 0.456; –ln L = 5073.4327). MP analysis resulted in 205 equally MP trees of which the 66 shortest were 628 steps long (rescaled consistency index = 0.699; homoplasy index = 0.463; –ln L between 5427.6007 and 5438.4730; MP trees not shown). These MP trees were nine steps longer than the ML tree, but the topology was essentially the same as that of the ML tree.

The ML tree shows a well-supported (94%) clade with all sequences from specimens with a morphology conforming that of *H. opuntia*. The *H. opuntia* clade revealed considerable intraspecific variation, but little phylogenetic structure was recovered among the sequences; only two internal clades obtained any support above the 50% threshold.

All sequences from specimens belonging to the *distorta–hederacea* complex grouped in a clade with 76% ML-bootstrap support as nearest sister to the *H. opuntia* clade. Sequence variation within the *distorta–hederacea* clade was comparable with that within the *H. opuntia* clade as illustrated by similar overall branch lengths in the two clades, but phylogenetic structure was better resolved in the former; several internal clades obtained support. Sequences from lax thalli with small segments (morphologies 2a–2c) were all but one recovered in the first major clade of the *distorta–hederacea* complex (Fig. 3a), whereas those obtained from stiffer thalli with relatively large segments (morphologies 1a–1b) were found at the basal polytomy of the complex (Fig. 3a). Phylogenetic separation of morphs was incomplete: Specimens 98–135 and 98–142 showed an intermediate morphology, and specimen 98–152 with its lax thallus and small segments was recovered among the stiff thalli with large segments in the lower polytomy. The previously described further division (indicated with a, b, or c) within the two major morphological groups did not reveal clear grouping in the phylogeny.

Sequences of *H. minima* were recovered in a clade as sister to the clade with *H. opuntia* and the *distorta–hederacea* complex. Differences among sequences in this clade were more pronounced than within the *H. opuntia* clade or within the *distorta–hederacea* complex. In fact, three genetically distinct groups separated by long branches and obtaining high bootstrap support were discernible within the *H. minima* clade.

Table 2 lists the distribution of ambiguities over the sequences of *H. minima*, *H. opuntia*, and the *distorta–hederacea* complex. Although about the same number of sequences has been included for *H. opuntia* and the *distorta–hederacea* complex, the former showed about twice as many ambiguities than the latter. Y was the most frequent ambiguity encountered across all sequences, followed by R, M, and W. Table 2 also lists the distribution of ambiguities over the different sequence regions;

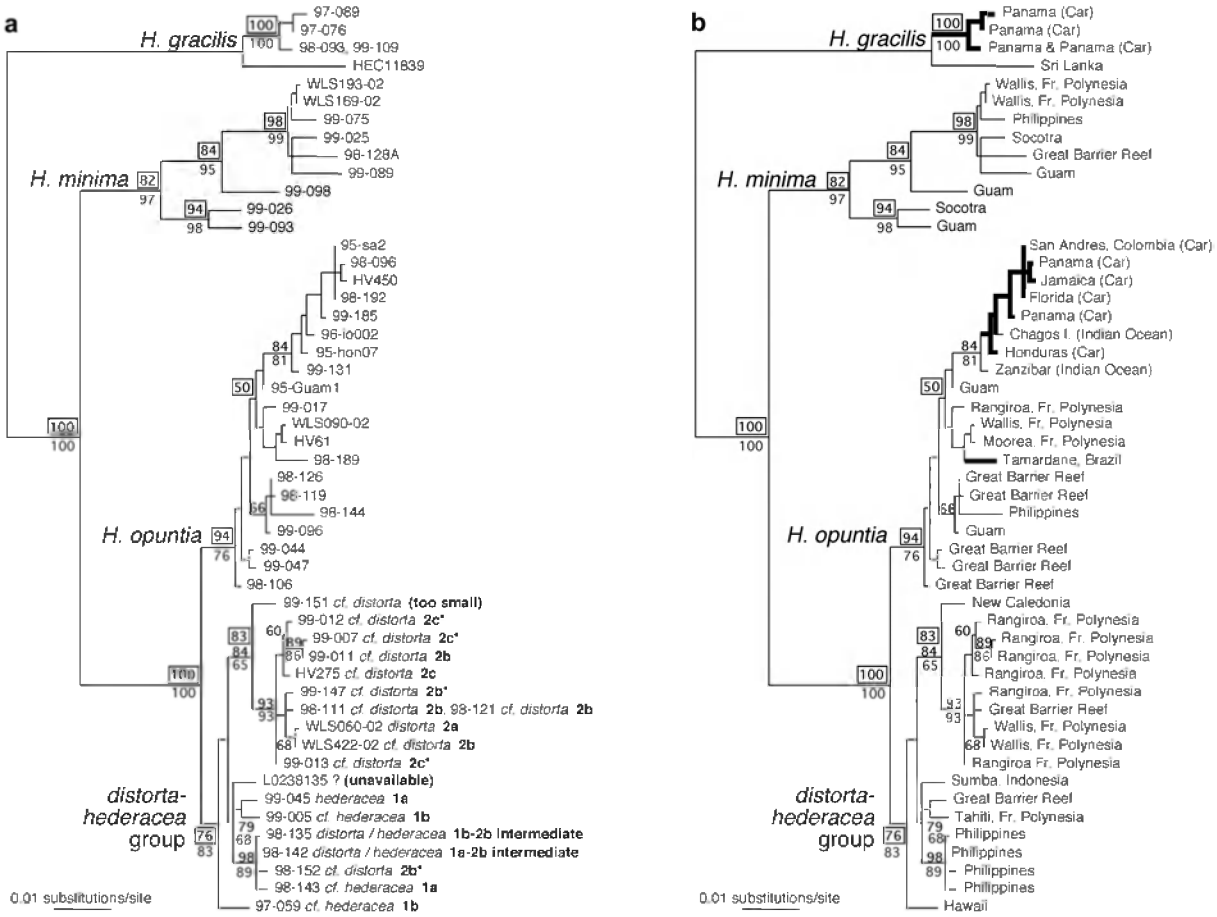

Fig. 3. (a) Maximum likelihood tree inferred from partial nuclear rDNA cistron data of *Halimeda minima*, *H. opuntia*, the *distorta–hederacea* group, and *H. gracilis*. The latter have been treated as outgroup (see Table 2). Car, Caribbean; Fr., French. Bootstrap values greater than or equal to 50% are indicated to the left of the clade. The ML and MP bootstrap values are indicated above and below branches, respectively. The ML bootstrap values not encased in a box have been generated by analyses of sequences within the *H. opuntia* clade or within the *distorta–hederacea* clade; values encased in a box have been generated in the global ML analysis (see text). Specimen numbers are explained in Table 1. Identification of specimens within the *distorta–hederacea* complex into morphological subgroups is indicated behind the specimen numbers (meaning of 1a–2c, see text). An asterisk denotes that only a few segments were available for study. The topology is available from TreeBASE under the same accession number as the alignment. (b) Area phylogram representation of a. Collection regions are indicated at end nodes. For more detailed information on collection sites, see Table 1. Car, Caribbean; Fr., French. The most parsimonious explanation for the occurrence of Atlantic specimens has been marked as thickened branches.

ambiguities were encountered mainly in the ITS2 region of the *distorta–hederacea* complex and *H. opuntia*; they were far less frequent in the ITS2 of *H. minima*, and they were rare in the other sequence regions. Ambiguities were encountered at positions in the alignment where the remaining sequences belonging to the same species contained either one or the other base of which the particular ambiguity was composed. As an example, positions showing ambiguity Y in some *H. opuntia* sequences contained C or T in the remaining sequences of this species.

Table 2. Distribution of ambiguities over the alignment.

Species	*Halimeda opuntia*	*Halimeda distorta complex*	*Halimeda minima*	Total
Ambiguity				
R (AG)	21	8	1	30
Y (CT)	51	20	8	79
S (CG)	2	4	0	6
W (AT)	9	8	0	17
K (GT)	3	1	0	4
M (AC)	8	11	1	20
N	11	1	3	15
Total	105	53	13	171
Sequences	23	18	13	54
No. positions showing ambiguities in:				
SSU	1	2	1	
Insert	5	1	2	
ITS1	6	8	3	
5.8S	0	0	0	
ITS2	27	19	2	

Phylogeography

In the area phylogram in Figure 3b, sample sites (Table 1) have been indicated at the end nodes of the tree in Figure 3a to infer the most parsimonious phylogeographic explanation of their distribution. All sequences of *H. minima* and the *distorta–hederacea* complex were obtained from Indo-Pacific specimens. Within the *distorta–hederacea* complex, Philippine specimens grouped together and so did many but not all French Polynesian ones. Sequences of *H. opuntia* showed a basal Pacific grade with a well-supported (84%ML, 81%MP) clade with specimens from the Caribbean and Indian Ocean. Although the Caribbean sequences form a grade with one from the Indian Ocean among them, monophyly for the Caribbean sequences is not rejected because of the total lack of bootstrap support within this clade. The sequence of a Brazilian specimen grouped with Pacific neighbors and not with the Caribbean ones, though monophyly for Atlantic sequences is not strictly rejected because all clades separating the well-supported clade with Caribbean sequences from the Brazilian one did not obtain sufficient support.

Discussion

Classical versus genealogical interpretation of species boundaries

Our major morphological subdivision of the specimens corresponds with the phylogenetic one; all sequences of the specimens belonging to our *H. opuntia* morph form a clade and so do those in the *distorta–hederacea* complex and those in the *H. minima* morphological group. Nonetheless, conflict occurs between the classical and phylogenetic interpretation of species in the studied group for two reasons. First, well-supported lineages exists within the *H. minima* clade and the *distorta–hederacea* complex, suggesting the existence of genetically separated populations or even biologically distinct taxa therein. Second, species as perceived and delineated by classical taxonomy (Hillis-Colinvaux 1980) appear to conflict with our phylogenetic clades and morphological groups.

Specimens assignable to *H. minima* are genetically and morphologically distinct from the group of specimens assignable to *H. opuntia* and the *H. distorta–hederacea* complex. Results support those in Verbruggen and Kooistra (2004) that *H. minima* consists of at least two genetically distinct lineages, that variation among the sequences within the clades is comparable to that within other *Halimeda* species, and that each lineage seems to be widely distributed. Therefore, we believe that there exist at least two biologically distinct species in *H. minima*. The *H. minima* group is morphologically diverse, and morphological patterns within this group should be addressed with a more sizable set of specimens, including *H. howensis*, *H. renschii*, and *H. velasquezii*.

Halimeda opuntia constitutes a monophyletic taxon. The tightly packed cushions composed of reniform segments encountered on wave-exposed sites and brittle networks of tripartite segments found in mangles (see illustrations in Littler and Littler 2000 and Fig. 1, c–e) do not show any grouping in the tree and probably result entirely from plasticity. Moreover, if cushions found on exposed reef flats are maintained in shaded aquaria, they sprout brittle thalli like those encountered in mangles. Similar morphological plasticity under influence of environmental factors has been demonstrated in *H. cylindracea* Decaisne (Gilmartin 1960).

Hillis-Colinvaux (1980) merged all forms described in *H. opuntia* under a single species, and at first sight our results prove her right. Nonetheless, Hillis-Colinvaux' interpretation of *H. opuntia* may have been too broad. *Halimeda distorta* (our morph 2a) is described very narrowly in her monographs, whereas our morphs 2b and 2c do not seem to be represented in her work. The segments of these morphs are often tripartite like those of *H. opuntia* growing in low light conditions. Furthermore, distal segments of morph 2b resemble those of typical *H. opuntia* cushions. Hillis-Colinvaux (1980) stressed that very few specimens of *H. distorta* were at her disposal. Given the fact that our morphs 2b and 2c are relatively common in Pacific atolls, a region well studied by Hillis-Colinvaux, we suspect that she

was misguided by the resemblance between both species and included our morphs 2b and 2c in *H. opuntia*.

In the *distorta–hederacea* complex, morphotypes seem to correlate with evolutionary history because the clade, including lax specimens with relatively small segments (including *H.* cf. *distorta*), is distinct from the remaining grade with stiff specimens and large segments (including *H.* cf. *hederacea*). The specimens resembling the types of *H. distorta* (WLS060-02) and *H. hederacea* (98–143) are recovered in the clade and the basal grade, respectively, but not all specimens in the clade resemble the type of *H. distorta* and neither do all those in the basal group resemble that of *H. hederacea*. Apparently, the type specimens are just morphs within one or two morphologically more broadly defined species inside the *distorta–hederacea* complex. The absence of any monophyly among the observed varieties suggests that these are part of plasticity ranges like those observed in *H. opuntia*; in fact, many in-between cases were noted already.

The taxonomic history of the entity *H. hederacea* has been a dynamic one. Barton (1901) recognized *H. opuntia* forma *hederacea* as a distinct form within *H. opuntia*. Colinvaux (1968) recognized it as *H. hederacea*, but merged it with Atlantic *H. copiosa* one year thereafter (Colinvaux 1969). Recently, Kooistra et al. (2002) demonstrated that Atlantic and Indo-Pacific *H. copiosa* are cognates, distantly related entities that have converged upon comparable thallus habit and anatomy; therefore, they proposed to reestablish *H. hederacea* provisionally. The taxonomic history of *Halimeda distorta* is somewhat more straightforward. First, Yamada (1941, 1944) described it as a form of *H. incrassata* (Ellis) Lamouroux, and subsequently Colinvaux (1968) elevated this form to the species level.

The absence of a tight correlation between morphology and phylogeny in the *H. distorta–hederacea* complex calls for a re-taxonomization of the group. Even though morphotypes correlate with clades and grades, the relatively low support of the different subgroupings and the existence of specimens showing intermediate morphologies leave us with a lack of evidence to sustain the distinction between *H. hederacea* and *H. distorta*. Therefore, we propose the provisional merger of both species. Because the formae *H. incrassata* forma *distorta* and *H. opuntia* forma *hederacea* were elevated to the specific rank in the same study, either name can be used. We are of the opinion that *distorta* is the more appropriate one for two reasons. First, the epithet *distorta* means distorted, indicating that segments are not entirely flat. This is the case in a majority of our specimens, either in the basal or the distal part. Only a small part of the specimens has ivy leaf-like segments, making the *hederacea* epithet less appropriate. Second, the denomination *hederacea* could bring about confusion with *H. copiosa*. The latter species occurs exclusively in the Atlantic Ocean, whereas the *hederacea–distorta* complex is restricted to the Indo-Pacific. Yet the species *H. hederacea* was described by Colinvaux (1968) based on a combination of Indo-Pacific and Atlantic specimens. The Atlantic specimens belong to *H. copiosa* sensu Kooistra et al. (2002). In our proposal, *H. copiosa* refers to Atlantic specimens corresponding to the description in Goreau and Graham (1967) and *H. distorta* refers to all Indo-Pacific specimens corresponding to our morphs 1a, 1b, 2a, 2b, and 2c and their intermediates (Fig. 2, a–j).

Discordances between classical and genealogical perceptions of species need to be stressed. Although for *H. opuntia* both perceptions seem to correspond well, classical *H. minima* appears to be under-taxonomized, whereas the *H. distorta–hederacea* group either has been over-taxonomized or has been taxonomized using the wrong morphological characters. The existence of several genetically distinct taxa within morphologically perceived species has also been observed in other *Halimeda* lineages (Kooistra et al. 2002). All these cases represented genetically distinct Atlantic and Indo-Pacific taxa that had converged upon one another morphologically, possibly because they grow in highly similar environments. Cryptic and pseudocryptic species have been noted also in other green algal groups (Angeler et al. 1999, Coleman 2001, Durand et al. 2002, O'Kelly et al. 2004).

Additional information on species boundaries could be acquired by studying reproductive events and anatomical characters. In a group of closely related *Halimeda* species (Atlantic *H. incrassata*, *H. monile* (Ellis et Solander) Lamouroux, and *H. simulans* Howe), the timing of concerted spawning differed between species (Clifton 1997, Clifton and Clifton 1999). A similar approach combined with interfertility studies could provide insights into the nature of subgroups uncovered in the present study. Furthermore, studies analyzing both morphometric and DNA sequence data (Verbruggen et al. 2005) can reveal which morphological characters can be used to diagnose different species and their internal clades.

Intraspecific and intraindividual sequence variation

If the well-supported clades within the *H. distorta–hederacea* complex and within *H. minima* represent biologically distinct species, then considerable sequence variation still abounds within each of these species. Such high intraspecific variation is also encountered within monophyletic morphologically defined species in other *Halimeda* lineages (Verbruggen and Kooistra 2004, unpublished data) and within their distant bryopsidalean relative *Caulerpa racemosa* (Forsskål) C. Agardh (Famà et al. 2000, Durand et al. 2002). Possible explanations for such high sequence variation are a high mutation rate, poorly performing concerted evolution (Dover 1982, Arnheim 1983, Jorgensen and Cluster 1988), ancestral polymorphism in arising species (Durand et al. 2002), and hybridization and polyploidization events (Scholin et al. 1995, Wendel et al. 1995).

Lineage-specific high mutation rates on the rDNA sequences could explain the high intraspecific sequence variation observed in both *Halimeda* and *Caulerpa* (Famà et al. 2000, Durand et al. 2002, Verbruggen and Kooistra 2004, this study) as well as a highly elevated substitution rate in nuclear SSU rDNA sequences of Bryopsidalean algae in general (Zechman et al. 1999). If elevated rates affect the SSU, then the same may be true for the far less conserved ITS sequences.

Concerted evolution generally performs poorly if organisms reproduce exclusively clonally or if the rDNA sequences occur scattered throughout the genome. *Halimeda* species, and particularly members of the section *Opuntia*, can grow clonally for extended periods (Hillis-Colinvaux 1980, Walters et al. 2002), but generally populations also experience frequent reproductive events during which a large part of the biomass is shed as gametes (Hillis-Colinvaux 1980, Drew and Abel 1988, Clifton and Clifton 1999). Given such frequent and massive sexual reproduction, one would expect rapid reshuffling and homogenization of all copies along a chain of rDNA sequences (Hillis and Dixon 1991).

Hybridization events can explain the observed intraindividual sequence variation (Table 2) and the apparent lack of intraspecific phylogenetic structure among sequences within *Halimeda*. Hybridization may have been more extensive in *H. opuntia* than in the *H. distorta–hederacea* complex because despite comparable sequence variation (as illustrated by similar branch lengths in the *H. opuntia* clade and the clade with the distorta complex), phylogenetic resolution is worse among the sequences of *H. opuntia*, and these sequences show a markedly higher number of intraindividual polymorphisms (Table 2). Similarly, high polymorphism and ill-defined species boundaries have been assigned to hybridization in corals (Van Oppen et al. 2001).

Phylogeographic structure within the *distorta–hederacea* and *opuntia* clades

Although the results of this study support the distinctness of the *H. opuntia* clade from the one with *H. distorta–hederacea* complex, it has not improved phylogeographic resolution within these two clades. Both the huge distribution ranges and the apparent paucity of phylogeographic patterning within the clades of *H. opuntia* and the *H. distorta–hederacea* complex suggest that *Halimeda* disperses over large distances and that dispersion is apparently ongoing and frequent. Mature *Halimeda* thalli are unlikely long-distance travelers because they are calcified and therefore sink rapidly if they become

dislodged (Walters et al. 2002). Yet it might be the propagules and the juvenile uncalcified thalli (Meinesz 1980) that do most of the traveling (Kooistra et al. 2002).

Interoceanic dispersal

Our data suggest that *H. opuntia* is of Indo-Pacific origin because its nearest neighbor taxa (the *distorta–hederacea* complex and *H. minima*) are all strictly Indo-Pacific. Moreover, within the *H. opuntia* clade in Figure 3b, all sequences from Caribbean specimens and two from Indian Ocean specimens form a well-supported clade within a grade of Pacific sequences. *Halimeda opuntia* appears to have settled the Brazilian coast independently from the region comprising the Caribbean and Bahamas because the sequence of the Brazilian specimen is distinct from those of Caribbean specimens and appears in a different part of the phylogeny. However, bootstrap support for the various clades in the *H. opuntia* clade is insufficient to confirm independent dispersal. The data suggest that the Caribbean founders arrived from the Indian Ocean because sequences of specimens from that region are recovered in the basal part of the Indo-Caribbean clade. Yet, this inference is weak because only two specimens from the Indian Ocean were included.

Halimeda opuntia may have arrived in the Caribbean, Bahamas, and Brazil as a hitchhiker in the fouling biota on ship hulls. It is now a common constituent of western Atlantic vegetations, forming nascent biohermal structures in lagoons and dense sprawls over leeward reef slopes (Hillis-Colinvaux 1980). The very first collection of *H. opuntia*, from Jamaica, at the close of the 17th century (Sloane 1707) proves its presence in the Caribbean three centuries ago. Yet interoceanic shipping commenced about another two centuries earlier, at the end of the 15th century. The possibility of an arrival in the western Atlantic before the closure of the Panama Isthmus at about 3.1 Ma B.P. (Coates and Obando 1996) is unlikely because that event could be linked to the separation of Atlantic and Indo-Pacific clades deeper down in the *Halimeda* phylogeny (Kooistra et al. 2002), and one of these Indo-Pacific clades gave rise to *H. opuntia*.

Evidence from the fossil stratigraphy also suggests recent settlement of *H. opuntia* in the Caribbean and Bahamas. Calcified segments of this species accumulate between 1 and 2 m per millennium (Drew and Abel 1985, Hudson 1985, Freile 2004). At Pacific undisturbed sites, extensive deposits of segments belonging to *H. opuntia* and its sister, *H. distorta* (Finckh 1904, Drew and Abel 1985), must have accrued over several 100,000 years. Instead, layers of *H. opuntia* segments at Atlantic locations (Hudson 1985, Andersen and Boardman 1989) are no more than 1 m thick, suggesting occurrence for a millennium at the most. As an example, modern day channel sands of Pigeon Creek (San Salvador, Bahamas) consist of up to 50% *Halimeda* segments with a considerable portion of those represented by *H. opuntia* (Mitchell 1986). In contrast, a nearby and ecologically comparable Sangamon interglacial unit contains only small amounts of *Halimeda* segments, but there is no trace of *H. opuntia* (Thalman and Teeter 1983).

The notion that extant *H. opuntia* is not a western Atlantic native is relevant for paleontologists and ecologists alike. Undisturbed layers of fossil segments may allow more precise dating of the arrival as well as reconstruction of how local biota adapted to the newcomer over a period spanning several centuries. Generally, species are considered to be nonindigenous if scientific records exist from the times predating their arrival. Unfortunately, however, human meddling with the global marine biodiversity dates further back than keen scientific interest in this biodiversity and "important constituents of the local seaweed flora" may well be historic invaders.

Acknowledgements

Llewellya W. Hillis is acknowledged for stimulating W. K. to study *Halimeda* and for funding (A. W. Mellon Foundation and Scholarly Studies). W. K. thanks STRI for providing research infrastructure and additional grants. H. V. is indebted to the Bijzonder Onderzoeksfonds (Ghent University grant

011D9101), the Fund for Scientific Research Flanders (grant 3G002496), C. Payri, P. Vanai, and the Environmental Service of Wallis and Futuna for facilitating fieldwork on Uvea Island, and C. & T. Leigh for facilitating fieldwork in Jamaica. We thank D. Freile for providing information on fossils and P. Goetghebeur for comments on nomenclature. The data set would not have been obtained without the collections of specimens by K. Arano, E. Coppejans, O. Dargent, E. Drew, F. Gurgel, O. Gussmann, L. Hillis, L. Kirkendale, F. Leliaert, P. Marshall, J. Maté, C. Payri, R. Robertson, P. Skelton, M. Waycott, S. Williams, B. Wysor, and G. Zuccarello.

References

Andersen, C. B. & Boardman, M. R. 1989. The depositional evolution of Snow Bay, San Salvador. *In* Mylroie, J. E. [Ed.] *Proc. of the 4th Symp. on the geology of the Bahamas.* Bahamian Field Station, San Salvador, Bahamas, pp. 7-22.

Angeler, D. G., Schagerl, M. & Coleman, A. W. 1999. Phylogenetic relationships among isolates of *Eudorina* species (Volvocales, Chlorophyta) inferred from molecular and biochemical data. *J. Phycol.* 35:815-23.

Arnheim, N. 1983. Concerted evolution of multigene families. *In* Nei, M. & Koehn, M. [Eds.] *Evolution of genes and proteins.* Sinauer Associates, Sunderland, MA, pp. 38–61.

Bandeira-Pedrosa, M. E., Bouzon, Z. L., Pereira, S. M. B. & Oliveira, E. 2003. Ultrastructure of some species of *Halimeda* (Bryopsidales, Chlorophyta) from Brazil. *Cryptogamie, Algologie* 24:219-31.

Barton, E. S. 1901. *The genus* Halimeda. Monograph LX of: Uitkomsten op zoologisch botanisch oceanographisch en geologisch gebied verzameld in Nederlandsch Oost-Indie 1988-1900 aan boord H. M. Siboga onder commando van luitenant ter zee 1e kl. G. F. Tydeman, uitgegeven door Dr. Max Weber, Prof. In Amsterdam, Leider der Expeditie. E. J. Brill, Publishers and Printers, Leiden. 32 pp + 4 pls.

Clifton K.E. 1997. Mass spawning by green algae on coral reefs. *Science* 275:1116–8

Clifton, K. E. & Clifton, L. M. 1999. The phenology of sexual reproduction by green algae (Bryopsidales) on Caribbean coral reefs. *J. Phycol.* 35:24-34.

Coates, A. G. & Obando, J. A. 1996. The geologic evolution of the Central American Isthmus. *In* Jackson, J. B. C., Budd, A. F. & Coates, A. G. [Eds.] *Evolution and environment in Tropical America.* University of Chicago Press, Chicago, pp. 21-56.

Coleman, A. W. 2001. Biogeography and speciation in the *Pandorina/Volvulina* (Chlorophyta) superclade. *J. Phycol.* 37:836-51.

Colinvaux, L. Hillis. 1968. New species of *Halimeda*: a taxonomic reappraisal. *J. Phycol.* 4:30-5.

Colinvaux, L. Hillis. 1969. *Halimeda copiosa* and *Halimeda hederacea*. *J. Phycol.* 5:88.

de Senerpont Domis, L.N., Famà, P., Bartlett, A.J., Prud'homme van Reine, W.F., Armenta-Espinosa, C., Trono Jr., G.C. 2003. Defining taxon boundaries in members of the morphologically and genetically plastic genus *Caulerpa* (Caulerpales, Chlorophyta). *J. Phycol.* 39:1019–37

Dover, G. 1982. Molecular drive: a cohesive mode of species evolution. *Nature* 299:111-7.

Drew, E. A. & Abel, K. M. 1985. Biology, sedimentology and geography of the fast inter-reefal *Halimeda* meadows within the Great Barrier Reef Province. *Proc. 5th Int. Coral Reef Symp.* 5:15-20

Drew, E. A. & Abel, K. M. 1988. Studies on *Halimeda*. II: reproduction, particularly the seasonality of gametangia formation, in a number of species from the Great Barrier Reef Province. *Coral Reefs* 6:207-18.

Durand, C., Manuel, M., Boudouresque, C. F., Meinesz, A., Verlaque, M. & LeParqo, Y. 2002. Molecular data suggest a hybrid origin for the invasive *Caulerpa racemosa* (Caulerpales, Chlorophyta) in the Mediterranean Sea. *J. Evol. Biol.* 15:122-33.

Famà, P., Olsen, J. L., Stam, W. T. & Procaccini, G. 2000. High levels of intra- and inter-individual polymorphism in the rDNA ITS1 of *Caulerpa racemosa* (Chlorophyta). *Eur. J. Phycol.* 35:349-56.

Finckh, A. E. 1904. Biology of the reef-forming organisms at Funafuti Atoll. *In* Anonymous [Ed.] *Royal Society of London, Coral reef committee report. The Atoll of Funafuti, borings into a coral reef and the results*. The Royal Society of London, London, UK, pp. 125-50.

Freile, D. 2004. Carbonate productivity rates of *Halimeda* at two different environments, San Salvador Island, Bahamas. Proceedings of the 11th Symposium on the Geology of the Bahamas and Other Carbonate Regions. pp. 95-106. Gerace Research Center, San Salvador, Bahamas.

Gilmartin, M. 1960. The ecological distribution of the deep water algae of Eniwetok Atoll. *Ecology* 41:210-21.

Goreau, T.F. & Graham, E.A. 1967. A new species of *Halimeda* from Jamaica. *Bull. Mar. Sci.* 17: 432– 441.

Hillis, D. M. & Dixon, M. T. 1991. Ribosomal DNA: molecular evolution and phylogenetic inference. *Q. Rev. Biol.* 66:411-53.

Hillis, L. W., Engman, J. A. & Kooistra, W. H. C. F. 1998. Morphological and molecular phylogenies of *Halimeda* (Chlorophyta, Bryopsidales) identify three evolutionary lineages. *J Phycol.* 34:669-81.

Hillis-Colinvaux, L. 1980. Ecology and taxonomy of *Halimeda*: primary producer of coral reefs. *Adv. Mar. Biol.* 17:1-327.

Hudson, J. H. 1985. Growth rate and carbonate production in *Halimeda opuntia*: Marquesas Keys, Florida. *In* Toomey, D. F. & Nitecki, M. H. [Eds.] *Paleoalgology: contemporary research and Applications.* Springer Verlag, Heidelberg, Germany, pp. 257-63.

Jorgensen, R. A. & Cluster, P. D. 1988. Modes and tempos in the evolution of nuclear ribosomal DNA: new characters for evolutionary studies and new markers for genetic and population studies. *Ann. Missouri Bot. Gard.* 75:1238-47.

Kooistra, W. H. C. F., Coppejans, E. G. G. & Payri, C. 2002. Molecular systematics, historical ecology and phylogeography of *Halimeda* (Bryopsidales). *Mol. Phylogen. Evol.* 24:121-38.

Kraft, G.T. 2000. Marine and estuarine benthic algae (Chlorophyta) of Lord Howe Island, South-western Pacific. *Austr. Syst. Bot.* 13: 509–648.

Littler, D. S. & Littler, M. M. 2000. *Caribbean reef plants: an identification guide to the reef plants of the Caribbean, Bahamas, Florida and Gulf of Mexico*, Offshore graphics Inc., Washington D.C, 542 pp.

Meinesz, A. 1980. Connaissances actuelles et contribution à l'étude de la reproduction et du cycle des Udotéacées (Caulerpales, Chlorophytes). *Phycologia* 19:110-38.

Mitchell, S. W. 1986. Sedimentology of Pigeon Creek, San Salvador Island, Bahamas *In* Curran, H. A. [Ed.] *Proc. of the 3rd Symp. on the Geol. of the Bahamas.* Bahamian Field Station, San Salvador, Bahamas, pp. 215-30.

O'Kelly, C. J., Wysor, B. & Bellows, W. K. 2004. Gene sequence diversity and the phylogenetic position of algae assigned to the genera *Phaeophila* and *Ochlochaete* (Ulvophyceae, Chlorophyta). *J. Phycol.* 40:789-99.

Posada, D. & Crandall, K. A. 1998. Modeltest: testing the model of DNA substitution. *Bioinformatics* 14:817–8.

Scholin, C.A., Hallegraeff, G. M. & Anderson, D.M. 1995. Molecular evolution of the *Alexandrium tamarense* 'species complex' (Dinophyceae): Dispersal in the North American and West Pacific regions. *Phycologia* 34:472-85.

Sloane, H. 1707. *A Voyage to the Islands Madera, Barbados, Nieves, S. Christophers and Jamaica, with the Natural History of the Herbs and Trees, Four-footed Beasts, Fishes, Birds, Insects, Reptiles, &c. of the last of those Islands*. Vol. 1. Printed by the British Museum for the author, London, U.K. 264 pp.

Swofford, D. L. 2002. PAUP* *Phylogenetic Analysis Using Parsimony (* and other methods) Version 4.0b10*, Sinauer Associates Inc., Sunderland, Massachusetts.

Taylor, W.R. 1950. Plants of Bikini and other northern Marshall Islands. Algae: Chlorophyceae. Univ. of Michigan Press, Ann Arbor, Michigan, 218 pp.

Taylor, W. R. 1960. *Marine algae of the Eastern tropical and sub-tropical coasts of the Americas.* Univ. of Michigan Press, Ann Arbor, Michigan, 870 pp.

Thalman, K. L. & Teeter, J. W. 1983. A Pleistocene estuary and its modern analogue, San Salvador, Bahamas. *In* Gerace, D. T. (Ed.) *Proc. of the 1st Symp. on the Geol. of the Bahamas.* Bahamian Field Station, San Salvador, Bahamas, pp. 18-21.

Van Oppen, M. J. H., McDonald, B. J., Willis, B. & Miller, D. J. 2001. The evolutionary history of the coral genus *Acropora* (Scleractinia, Cnidaria) based on a mitochondrial and a nuclear marker: reticulation, incomplete lineage sorting, or morphological convergence? *Mol. Biol. Evol.* 18:1315-29.

Verbruggen, H. & Kooistra, W.H.C.F. 2004. Morphological characterization of lineages within the calcified tropical seaweed genus *Halimeda* (Bryopsidales, Chlorophyta). *Eur. J. Phycol.* 39:213-28.

Verbruggen, H., De Clerck, O., Cocquyt, E., Kooistra, W.H.C.F. & Coppejans, E. (2005) Morphometric taxonomy of siphonous green algae: a methodological study within the genus *Halimeda* (Bryopsidales). *J. Phycol.*: 126–139.

Veron, J. E. N. 1995. *Corals in space and time: the biogeography and evolution of the Scleractinia*, Cornell University Press, Ithaca, 321 pp.

Walters, L. J., Smith, C. M., Coyer, J. A., Hunter, C. L., Beach, K. S. & Vroom, P. S. 2002. Asexual propagation in the coral reef macroalga *Halimeda* (Chlorophyta, Bryopsidales): production, dispersal and attachment of small fragments. *J. Exp. Mar. Biol. Ecol.* 278:47-65.

Wendel, J.F., Schnabel, A. & Seelanan, T. 1995. Bidirectional interlocus concerted evolution following allopolyploid speciation in cotton (*Gossypium*). *PNAS* 92: 280–284.

Yamada, Y. 1941. Species of *Halimeda* in the South Sea. *Kagaku Nanyo* 4:108-21.

Yamada, Y. 1944. New Caulerpas and Halimedas from Micronesica. *Scientific papers of the Institute of Algological Research of Hokkaido University.* 3:27-9.

Zechman, F. W., Kooistra, W. H. C. F., Olsen, J. L. & Stam, W. T. 1999. Current perspectives on the phylogeny of ulvophycean green algae. *In* Anonymous [Ed.] *Abstracts of the XVI International Botanical Congress*. St. Louis, Missouri. p. 144.

Evolution and phylogeography of the *Halimeda cuneata–discoidea–tuna* cryptic species complex

Heroen Verbruggen, Olivier De Clerck, Tom Schils, Wiebe H.C.F. Kooistra & Eric Coppejans

Manuscript submitted

Abstract

Nuclear ribosomal and plastid DNA sequences of specimens belonging to section *Halimeda* of the pantropical green seaweed genus *Halimeda* show that the group under scrutiny contains many more genetically delineable species than those recognized by classical taxonomy. Discordances between phylograms inferred from nuclear and plastid DNA sequences suggest that reticulate evolution has been involved in speciation within the clade. Nonetheless, our data do not allow ruling out certain alternative explanations for the discordances. Several pseudo-cryptic species are restricted to the margins of the generic distribution range, indicating that gene flow at distributional extremities is low enough to allow genetic differentiation and speciation. In a clade of *H. cuneata* sibling species from widely separated subtropical localities in the Indian Ocean, the South African sibling branches off first, leaving the Arabian and West Australian species as closest relatives. We hypothesize that geographic isolation of the siblings may have taken place following Pleistocene or Pliocene periods of climatic cooling during which subtropical species occupied larger distribution ranges. A more basal separation of Atlantic, Indo-Pacific, and Mediterranean species indicates vicariance. The alternative events that could have caused this vicariance are discussed.

Introduction

In the tropical marine realm, patterns and processes of speciation are seldom obvious. A striking contradiction in this context is that while marine populations are presumed to be more open than their terrestrial counterparts as a consequence of genetic remixing brought about by ocean currents, many species show large genetic differences between geographically separated populations (e.g. McMillan & Palumbi, 1995; Duke et al., 1998; Lessios et al., 2003), sometimes to such a degree that geographic entities deserve species status (e.g. Pakker et al., 1996; Muss et al., 2001; De Clerck et al., 2005). Additionally, several marine species have been shown to contain cryptic diversity unlinked with geography (Knowlton 1993).

Marine macroalgae abound in almost all coastal habitats. Despite their high diversity and abundance, the patterns of their evolution and processes involved in their speciation have not yet been intensively studied. The green algal genus *Halimeda*, the focus of this paper, is among the better studied (Kooistra et al., 2002; Verbruggen & Kooistra, 2004; Kooistra & Verbruggen, 2005; Verbruggen et al., 2005c).

Halimeda is a common inhabitant of tropical and warm-temperate marine environments and a prominent primary producer, source of food and habitat, and carbonate sand producer (Hillis-Colinvaux, 1980). The algal body of *Halimeda* is composed of flattened, green, calcified segments interconnected

by uncalcified nodes (Lamouroux, 1812; Hillis-Colinvaux, 1980). From the anatomical point of view, the entire algal body consists of a single, tubular cell that branches to form an organized network of siphons (Barton, 1901; Hillis-Colinvaux, 1980). Sexual reproduction occurs periodically (Drew & Abel, 1988) and gametes are released into the water column during mass spawning events (Clifton, 1997). Sympatric species have been shown to spawn in slightly different timeframes (Clifton, 1997; Clifton & Clifton, 1999). Reproduction is followed by death of the alga, after which the calcified segments disconnect from one another and contribute to the sediment (Meinesz, 1980; Freile et al., 1995). These segments endure in the fossil record and often make up the bulk of the carbonate structure of tropical reefs (Bassoullet et al., 1983; Hillis-Colinvaux, 1986).

Kooistra et al. (2002) examined the phylogeny, biogeography and historical ecology of the genus on the basis of partial nuclear ribosomal cistron sequences of 28 out of the 33 species recognized at that time. Sequences grouped in five clear-cut clades, which subsequently formed the foundation of a new sectional subdivision (Verbruggen & Kooistra, 2004). Kooistra et al. (2002) also showed that the generic subdivision was correlated with ecological properties such as growth on unconsolidated substrates and in sheltered localities. Finally, it was shown that each of the five lineages featured distinct Atlantic and Indo-Pacific subgroups, indicating that vicariance has been at play.

The focus of this study is on section *Halimeda* of the genus, and more particularly on the species *H. cuneata*, *H. discoidea*, and *H. tuna* (species authorities in Appendix 1). Within this section, eleven species are currently recognized, the majority of which are epilithic and occur in wave-affected habitats (Verbruggen & Kooistra, 2004). *Halimeda cuneata*, *H. discoidea* and *H. tuna* are morphologically plastic species and the boundaries between these species are not always clear. Several species of *Halimeda* section *Halimeda* range throughout either the tropical Indo-Pacific or the Caribbean. *Halimeda discoidea* and *H. tuna* are pantropical and the latter species also occurs in the Mediterranean Sea (Hillis-Colinvaux, 1980). *Halimeda cuneata* has a disjunct distribution in the subtropical parts of the Indian Ocean, with populations in Australia, SE Africa, SW Madagascar and the Arabian Sea (Hillis-Colinvaux, 1980) and has recently been reported from Brazil (Bandeira-Pedrosa et al., 2004). In former studies, the molecular phylograms of section *Halimeda* were ill-resolved (Kooistra et al., 2002; Verbruggen & Kooistra, 2004). Cryptic diversity was revealed within *H. discoidea* and *H. tuna*: the former consisted of separate Atlantic and Indo-Pacific units and the latter showed strong divergence between specimens from the Caribbean and Mediterranean Seas (Kooistra et al., 2002; Verbruggen & Kooistra, 2004).

The goals of this study are (1) to evaluate monophyly of species within *Halimeda* section *Halimeda* using molecular tools, (2) to elucidate the phylogenetic history of the section using plastid DNA markers (*tuf*A, *rps*19–*rps*3 and *rpl*5–*rps*8–*inf*A) and nuclear ribosomal sequences (18S–ITS1–5.8S–ITS2), and (3) to examine biogeographic patterns within the section as a whole and phylogeographic patterns within *H. discoidea* and *H. cuneata*.

Materials and methods

Taxa of *Halimeda* section *Halimeda* were collected throughout most of their distribution ranges. Vouchers were deposited in the Ghent University Herbarium (GENT). Identifications followed Hillis-Colinvaux (1980), Ballantine (1982) and Noble (1986) and, for *H. cuneata* forms, Barton (1901) and Littler & Littler (2003). We were unable to obtain specimens suitable for DNA analysis of three species of section *Halimeda* (*H. gigas*, *H. scabra*, and *H. xishaensis*). *Halimeda gigas* was represented in the studies of Kooistra et al. (2002) and Verbruggen & Kooistra (2004), but these specimens belong to *H. cuneata* f. *undulata*, an entity not recognized in the monographic work these authors used for their identifications (Hillis-Colinvaux 1980). Extraction of DNA followed Kooistra et al. (2002). The nuclear ITS1–5.8S–ITS2 region was amplified according to Kooistra et al. (2002) and plastid partial *rps*19–*rps*3 (UCP7) according to Provan et al. (2004). Amplified products were sequenced with an

ABI Prism 3100 automated sequencer (Applied Biosystems, Foster City, CA) and submitted to Genbank (accession numbers in Appendix 1). For a subset of specimens, additional sequences were obtained (plastid partial *tuf*A: Famà et al. [2002]; plastid *rpl*5–*rps*8–*inf*A [UCP3]: Provan et al. [2004]; nuclear 18S rDNA: Kooistra et al. [2002]).

Partial *rps*19–*rps*3 and *tuf*A DNA sequences were aligned on the basis of a blueprint created by alignment of these regions' amino acid sequences using ClustalW 1.82 at the EBI (European Bioinformatics Institute) server, with default settings. Alignment of the *rpl*5–*rps*8–*inf*A plastid region was more complex. Open reading frames were assessed using ORF Finder at the NCBI (National Center for Biotechnology Information) server. The initiation codon of *rps*8 was situated within the *rpl*5 gene in all ingroup sequences, so that a few (4–17) base pairs were used for both genes. The region of overlap was duplicated for alignment. Between *rps*8 and *inf*A, a small (5–32 base pairs) spacer was present. Amino acid sequences corresponding to the different genes were aligned using ClustalW 1.82 at the EBI server, with default settings. The obtained amino acid alignment was used as a blueprint for DNA sequence alignment. The *rps*8–*inf*A spacer was excluded from the alignment. After alignment, sequence blocks of all plastid regions (*tuf*A, *rps*19–*rps*3 and *rpl*5–*rps*8–*inf*A) were concatenated. Nuclear ribosomal DNA sequences were aligned by eye. Alignments are available from the first author upon request (will be submitted to Treebase after acceptance).

Neighbor joining analysis was applied to the *rps*19–*rps*3 and ITS1–5.8S–ITS2 alignments to aid identification of groups of specimens at the species level. The NJ analyses were carried out in PAUP* 4.0b10 (Swofford, 2003), using the ML distance measure. Likelihood parameter settings were determined using Modeltest 3.5 (Posada & Crandall, 1998). Other search options were: starting trees obtained by stepwise random sequence addition, TBR branch swapping, maximum 10^3 rearrangements per addition-sequence replicate, and 250 addition-sequence replicates. NJ bootstrapping analysis (500 replicates) was carried out with five addition-sequence replicates per bootstrap replicate. Maximum parsimony (MP) and maximum likelihood (ML) analyses were carried out using the same software and settings except (1) maximum 10^6 rearrangements per addition-sequence replicate for MP analysis, (2) a NJ starting tree for ML analysis, and (3) 25 addition-sequence replicates for MP and ML analysis. Bootstrapping was not carried out under the MP and ML criteria. The combined plastid and 18S–ITS1–5.8S–ITS2 sequence alignments were subjected to heuristic ML analysis in PAUP* 4.0b10, with base-substitution models determined by Modeltest 3.5. Settings were as mentioned above for NJ analysis. Heuristic ML bootstrapping (100 replicates) was carried out with five addition-sequence replicates per bootstrap replicate. Bayesian posterior probabilities to indicate statistical support for interior branches were calculated using MrBayes v3.0B4 (Ronquist & Huelsenbeck, 2003). The different genes and regions (plastid *tuf*A, *rps*19, *rps*3, *rpl*5, *rps*8 and *inf*A; and nuclear 18S, ITS1, 5.8S and ITS2) were subjected to MrModeltest 2.0 (Nylander, 2004) independently and optimal substitution models were specified to MrBayes for each gene separately (Ronquist & Huelsenbeck, 2003). Analyses were run with four Markov chains for 10^6 generations, with a tree saved every 100th generation. The first 1000 trees were discarded as burn-in. Identical ML and BI analyses were carried out on an alignment of combined plastid sequences after exclusion of all positions showing gaps in the ingroup. A single *H. gracilis* sequence was used as outgroup in all above analyses (Appendix 1). Sequences of Indo-Pacific *H. discoidea* were subjected to heuristic ML analysis in PAUP* 4.0b10 and Bayesian analysis in MrBayes v3.0B4, with base-substitution models determined by MrModeltest 2.0. All settings for ML and BI were as mentioned above, but no outgroup was specified.

Significance of length differences between trees obtained by the analyses described above and user-defined trees was assessed using the Shimodaira-Hasegawa (SH) test (Shimodaira & Hasegawa, 1999; Goldman et al., 2000) implemented in PAUP* 4.0b10, with resampling-estimated log-likelihood (RELL) optimization and 1000 bootstrap replicates.

Table 1. Length, variability, base composition, and selected substitution models of the molecular markers[a].

	*rps*19–*rps*3[c]	ITS1–5.8S–ITS2[c]	18S– ITS1–5.8S–ITS2[d]	*tuf*A	*rpl*5-*rps*8-*inf*A
sequence length[b]	549–603	443–476	1671–1700	858	623–677
alignment length	660	528	1756	858	735
constant positions	385	350	1515	589	425
variable positions	275	178	241	249	310
parsimony informative positions	210	145	119	153	153
A	40.37%	22.83%	20.85%	36.89%	31.24%
C	14.89%	31.05%	27.38%	11.39%	17.21%
G	14.62%	28.95%	31.44%	20.55%	17.65%
T	30.12%	17.17%	20.33%	31.17%	33.90%
selected substitution model	TVM+G	GTR+I+G	18S: GTR+I+G ITS1: K80+G 5.8S: K80+I+G ITS2: HKY+G	GTR+I+G	*rpl*5: GTR+G *rps*8: GTR+G *inf*A: JC+G

[a] the selected model for the concatenated plastid dataset as a whole was GTR+I+G
[b] ingroup sequences only
[c] statistics of the dataset with all specimens; Modeltest ran without distinction between regions
[d] the selected model for the 18S–ITS1–5.8S–ITS2 dataset as a whole was GTR+I+G

Results

Identifications and DNA sequences

Specimen identifications are presented in Appendix 1. Information on length, variability, and base composition of the molecular markers can be found in Table 1. Different species exhibited markedly divergent ITS1–5.8S–ITS2 and partial *rps*19–*rps*3 sequences. Within each of the species *H. cuneata*, *H. discoidea* and *H. tuna*, two or more genotypic groups were present. Sequences within such genotypic groups differed in only one or a few positions (or not at all) while sequences among genotypic groups differed more substantially (Figure 1). Modeltest revealed differences in optimal base substitution models among regions (Table 1).

Cryptic species diversity

The phylograms resulting from NJ analysis of partial *rps*19–*rps*3 and ITS1–5.8S–ITS2 sequences are presented in Figures 2 and 3, respectively. The specimens clustered in a number of dense clades

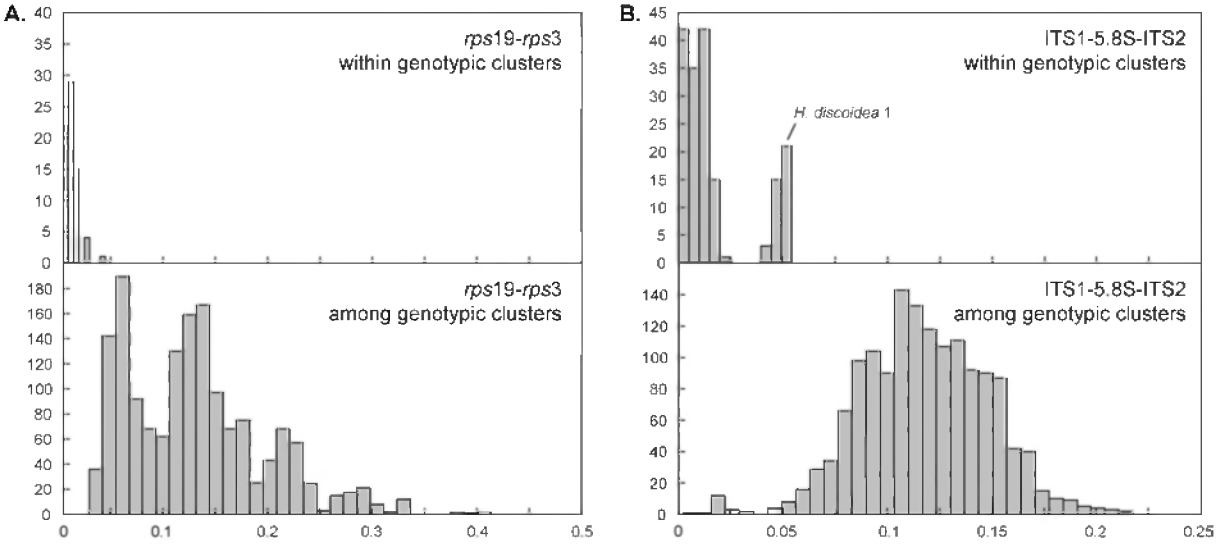

Figure 1. Pairwise corrected distances of *rps*19–*rps*3 (A) and ITS1–5.8S–ITS2 (B) sequence data. Top panels show the distribution of p-distances between specimens belonging to the same genotypic cluster; lower panels represent the distribution of distances between specimens belonging to different genotypic clusters. The secondary peak marked "*H. discoidea* 1" in the top panel of B consists of divergences between Omanese and Indo-Pacific specimens of genotypic cluster *H. discoidea* 1.

(boxed in figures) with little or no internal structure. These clades corresponded to genotypic groups recognized in the sequence alignments. Branches leading to different genotypic clusters were of variable length and obtained high support (bootstrap proportion generally > 90 and often 100). The ML and MP topologies were highly similar to the NJ trees, showing dense clusters of specimens identical to those recognized in the NJ trees and branch lengths highly comparable to those of the NJ trees. All clades receiving bootstrap support in the NJ tree were present in the obtained ML tree and the majority rule consensus tree of all obtained equally MP trees. These patterns of similarity were observed for the plastid and nuclear datasets.

Several species turned out to comprise two or more genotypic clusters. *Halimeda tuna* sequences separated in two distinct clades and *H. discoidea* consisted of three divergent genotypic clusters. Within the genetic diversity of *H. cuneata*, seven distinct clusters were disclosed. Sequences of *H. cuneata* f. *digitata* were recovered within the *H. discoidea* 1 clade.

Genotypic clusters within morphologically perceived species generally accorded with geographic origin of the samples. Of the two *H. tuna* clades, one contained specimens collected in the Caribbean Sea (*H. tuna* 1) and the second contained specimens collected in the Mediterranean Sea (*H. tuna* 2). Specimens belonging to *H. cuneata* 1 and 2 were all collected in SE Africa; those of *H. cuneata* 3

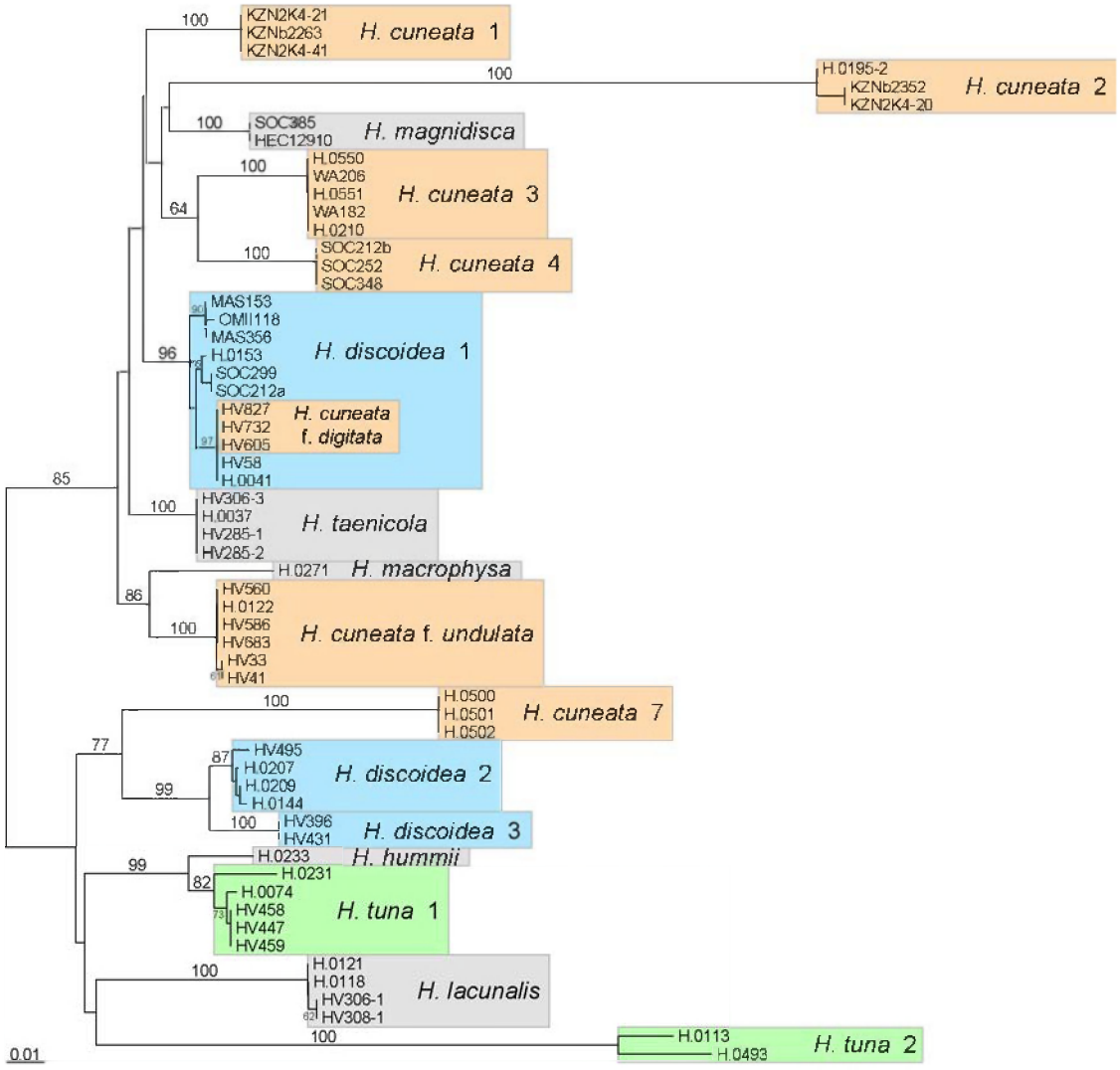

Figure 2. Neighbor joining phylogram inferred from *rps*19–*rps*3 sequences of 60 *Halimeda* specimens (score = 1.13797). The outgroup was removed from the tree. Bootstrap proportions exceeding 50% are indicated at branches.

came from SW Australia, and specimens of *H. cuneata* 4 originated from the Arabian Sea (Socotra). Specimens of *H. cuneata* f. *undulata* were collected from several places in the Indo-Pacific, and specimens belonging to *H. cuneata* 7 came from Brazilian populations. Within *H. discoidea*, genotypic cluster 1 contained specimens from throughout the Indo-Pacific. Specimens of the second genotypic cluster were collected throughout the Atlantic, and specimens of genotypic cluster 3 originated from the Caribbean Sea. *Halimeda discoidea* 1 split up into two widely divergent clades in the ITS1–5.8S–ITS2 phylogram. These clades were not regarded separate genotypic clusters because they did not show strong divergence in the *rps*19–*rps*3 data.

The phylogeographic structure of *H. discoidea* 1 (including *H. cuneata* f. *digitata*) is presented in Figure 4. Sequences of the ITS1–5.8S–ITS2 region formed three main groups (Figure 4A). The first, most widely ranging group contained specimens from the tropical parts of the Indian and Pacific Oceans. The second and third group contained two specimens from Socotra and three specimens from Oman, respectively. The *rps*19–*rps*3 tree (Figure 4B) contained less sequences but also showed distinctness of Omanese and Socotran sequences. Philippine and French Polynesian sequences formed a clade widely divergent from the other sequences. The Hawaiian specimen, which was contained in the

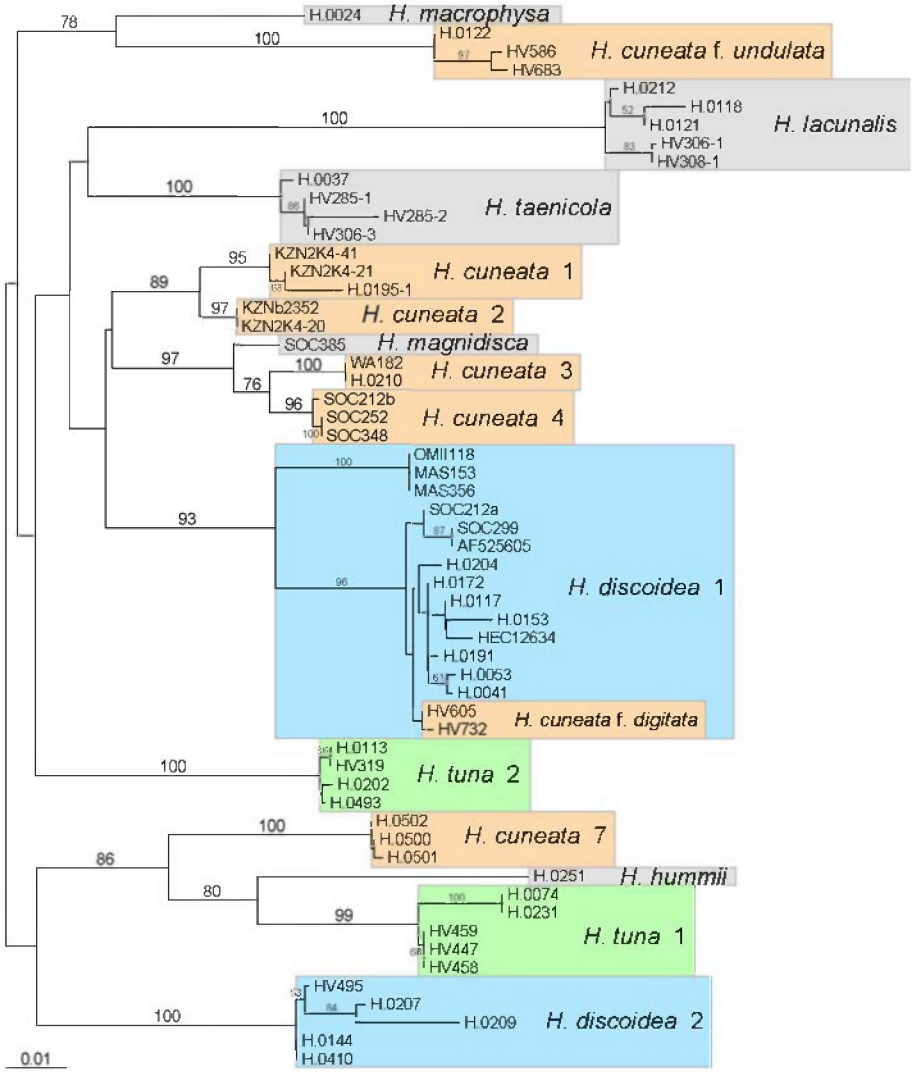

Figure 3. Neighbor joining phylogram inferred from ITS1–5.8S–ITS2 sequences of 59 *Halimeda* specimens (score = 0.90205). The outgroup was removed from the tree. Bootstrap proportions exceeding 50% are indicated at branches.

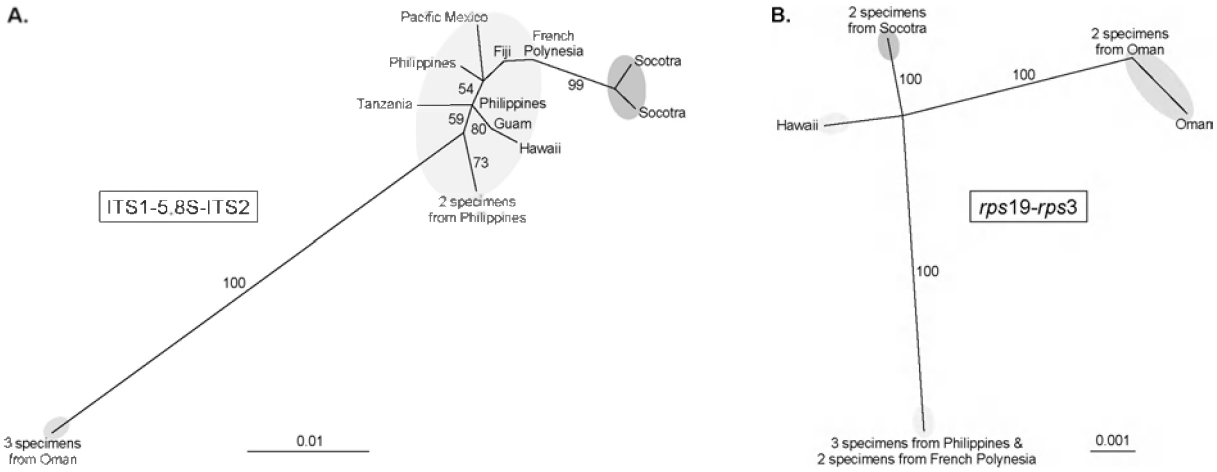

Figure 4. Internal phylogeny of *H. discoidea*. (A) Single ML tree inferred from ITS1–5.8S–ITS2 sequences (–ln L = 817.15664). (B) Single ML tree inferred from *rps*19–*rps*3 sequences (–ln L = 795.24718). Bayesian posterior probabilities exceeding 50% are indicated at branches.

tropical group of the ITS1–5.8S–ITS2 tree, was not contained in the clade with the Philippine and French Polynesian specimens in the *rps*19–*rps*3 phylogram.

Phylogenies, topological discordances and historical biogeography

Figure 5 shows the phylograms inferred from concatenated plastid and 18S–ITS1–5.8S–ITS2 sequences. Exclusion of gap sites from the concatenated plastid data did not influence topology and had little impact on support, short branches generally obtaining slightly less support. Sequences grouped in two major clades in both phylograms. Whereas the upper clade was strictly Indo-Pacific, the lower clade contained a Mediterranean species, an Indo-Pacific species, and all Atlantic–Caribbean species. The lower clade consisted of 4 lineages among which relationships remained unresolved. *Halimeda hummii* and *H. tuna* formed a well-supported group in both phylograms, as did *H. discoidea* 2 and 3. *Halimeda cuneata* 7 was recovered as closest sister to the *H. discoidea* 2–3 group in the plastid tree but as closest sister of the *H. hummii–tuna* clade in the nuclear phylogram.

Within the upper, Indo-Pacific lineage, phylogenetic structure was well-resolved in the plastid phylogram. There were three main species clusters. The first comprised *H cuneata* 1, *H. magnidisca*, and *H. discoidea* 1; the second comprised three subtropical *H. cuneata* haplotypes (2, 3 and 4 – in gray box); and the third comprised *H. taenicola*, *H. cuneata* f. *undulata* and *H. macrophysa*. In the clade comprising the three subtropical *H. cuneata* entities (gray box), the SE African entity (2) branched off first, leaving the SW Australian (3) and Arabian (4) entities as closest sisters. In the nuclear tree, the Indo-Pacific lineage was relatively poorly resolved, and structured differently than in the plastid phylogram. *Halimeda cuneata* 1 and 2 clustered, and so did *H. cuneata* 3 and 4 together with *H. magnidisca*. As was the case in the plastid tree, *H. cuneata* f. *undulata* and *H. macrophysa* were sisters.

Topological discordances among trees were tested for significance using the Shimodaira-Hasegawa test. In two of six cases, clades obtained by ML analysis of one dataset were rejected by the other dataset (Figure 6). Additionally, for the strictly subtropical *H. cuneata* clade in the plastid tree, the alternative topology with the Australian entity taking a basal position and the SE African and Arabian entities as closest sisters was tested against the original topology. This alternative was significantly worse than the original tree (length difference = 14.14948; p = 0.017).

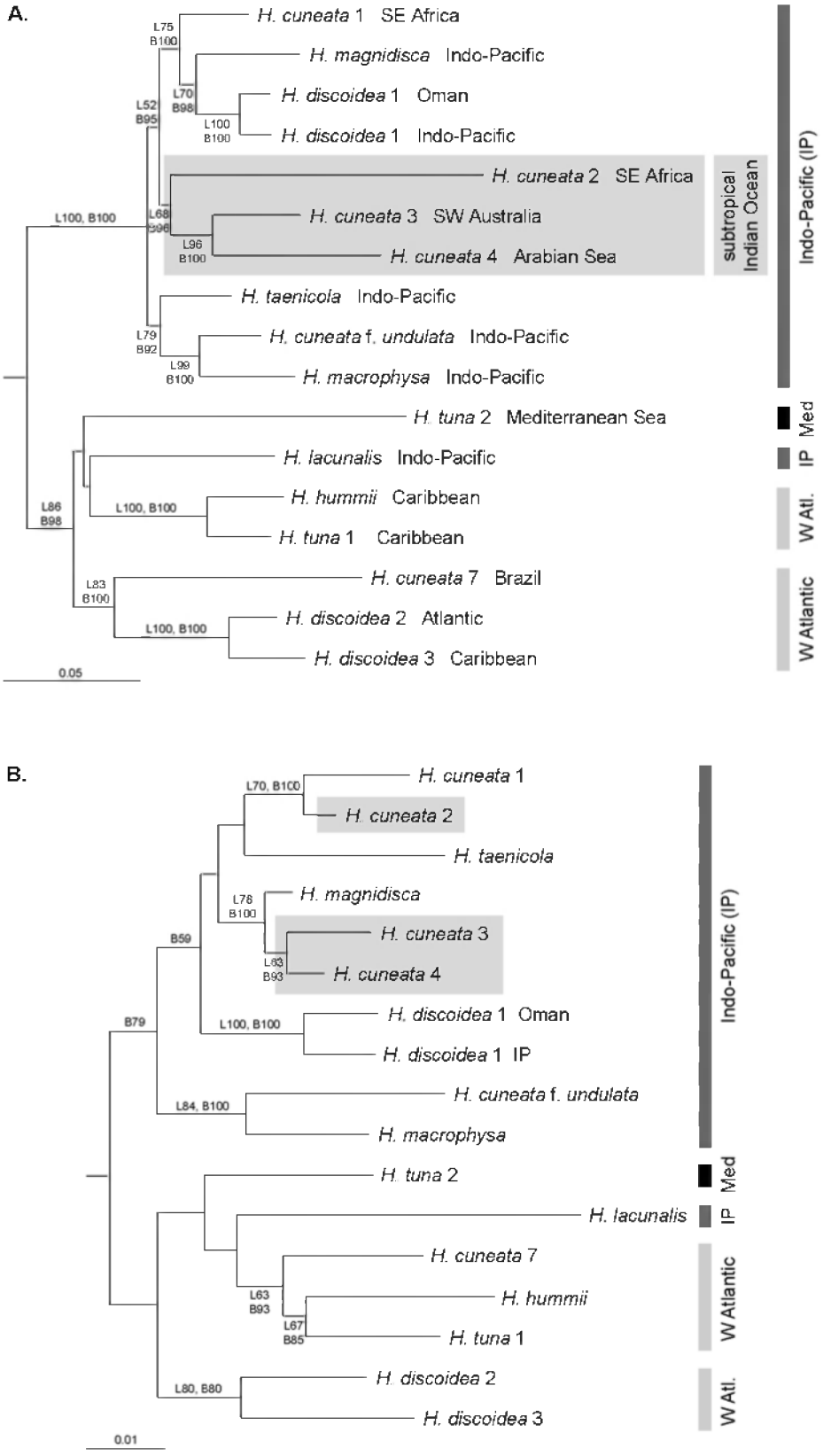

Figure 5. ML phylograms inferred from chloroplast and nuclear ribosomal DNA sequences. (A) ML tree of combined chloroplast data of 17 *Halimeda* taxa. –ln L = 11579.11. (B) ML tree inferred from nuclear ribosomal DNA data of 17 *Halimeda* taxa. –ln L = 5113.61. Outgroup was pruned from the trees. ML bootstrap proportions (L...) and Bayesian posterior probabilities (B...) for clades (expressed in %) that exceeded 50 are indicated at the appropriate branches. Scalebars are in substitutions per site.

Discussion

The obtained molecular phylogenetic data broach several issues about the evolutionary history of *Halimeda* section *Halimeda*. First, the *rps*19–*rps*3 and ITS1–5.8S–ITS2 phylograms show that the group under scrutiny contains many more genetically delineable species than those recognized by classical taxonomy. Second, the topological discordances between nuclear and plastid phylograms are suggestive of reticulate speciation. Third, the fact that some cryptic species are restricted to the margins of the generic distribution range alludes to the importance of peripatric isolation. Fourth, the separation of Indo-Pacific from Atlantic species in the phylograms confirms the idea of vicariance. Finally, the topology of *H. cuneata* reveals information about the historical biogeography of subtropical locations in the Indian Ocean. In what follows, these five topics will be addressed in more detail.

Cryptic species

Our data leave no doubt about the inadequacy of current species delineations in *Halimeda* section *Halimeda*. Assuming that each densely packed genotypic cluster in Figures 2 and 3 constitutes a species implies the existence of sixteen rather than eight species in the examined group. Kooistra et al. (2002) and Verbruggen & Kooistra (2004) first revealed the existence of widely divergent genealogical species within morphological *Halimeda* species. In their analyses, Atlantic and Indo-Pacific specimens of certain species were recovered in different clades. This inter-oceanic cryptic diversity is corroborated by our data. Additionally, we reveal the existence of a second level of formerly unrecognized species diversity in the species *H. discoidea* and *H. cuneata*, situated within ocean basins. A similar pattern was found previously for *H. minima* (Kooistra et al., 2002; Kooistra & Verbruggen, 2005) and Indo-Pacific *H. incrassata* (Verbruggen et al. 2005c).

Our findings suggest that morphology-based taxonomical practices have not provided the resolution to detect differences between certain genealogical species. Yet morphological differences between populations which now turn out to be distinct genealogical species were noted before but considered insufficient for recognition as separate species. For example, small morphological differences between Mediterranean and Caribbean populations of *H. tuna* have been reported but the species was not split because of high levels of intra-regional morphological plasticity (Hillis, 1959; Hillis-Colinvaux, 1980). Molecular analyses reveal that Mediterranean and Atlantic populations are distinct and justify recognition of both entities at the specific rank (Kooistra et al., 2002; this study). Similarly, Bandeira-Pedrosa et al. (2004) considered the option that Brazilian *H. cuneata* (clade 7 of the present study)

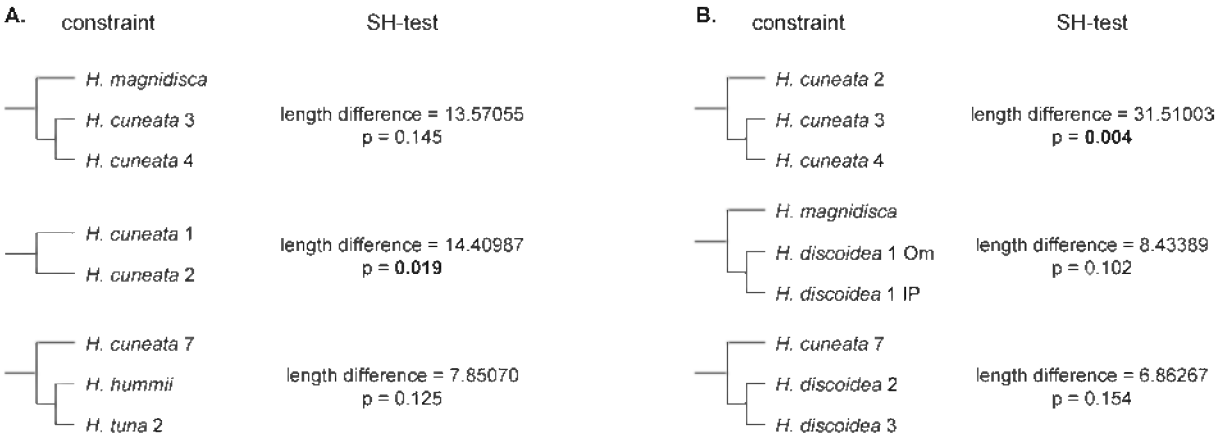

Figure 6. Discordances between chloroplast and nuclear markers: Shimodaira-Hasegawa test results. Panel A shows species relationships suggested by the 18S–ITS1–5.8S–ITS2 data that did not conform to the plastid topology. These relationships were used as constraints for ML analysis of the concatenated plastid data. The significance of length difference between such constrained trees and the original plastid topology of Fig. 5A were tested using the SH-test. Length differences and levels of significance are listed. Similarly, clades species relationships suggested by the plastid dataset were tested against nuclear data (panel B).

evolved independently from the Indo-Pacific diversity of this species but nevertheless refrained from describing it as a new species. Our sequence data show that the Brazilian population has Atlantic roots demonstrating yet another case of parallel evolution in the Atlantic and Indo-Pacific ocean basins.

Taxonomists are now facing the challenge of elucidating whether and how morphology and molecular phylogenetics can be reconciled. Within *Halimeda* and its relative *Caulerpa*, the combined action of molecular and morphometric tools has been successful at defining morphological boundaries between pseudo-cryptic species (de Senerpont-Domis et al., 2003; Verbruggen et al., 2005a, b, c).

Topological discordances: possible reticulate speciation

Reticulate speciation causes the genome of the daughter species to contain traces from both parental species. The nuclear DNA of the daughter species will be a mixture of the genomes of both parent taxa. Nuclear ribosomal DNA, however, will in many cases be homogenized by interlocus concerted evolution during the next couple of generations (Liao, 1999; Small et al., 2004). Plastid inheritance is clonal, and in normal circumstances only one parent contributes the entire plastid genome. As a consequence of these different modes of nrDNA and plastid DNA inheritance, reticulate evolutionary events can cause topological differences among trees inferred from nrDNA and plastid DNA sequences. In contrast to higher plants, where reticulate evolution is well-studied (Linder & Rieseberg, 2004), the roles of hybrid speciation and introgression in green algal diversification have not been thoroughly assessed. However, karyological (Kapraun, 1993, 1994; Kapraun & Buratti, 1998), and molecular (Durand et al., 2002) studies suggest that they may be at play. Artificial hybrids between the green microalgae *Eudorina* and *Pleodorina*, which have been kept in culture for decades and are capable of reproduction, have been studied (Coleman, 2002, and references therein). However, such hybrids are not known to occur in the wild.

Of the topological discordances between nuclear and plastid phylograms in the present study, only the position of *H. cuneata* 2 was truly conflicting according to Shimodaira-Hasegawa tests. The fact that *Halimeda* is a broadcast spawner (Clifton, 1997) could promote hybridization between sympatric species in the absence of intrinsic reproductive barriers. In the *H. incrassata–monile–simulans* species group, gametes are released in species-specific time intervals, which is suggestive of hybridization avoidance (Clifton, 1997; Clifton & Clifton, 1999; Kooistra et al., 2002). Despite these arguments in favor of reticulate evolution, several other possibilities cannot be excluded. Incomplete lineage sorting, the complexity of ITS sequence alignment, and amplification and sequencing of paralogous sequences or pseudogenes are all known to limit the phylogenetic utility of rDNA–ITS sequence data (Alvarez & Wendel, 2003), and are valid and non-refutable alternative explanations for the observed pattern. The limited data at hand do not allow us to unequivocally single out the causes of topological discordances (Holder et al., 2001). In order to discern between the possibilities, karyological, genomic, and single-copy nuclear sequence data could be utilized (Hegarty & Hiscock, 2005).

Geographic speciation modes

Several geographic modes of speciation have been put forward (reviewed in e.g. Coyne & Orr, 2004). Allopatric or vicariant speciation is caused by divergent evolution of geographically isolated populations. Parapatric speciation is a variant hereof, in which speciation of adjacent populations takes place in the presence of (a limited amount of) gene flow. In peripatric speciation a small, peripheral population diverges from the main population. In sympatric speciation, species formation occurs within the range of the parental species.

The *Halimeda* section under study may represent examples of several of these geographic modes of speciation. The cryptic species contained within *H. cuneata*, *H. discoidea* and *H. tuna* often appear to occupy non-overlapping distribution ranges. The most marked examples are *H. tuna*, of which the pseudo-cryptic species in the Mediterranean Sea and Atlantic Ocean are distinct, and *H. cuneata*,

which has isolated cryptic species in Brazil, SE Africa, the Arabian Sea, and Western Australia. Even though our sampling sizes and density may be on the low side to be entirely convincing of non-overlapping ranges, our current data strongly suggest this. For what follows, we will assume that the different cryptic species are limited to the distribution ranges outlined above. Under this assumption, it can be concluded that allopatric speciation is be the most common mechanism of cryptic species formation within the section under study. Cryptic endemicity, the partitioning of cryptic species among geographical locations, is fairly common in marine algae (e.g. Pakker et al., 1996; Gurgel et al., 2003; De Clerck et al., 2005) and sedentary marine animals (e.g. Muss et al., 2001; Carlin et al., 2003).

The phylogeographic structure of *H. discoidea* 1 is suggestive of incipient peripatric speciation of an Omanese population. Seasonal coastal upwelling of cold water along the southern coast of the Arabian peninsula, from which *H. discoidea* is absent except at the mouth of the Gulf of Oman, may contribute to genetic isolation of warm water populations from the tropical Indian Ocean and the Gulf of Oman. *H. discoidea* 2 and 3 are sympatric in much of the Caribbean basin (HV, unpublished results). Whereas specimens from genotypic cluster 2 are most commonly found in shallow bays and lagoons, our specimens from genotypic cluster 3 all originated from deeper waters (15–50 m) along outer reef slopes, suggesting that these species originated sympatrically by habitat shift. *Halimeda cuneata* 1 and 2 are also sympatric but do not show obvious ecological differences.

Interestingly, in cases of cryptic species diversity within the Indo-Pacific and within the Atlantic Ocean, cryptic species with restricted distribution ranges are confined to the edges of the generic distribution range, often in regions characterized by colder temperatures (Arabian Sea, SE Africa, SW Australia). The distribution range of marine green algae is known to be strongly governed by temperature (van den Hoek, 1982). Species intolerant of tropical temperatures may thus show antitropical populations, and genetic isolation of such populations may be promoted through the absence of suitable stepping stones in the tropics and the small average dispersal distances of most marine algae (cf. Kinlan & Gaines, 2003).

Global biogeography

The basal division of sequences in an Indo-Pacific and a (mainly) Atlantic clade conforms to the results of previous studies (Kooistra et al., 1999; Kooistra et al., 2002; Verbruggen & Kooistra, 2004; Verbruggen et al. submitted). A number of vicariance events are commonly invoked to explain Atlantic–Indo-Pacific sister relationships. The earliest event is the widening of the central Atlantic Ocean (Jurassic – Smith et al., 1994). The second is the closure of the Tethys Sea in the Middle East (Miocene – Rögl & Steininger, 1984). The third event, situated in the Pliocene, is the rise of the Central American Isthmus (Coates & Obando, 1996). The fourth and most recent barrier between the Atlantic and Indo-Pacific oceans for tropical organisms was the intensification of the Benguela upwelling in South Africa (late Pliocene – Marlow et al., 2000).

The first scenario can be falsified with the fossil record: there have been no reports of the genus in the Caribbean before the Miocene except for one (Beckmann & Beckmann, 1966; cited after Bassoullet et al., 1983), the age of which was questioned by Bassoullet et al. (1983). Similarly, the third and fourth scenarios can be considered unlikely because the occurrence of such recent events relatively deep in the phylogeny disaccord with the presence of extant species in Plio- and Miocene deposits (Bassoullet et al., 1983; Dragastan et al., 2002). However, given the potential of *Halimeda* species to converge onto the same morphology (Kooistra et al., 2002; Verbruggen et al., 2005c), reports of extant species from the fossil record should be treated with extreme caution (Kooistra et al., 2002).

Besides the fossil record, the evolutionary position of Mediterranean *H. tuna* 2 can contribute to the discussion. The relatively basal position of this species in the lower clade suggests that this species is a paleo-endemic from the time that the Mediterranean Sea was formed rather than a recent invader from the Atlantic. This would imply that the vicariance event that caused the split in our trees was asso-

ciated with the closure of the Tethys Sea in the Middle East. This scenario has two flaws. First, it requires assuming that *Halimeda* persisted in the Mediterranean Sea during the Messinian crisis (Duggen et al., 2003), during which the Mediterranean Sea almost completely dried up. Second, a more derived position of Mediterranean *H. tuna* may be concealed by extinction. In the latter case, it is not unthinkable that the vicariance at the base of the observed pattern was the rise of the Central American Isthmus as suggested by Kooistra et al. (2002), and that the Mediterranean Sea was recolonized from the Atlantic Ocean after the Messinian crisis.

In conclusion, each scenario has its pros and cons, and only more accurate information from the fossil record can discriminate between the events that could be at the base of the observed vicariance.

Biogeography of the subtropical Indian Ocean

The subtropical regions of the Indian Ocean (Arabian Sea, SE Africa, SW Australia) foster rich seaweed floras and high endemism (Phillips, 2001; Schils, 2002; Bolton et al., 2004). Moreover, biogeographic links between these regions have been described on the basis of shared taxa (Norris & Aken, 1984; Joosten & van den Hoek, 1986; Schils & Coppejans, 2003). Hommersand (1986) put forward three evolutionary-biogeographic scenarios that could explain the affinities between these distant floras. First, convergent evolution as a response to similar environments could cause the pattern. Second, common taxa could represent relics of a continuous distribution along the Cretaceous coast of Gondwanaland that was fragmented by the northward migration of Africa, Australia, and the Indian subcontinent. Third, the links could have come about through dispersal of species from their origin in SW Australia to SE Africa and the Arabian Sea through the Indian Ocean during Plio- or Pleistocene periods of global cooling (Figure 7).

Interpretation of the origin and topology of the subtropical *H. cuneata* 2–4 clade of Figure 5A may provide additional information on the subtropical floristic similarities. That this clade is scattered in the nuclear tree (Figure 5B) should not hinder biogeographic interpretation. If the discordances were caused by reticulate speciation, biogeographic inference is a matter of reconciling information from both trees, taking into account that both parental species of species with discordant positions must have been sympatric. Alternatively, if the discordances between our trees were caused by incomplete lineage sorting, rDNA paralogues–pseudogenes or ITS alignment errors, one would expect the plastid tree to provide the more accurate representation of evolutionary history because (1) the clonal inheritance of plastid DNA shows faster coalescence through a smaller effective population size (Small et al., 2004), (2) no paralogues or pseudogenes are known for plastid genes in the ulvophycean algae, and (3) alignment of plastid genes is trouble-free and leaving out gaps did not influence the obtained topology.

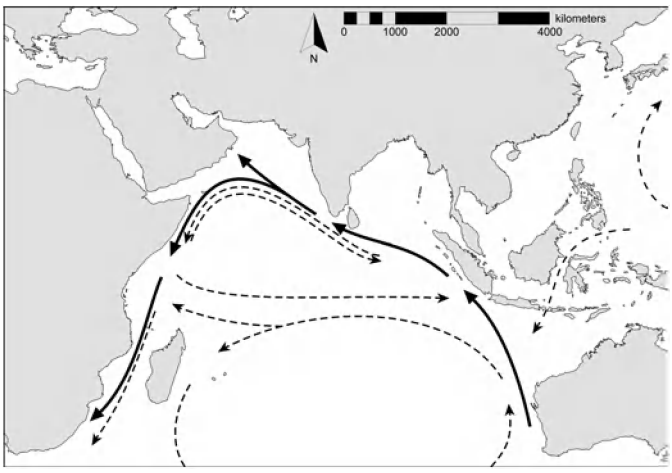

Figure 7. Map of the Indian Ocean showing present-day surface currents (dashed lines) and the migration path from SW Australia to SE Africa (bold solid lines) proposed by Hommersand (1986). The opposing surface currents in the Arabian Sea represent the SW monsoon current (Somali current – W to E) and the NE monsoon current (E to W). Map outline from ReefBase (www.reefbase.org); current patterns after Gordon & Fine (1996), Kemp (1998) and Pidwirny (2004); migration path after Hommersand (1986).

Morphological convergence, the first possible cause put forward by Hommersand (1986), is not an issue for biogeographic interpretation within the *H. cuneata* 2–4 species group because this group is monophyletic (with relatively high support) in the plastid phylogram. Neither does *H. cuneata* 2–4 fit the second scenario

because it would imply that the 18S region of *Halimeda* evolves much slower than that of other green algal lineages (e.g. Olsen et al., 1994) while in reality *Halimeda* and its allies show higher mutation rates (Zechman et al., 1999; Kooistra et al., 2002). Furthermore, because the fossil record shows very little species diversification until the Late Cretaceous – Paleocene (Hillis, 2001), it is against all probability that a derived clade such as *H. cuneata* 2–4 would date back to the Early Cretaceous coasts of Gondwanaland.

Hommersand's third hypothesis, migration of species across low latitudes during periods of global cooling in the Plio- or Pleistocene thus seems the most probable and has been corroborated by molecular clock analyses of antitropical fish, echinoderm and mollusk species (Hilbish et al., 2000; Burridge, 2002; Waters & Roy, 2003). However, the basal position of the SE African sequence counters Hommersand's proposed migration path from SW Australia to the Arabian Sea and SE Africa. An alternative interpretation could be that migration acted the other way around or that the populations we see now are relics of a population with a much wider distribution at times that the sea surface at low latitudes was colder.

Acknowledgements

We are grateful to E. Cocquyt, C. De maire, C. VanKerckhove and A. Vierstraete for laboratory and administrative assistance. We thank K. Arano, C. Battelli, P. Colinvaux, Y. De Jong, R. Diaz, C. Galanza, S. Guimaraes, O. Gussmann, R. Haroun, I. Hendriks, L. Hillis, L. Kirkendale, T. & C. Leigh, F. Leliaert, J. Maté, A. Maypo, A. N'Yeurt, D. Olandesca, F. Parrish, K. Pauly, C. Payri, G. Procaccini, W. Prud'homme van Reine, E. Tronchin, S. Wilson and B. Wysor for providing specimens and/or assistance during field work. We thank Jenny Bryant (British Museum – Natural History) for providing pictures of the type material of *H. cuneata*. Funding was provided by BOF (Ghent University, grant 011D9101), FWO-Flanders (grants G.0136.01 and G.0142.05; postdoctoral fellowship grants to ODC and TS), the Flemish Government (BIL 01/46) and the King Leopold III Fund for Nature Exploration and Conservation.

References

Alvarez, I., Wendel, J.F., 2003. Ribosomal ITS sequences and plant phylogenetic inference. Mol. Phylogen. Evol. 29, 417–434.

Ballantine, D.L., 1982. *Halimeda hummii* sp.nov., *Halimeda cryptica* v. *acerifolia* var.nov. (Caulerpales, Chlorophyta), and additional records of *Halimeda* species from Puerto Rico. J. Phycol. 18, 86–91.

Bandeira-Pedrosa, M.E., Pereira, S.M.B., Bouzon, Z.L., Oliveira, E.C., 2004. *Halimeda cuneata* (Bryopsidales, Chlorophyta), a new record for the Atlantic Ocean. Phycologia 43, 50–57.

Barton, E.S., 1901. The genus *Halimeda*. Siboga Expedition Monograph 60. Brill, Leiden.

Bassoullet, J.P., Bernier, P., Deloffre, R., Genot, P., Poncet, J., Roux, A., 1983. Les algues Udoteacées du Paléozoique au Cénozoique. Bulletin Des Centres De Recherches Exploration-Production Elf-Aquitaine 7, 449–621.

Beckmann, J.-P., Beckmann, R. (1966) Calcareous algae from the Cretaceous and Tertiary of Cuba. Schweizerische Paläontologische Abhandlungen 85, 45 pp.

Bolton, J.J., Leliaert, F., De Clerck, O., Anderson, R.J., Stegenga, H., Engledow, H.E., Coppejans, E., 2004. Where is the western limit of the tropical Indian Ocean seaweed flora? An analysis of intertidal seaweed biogeography on the east coast of South Africa. Mar. Biol. 144, 51–59.

Burridge, C.P., 2002. Antitropicality of Pacific fishes: molecular insights. Environ. Biol. Fish. 65, 151–164.

Carlin, J.L., Robertson, D.R., Bowen, B.W., 2003. Ancient divergences and recent connections in two tropical Atlantic reef fishes *Epinephelus adscensionis* and *Rypticus saponaceous* (Percoidei : Serranidae). Mar. Biol. 143, 1057–1069.

Clifton, K.E., 1997. Mass spawning by green algae on coral reefs. Science 275, 1116–1118.

Clifton, K.E., Clifton, L.M., 1999. The phenology of sexual reproduction by green algae (Bryopsidales) on Caribbean coral reefs. J. Phycol. 35, 24–34.

Coates, A.G., Obando, J.A., 1996. The geological evolution of the Central American Isthmus. In: Jackson, J.B.C., Budd, A.F., Coates, A.G. (Eds.) Evolution and environment in tropical America. University of Chicago Press, Chicago, pp. 21–56.

Coleman, A.W., 2002. Comparison of *Eudorina/Pleodorina* ITS sequences of isolates from nature with those from experimental hybrids. Am. J. Bot. 89, 1523–1530.

Coyne, J.A., Orr, H.A., 2004. Speciation. Sinauer, Sunderland.

De Clerck, O., Gavio, B., Fredericq, S., Bárbara, I., Coppejans, E., 2005. Systematics of *Grateloupia filicina* (Halymeniaceae, Rhodophyta), based on *rbc*L sequence analyses and morphological evidence, including the reinstatement of *G. minima* and the description of *G. capensis* spec. nov. J. Phycol. 41, in press.

de Senerpont-Domis, L.N., Famà, P., Bartlett, A.J., Prud'homme van Reine, W.F., Espinosa, C.A., Trono, G.C., 2003. Defining taxon boundaries in members of the morphologically and genetically plastic genus *Caulerpa* (Caulerpales, Chlorophyta). J. Phycol. 39, 1019–1037.

Dragastan, O.N., Littler, D.S., Littler, M.M., 2002. Recent vs. fossil *Halimeda* species of Angaur Island, Palau and adjacent western Pacific areas. Acta Palaeontologica Romaniae, Special publication no. 1. Cartea Universitara, University of Bucharest, Bucharest.

Drew, E.A., Abel, K.M., 1988. Studies on *Halimeda*. II: reproduction, particularly the seasonality of gametangia formation, in a number of species from the Great Barrier Reef Province. Coral Reefs 6, 207–218.

Duggen, S., Hoernle, K., Van Den Bogaard, P., Rüpke, L., Phipps Morgan, J., 2003. Deep roots of the Messinian salinity crisis. Nature 422, 602–606.

Duke, N.C., Benzie, J.A.H., Goodall, J.A., Ballment, E.R., 1998. Genetic structure and evolution of species in the mangrove genus *Avicennia* (Avicenniaceae) in the Indo-West Pacific. Evolution 52, 1612–1626.

Durand, C., Manuel, M., Boudouresque, C.F., Meinesz, A., Verlaque, M., Le Parco, Y., 2002. Molecular data suggest a hybrid origin for the invasive *Caulerpa racemosa* (Caulerpales, Chlorophyta) in the Mediterranean Sea. J. Evol. Biol. 15, 122–133.

Famà, P., Wysor, B., Kooistra, W.H.C.F., Zuccarello, G.C., 2002. Molecular phylogeny of the genus *Caulerpa* (Caulerpales, Chlorophyta) inferred from chloroplast *tuf*A gene. J. Phycol. 38, 1040–1050.

Freile, D., Milliman, J.D., Hillis, L. (1995) Leeward bank margin *Halimeda* meadows and draperies and their sedimentary importance on the western Great Bahama bank slope. Coral Reefs 14, 27–33.

Goldman, N., Anderson, J.P., Rodrigo, A.G., 2000. Likelihood-based tests of topologies in phylogenetics. Syst. Biol. 49, 652– 670.

Gurgel, C.F.D., Liao, L.M., Fredericq, S., Hommersand, M.H., 2003. Systematics of *Gracilariopsis* (Gracilariales, Rhodophyta) based on *rbc*L sequence analyses and morphological evidence. J. Phycol. 39, 154–171.

Hegarty, M.J., Hiscock, S.J., 2005. Hybrid speciation in plants: new insights from molecular studies. New Phytol. 165, 411– 423.

Hilbish, T.J., Mullinax, A., Dolven, S.I., Meyer, A., Koehn, R.K., Rawson, P.D., 2000. Origin of the antitropical distribution pattern in marine mussels (*Mytilus* spp.): routes and timing of transequatorial migration. Mar. Biol. 136, 69–77.

Hillis, L., 1959. A revision of the genus *Halimeda* (order Siphonales). Pub. Inst. Mar. Sci. 6, 321–403.

Hillis, L.W., 2001. The calcareous reef alga *Halimeda* (Chlorophyta, Bryopsidales): a cretaceous genus that diversified in the Cenozoic. Palaeogeogr. Palaeocl. 166, 89–100.

Hillis-Colinvaux, L., 1980. Ecology and taxonomy of *Halimeda*: primary producer of coral reefs. Adv. Mar. Biol. 17, 1–327.

Hillis-Colinvaux, L., 1986. Historical perspectives on algae and reefs: Have reefs been misnamed? Oceanus 29, 43–49.

Holder, M.T., Anderson, J.A., Holloway, A.K., 2001. Difficulties in detecting hybridization. Syst. Biol. 50, 978–982.

Hommersand, M.H., 1986. The biogeography of the South African marine red algae: a model. Bot. Mar. 24, 257–270.

Joosten, A.M.T., van den Hoek, C., 1986. World-wide relationships between red seaweed floras: a multivariate approach. Bot. Mar. 29, 195–214.

Kapraun, D.F., 1993. Karyology of marine green algae. Phycologia 32, 1–21.

Kapraun, D.F., 1994 Cytophotometric estimation of nuclear DNA contents in thirteen species of the Caulerpales (Chlorophyta). Cryptogamic Botany 4, 410–418.

Kapraun, D.F., Buratti, J.R., 1998. Evolution of genome size in the Dasycladales (Chlorophyta) as determined by DAPI cytophotometry. Phycologia 37, 176–183.

Kinlan, B.P., Gaines, S.D., 2003. Propagule dispersal in marine and terrestrial environments: A community perspective. Ecology 84, 2007–2020.

Knowlton, N., 1993. Sibling species in the sea. Annu. Rev. Ecol. Syst. 24, 189–216.

Kooistra, W.H.C.F., Caldéron, M., Hillis, L.W., 1999. Development of the extant diversity in *Halimeda* is linked to vicariant events. Hydrobiologia 398, 39–45.

Kooistra, W.H.C.F., Coppejans, E.G.G., Payri, C., 2002. Molecular systematics, historical ecology, and phylogeography of *Halimeda* (Bryopsidales). Mol. Phylogen. Evol. 24, 121–138.

Kooistra, W.H.C.F., Verbruggen, H., 2005. Genetic patterns in the calcified tropical seaweeds *Halimeda opuntia*, *H. distorta*, *H. hederacea* and *H. minima* (Bryopsidales, Chlorophyta) provide insights in species boundaries and inter-oceanic dispersal. J. Phycol. 41, 177–187.

Lamouroux, J.V.F., 1812. Extrait d'un mémoire sur la classification des Polypiers coralligènes non entièrement pierreux. Nouveaux Bulletin des Sciences, par la Société Philomathique de Paris 3, 181–188.

Lessios, H.A., Kane, J., Robertson, D.R. 2003. Phylogeography of the pantropical sea urchin *Tripneustes*: Contrasting patterns of population structure between oceans. Evolution 57, 2026–2036.

Liao, D.Q., 1999. Concerted evolution: Molecular mechanism and biological implications. Am. J. Hum. Genet. 64, 24–30.

Linder, C.R., Rieseberg, L.H. 2004. Reconstructing patterns of reticulate evolution in plants. Am. J. Bot. 91, 1700–1708.

Littler, D.S., Littler, M.M., 2003. South Pacific reef plants. OffShore Graphics, Washington DC.

Marlow, J.R., Lange, C.B., Wefer, G., Rosell-Mele, A., 2000. Upwelling intensification as part of the Pliocene-Pleistocene climate transition. Science 290, 2288–2291.

McMillan, W.O., Palumbi, S.R., 1995. Concordant evolutionary patterns among Indo-West Pacific butterflyfishes. Proc. Roy. Soc. London, Ser. B – Biol. Sci. 260, 229–236.

Meinesz, A., 1980. Connaissances actuelles et contribution a l'etude de la reproduction et du cycle des Udoteacees (Caulerpales, Chlorophytes). Phycologia 19, 110–138.

Muss, A., Robertson, D.R., Stepien, C.A., Wirtz, P., Bowen, B.W., 2001. Phylogeography of *Ophioblennius*: The role of ocean currents and geography in reef fish evolution. Evolution 55, 561–572.

Noble, J.M., 1986. *Halimeda magnidisca* (Caulerpales, Chlorophyta), a new species from the Great Barrier Reef, Australia. Phycologia 25, 331–339.

Norris, R.E., Aken, M.E., 1984. Marine benthic algae new to South Africa. S. Afr. J. Bot. 51, 55–65.

Nylander, J.A.A., 2004. MrModeltest v2.0. Department of Systematic Zoology, Uppsala University, Sweden.

Olsen, J.L., Stam, W.T., Berger, S., Menzel, D., 1994. 18S rDNA and evolution in the Dasycladales (Chlorophyta): modern living fossils. J. Phycol. 30, 729–744.

Pakker, H., Klerk, H., Hein van Campen, J., Olsen, J.L., Breeman, A.M., 1996. Evolutionary and ecological differentiation in the pantropical to warm-temperate seaweed *Digenea simplex* (Rhodophyta). J. Phycol. 32, 250–257.

Phillips, J.A., 2001. Marine macroalgal biodiversity hotspots: why is there high species richness and endemism in southern Australian marine benthic flora? Biodivers. Conserv. 10, 1555–1577.

Posada, D., Crandall, K.A., 1998. Modeltest: testing the model of DNA substitution. Bioinformatics 14, 817–818.

Provan, J., Murphy, S., Maggs, C.A., 2004. Universal plastid primers for Chlorophyta and Rhodophyta. Eur. J. Phycol. 39, 43–50.

Rögl, F., Steininger, F.F., 1984. Neogene Paratethys, Mediterranean and Indo-Pacific seaways. Implications for the paleobiogeography of marine and terestrial biotas. In: Brenchley, P.J. (Ed.) Fossils and Climate. John Wiley & sons, New York, pp. 171–200.

Ronquist, F., Huelsenbeck, J.P., 2003. MrBayes 3: Bayesian phylogenetic inference under mixed models. Bioinformatics 19, 1572–1574.

Schils, T., 2002 Marine plant communities of upwelling areas within the Arabian Sea: A taxonomic, ecological and biogeographic case study on the marine flora of the Socotra Archipelago (Yemen) and Masirah Island (Oman). Doctoral thesis, Ghent University, Ghent.

Schils, T., Coppejans, E., 2003. Spatial variation in subtidal plant communities around the Socotra Archipelago and their biogeographic affinities within the Indian Ocean. Mar. Ecol. Prog. Ser. 251, 103–114.

Shimodaira, H., Hasegawa, M., 1999. Multiple comparisons of log-likelihoods with applications to phylogenetic inference. Mol. Biol. Evol. 16, 1114–1116.

Small, R.L., Cronn, R.C., Wendel, J.F., 2004, Use of nuclear genes for phylogeny reconstruction in plants. Aust. Syst. Bot. 17, 145–170.

Smith, A.G., Smith, D.G., Funnell, B.M., 1994. Atlas of Mesozoic and Cenozoic coastlines. Cambridge University Press, Cambridge.

Swofford, D.L., 2003. PAUP*. Phylogenetic Analysis Using Parsimony (*and other methods). Version 4. Sinauer Associates, Sunderland.

van den Hoek, C., 1982. The distribution of benthic marine algae in relation to the temperature regulation of their life histories. Biol. J. Linnean Soc. 18, 81–144.

Verbruggen, H. De Clerck, O., Cocquyt, E., Kooistra, W.H.C.F., Coppejans, E. 2005a. Morphometric taxonomy of siphonous green algae: a methodological study within the genus *Halimeda* (Bryopsidales). J. Phycol. 41, 126–139.

Verbruggen, H., De Clerck, O., Coppejans, E., 2005b. Deviant segments hamper a morphometric approach towards *Halimeda* taxonomy. Cryptogamie Algol. 26, in press.

Verbruggen, H., De Clerck, O., Kooistra, W.H.C.F., Coppejans, E., 2005c. Molecular and morphometric data pinpoint species boundaries in *Halimeda* section *Rhipsalis* (Bryopsidales, Chlorophyta). J. Phycol., accepted.

Verbruggen, H., Kooistra, W.H.C.F., 2004. Morphological characterization of lineages within the calcified tropical seaweed genus *Halimeda* (Bryopsidales, Chlorophyta). Eur. J. Phycol. 39, 213–228.

Verbruggen, H., N'Yeurt, A., Spalding, H., Vroom, P.S., submitted. Phylogeny and taxonomy of *Halimeda incrassata*, including the description of *H. kanaloana* and *H. heteromorpha* spp. nov. (Bryopsidales, Chlorophyta).

Waters, J.M., Roy, M.S., 2003. Global phylogeography of the fissiparous sea-star genus *Coscinasterias*. Mar. Biol. 142, 185–191.

Zechman, F.W., Kooistra, W.H.C.F., Olsen, J.L., Stam, W.T., 1999. Current perspectives on the phylogeny of ulvophycean green algae. Abstracts of the 16th International Botanical Congress, St. Louis, MI, p. 144.

Appendix 1. Specimen list.

Specimen numbers correspond to accession numbers in Ghent University Herbarium (GENT). Species authorities are *H. cuneata* Hering, *H. cuneata* f. *digitata* Barton, *H. cuneata* f. *undulata* Barton, *H. discoidea* Decaisne, *H. gigas* Taylor, *H. gracilis* Harvey ex J. Agardh, *H. hummii* Ballantine, *H. incrassata* (Ellis) Lamouroux, *H. lacunalis* Taylor, *H. macrophysa* Askenasy, *H. magnidisca* Noble, *H. minima* (Taylor) Colinvaux, *H. monile* (Ellis & Solander) Lamouroux, *H. scabra* Howe, *H. simulans* Howe, *H. taenicola* Taylor, *H. tuna* (Ellis & Solander) Lamouroux, *H. xishaensis* Dong & Tseng. Note that Kooistra et al. (2002) and Verbruggen & Kooistra (2004) identified H.0122 (their 99-102) as *H. gigas* Taylor. However, the specimen belongs to *H. cuneata* f. *undulata*, an entity not recognized in the taxonomic work used for species identification in these previous studies (Hillis-Colinvaux, 1980). The current identification of this material is based on Barton (1901) and Littler & Littler (2003). Specimens identified here as *H. magnidisca* and *H. cuneata* 4 deviated from the type material as described in Kooistra et al. (2002) and Verbruggen & Kooistra (2004).

genotypic cluster	number	geographical origin	*rps*19-*rps*3	SSU-ITS	*tuf*A	*rpl*5-*rps*8-*inf*A
H. cuneata 1	H.0195-1	Scottsburgh, South Africa		AF407256		
	KZN2K4-21	Palm Beach, KwaZulu Natal, South Africa	AY823860	AY823840	AY826353	AY826369
	KZN2K4-41	Marina Beach, KwaZulu Natal, South Africa	AY823861	AY823842		
	KZNb2263	Jesser Point, Sodwana, South Africa	AY823862			
H. cuneata 2	H.0195-2	Scottsburgh, South Africa	AY823863			
	KZN2K4-20	Palm Beach, KwaZulu Natal, South Africa	AY823864	AY823843		
	KZNb2352	Palm Beach, KwaZulu Natal, South Africa	AY823865	AY823841	AY826354	AY826370
H. cuneata 3	H.0210	Rottnest Island, Western Australia	AY823866	AY823844		
	H.0550	Rottnest Island, Western Australia	AY823867			
	H.0551	Rottnest Island, Western Australia	AY823868			
	WA182	Rottnest Island, Western Australia	AY823869	AY823838	AY826355	AY826371
	WA206	Carnac Island, Western Australia	AY823870			
H. cuneata 4	SOC212b	Socotra (Yemen)	AY823871	AY823845		
	SOC252	Socotra (Yemen)	AY823872	AF525595	AY826356	AY826372
	SOC348	Socotra (Yemen)	AY823873	AF525596		
H. cuneata 5 (f. *digitata*)	HV605	Mactan Island, Philippines	AY823874	AY823846		
	HV732	Uson Island, Philippines	AY823875	AY823847		
	HV827	Dancalan, Luzon, Philippines	AY823876			
H. cuneata 6 (f. *undulata*)	H.0122	Cocos Island, Guam	AY823877	AF407252	AY826357	AY826373
	HV33	Pongwe, Zanzibar, Tanzania	xxx			
	HV41	Ras Ruvula, Mnazi Bay area, Tanzania	xxx			
	HV560	Malapascua Island, Philippines	AY823878			
	HV586	Malapascua Island, Philippines	AY823879	AY823848		
	HV683	Catagbacan, Bohol, Philippines	AY823880	AY823849		
H. cuneata 7	H.0500	Espirito Santo State, Brazil	AY823881	AY823837	AY826358	AY826374
	H.0501	Espirito Santo State, Brazil	AY823882	AY823850		
	H.0502	Espirito Santo State, Brazil	AY823883	AY823851		
H. discoidea 1	no voucher	Rhiq di Katanan, Socotra (Yemen)		AF525605		
	H.0041	Moorea, French Polynesia	AY823887	AF525604		
	H.0053	Nukubiko Reef, Fiji		AF525600		
	H.0117	Cocos Island, Guam		AF525597		
	H.0153	Eastern Island, Midway, Hawaii (U.S.A.)	AY823888	AF525602		
	H.0172	Bolinao, Pangasinan, Philippines		AF525601		
	H.0191	Lapu Lapu, Mactan Island, Philippines		AF525599		
	H.0204	Puerto Vallarta Bay, Pacific Mexico		AF525598		
	HEC12634	Cairo, Zanzibar, Tanzania		AF525603		
	HV58	Paea, Tahiti, French Polynesia	xxx			
	MAS153	Masirah, Oman	AY823884	AY823852		
	MAS356	Masirah, Oman	AY823885	AY823853		
	OMII118	Sur, Oman	AY823886	AY823839	AY826359	AY826375
	SOC212a	Socotra (Yemen)	AY823889	AY823854		
	SOC299	Socotra (Yemen)	AY823890	AF407254	AY826360	AY826376
H. discoidea 2	H.0144	Florida, U.S.A.	AY823891	AF525585		
	H.0207	Gran Canaria, Canary Islands (Spain)	AY823892	AF407249	AY826361	AY826377
	H.0209	Sao Vicente, Cape Verde	AY823893	AF525587		
	H.0410	Isla Grande, Panama		AF525586		
	HV495	Discovery Bay, Jamaica	AY823894	AY823855		
H. discoidea 3	HV396	St. Ann's Bay, Jamaica	AY823895		AY826362	AY826378
	HV431	St. Ann's Bay, Jamaica	AY823896			
H. hummii	H.0233	Galeta, Panama	xxx			xxx
	H.0251	Portobelo, Panama		AF525583		
	H.0253	House Reef, San Blas, Panama			xxx	
H. lacunalis	H.0118	Bile Bay, Guam	AY823897	AF407246		
	H.0121	Agat, Guam	AY823898	AF525579	AY826363	AY826379
	H.0212	Guam		AF525580		
	HV306-1	Rangiroa, French Polynesia	AY823899	AY786519		
	HV308-1	Rangiroa, French Polynesia	AY823900	AY786520		

H. macrophysa	H.0024	Lizard Island, Great Barrier Reef, Australia		AF407251		
	H.0271	New Caledonia	xxx		xxx	xxx
H. magnidisca	HEC12910	Mnazi Bay, Tanzania	AY823901		AY826364	AY826380
	SOC385	Socotra (Yemen)	AY823902	AF407253		
H. taenicola	H.0037	Tahiti, French Polynesia	AY823903	AF407255		
	HV285-1	Rangiroa, French Polynesia	AY823904	AY786521	AY826365	AY826381
	HV285-2	Rangiroa, French Polynesia	AY823905	AY786522		
	HV306-3	Rangiroa, French Polynesia	AY823906	AY786523		
H. tuna 1	H.0074	Isla Colon, Panama	AY823909	AF525589		
	H.0231	Puerto Morelos, Mexico	AY823910	AF407248	AY826367	AY826383
	HV447	Discovery Bay, Jamaica	AY823911	AY823857		
	HV458	Lee Reef, St. Ann's Bay, Jamaica	AY823912	AY823858		
	HV459	Lee Reef, St. Ann's Bay, Jamaica	AY823913	AY823859		
H. tuna 2	H.0113	Naples, Italy	AY823907	AF407250	AY826366	AY826382
	H.0202	Malta		AF525588		
	H.0493	Piran, Slovenia	AY823908	AY823856		
	HV319	Rosas, Spain		AY786524		
outgroup: *H. gracilis*	HV317	Rangiroa, French Polynesia	AY823914	AY786526	AY826368	AY826384
	HEC11839	Beruwela, Sri Lanka		AF407257		

Part 4

Morphometric tools for *Halimeda* taxonomy

Morphometric taxonomy of siphonous green algae: a methodological study within the genus *Halimeda*

Heroen Verbruggen, Olivier De Clerck, Ellen Cocquyt, Wiebe H.C.F. Kooistra & Eric Coppejans

Journal of Phycology 41: 126–139 (2005)

Abstract

Species-level taxonomy of Bryopsidalean genera is often based on quantifiable morphological characters. Yet there are relatively few examples of statistically founded morphometric studies within this group of siphonous algae and macroalgae in general. Molecular phylogenetic studies have revealed cases of cryptic diversity in several Bryopsidalean genera and call for new approaches toward taxonomy. We present a combined molecular and morphometric approach toward *Halimeda* taxonomy using a selection of specimens representing the five natural lineages within the genus. A phylogeny was inferred from partial nuclear rDNA sequences (3' end of small subunit, internal transcribed spacer region 1, 5.8S, internal transcribed spacer region 2, and 5' end of large subunit) from our and previously studied specimens. Segment size and shape descriptors were acquired using different techniques, including landmark analysis and elliptic Fourier analysis. A broad range of anatomical structures was measured. Taxonomic utility of the different methods and characters was assessed using predictive discriminant analysis. Molecular data were used to delimit species groups. Segment morphological characters proved fairly good predictors for species membership, but anatomical variables yielded the best results. The good performance of morphometric taxon predictors offers perspectives, not only for future taxonomic case studies within problematic species complexes, but also for thorough examinations of the rich fossil record of *Halimeda*. Statistically founded morphometric studies can probably help elucidate taxonomic issues within other Bryopsidalean genera as well.

Introduction

Morphometric analysis, the mathematical investigation of shape, allows objective and statistically sound evaluation of morphological variation to answer a broad spectrum of biological questions. Macroalgae are at first sight less suited for morphometric investigation because their structures and branching patterns are marked by considerable stochastic variation and plasticity. Contrary to botanists and zoologists, phycologists do not have the habit of embracing morphometrics to answer their taxonomic and ecological questions. Nonetheless, during the last 5 years, a raise in interest for morphometrics could be observed (Sherwood and Sheath 1999, Kraan et al. 2001, Krellwitz et al. 2001, Collado-Vides 2002, Hubbard and Garbary 2002, Vieira and Necchi 2002, de Senerpont Domis et al. 2003, Kamiya et al. 2003, Vroom and Smith 2003, Vroom et al. 2003, Haywood et al. 2004, Murray et al. 2004). Achievements of these studies include reports of morphological differences between taxa and the description of taxon boundaries. In the present study, we explore the taxonomic utility of morphometric methods in the genus *Halimeda*. This genus belongs to the Bryopsidales, a group of algae characterized by siphonous thalli, each specimen essentially comprising a single giant multinucleate cell. The siphons branch, anastomose, and adhere to form very simple (e.g. *Derbesia*, *Bryopsis*) to highly complex (e.g. *Avrainvillea*, *Halimeda*) thalli. Within genera, direct observations of thallus shape and a limited number of anatomical characters and measurements are supposed to lead to accu-

rate taxonomic assignment. However, recent molecular studies showed morphological convergence and cryptic diversity (Kooistra 2002, Kooistra et al. 2002); that is, genetically distinct species cannot be keyed out with current procedures and insights in morphology. Yet these classical approaches may not use the anatomical and morphological information to the fullest.

The genus *Halimeda* is a particularly interesting target for morphometric studies because its thalli are composed of calcified segments with a particular shape (Fig. 1, a and b), and many anatomical structures can be quantified. Within segments, an inner medulla and an outer cortex can be discerned (Fig. 1, e–h). Medullar siphons are oriented along the thallus axis and string the segments together. These siphons branch laxly, with the main branch continuing toward the thallus apex and side branches giving rise to the cortex (Fig. 1, g and h). In the cortex, siphon branching is denser. This results in several layers of short, often inflated siphons called utricles. Peripheral utricles adhere (Fig. 1, c, d, g, and h) and enclose an intersiphonal space where aragonite precipitation occurs (Borowitzka and Larkum 1977).

Classical morphotaxonomy discerned 35 species in five sections (Dong and Tseng 1980, Hillis-Colinvaux 1980, Ballantine 1982, Noble 1986, Kraft 2000). Although sections were defined on the basis of patterns of siphon fusion at nodes between segments, species recognition within sections was primarily based on segment shape and cortical patterns. This taxonomy has been questioned by molecular phylogenetic studies based on partial rDNA sequence analysis. The evolutionary partitioning of the genus proved different from Hillis-Colinvaux' (1980) sectional subdivision (Verbruggen and Kooistra 2004), and several nonmonophyletic species and cases of cryptic diversity within species were revealed (Kooistra et al. 2002). The phylogenetic insights resulted in a revision of the sectional subdivision, which is now in accordance with major evolutionary directions within the genus. Each of the new sections can easily be recognized by unique combinations of synapo- and symplesiomorphies (Kooistra et al. 2002, Verbruggen and Kooistra 2004). Within lineages, some species can be easily recognized, whereas other species lump into morphocomplexes with or without internal molecular phylogenetic structure. In addition to the previously mentioned cases of nonmonophyly and hidden diversity, additional taxonomic problems occur (Noble 1987, Dargent 1997). Specimens are often difficult to identify with existing identification keys and taxonomic descriptions. This is probably due to a combination of three factors. First, traditional qualitative characters generally are not diagnostic for closely related species. Second, intraspecific morphological plasticity appears to be underestimated. Finally, there seems to exist a historical bias of taxonomy toward Caribbean species, with Indo-Pacific representatives fitted in without full consideration of morphological variation. A new approach toward the taxonomy of the genus is sorely needed.

Here we explored the utility of a combined molecular and morphometric approach toward species separation in *Halimeda*, using a limited number of specimens representing the five natural lineages within the genus. We aimed 1) to estimate the feasibility of morphometric taxonomy within the genus, 2) to gain insight in the taxonomic utility of different morphometric methods and characters at different taxonomic levels, 3) to narrow the range of techniques and measurements for future case studies within morphological species complexes, and 4) to discuss the potential of morphometric taxonomy in Bryopsidalean algae.

The first two questions were tackled by comparing the adequacy of clade membership prediction by a series of morphometrics (quantitative morphological characters) taken from segments and anatomical structures. Molecular information was used as an objective allocator of specimens to species-level groups; in other words, the species groups used were delimited on the basis of objective sequence data. Segment size and shape were digitized using landmark methods (Rohlf and Marcus 1993) and outline analysis (elliptic Fourier analysis [EFA]; Kuhl and Giardina 1982). The third question was raised

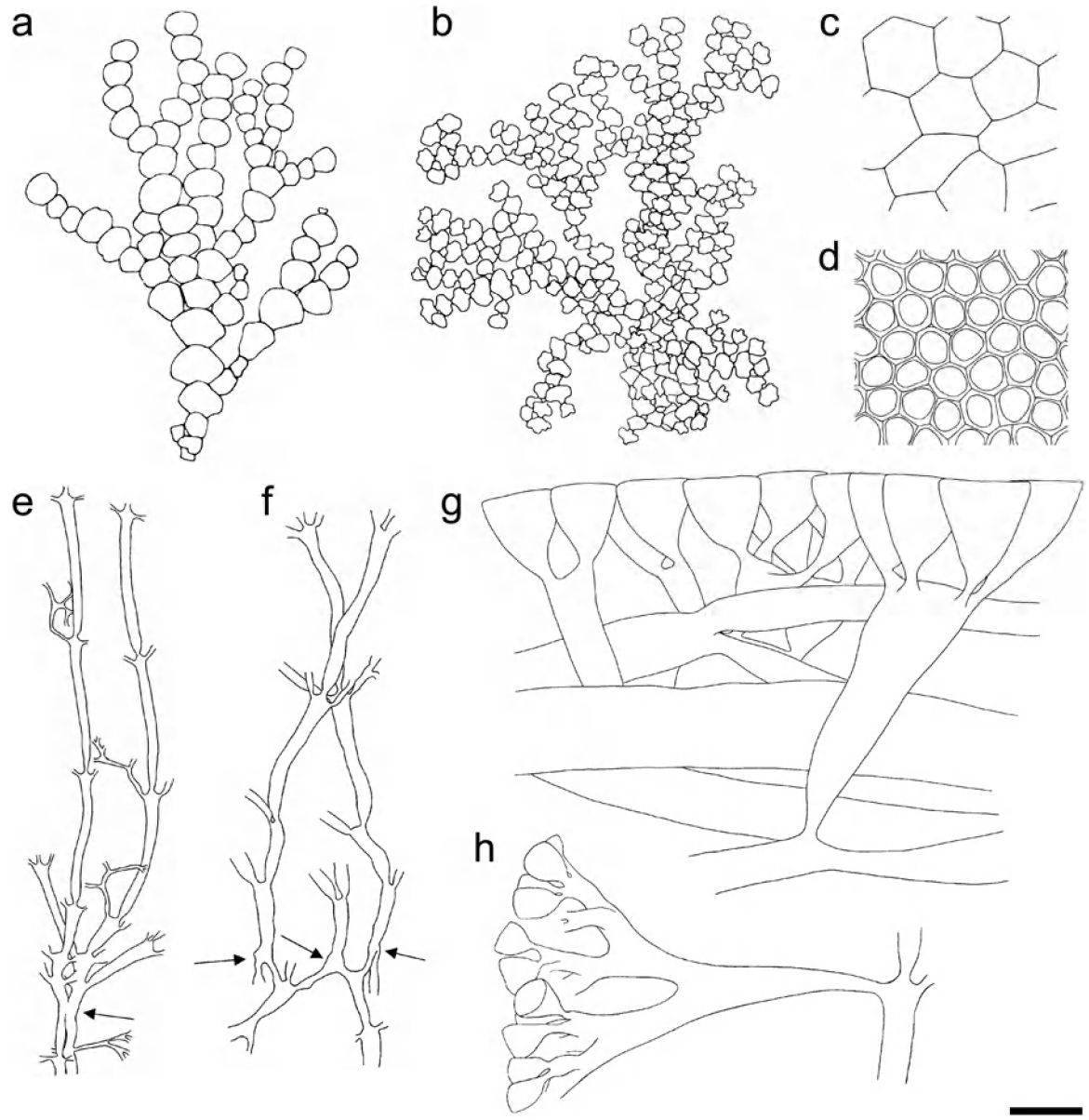

Fig. 1. Thallus morphology and anatomical details of a few *Halimeda* species used in this study. (a–b) Thallus morphology. (a) *H. lacunalis*, HV306-1. (b) *H. gracilis*, C&PvR13865B. (c–d) Surface view. (c) *H. tuna*, HV54. (d) *H. gracilis*, HV317. (e–f) Medulla and nodal region. (e) *H. opuntia*, HV19. (f) *H. tuna*, HV54. (g–h) Cortical region in cross-section. (g) *H. tuna*, HV54. (h) *H. micronesica*, WLS184-02. Arrows indicate the location of the node. Scale bars: 25 mm for thalli, 400 mm for medulla, 60 mm for cortical structures and surface views. (Adapted from Verbruggen and Kooistra 2004). All specimens deposited in GENT.

when dissecting segments and measuring their anatomical structures proved to be extremely time consuming. To approach this issue, the behavior of central and deviance measures of anatomical variables were examined in the light of specimen and segment sampling approaches. In a parallel study (Verbruggen et al. 2005), we reported on the exploratory statistics and so-called deviant segments and their influence on group membership prediction.

Materials and methods

Species sampling

Nine species were sampled covering the phylogenetic spectrum of the genus. From each of the large sections (*Rhipsalis*, *Halimeda*, and *Opuntia*), two or three species were chosen; from smaller sections (*Micronesicae* and *Pseudo-opuntia*), a single species was selected. Morphological species identifications were based on Hillis-Colinvaux (1980). For each species, two or three specimens were examined (Table 1). All specimens are deposited in the Ghent University Herbarium, Belgium (GENT).

Sequence analysis

DNA was extracted and amplified as described in Kooistra (2002). Sequences of the nuclear rDNA region were obtained (3' end of 18S, internal transcribed spacer [ITS] region 1, 5.8S, ITS2, and 5' end of 28S) following procedures in Kooistra (2002). Of specimens HV46b and H.0257, only partial sequences could be obtained. For HV46b it concerns ITS1, 5.8S, ITS2, and the 5' end of 28S; for H.0257 it concerns the 3' end of 5.8S, ITS2, and the 5' end of 28S. For specimen HV45, we were unable to obtain a sequence. Forward and reverse sequences were merged using Autoassembler, version 1.4.0 (Applied Biosystems, Foster City, CA, USA). Obtained sequences were added to the alignment of Kooistra (Kooistra et al. 2002, Verbruggen and Kooistra 2004) and were aligned manually in BioEdit, version 5.0.9 (Hall 1999). Unweighted maximum parsimony trees were inferred from the obtained alignment of specimens in Tables 1 and 2 using PAUP*, version 4.0.b10 (Swofford 2001) using the TBR branch-swapping algorithm. Gaps were treated as missing data, and starting trees were obtained via stepwise addition. Sequences of *Udotea flabellum* (Ellis and Solander) Howe and *Penicillus capitatus* Lamarck were used as outgroup (Kooistra et al. 2002, Verbruggen and Kooistra 2004). Bootstrap support (100 replicates) was obtained under the same criteria as the heuristic maximum parsimony analysis.

Morphometrics

Segment sampling

For morphometric examination of small specimens (less than about 100 segments) all segments were investigated. Of larger thalli, between 48 and 89 segments were sampled in series spanning the entire

Table 1. Specimens in the morphometric study. Given are their accession number in the GENT herbarium, geographic origin and Genbank accession number of their nuclear rDNA sequences.

section	species	GENT	geographic origin	ocean	Genbank
Rhipsalis	*H. borneensis*	HV18-1	Zanzibar Island (Tanzania)	Western Indian	AY786512
		HV183b	Tahiti, French Polynesia	Central Pacific	AY786513
	H. macroloba	HV38	Zanzibar Island (Tanzania)	Western Indian	AY786514
		HV45	Mnazi Bay, Tanzania	Western Indian	—
		HV206	Tahiti, French Polynesia	Central Pacific	AY786515
Micronesicae	*H. micronesica*	H.0014-1	Great Barrier Reef, Australia	Western Pacific	AY786516
		WLS184-02	Wallis Island (France)	Central Pacific	AY786517
		WLS420-02	Wallis Island (France)	Central Pacific	AY786518
Halimeda	*H. lacunalis*	HV306-1	Rangiroa, French Polynesia	Central Pacific	AY786519
		HV308-1	Rangiroa, French Polynesia	Central Pacific	AY786520
	H. taenicola	HV285-1	Rangiroa, French Polynesia	Central Pacific	AY786521
		HV285-2	Rangiroa, French Polynesia	Central Pacific	AY786522
		HV306-3	Rangiroa, French Polynesia	Central Pacific	AY786523
	H. tuna	H.0113-1	Naples, Italy	Mediterranean Sea	AF407248
		HV319	Rosas, Spain	Mediterranean Sea	AY786524
Pseudo-Opuntia	*H. gracilis*	HV312-1	Rangiroa, French Polynesia	Central Pacific	AY786525
		HV317-1	Rangiroa, French Polynesia	Central Pacific	AY786526
Opuntia	*H. goreauii*	H.0257	Bocas del Toro, Panama	Caribbean Sea	AY786527
		H.0258-1	Galeta, Panama	Caribbean Sea	AF525610
	H. opuntia	HV46b	Mnazi Bay, Tanzania	Western Indian	AY786528
		HV61	Moorea, French Polynesia	Central Pacific	AY649380

thallus length. For sprawling species (*H. gracilis* and *H. opuntia*), the basal reference segment was arbitrarily chosen.

Thallus structure

The position of segments within the thallus was determined as the distance of the segment to the basal segment (number of intermediate nodes). Segments were classified into three groups according to their location along the thallus axis: the lowermost 25% (thal_prt = 1), the central 50% (thal_prt = 2), and the uppermost 25% (thal_prt = 3). The binary variable apical was set to 1 for apical segments or 0 for nonapical segments. Noted was also whether segments were calcified or not. The local branching pattern was characterized by counting the number of sister segments and the number of daughter segments.

Segment morphology

Segment form was digitized from calibrated digital pictures of various thallus parts. After being numbered, individual segments were aligned horizontally with their base pointing downward (Fig. 2, a and b).

Categorical shape variables

From the segment pictures, a first set of six variables (Table 3: s7–s12) corresponding to characters traditionally used in taxonomic treatises of *Halimeda*, was gathered for specimens HV18-1, HV206, WLS184-02, HV285-1, HV319, HV312-1, H.0257, and HV46b.

Conventional measurements

Five landmarks were digitized using tpsDIG (version 1.31, Rohlf 2001a). Two landmarks were placed on the right and left sides of the segment's attachment zone (Fig. 2a); three more were placed at the left, top, and right extremities of the segment.

The following conventional size variables (segment length and width, the height where the width is maximal, and width of the attachment zone, variables s13–s17) were calculated from the landmark coordinate files using the following equations (visualized in Fig. 2b).

$$\text{length} = y4 - \frac{y1 + y2}{2}$$

$$\text{width} = x5 - x3$$

$$\text{homw} = \frac{y3 + y5}{2} - \frac{y1 + y2}{2}$$

$$\text{attach} = \sqrt{(y1 - y2)^2 + (x1 - x2)^2}$$

Segment thickness was measured using calipers. The five conventional variables presented a log-

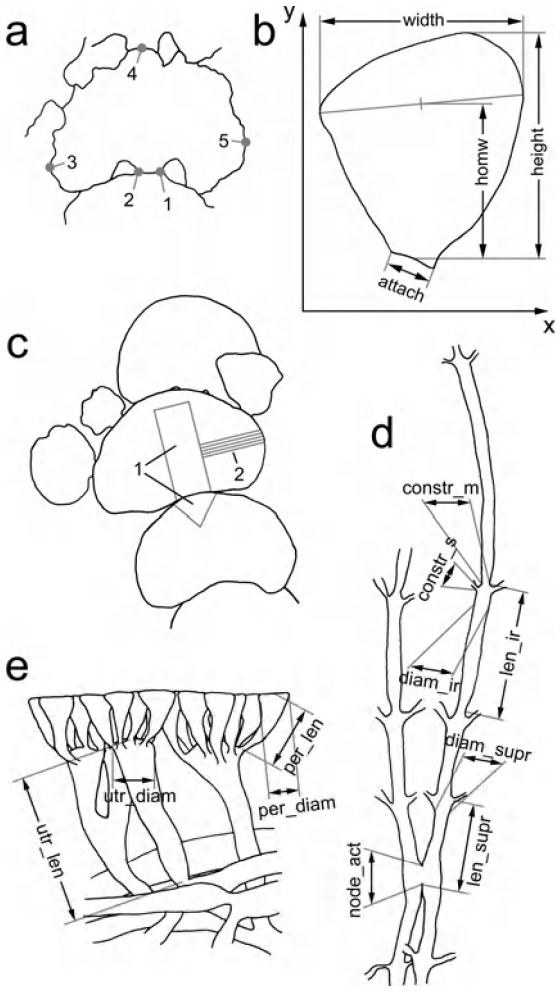

Fig. 2. Explanation of methods. (a) Digitized landmarks 1–5. (b) Size properties of segments as calculated from the landmark coordinates. The fifth segment size variable, thickness, is not shown. (c) Dissection of a segment. The gray lines illustrate the part cut out for node dissection (1) and the slices made for observations of the cortex (2). (d) Measurements made on medullar structures. (e) Measurements made on cortical structures. In the case shown here, utr_len and utr_diam (general notation used during data acquisition) correspond to sec_len and sec_diam, respectively (because it concerns a secondary utricle). The variable per_surf is not shown.

normal distribution and were transformed using the neperian logarithm (ln) for all analyses that required it.

Ratio shape variables

Using untransformed size variables, five ratios expected to provide useful segment shape information were calculated: segment length over segment width, width of attachment zone over segment width, height of maximal segment width over segment length, segment thickness over segment length, and segment thickness over width of attachment zone (Table 3, s18–s22).

Landmark analysis

We carried out a geometric landmark analysis (Bookstein 1989, 1991, Rohlf and Marcus 1993) on the group of landmarks described above. This type of analysis extracts the variation in geometric configu-

Table 2. List of previously published sequences used in our phylogeny. For specimens housed in the Ghent University herbarium, their accession number in this herbarium is given. For the biphyletic species (see Kooistra et al. 2002), the geographic origin is indicated after the species epiteth with CAR for Caribbean, ATL for Atlantic, IP for Indo-Pacific, and MED for Mediterranean.

species	GENT	geographic location	ocean	Genbank
H. borneensis	HEC12603b	Zanzibar, Tanzania	Western Indian	AF525559
H. borneensis	H.0267	New Caledonia	Western Pacific	AF525550
H. melanesica	no voucher	Taka Garlarang, Indonesia	Western Pacific	AF407237
H. incrassata IP	PH197	Cebu, Philippines	Western Pacific	AF407241
H. incrassata IP	H.0045	Rangiroa, French Polynesia	Central Pacific	AF525573
H. macroloba	H.0157	Pangasinan, Philippines	Western Pacific	AF525560
H. macroloba	H.0038	Tahiti, French Polynesia	Central Pacific	AF525563
H. cylindracea	SOC364	Socotra, Yemen	Western Indian	AF525546
H. cylindracea	H.0018	Great Barrier Reef, Australia	Western Pacific	AF525548
H. simulans	H.0367	Panama	Caribbean Sea	AF407235
H. incrassata CAR	H.0181	Florida, U.S.A.	Caribbean Sea	AF525537
H. incrassata CAR	H.0179	Bahamas	Caribbean Sea	AF407233
H. monile	H.0228	Yucatan, Mexico	Caribbean Sea	AF407234
H. cryptica	H.0237	Discovery Bay, Jamaica	Caribbean Sea	AF407244
H. micronesica	no voucher	Great Barrier Reef, Australia	Western Pacific	AF407243
H. fragilis	H.0125	Bile Bay, Guam	Western Pacific	AF407245
H. hummii	H.0253	San Blas, Panama	Caribbean Sea	AF525581
H. discoidea ATL	H.0207	Gran Canaria, Canary Islands	Eastern Altantic	AF407249
H. tuna MED	H.0113	Naples, Italy	Mediterranean Sea	AF407250
H. tuna ATL	H.0231	Puerto Morelos, Mexico	Caribbean Sea	AF407248
H. lacunalis	H.0121	Agat Bay, Guam	Western Pacific	AF525579
H. magnidisca	SOC252	Socotra, Yemen	Western Indian	AF525595
H. magnidisca	SOC348	Socotra, Yemen	Western Indian	AF525596
H. discoidea IP	SOC299	Socotra, Yemen	Western Indian	AF407254
H. discoidea IP	H.0041	Moorea, French Polynesia	Central Pacific	AF525604
H. taenicola	H.0037	Tahiti, French Polynesia	Central Pacific	AF407255
H. cuneata	no voucher	W Australia	Eastern Indian	AF525606
H. macrophysa	H.0271	New Caledonia	Western Pacific	AF525590
H. gigas	H.0122	Cocos Island, Guam	Western Pacific	AF407252
H. gracilis IP	HEC11839	Beruwala, Sri Lanka	Central Indian	AF407257
H. lacrimosa	H.0308	Bahamas	Caribbean Sea	AF407258
H. gracilis CAR	H.0405	Isla Grande, Panama	Caribbean Sea	AF525609
H. minima	SOC384	Socotra, Yemen	Western Indian	AF407263
H. minima	PH526	Mindanao, Philippines	Western Pacific	AF525618
H. minima	H.0382	Apra Harbor, Guam	Western Pacific	AF407265
H. renschii	C&PvR13855B	Madang, Papua New Guinea	Western Pacific	AF407262
H. opuntia	H.0262	Tamandare, Brazil	Western Atlantic	AF525639
H. opuntia	HEC12584	Zanzibar, Tanzania	Western Indian	AF525629
H. distorta	no voucher	Cebu, Philippines	Western Pacific	AF525652
H. distorta	H.0280	New Caledonia	Western Pacific	AF525641
H. hederacea IP	H.0475	Great Barrier Reef, Australia	Western Pacific	AF407269
Penicillus capitatus	H.0349	San Blas, Panama	Caribbean Sea	AF407271
Udotea flabellum	H.0415	Portobelo, Panama	Caribbean Sea	AF407270

ration of a set of landmarks that are superimposed on each of the specimens and codes this variation in a series of continuous variables (partial warps). The whole analysis up until the extraction of partial warp scores was performed with tpsRELW (version 1.31, Rohlf 2001b). Landmark configurations were aligned using the general orthogonal least-squares method (Rohlf and Slice 1990). The configuration of averaged landmarks was chosen to be the point of tangency between Kendall's shape space and tangent space (Rohlf et al. 1996). The relation between Procrustes distances and the linear distances in tangent space was evaluated for linearity using tpsSMALL (version 1.19, Rohlf 1998). Partial warp scores were computed with alpha set to zero so as not to weigh the partial warps (Rohlf 1993). Uniform shape changes (s23 and s24) were computed following Bookstein (1996). Nonuniform, localizable shape changes are coded in variables s25–s28.

Elliptic Fourier analysis

In EFA (Kuhl and Giardina 1982), shape characteristics of the outline of the studied object are translated into mathematical variables. The resulting number of variables is proportional to the desired degree of precision between the original outline and the closed contour captured in the variables.

Table 3. List of segment morphological variables. The variable group to which they belong are indicated on the right hand side.

	variable	description	
s1	dis_base	location of the segment in the thallus: measured in # of nodes from the basal segment	thallus structure variables
s2	thal_prt	thallus part the segment is located in	
s3	apical	is the segment apical? (binary variable)	
s4	calcif	is the segment fully calcified? (binary variable)	
s5	no_sist	number of sister segments	
s6	no_daugh	number of daughter segments	
s7	form_seg	categorical segment form: reniform, ovate, elliptical, obovate, cuneate, rectangular	categorical shape variables
s8	seg_widt	categorical variable for relative segment width: narrow, medium, broad	
s9	stalk	categorical variable describing the proximal stalk zone: absent, intermediate, present	
s10	form_bas	categorical variable for the form of the segment base: auriculate to acute in five steps	
s11	lobedne	categorical variable describing the segment's lobedness: absent, shallow, medium, deep	
s12	numlobes	number of lobes: 1 to 6 (six meaning many)	
s13	length	segment length (mm); L_length is neperian logarithm hereof	conventional measurements
s14	width	segment width (mm); L_width is neperian logarithm hereof	
s15	attach	width of attachment zone (mm); L_attach is neperian logarithm hereof	
s16	homw	height of maximal segment width (mm); L_homw is neperian logarithm hereof	
s17	thick	segment thickness (mm); L_thick is neperian logarithm hereof	
s18	len_wd	relative segment width: length over width ratio	ratio shape variables
s19	att_wd	relative width of attachment zone: attach over width ratio	
s20	homw_len	relative height of maximal width: homw over length ratio	
s21	thk_len	relative segment thickness: thickness over length ratio	
s22	thk_att	ratio of segment thickness over the width of the attachment zone	
s23	pw_uniX	uniform shape change score X	partial warp scores
s24	pw_uniY	uniform shape change score Y	
s25	pw_1X	partial warp score 1X	
s26	pw_1Y	partial warp score 1Y	
s27	pw_2X	partial warp score 2X	
s28	pw_2Y	partial warp score 2Y	
s29-s68	fc1a-10d	set of 40 fourier coefficients (10 harmonics, 4 series)	fourier

Segment outlines were traced manually from the aligned segment images. The outlines were then rotated 90 degrees clockwise to facilitate their digitization using the center of the attachment zone as a fixed starting point (tpsDIG version 1.31, Rohlf 2001a). All points along the segment outlines were saved. Visual inspection of the degree to which outlines reconstructed from Fourier coefficients corresponded to the original outlines (EFAWin, Isaev 1995), suggested that 10 harmonics captured the major shape properties of the segments. Coefficients for 10 harmonics were extracted with Morpheus et al. (Slice 2000). The Morpheus et al. software was set to remove size differences. Rotational correction was omitted because the visual alignment already present in the outline pictures was more appropriate. The program was set to use the first coordinate couple as a fixed starting point. All 40 variables resulting from the analysis (four per harmonic, fc1a–fc10d, s29–s68) were added to the data set.

Dissection procedures for siphonal structures

Five to eight randomly chosen segments per specimen were decalcified in a 20% HCl solution and rinsed in tap water. From the central-axial region of the segment, a long and relatively narrow piece, extending into the preceding segment over the node connecting both segments, was excised (Fig. 2, c, 1). The cortex was scraped away from the excised fragment with a scalpel. The cortex piece was then

Table 4. List of anatomical variables. The variable group to which they belong are indicated on the right hand side.

	variable	description	
a1	len_ir	distance between two subsequent ramifications (µm)	medullar properties
a2	diam_ir	medullary siphon diameter (µm)	
a3	l_d_ir	length over diameter ratio of the siphon segment: len_ir / dia_ir	
a4	constr_m	constriction of main branch diameter (µm)	
a5	constr_s	constriction of side branch diameter (µm)	
a6	frac_di	fraction dichotomous ramifications	
a7	frac_tri	fraction trichotomous ramifications	
a8	frac_qua	fraction quadrichotomous ramifications	
a9	len_supr	distance from below node to supranodal ramification (µm)	nodal prop's
a10	diam_supr	thickness of the supranodal interramification (µm)	
a11	node_act	actual pore size or node height (µm)	
a12	per_surf	surface diameter peripheral utricle (µm)	peripheral utricles
a13	per_len	length (height) of peripheral utricle (µm)	
a14	per_diam	diameter of peripheral utricle (µm)	
a15	per_l_d	relative length of the peripheral utricle: per_len over per_diam ratio	
a16	per_adh	distance over which peripheral utricles adhere (µm)	
a17	sec_len	length (µm) of the secondary utricle	secondary utricles
a18	sec_diam	maximal diameter (µm) of the secondary utricle	
a19	sec_l_d	relative length of secondary utricle: sec_len over sec_diam ratio	
a20	sec_2_succ	fraction of measured secondary utricles carrying two peripheral utricles	
a21	sec_3_succ	fraction of measured secondary utricles carrying three peripheral utricles	
a22	sec_4_succ	fraction of measured secondary utricles carrying four peripheral utricles	
a23	sec_5p_succ	fraction of measured secondary utricles carrying five or more peripheral utricles	
a24	ter_len	length (µm) of the tertiary utricle	tertiary utricles
a25	ter_diam	maximal diameter (µm) of the tertiary utricle	
a26	ter_l_d	relative length of tertiary utricle: ter_len over ter_diam ratio	
a27	ter_2_succ	fraction of measured tertiary utricles carrying two secondary utricles	
a28	ter_3_succ	fraction of measured tertiary utricles carrying three secondary utricles	
a29	ter_4_succ	fraction of measured tertiary utricles carrying four secondary utricles	
a30	ter_5p_succ	fraction of measured tertiary utricles carrying five or more secondary utricles	

placed on a microscope slide to yield a surface view. The medullar part that remained after removal of the cortex was prepared for examination as follows. For specimens belonging to section *Rhipsalis* (sensu Verbruggen and Kooistra 2004) the nodal region was sectioned longitudinally. Sections were placed on a microscope slide in clear Karo corn syrup diluted with water, and the siphons above and below the node were spread open using dissecting needles. For specimens belonging to the other sections, siphons were spread open so that nodal structure became clear. The cortex was examined in cavity slides using thick transverse cuts (Fig. 2, c, 2).

Medulla and node

From the medulla, seven types of measurements were taken (see Fig. 2d for a visualization and Table 4 for a list). Cell walls were included in the measurements. When connecting siphon segments were measured, the sequence in which they occurred was noted as well. The whole slide was screened for medullar ramifications; the fraction of dichotomous, trichotomous, and quadrichotomous ramifications was calculated from their counts.

Cortex

The surface diameter of peripheral utricles was measured from the scraped-off cortex part that was fixed in surface view. Another set of peripheral utricles was drawn in side view (camera lucida), and the utricles' length, width, and length-over-width ratio were computed from scanned images of these drawings (Fig. 2e). If peripheral utricles adhered to their neighbors, the height of the adhesion zone was recorded. For subperipheral utricles, we recorded length, diameter, the ratio between the former two, and the number of daughter utricles (Fig. 2e). Only the data for secondary and tertiary utricles was retained for analysis (variables a17–a23 for secondary utricles and a24–a30 for tertiary utricles). If measured utricles were connected to each other, their sequence in the series was noted.

Where possible, at least 10 replicate measurements (per segment) were made (e.g. measurements on 10 random peripheral utricles). These replicate measurements were averaged to yield a single value for each segment. All anatomical observations were made with a BX51 light microscope (Olympus Europe, Hamburg, Germany).

Statistical analyses

Taxonomic utility of the data

To test the taxonomic utility of the data set as a whole and its separate components, discriminant analyses (DAs) were performed using the GDA module of Statistica 6.0 (StatSoft Inc., Tulsa, OK, USA) with a priori groups corresponding to species clusters found in the molecular phylogeny. The percentage of correctly classified segments in DA was used as a measure of taxonomic power. Assumptions for DA were met except for some cases of heteroscedasticity. Because DA is fairly robust against violation of the homoscedasticity assumption (Lachenbruch 1975, Klecka 1980), in particular when violation is not due to outliers (which was not the case in our data), we further disregarded this assumption. Multicollinearity issues are touched on in Results. Segments from the basal thallus region and apical and noncalcified segments were excluded from all DAs (Verbruggen et al. 2005).

Segment morphology

Classification success of six DA models was compared. These models differed in the variable sets they included (conventional size, ratio shape sensu stricto + partial warp scores, Fourier coefficients, and combinations of these; see Fig. 4 for a complete list of combinations used). All effects were entered at once, prior probabilities were set to equal, and cross-validation was set so that 50% randomly chosen segments were used to build the model and the remaining segments were used to evaluate it. This procedure was repeated 20 times with different randomizations of segments used for model building and for testing. First, models were built to yield maximal separation of all nine species in the study (here-

after called nine-species models/analyses). Afterward, models were built for maximal separation of (closely related) taxa within individual sections (*H. macroloba* vs. *H. borneensis*, *H. tuna* vs. *H. taenicola* vs. *H. lacunalis*, and *H. opuntia* vs. *H. goreauii*; hereafter called within-section models/analyses). Because the data set of categorical shape variables was incomplete, we tested its taxonomic utility separately, on a subset of the data. Classification success of DA models based on categorical variables was compared with that of models based on ratio shape variables, partial warp scores, and Fourier coefficients. Additional models, embodying categorical variables and ratio shape variables or Fourier coefficients, were built and compared with models in which a single variable set was used.

Anatomy

Similarly for the anatomical data, a DA approach was used to determine the utility of the different variables. Anatomical structures not present in all nine species were omitted from nine-species analyses (basic models). For these analyses, we used four variable groups and different combinations of these groups: 1) the medullar, a1–a6; 2) the nodal zone, a9 and a10; 3) the peripheral utricles, a12–a15; and 4) the subperipheral utricles, a17–a20. Discriminant analyses were performed in a non-stepwise manner with equal prior probabilities and without cross-validation. For some within-section models, additional variables could be included (extended models). For DAs within sections *Rhipsalis* and *Opuntia*, actual node height (a11) was added to the models with nodal variables. Peripheral utricle models were expanded with the distance over which utricles adhere (a16). Finally, within-section models were expanded with the tertiary utricle variables a24–a27 for sections *Rhipsalis* and *Opuntia*.

Redundancy between anatomical variables within variable groups was traced using principal components analysis biplots and r^2 values of their linear regressions. One of both variables in the well-fitting linear regressions was subsequently left out of the discriminant models described above to evaluate its influence on classification success. Between-variable-group redundancy was examined by running canonical correlation analyses of all pairs of variables sets.

Sampling segments for anatomical investigation

Of all three representatives of *H. taenicola* in this study, five segments were dissected and 10 within-segment replicate measurements of each of the anatomical variables were taken. The data set comprising all 150 measurements per structure was considered to represent the statistical population. Four types of randomized subsets were created from the original data by retaining different numbers of specimens, numbers of segments per species, and/or numbers of replicate measurements per segment. The properties of the four subset types, together with their abbreviations, are listed in Table 5. Per subset type, 50 random subsets were created using self-written algorithms. In choosing which types of subsets to compare, we strived for equal total measuring effort (Table 5, fourth column). The anatomical variables examined were a1–a5, a9, and a12–a15.

After calculating the Euclidean distances between the means and SDs of the different subsets and those of the statistical population, patterns in these distances were visualized with the aid of mean and whisker plots. To test for differences between different segment sampling strategies, one-way analysis of variance tests and Tukey HSD post-hoc tests (Zar 1999) were carried out.

Table 5. Summary of the different subset-types created to assess how their means and standard deviations approximate that of the statistical population. The first column lists the number of (randomly chosen) specimens retained in the subset. The second column specifies how many segments were randomly chosen from each of the specimens. The third column lists the number of replicate measurements taken from each of the segments. The fourth and fifth columns list the total sample size (total number of replicates) and the abbreviation of the subset type used throughout the paper. This abbreviation consists of a series of three numbers representing (in this order) the content of column 1, 2 and 3.

specimens	segments	replicates	total replicates	abbreviation
2	1	10	20	**2-1-10**
1	2	10	20	**1-2-10**
2	2	5	20	**2-2-5**
3	1	7	21	**3-1-7**

Results

Molecular phylogeny, species identification, and the morphometric data set

Figure 3 presents 1 of 105 equally most parsimonious trees. Bootstrap values larger than 50 are indicated below branches. The phylogeny supports the five sections of the genus sensu Verbruggen and Kooistra (2004) and illustrates the representation of each of these five sections in our morphometric study (gray boxes). All specimens used in our morphometric analyses fell within existing species clades or were closely associated sisters to them. For all but two specimens, morphology- and sequence-based identifications corresponded. Only specimens HV183b and HV18-1 keyed out as *H. simulans* but clustered within the *H. borneensis* clade. We followed Kooistra et al. (2002) in their opinion that these look-alike species are geographically restricted and cling to the *H. borneensis* denomination for these Indo-Pacific specimens.

Of the 21 specimens listed in Table 1, 1346 segments were digitized. For each of these segments, values for 62 variables related to morphology and local thallus structure were generated (6 thallus structure variables, 5 size variables, 5 ratio variables, 6 partial warp scores, 40 Fourier coefficients). An additional six categorical variables were coded for a subset of 536 segments. In total, 104 segments were dissected. This resulted in measurements being taken of 2193 utricles (of which 1008 were peripheral), 982 medullar siphon branches, and 827 nodal structures.

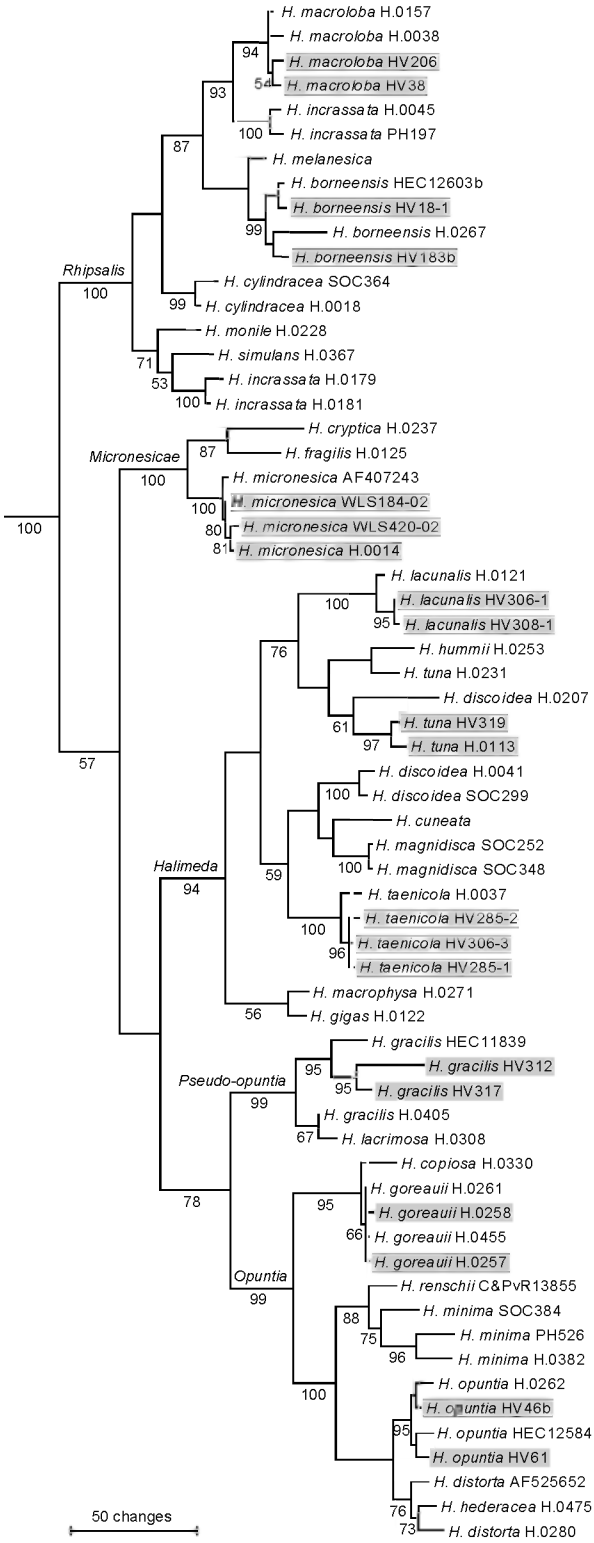

Fig. 3. Phylogeny of *Halimeda* taxa used in this study. One of 105 most parsimonious trees (1506 steps). Maximum parsimony bootstrap values 450 are indicated below and section names above internodes. The outgroup taxa were removed from the tree. Taxa used in the morphometric study are in gray boxes.

Taxonomic utility: matrix ill-conditioning

Discriminant analysis reported matrix ill-conditioning (problematic levels of multicollinearity) when multiple variable groups were combined in one predictive model. Initial analyses pointed out that a number of variables could be discarded without loss of discriminative power. Segment size variability was efficiently captured by two variables, the log-transforms of segment length and thickness. Furthermore, partial warp scores proved to be closely related to ratio variables; many of them showed nearly perfect correlations (Verbruggen et al. 2005: Fig. 1). Therefore, these two variable sets

were merged and a number of ratios (s18–s20) were excluded from all further analyses. Their notation in Figures 4 and 5 is "ratio s.s. + landmark." For DAs based on anatomical data, multicollinearity was not an issue of importance.

Segment morphology

Classification success in DA varied strongly between species and methods. The models' performance was poor for species of section one (*H. macroloba* and *H. borneensis*). Rather than being misclassified within the lineage, their segments were most often mistaken for segments of section *Halimeda* species. For the other species, classification success was considerably higher. The upper graph of Figure 4 shows the overall classification success for the six combinations of morphometric variables used. The percentage correctly classified segments varied between 50% and 70%. Of the individual variable sets, Fourier coefficients performed best. The combination of ratio shape variables and partial warp scores had the poorest differentiating power. All models with more than one variable group showed significantly more correct allocations. Nevertheless, results were far from additive, indicating considerable redundancy between variable sets. Including Fourier coefficients in any of these nine-species models significantly increased its taxonomic power.

When the success of classification into species groups was examined within each of the sections separately, patterns somewhat different from those observed previously were obtained. These within-section patterns were highly uniform for the three sections examined. The lower graph of Figure 4 shows the taxonomic power of the different models for section *Halimeda* (*H. lacunalis*, *H. taenicola*, and *H. tuna*). Compared with nine-species models, overall classification success was higher, and the contribution of the different variable sets to the taxonomic power of the model differed. The most remarkable difference is that adding Fourier coefficients to a model now decreased its taxonomic power, whereas in nine-species models this always led to an increase in classification success.

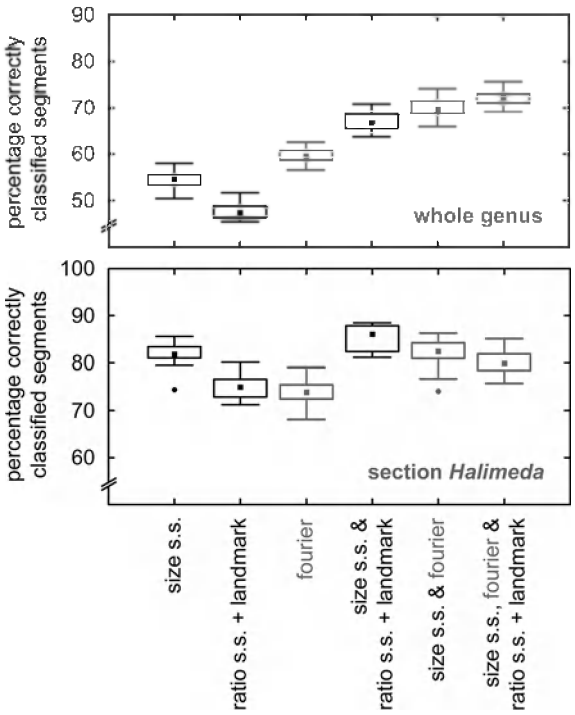

Fig. 4. Classification success of DA models constructed using different combinations of segment morphological variables (abscissa). The graphs depict the percentage of segments that were assigned to the species to which they belong. In the upper graph, the DA models were built for maximal discrimination between species within the whole genus; in the lower graph, only species belonging to section Halimeda were retained for DA. Models containing Fourier coefficients are in gray. The central squares indicate median values, the boxes are the 25 percentiles, the whiskers refer to nonoutlier range, and the outer dots represent outliers.

We also assessed the taxonomic utility of the categorical shape variables, using the subset of data for which these variables were available (Fig. 5). On average, categorical variables scored 47.5% correct classifications, significantly less than any other model tested. The combination of ratio variables (sensu stricto) and partial warps scored somewhat higher, but it was Fourier coefficients and models incorporating several variable sets that performed best. When categorical shape predictors were combined with ratio shape variables and partial warps or with Fourier coefficients (last two cases in Fig. 5), it became clear that categorical variables added power to the DA model based on ratio shape variables but not to that based on Fourier coefficients. The significance levels of the differences between

simple models and models enriched with categorical shape predictors were < 0.001 and 0.999 for the ratio and landmark model and the Fourier model, respectively (Tukey HSD test).

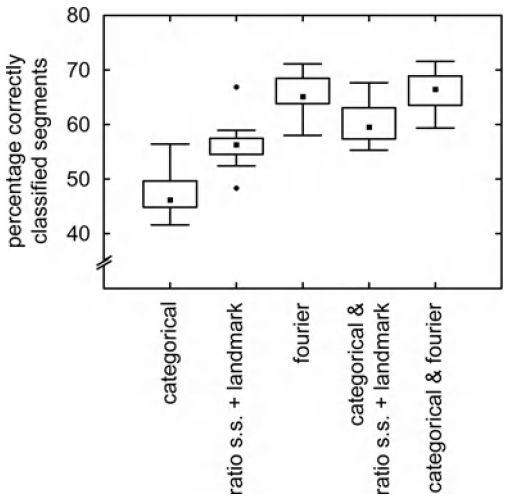

Fig. 5. DA with categorical segment shape descriptors. The different combinations of segment morphological variables used in the DA models are indicated along the abscissa. The graphs depict the percentage of segments that were assigned to the species group to which they belong. The central dots indicate median values, the boxes are the 25 percentiles, the whiskers refer to nonoutlier range, and the outer dots represent outliers.

Anatomy

Table 6 summarizes the results of the anatomy-based predictive discriminant models. Overall classification success was high: Models based on more than one variable group always yielded more than 90% correct classifications. In nine-species models, segments were most often misclassified as a species belonging to another section rather than to the same section. An examination of the factor structures of the models indicated that the different diameter measures of medullar and cortical siphons had a high differentiating power. The anatomy model (7) had primary and secondary roots with high loadings of the cortical variables, indicating their relative importance for discriminating between species at this taxonomic level. Within-section predictive DA always exceeded 90% classification success; models with more than one variable group even resulted in 100% correct allocations (except for one model in section *Halimeda*).

The results of the reruns of DAs without some of the strongly correlated variables were not uniform throughout the genus but generally resulted in a decrease of discriminatory power. As an example we elaborate the results for the set of medullar variables. Internal redundancy in this variable set was high. The first two principal components of a PCA carried out on this variable set represented 80% of the total variability in the data. Variables a4, a5, and a6 clustered close together in the biplot. For nine-species analyses, the DA model with all medullar (s.s.) variables included yielded a classification success of 87.3%. Leaving out variable a5 reduced this value to 84.1%, whereas omitting variables a4 or a6 had stronger effects (reduction to 76.2% and 79.4%, respectively). With both variables a5 and a6

Table 6. Classification success of the DA models based on anatomical data, given as the percentage of segments assigned to the species group they actually belong to. For certain individual sections, different b and e scores are given. These letters stand for basic models (including only variables measurable throughout the whole genus) and extended models (including variables measurable in this section but not throughout the genus), respectively.

	nine species	section *Rhipsalis*	section *Halimeda*	section *Opuntia*
1 – medullar structures	87.3	100	87.0	100
2 – nodal structures	58.7	b: 91.7	82.6	b: 90.9
		e: 100		e: 100
3 – peripheral utricles	84.1	b: 100	b: 91.3	b: 100
		e: 100	e: 91.3	e: 100
4 – subperipheral utricles	69.8	b: 91.7	87.0	b: 90.9
		e: 91.7		e: 100
5 – medulla s.l. (1–2)	90.5	b: 100	100	b: 100
		e: 100		e: 100
6 – cortex (3–4)	93.7	b: 100	95.6	b: 100
		e: 100		e: 100
7 – anatomy (1–4)	100	b: 100	100	b: 100
		e: 100		e: 100

left out, classification success was 79.4%. For analyses within sections *Opuntia* or *Rhipsalis*, there were no observable effects of leaving out any of the variables a4, a5, and a6 or any of their combinations. In section *Halimeda*, however, classification success was left unaffected when omitting variables a4 or a6, whereas leaving out a5 resulted in a slight increase from 87.0% to 91.3%. Removal of variable a3, which had low loadings on the roots of the different models, reduced classification success from 87.3% to 81.0% for nine-species models and did not alter the performance of within-section models.

Redundancy between variable groups was evident as well. Canonical analyses run between each two sets of anatomical variables revealed that between 28% and 70% of the variability within one variable set was accounted for by the other variable set. Mutual redundancy of variable groups based on similar structures and on locally adjacent structures was higher.

Sampling segments for anatomical investigation

The upper graph of Figure 6 depicts the distances between the mean values of the different subsets and the statistical population. The lower graph of Figure 6 shows the distances for the SDs. The patterns shown in these graphs were representative of those found for most variables studied. Both for means (upper graph) and SDs (lower graph), the y values of the 2-1-10 and 1-2-10 sampling strategies were higher than those of the 2-2-5 and 3-1-7 sampling methods. These differences were, however, generally nonsignificant (Tukey HSD tests). For the most part, the distances from the population score were significantly different (higher) only for the second sampling method (1-2-10).

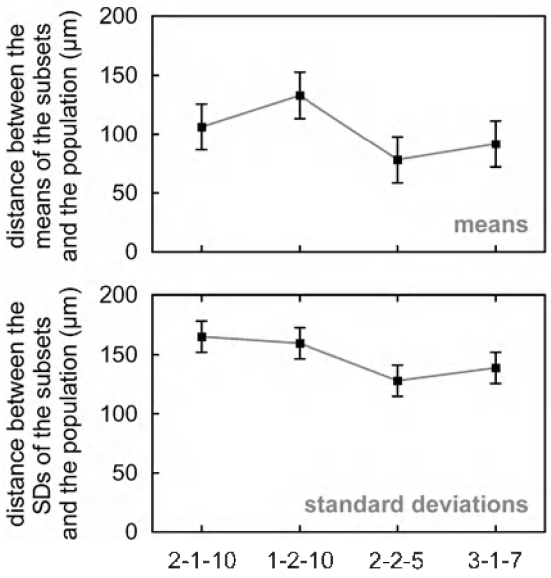

Fig. 6. The upper graph shows the Euclidean distances between the mean values of the variable diam_ir for the different types of subsets described in Table 3 and the mean of the statistical population. The lower graph depicts the Euclidean distances between the SDs of the variable diam_ir for the different types of subsets and the SD of the statistical population. The filled square and whiskers represent the mean distance ± 1 SD for the population of 50 random subsets of each given type.

Discussion

The days that *Halimeda* species were described solely on the basis of what their segments looked like lie far behind us. Soon after taxonomists started examining the anatomy of the thalli (Askenasy 1888), they realized that this was the key to a firm taxonomy, and the first measurements of anatomical structures appeared in literature (Barton 1901, Howe 1907). With both revisions of Hillis (1959, Hillis-Colinvaux 1980), even more emphasis was placed on anatomical characters. Molecular studies have now unveiled that these anatomical characters have not engendered an evolutionary correct classification (Kooistra et al. 2002, Verbruggen and Kooistra 2004). For example, the species *H. incrassata*, *H. copiosa*, and *H. discoidea* each consist of two unrelated species (Kooistra et al. 2002). Furthermore, within the species *H. minima*, *H. tuna*, and the *H. distorta* complex, significant phylogenetic structure indicates cryptic species diversity (Kooistra et al. 2002, Kooistra and Verbruggen 2005, Verbruggen and Kooistra 2004). Verbruggen and Kooistra (2004) advocated the use of quantitative morphological characters in taxonomical analyses. The method presented in the present study, which unites molecular information and morphometric data of segments and anatomy, permits distinction of the different species with high accuracy.

Segment morphology was regarded by Hillis-Colinvaux (1980) as an "exceedingly variable character" of limited utility in *Halimeda* systematics. Where used in taxonomy, segments are typified only by simple linear measurements and a descriptive expression of shape. Our results show that linear measurements are good predictors of species membership (Fig. 4). Shape descriptors, whether based on ratios of linear measurements or on geometric morphometric analyses, are in themselves of slightly lower taxonomic utility. When shape and size information are combined, DA models can pinpoint optimally to which species a specimen belongs.

Categorical shape variables, coding characters used in traditional taxonomy, are no match for morphometric variable sets. But here again, models incorporating both types of data performed best. An interesting result in this context was that adding categorical variables to different discriminant models had discrepant outcomes. For the ratio- and landmark-based discriminant model, higher classification success was achieved, whereas no effect was observed for the DA model based on Fourier coefficients. This is not surprising: the five landmarks on which ratio shape variables are based (Fig. 2a) were unable to capture certain segment properties that are embodied by the categorical shape variables (e.g. auriculate base, presence of a stalk). Conversely, Fourier coefficients are based on complete outlines of segments and are able to capture all properties coded in the categorical shape variables.

Comparing nine-species and within-section analyses yields information on the contrasts in performance of discriminant models in broad- versus narrow-scale taxonomy. The most important result in this context was that nine-species models reacted positively to the addition of Fourier coefficients, whereas within-section designs reacted negatively. Yet it is obvious that models solely based on Fourier coefficients achieved higher levels of classification success than those based solely on ratio shape variables and partial warps on both taxonomic scales. The latter finding implies that Fourier coefficients hold taxonomically useful information that is not present in the ratio shape variables or partial warps. But then why do within-section models enriched with Fourier coefficients perform worse than their more basic counterparts? In part, this is because those shape attributes coded in Fourier coefficients and not in the other shape data sets are largely uninformative at this taxonomic level. Furthermore, variables inherently incorporate a certain amount of noise and, in our case, lead to enhanced levels of multicollinearity. Therefore, adding a substantial amount of variables to discriminant models can lead to a reduction of their performance by lowering the accuracy and/or precision of regression coefficient estimation (Grapentine 1997).

In the progression of *Halimeda* studies, it was soon conceived that ecological factors can have a strong influence on segment morphology and that, for solving taxonomic issues, emphasis could better be placed on anatomical characters. At first, attention was paid to nodal fusion patterns (Barton 1901). Cortex structure and utricle dimensions soon followed as prime characters for species delineation (Barton 1901, Howe 1907). We did not include structural patterns in our analyses; instead, we concentrated on the dimensions of the different anatomical structures. Our results support the notion that anatomical information is a valuable species delineator. Classification success increased with expansion of the predictor variable content of the models, often reaching 100% in within-section analyses. The achievements and the buildup of the models show that cortical variables (particularly utricle length and diameter) have a high discriminative potential. This result justifies the importance traditional taxonomists attached to these measurements.

Optimization of the procedures

One of the missions of this study was to attain a time-efficient protocol for future case studies by reducing the number of methods applied and measurements taken while maintaining the achievement of predictive DAs. Our results provide clear information on which methods and measurements to abandon for narrow-scale investigations. The reduction of within-section classification success after addition of Fourier coefficients suggests that outline analysis can be dropped without devaluating the tax-

onomy-beneficial information content of the data. In addition to this, EFA is labor intensive because segment outlines have to be traced manually. Automatic detection is virtually impossible because segments are often superimposed and cannot be distinguished by a brightness threshold. Furthermore, the attachment zone between mother and daughter segments is hard to detect automatically. Isolating segments would solve these problems but is, because of its destructive nature, unjustifiable when using historic or rare herbarium materials.

The process of excluding variables from the anatomical data was not as straightforward as it was for the morphological data. In spite of the fact that redundancy levels were high and that discarding certain variables did not substantially alter the classification success, results were not homogenous throughout the phylogenetic spectrum of the genus. Only the width of medullar side branches at their constriction appears superfluous throughout all lineages within the genus and is thus eligible for exclusion from future studies.

Despite not being able to eliminate a subset of anatomical measurements, time-efficiency of anatomical data gathering can be substantially improved. Our analysis of the behavior of central and deviance measures of a number of representative anatomical variables as a function of specimen and segment sampling approaches, although possibly impeded by small sampling size, indicates that dissecting fewer segments per specimen and more specimens per population better approximates the variability found within that population than dissecting more segments per specimen from a small number of specimens. Because dissecting and preparing a segment is approximately equally time consuming as measuring 10 replicates of all anatomical structures in the slide, reducing the number of segments per specimen is a time saver. Of course, when picking out a limited amount of segments per specimen, this should be done minimizing the risk of those segments being deviant. Consequently, apical segments, noncalcified segments, and segments from the basal thallus region should be precluded (Verbruggen et al. 2005).

Perspectives

The molecular phylogenetic studies of Kooistra point out several groups of species that require additional taxonomic attention (Kooistra et al. 1999, 2002). It mostly concerns phylogenetically distant look-alikes with fuzzy species delineations (e.g. *H. borneensis–simulans*, *H. copiosa–hederacea*) and morphospecies that are nonmonophyletic (e.g. *H. incrassata*, *H. discoidea*, *H. tuna*, *H. gracilis*) or embody cryptic diversity (e.g. *H. minima*, *H. hederacea–distorta* complex). Traditional taxonomic practices have provided insufficient arguments to lead to an evolutionary correct classification of the phyletic entities within each of these species groups. It is self-evident that this does not imply the absence of morphological differences between the phyletic entities. On the contrary, subtle anatomical differences between genetically distinct entities of *H. tuna* and *H. discoidea* were observed (Hillis 1959, Hillis-Colinvaux 1980). These findings strengthen our belief that a morphometric approach embodying precise measurements and thorough statistical analyses can aid the taxonomy of each of the problematic morphocomplexes.

In this context, the application of DAs on morphometric data, with a priori groups defined on the basis of molecular data, opens a variety of perspectives. First, it permits evaluating whether species differences actually exist. This can be evaluated by means of multivariate analysis of variance (or nonparametric alternatives) or by checking whether the number of accurate designations in DA exceeds that expected by chance alone. Second, it allows pinpointing morphometric variables that provide strong differentiating power. These variables can then be translated into diagnostic characters by which specimens can be identified. Alternatively, a computer-assisted identification system could be established. This system could be trained (calibrated) using the existing database of segment pictures. Via automated contour extraction of digitized isolated segments, new specimens could then be identified using an automated classification procedure (e.g. neural networks). Our results indicate that for such

an approach to yield high levels of correct classification, several segments per specimen must be included.

The present study used within-section DAs to estimate the feasibility of morphometric taxonomy of closely related species. The high levels of adequate group membership prediction are promising for actual case studies. Nonetheless, two things must be stressed here. First, the sample size of this study was far too small to draw firm taxonomic conclusions. Adding specimens will undoubtedly increase the ranges of most variables and consequently alter the DA models. Second, species sampling in this study did not include actual problem clades. To some extent this limits the value of the predictive extrapolation toward puzzling morphocomplexes, but, on the other hand, the broad-scale sampling presented here is essential for the development of a sound morphometric modus operandi.

Not only does the finding that morphometrics allows species identification in our data set appear to be promising for future taxonomic case studies in extant representatives, it also pleads for a more standardized approach of the *Halimeda* fossil record. Of particular interest are the ambiguous species ages. Kooistra et al. (2002) estimated these to be less than 3 million years, whereas several paleontological studies report extant species from Miocene (Dragastan et al. 2002), Eocene (Dragastan and Soliman 2002), and Cretaceous (Dragastan et al. 2002, and references therein) deposits. Meticulous morphometric comparisons of extant and fossil *Halimeda* specimens could be used as additional information in this matter.

Finally, we wish to broaden the discussion toward Bryopsidalean algae. Within individual genera of this group, basic anatomical architecture is fairly homogeneous, whereas finer structural elements exhibit variation that is considered to be taxonomically useful (Silva 1959a,b, Ducker 1967, Farghaly and Denizot 1979, Olsen-Stojkovich 1985, Kraft 1986, Littler and Littler 1990, 1992, Krellwitz et al. 2001, de Senerpont Domis et al. 2003). On the other hand, traditional morphotaxonomic insights have been refuted by phylogenetic studies (Kooistra 2002, Kooistra et al. 2002). Recent morphometric studies on Bryopsidalean algae (Krellwitz et al. 2001, Hubbard and Garbary 2002, de Senerpont Domis et al. 2003, this study, unpublished data) prove that the combination of architectural constancy and fine-structural variability within genera permits establishing a morphometric method that is applicable to a variety of species yet provides accurate taxonomic resolution. In conclusion, most current evidence agrees that the shaky species-level taxonomy of Bryopsidalean algae benefits from studies founded on a combination of molecular phylogenetics and statistically founded morphometrics.

Acknowledgements

H.V. is indebted to the Bijzonder Onderzoeksfonds (Ghent University, grant 011D9101) and O.D.C. to the Fund for Scientific Research Flanders (grant 3G002496 and postdoctoral research grant). P. Colinvaux, L. Hillis, A. N'Yeurt, and G. Procaccini are acknowledged for specimen collection. H. V. thanks C. Payri, P. Vanai, and the Environmental Service of Wallis and Futuna for facilitating fieldwork on Uvea Island. The comments from the associate editor M. Kamiya and two anonymous referees are greatly appreciated.

References

Askenasy, E. 1888. Algen. *In*: Die Forschungsreise S.M.S. Gazelle Th. 4, Bot., Berlin.

Ballantine, D.L. 1982. *Halimeda hummii* sp.nov., *Halimeda cryptica* v. *acerifolia* var.nov. (Caulerpales, Chlorophyta), and additional records of *Halimeda* species from Puerto Rico. *J. Phycol.* 18: 86–91

Barton, E.S. 1901. The genus *Halimeda*. *Monographs of the Siboga Expedition* 60. Brill, Leiden, The Netherlands. 32 pp.

Bookstein, F.L. 1989. Principal warps: thin-plate splines and the decomposition of deformations. *IEEE T. Pattern Anal.* 11: 567–85

Bookstein, F.L. 1991. Morphometric tools for landmark data. *Cambridge University Press*. 435 pp.

Bookstein, F.L. 1996. Standard formula for the uniform shape component in landmark data. *In* Marcus L.F., Corti M., Loy A., Naylor G.J.P. and Slice D.E. (eds.) *Advances in Morphometrics*. Nato ASI series A: Life sciences vol 284. Plenum Press, New York, U.S.A. and London, U.K. pp. 153–68

Borowitzka, M.A. and Larkum, A.D.W. 1977. Calcification in the green alga *Halimeda*. V. An ultrastructure study of the thallus development. *J. Phycol.* 13: 6–16.

Collado-Vides, L. 2002. Morphological plasticity of *Caulerpa prolifera* (Caulerpales, Chlorophyta) in relation to growth form in a coral reef lagoon. *Bot. Mar.* 45: 123–9

Dargent, O. 1997. Etude systématique du genre *Halimeda* (Caulerpales, Bryopsidophycées), dans la zone de contact entre l'Océan Indien et l'Océan Pacifique. MSc thesis, Université Pierre et Marie Curie (Paris VI), Paris, France. 30 p.

de Senerpont Domis, L.N., Famà, P., Bartlett, A.J., Prud'homme van Reine, W.F., Armenta-Espinosa, C., Trono Jr. G.C. 2003. Defining taxon boundaries in members of the morphologically and genetically plastic genus *Caulerpa* (Caulerpales, Chlorophyta). *J. Phycol.* 39: 1019–37

Dong, M. & Tseng, C.K. 1980. Studies on some marine green algae from the Xisha Islands, Guandong Province, China. II. *Stud. Mar. Sin.* 17: 1–10.

Dragastan, O.N. and Soliman, H.A. 2002. Paleogene calcareous algae from Egypt. *Micropaleontology* 48: 1–30

Dragastan, O.N., Littler, D.S. and Littler, M.M. 2002. Recent vs. fossil *Halimeda* species of Angaur Island, Palau and adjacent western Pacific areas. *Acta Palaeontologica Romaniae. Special publication no. 1.* Cartea Universitara, University of Bucharest, Bucharest, Romania. 20 pp.

Ducker, S.C. 1967. The genus *Chlorodesmis* (Chlorophyta) in the Indo-Pacific region. *Nova Hedwigia* 13: 145–82

Farghaly, M.S. and Denizot, M. 1979. Le genre *Rhipiliopsis*. Définition et place dans les Caulerpales (Chlorophycées). *Rev. Algol.* 14: 169–84

Grapentine, T. 1997. Managing multicollinearity: Real-world survey data can create surrealistic analytic models. *Grapentine Company On-line Publications*. http://www.grapentine.com/articles/multicol.pdf

Hall, T.A. 1999. BioEdit: a user-friendly biological sequence alignment editor and analysis program for Windows 95/98/NT. Version 5.0.9. *Nucl. Acids. Symp. Ser.* 41: 95–8

Haywood, A.J., Steidinger, K.A., Truby, E.W., Bergquist, P.R., Bergquist, P.L., Adamson, J. and MacKenzie, L. 2004. Comparative morphology and molecular phylogenetic analysis of three new species of the genus *Karenia* (Dinophyceae) from New Zealand. *J. Phycol.* 40: 165–79

Hillis, L.W. 1959. A revision of the genus *Halimeda* (order Siphonales). *Publ. Inst. Mar. Sci.* 6: 321–403

Hillis-Colinvaux, L. 1980. Ecology and taxonomy of *Halimeda*: primary producer of coral reefs. *Adv. Mar. Biol.* 17: 1–327

Howe, M.A. 1907. Phycological studies - III. Further notes on *Halimeda* and *Avrainvillea* (pro parte: Halimeda). *Bull. Torrey Bot. Club* 34: 491–516

Hubbard, C.B. and Garbary, D.J. 2002. Morphological variation of *Codium fragile* (Chlorophyta) in Eastern Canada. *Bot. Mar.* 45: 476–85

Isaev, M. 1995. *EFAWin*. Windows shell for EFA. Free for download from http://life.bio.sunysb.edu/morph/

Kamiya, M., Zuccarello, G.C. and West, J.A. 2003. Evolutionary relationships of the genus *Caloglossa* (Delesseriaceae, Rhodophyta) inferred from large-subunit ribosomal RNA gene sequences, morphological evidence and reproductive compatibility, with description of a new species from Guatemala. *Phycologia* 42: 478–97

Klecka, W.R. 1980. *Discriminant analysis*. Sage, Beverly Hills, CA. 71 pp.

Kooistra, W.H.C.F. 2002. Molecular phylogenies of Udoteaceae (Bryopsidales, Chlorophyta) reveal nonmonophyly for *Udotea*, *Penicillus* and *Chlorodesmis*. *Phycologia* 41: 453–62

Kooistra, W.H.C.F., Caldéron, M. and Hillis, L.W. 1999. Development of the extant diversity in *Halimeda* is linked to vicariant events. *Hydrobiologia* 398: 39–45

Kooistra, W.H.C.F., Coppejans, E.G.G. and Payri, C. 2002. Molecular systematics, historical ecology and phylogeography of *Halimeda* (Bryopsidales). *Mol. Phylogen. Evol.*, 24: 121–38

Kooistra, W.H.C.F. and Verbruggen, H. 2005. Genetic patterns in the calcified tropical seaweed species *Halimeda opuntia*, *H. distorta, H. hederacea*, and *H. minima* (Bryopsidales, Chlorophyta) provide new views on species boundaries and inter-oceanic dispersal. *J. Phycol.*: 177–187.

Kraan, S., Rueness, J. and Guiry, M.D. 2001. Are North Atlantic *Alaria esculenta* and *A. grandifolia* (Alariaceae, Phaeophyceae) conspecific? *Eur. J. Phycol.* 36: 35–42

Kraft, G.T. 1986. The green algal genera *Rhipiliopsis* A. and E.S. Gepp and *Rhipiliella* gen. nov. (Udoteaceae, Bryopsidales) in Australia and the Philippines. *Phycologia* 25: 47–72

Kraft, G.T. 2000. Marine and estuarine benthic algae (Chlorophyta) of Lord Howe Island, South-western Pacific. *Austral. Syst. Bot.* 13: 509–648

Krellwitz, E.C., Kowallik, K.V. and Manos, P.S. 2001. Molecular and morphological analyses of *Bryopsis* (Bryopsidales, Chlorophyta) from the western North Atlantic and Caribbean. *Phycologia* 40: 330–9

Kuhl, F.P. and Giardina, C.R. 1982. Elliptic Fourier features of a closed contour. *Computer Graphics and Image Processing* 18: 236–58

Lachenbruch, P.A. 1975. *Discriminant Analysis*. Hafner Press, New York. 128 pp.

Littler, D.S. and Littler, M.M. 1990. Systematics of *Udotea* species (Bryopsidales, Chlorophyta) in the tropical western Atlantic. *Phycologia* 29: 206–52

Littler, D.S. and Littler, M.M. 1992. Systematics of *Avrainvillea* (Bryopsidales, Chlorophyta) in the tropical western Atlantic. *Phycologia* 31: 375–418

Murray, S., Jorgensen, M.F., Daugbjerg, N. & Rhodes, L. 2004. *Amphidinium* revisited. II. Resolving species boundaries in the *Amphidinium operculatum* species complex (Dinophyceae), including the descriptions of *Amphidinium trulla* sp nov and *Amphidinium gibbosum* comb. nov. *J. Phycol.* 40: 366–82

Noble, J.M. 1986. *Halimeda magnidisca* (Caulerpales, Chlorophyta), a new species from the Great Barrier Reef, Australia. *Phycologia* 25: 331–9

Noble, J.M. 1987. A taxonomic study of the genus *Halimeda* Lamouroux (Chlorophyta, Caulerpales) from the Heron Island region of the southern Great Barrier Reef, Australia. Masters degree thesis, University of Melbourne, Melbourne, Australia. 200 pp.

Olsen-Stojkovich, J. 1985. A systematic study of the genus *Avrainvillea* Decaisne (Chlorophyta, Udoteaceae). *Nova Hedwigia* 41: 1–68

Rohlf, F.J. 1993. Relative warp analysis and an example of its application to mosquito wings. *In*: Marcus L.F., Bello E. Garcia-Valdecasas A. (eds.). *Contributions to Morphometrics*. Museo Nacional de Ciencias Naturales (CSIC) Vol. 8, Madrid, Spain. pp. 131–59

Rohlf, F.J. 1998. *tpsSMALL* version 1.19. State University of New York at Stony Brook, Stony Brook, NY. Downloadable from http://life.bio.sunysb.edu/morph/

Rohlf, F.J. 2001a. *tpsDIG* version 1.31. State University of New York at Stony Brook, Stony Brook, NY. Free for download from http://life.bio.sunysb.edu/morph/

Rohlf, F.J. 2001b. *tpsRELW* version 1.31. State University of New York at Stony Brook, Stony Brook, NY. Free for download from http://life.bio.sunysb.edu/morph/

Rohlf, F.J. and Marcus, L.M. 1993. A revolution in morphometrics. *Trends Ecol. Evol.* 8: 129–32

Rohlf, F.J. and Slice, D.E. 1990. Extensions of the Procrustes method for the optimal superimposition of landmarks. *Syst. Zool.* 39: 40–59

Rohlf, F.J., Loy, A. and Corti, M. 1996. Morphometric analysis of old world Talpidae (Mammalia, Insectivora) using partial-warp scores. *Syst. Biol.* 45: 344–62

Sherwood, A.R. and Sheath, R.G. 1999. Biogeography and systematics of *Hildenbrandia* (Rhodophyta, Hildenbrandiales) in North America: inferences from morphometrics and rbcL and 18S rRNA gene sequence analyses. *Eur. J. Phycol.* 34: 523–32

Slice, D.E. 2000. *Morpheus et al.* Software for morphometric research. Beta version of 01/31/2000. Free for download from http://life.bio.sunysb.edu/morph/morpheus/

Silva, P.C. 1959a. The genus *Codium* (Chlorophyta) in South Africa. *The Journal of South African Botany* 15: 103–65

Silva, P.C. 1959b. *Codium* (Chlorophyta) in the tropical Western Atlantic. *Nova Hedwigia* 1: 497–536

Swofford, D.L. 2001. PAUP* Phylogenetic Analysis Using Parsimony (*and other methods) Version 4.0.b10. Sinauer Associates Inc., Sunderland, MA.

Verbruggen, H. and Kooistra, W.H.C.F. 2004. Morphological characterization of lineages within the calcified tropical seaweed genus *Halimeda* (Bryopsidales, Chlorophyta). *Eur. J. Phycol.* 39: 213–28

Verbruggen, H., De Clerck, O. and Coppejans, E. 2005. Deviant segments hamper a morphometric approach towards *Halimeda* taxonomy. *Cryptogamie Algologie* 26: in press.

Vieira, J. and Necchi, O. 2002. Microhabitat and plant structure of Characeae (Chlorophyta) populations in streams from Sao Paulo State, southeastern Brazil. *Cryptogamie Algologie* 23: 51–63

Vroom, P.S. and Smith, C.M. 2003. Reproductive features of Hawaiian *Halimeda velasquezii* (Bryopsidales, Chlorophyta), and an evolutionary assessment of reproductive characters in *Halimeda*. *Cryptogamie Algologie* 24: 355–70

Vroom, P.S., Smith, C.M., Coyer, J.A., Walters, L.J., Hunter, C.L., Beach, K.S. and Smith, J.E. 2003. Field biology of *Halimeda tuna* (Bryopsidales, Chlorophyta) across a depth gradient: comparative growth, survivorship, recruitment, and reproduction. *Hydrobiologia* 501: 149–66

Zar, J.H. 1999 *Biostatistical Analysis.* Fourth edition. Prentice-Hall, Upper Saddle River, NJ. 663 pp.

Deviant segments hamper a morphometric approach towards *Halimeda* taxonomy

Heroen Verbruggen, Olivier De Clerck & Eric Coppejans

Cryptogamie Algologie 29: accepted (2005)

Abstract

Traditional taxonomy of the segmented green algal genus *Halimeda* is largely based on descriptive expressions of thallus habit, segment shape and anatomical structures. In the course of the last decade, molecular phylogenetic studies have revealed non-monophyly and cryptic diversity in several species. In an attempt to tackle the taxonomic problems that were raised by these molecular studies, a combined molecular and morphometric method was developed. In this study, a morphometric pilot data set is explored. This resulted in the discovery of segments aberrant in morphology and/or anatomy. These are primarily apical and non-calcified segments, and segments from the basal part of the algal body. To answer the question whether incorporation of deviant segments into a morphometric dataset has a negative effect on its taxonomic value, a discriminant analysis approach was used. The a priori groups for discriminant analysis were determined by molecular methods, i.e. independent from morphology. Comparison of discriminant analyses that included and excluded deviant segments demonstrated the negative influence of such segments on the taxonomic power of the data. Omitting non-calcified and apical segments and segments from the basal thallus region yielded the same results as the exclusion of all deviant segments, irrespective of their location in the algal body. This result permits a simple recommendation towards precluding these types of segments from further studies.

Introduction

The chlorophyte genus *Halimeda* is ubiquitous throughout the tropics (Taylor, 1960; Hillis-Colinvaux, 1980; Littler & Littler, 2000, 2003). Its segmented thalli consist of a single giant tubular cell (siphon) that branches and anastomoses to form one of the most architecturally complex algal bodies within the order Bryopsidales (Vroom et al., 1998). The medulla consists of lengthwise siphons that branch off into the cortex, where they form series of short, inflated branches called utricles.

In current *Halimeda* taxonomy, sections and species are defined using descriptive expressions of thallus habit, segment shape and anatomical structures (Hillis-Colinvaux, 1980; Verbruggen & Kooistra, 2004). In addition, measurements of segment size and a limited number of anatomical structures are usually specified, and aid to distinguish between certain species. Although the major evolutionary lineages within the genus can be recognized with relative ease (Verbruggen & Kooistra, 2004), within these lineages species are often difficult to identify with existing identification keys and morphological insights. Additionally, molecular phylogenetic studies have shown that several species are nonmonophyletic or incorporate hidden diversity (Kooistra et al., 1999; 2002; Kooistra & Verbruggen, 2005). It is clear that classical approaches do not provide systematicians with the acumen needed to come to an evolutionarily correct species-level taxonomy. This appears not to be the case for *Halimeda* alone; more and more cases of cryptic diversity and erroneous species boundaries within all three major marine macroalgal groups have become evident (e.g. Siemer et al., 1998; van der Strate et al., 2002; Zuccarello et al., 2002; Zuccarello & West, 2003; Saunders & Lehmkuhl, 2003). If we strive

for a correct morphological interpretation of species boundaries, new methods of examining and interpreting morphology are needed.

In this and a parallel paper (Verbruggen et al., 2005), we introduce a combined molecular and morphometric approach towards *Halimeda* taxonomy. While Verbruggen et al. (2005) concentrate on the taxonomic utility of the different methods and variables; the focus of this study is on exploration of the morphometric data and on the study of deviant segments within the thallus. More specifically, we identify and characterize deviant segments. Thereafter, their influence on the taxonomic power of the morphometric data is assessed and suggestions towards the exclusion of certain groups of segments from further studies are put forward.

Materials and methods

The procedures for segment dissection and the morphometric methods employed are explained in more detail in Verbruggen et al. (2005). We will here restrict ourselves to a short overview of the molecular and morphometric dataset and expand on the statistical analyses used to address this paper's questions. For the tables listing the morphometric variables, we refer to Verbruggen et al. (2005: tables 3 & 4). Notations of the type s?? or a?? refer to variable numbers in these tables (in this notation ?? are numbers, while s and a stand for segment morphological and anatomical variables, respectively).

Species sampling, sequence analysis and morphometrics

Twenty-one specimens from nine species spanning the phylogenetic range of the genus were examined (Table 1). All specimens were deposited in the Ghent University Herbarium, Belgium (GENT). Specimens were assigned to species-level groups by sequencing the nuclear ribosomal DNA (SSU, ITS1, 5.8S, ITS2 and partial LSU) and determining the species-level clade to which they belong in a phylogenetic tree (Verbruggen et al., 2005 and references therein).

The morphometric study involved gathering segment morphological and anatomical variables. For analyses of segment morphology, small plants (< 100 segments) were studied in their entirety, whereas series of segments spanning the entire thallus length were studied for larger specimens (totalling between 48 and 89 segments studied per specimen).

The position of segments within the thallus was determined as the distance of the segment to the basal segment (number of intermediate nodes; variable s1). Segments were classified in three groups according to their location along the thallus axis: the lower-most 25% (s2 = 1), the central 50% (s2 = 2), and the apical-most 25% (s2 = 3). The binary variable apical (s3) was set to 1 for apical segments or 0 for non-apical segments. It was also noted whether the segments were calcified or not (s4). The local branching pattern was characterized by counting the number of sister segments (s5) and the number of daughter segments (s6).

Table 1. Specimens in the morphometric study. Given are their accession number in the GENT herbarium and geographic origin.

section	species	GENT	geographic origin
Rhipsalis	*H. borneensis*	HV18-1	Zanzibar Island (Tanzania)
		HV183b	Tahiti, French Polynesia
	H. macroloba	HV38	Zanzibar Island (Tanzania)
		HV45	Mnazi Bay, Tanzania
		HV206	Tahiti, French Polynesia
Micronesicae	*H. micronesica*	H.0014-1	Great Barrier Reef, Australia
		WLS184-02	Wallis Island (France)
		WLS420-02	Wallis Island (France)
Halimeda	*H. lacunalis*	HV306-1	Rangiroa, French Polynesia
		HV308-1	Rangiroa, French Polynesia
	H. taenicola	HV285-1	Rangiroa, French Polynesia
		HV285-2	Rangiroa, French Polynesia
		HV306-3	Rangiroa, French Polynesia
	H. tuna	H.0113-1	Naples, Italy
		HV319	Rosas, Spain
Pseudo-Opuntia	*H. gracilis*	HV312-1	Rangiroa, French Polynesia
		HV317-1	Rangiroa, French Polynesia
Opuntia	*H. goreauii*	H.0257	Bocas del Toro, Panama
		H.0258-1	Galeta, Panama
	H. opuntia	HV46b	Mnazi Bay, Tanzania
		HV61	Moorea, French Polynesia

All segments were digitally photographed, numbered, and aligned with their base pointing

downwards. Six qualitative characters used in traditional taxonomy were gathered for a subset of the specimens (Verbruggen et al., 2005: table 3: s7–s12). These variables are referred to as categorical shape variables. Using landmarks superimposed on the digital segment pictures, a series of size properties of the segments were calculated (Verbruggen et al., 2005: figure 2a, 2b and table 3: s13–s17). These variables are called conventional measurements; they showed a log-normal distribution and were transformed using the neperian logarithm (= logarithm with e as base) when necessary. The ratio shape variables were calculated from the conventional measurements; they are ratios of conventional measurements (Verbruggen et al., 2005: table 3: s18–s22). A geometric landmark analysis (Bookstein, 1989, 1991; Rohlf & Marcus, 1993) was carried out on the landmarks under the conditions specified in Verbruggen et al. (2005). Partial warp scores were extracted and saved to variables s23–s28. An elliptic Fourier analysis (Kuhl & Giardina, 1982) was carried out on the digitized segment outlines in Morpheus et al. (Slice, 2000) with settings as in Verbruggen et al. (2005). The ten extracted harmonics yielded a total of 40 fourier coefficients (Verbruggen et al., 2005: table 3: s29–s68).

From each specimen, between five and eight segments spanning the thallus from the basal to the apical region dissected. In total, data was gathered for 30 variables (Verbruggen et al., 2005: table 4: a1–a30). Ten replicate measurements were made for all structures. The different measurements are visualized in Verbruggen et al. (2005: figures 2d & 2e). Measurements were taken from the medullar filaments throughout the segment (a1–a8) and at the node (a9–a11). Utricular properties were recorded from the outer three layers (a12–a16, a17–a23 and a24–a30 for the peripheral, secondary and tertiary utricles, respectively).

Exploratory analyses

A number of correlation-matrix based principal components analyses (PCA) were performed on a subset of segments and variables. The first analysis was carried out on the conventional measurements, ratio shape variables and partial warp scores (s13–s28). All segments were included in this analysis. The second PCA included only anatomical variables. It concerns medullar and nodal characters a1–a6, a9 and a10, the variables associated with the peripheral utricles except a16, and some associated with the secondary utricles (a17–a20). Variables a11 and a16 were omitted because they were not applicable throughout the genus. The tertiary utricles were left out for the same reason. Variables a7 and a8 were left out because they are dependent on a6 (a6 + a7 + a8 = 1). In this analysis, only dissected segments were included. The third ordination is a combined analysis of segment morphological and anatomical data (s13–s28, a1–a6, a9, a10, a17–a20). Only dissected segments were included. A fourth ordination was carried out on the combined data set plus the thallus structure variables (s1–s6). In this analysis too, only dissected segments were included. All ordinations were carried out with the PCA&CA module of Statistica 6.0 (Statsoft Inc., Tulsa, OK).

Calculation of segment deviation and identification of deviant segments

The deviation of a segment within the specimen to which it belonged was estimated as the Euclidian distance between the segment and its specimen mean in the space spanned by the axes of ordinations of different subsets of variables.

Segment morphology

Deviation in segment size was calculated for each segment as the Euclidian distance between the position of the segment in question and the specimen mean in the multivariate space spanned by all four principal components resulting from a PCA of the log-transformed s13–s15 and s17. To calculate deviation in segment shape, the same procedure was used in the multivariate space spanned by the 23 principal components resulting from a PCA of ratio shape variables, partial warp scores, and fourier coefficients (first three harmonics only). A single measure of deviation of segment morphology was calculated by assessing the multivariate distances between the segments in question and the specimen

mean in the space spanned by the four principal components from the segment size PCA above and the first four principal components from the segment shape PCA above. The three measures of segment morphology deviation explained above were calculated for all 1346 segments in the study.

Anatomy

The Euclidian distance between the location of the specimen mean and the segment in the multivariate space spanned by all seven principal components resulting from a PCA of variables a12–a15 and a17–a19 was calculated as a measure of deviation in cortical structure. The deviation in medullar structures was based on the multivariate distances in the space spanned by the axes of the PCA of a1–a5 and a9–a10. The general measure of anatomical deviation was calculated for the space spanned by the first four principal components of both anatomy-based PCAs described above. The three measures of anatomical deviation were calculated for all 104 dissected segments.

For all six types of deviation, segments with the 10% highest Euclidean distances were considered seriously deviant.

Typification of the seriously deviant segments

In order to typify the seriously deviant segments, their frequency patterns against thallus part (s2), apicality (s3), and calcification state (s4) were analysed. We used chi-square tests to test for significant deviations from the expected frequencies. Since for some cells in some tables the expected frequency exceeded the absolute value of the difference between the observed and expected frequency, log-likelihood ratio tests were used in addition to the chi-square tests. The G-values listed in Table 2 are equal to the double of the sum of all log-likelihood ratios in the table. For contingency tables containing cells with counts less than five, chi-square and G-statistics were computed using Yates' correction. To complete the picture, ANOVA was used to test whether or not the deviation measures differed significantly between segments with different states of thallus part (s2), apicality (s3) and calcification state (s4). The effect of thallus part was tested using single-factor ANOVAs and differences were pointed out using Tukey HSD post-hoc comparisons. The effects of apicality and presence of calcification were tested together in main-effects ANOVAs (no interactions). Segments from the basal thallus region were excluded from this analysis since apical and non-calcified segments usually don't occur in this region.

Influence of deviant segments on taxonomic power

Taxonomic power of the morphometric data was estimated by comparing the adequacy of group membership prediction of segments in discriminant analysis (DA). Species-level clades from the molecular phylogeny were used as the a priori groups for the DA. To assess the influence of deviant segments, three different DA models for discriminating between the nine species in the study were built from a selection of segment morphological variables (s13, s17, s21–s28). The three models differed in the segments that they included. The first model included all segments; the second model included only segments that were not seriously deviant; and the third model excluded segments from the basal thallus region, apical segments and non-calcified segments. Henceforth, these latter three segment types will be abbreviated as B-segments (basal zone), A-segments (apical) and N-segments (non-calcified), and the union of these segment types as BAN-segments. All effects were entered at once, prior probabilities were set to equal and cross-validation was set so that 50% randomly chosen segments were used to build the model and the remaining segments were used to evaluate it. This procedure was repeated 20 times with different randomizations of which segments to use for model building and which for testing.

For the anatomy, a similar approach was used. The same three DA models were built using variables a1–a5, a9, a10, a12–a15, a17–a19. Again, we performed DA in a non-stepwise manner with equal prior probabilities. Owing to the relatively low number of segments after the removal of BAN-

segments, we chose not to use cross-validation to test the anatomy-based model. So in all three cases, all available segments (except those excluded by the model of course) were used to build and test the model.

Although most assumptions for DA were met, heteroscedasticity (nonconstant variance) was an issue. Because DA is robust against violation of the heteroscedasticity assumption (Lachenbruch, 1975; Klecka, 1980), we further disregarded this assumption (see also Verbruggen et al., 2005). Owing to the meticulous selection of variables for our models, multicollinearity was not an issue (see also Verbruggen et al., 2005). All DAs were performed using the GDA module of Statistica 6.0 (Statsoft Inc., Tulsa, OK).

The classification successes of the three discriminant models based on morphological data were compared using a one-way ANOVA and a Tukey HSD post-hoc test. Both these analyses were carried out in the ANOVA module of Statistica 6.0 (Statsoft Inc., Tulsa, OK).

Results

Molecular phylogeny

Figure 3 from Verbruggen et al. (2005) shows the placement of specimens used in our morphometric analyses within a phylogeny of the genus. All our specimens clustered within or as the closest sister to existing species clades.

Basic statistics

The dataset consisted of 21 specimens (Table 1). From a total of 1346 segments, data for 62 variables relating to the morphology of the segment and local thallus structure were gathered (6 thallus structure variables, 5 size variables, 5 ratio variables, 6 partial warp scores, 40 fourier coefficients). In addition, six categorical variables were coded for a subset of 536 segments. Within the 104 segments that were dissected, a total of 2193 utricles were measured. Of these, 1008 were peripheral. From the slides with the medullar siphons, data was gathered from 827 nodal structures and 982 medullar siphon branches.

Ordinations

Fig. 1 shows the biplots of the PCAs performed on the segment morphological (Fig. 1a), anatomical (Fig. 1b), and combined (Fig. 1c) data sets. In all three PCAs the first two principal components accounted for about 50% of the total variance. The biplot of the segment morphological data (Fig. 1a) showed no separation between species. Although species clusters were clearly present, they showed large overlap, both between closely and distantly related taxa. As for the variables, the distinction between the size descriptors (fourth quadrant; e.g. L_length, L_attach) and the shape descriptors (first and third quadrant; e.g. att_wd, pw_2X) was clear. Nonetheless, certain shape aspects were correlated with size (e.g. pw_uniY and L_width).

In the PCA biplot of anatomical data (Fig. 1b) species clusters showed substantially less overlap than was the case for the segment morphological data. In general, closely related species clustered together. *Halimeda gracilis* fell out of the bunch because of its high loadings on the second principal component.

The third graph (Fig. 1c) was based on segment morphological and anatomical data. Segment size and shape variables were located primarily in the first and third quadrants whereas anatomical variables concentrated in the second quadrant. The first axis was strongly correlated with variables measuring the size of segments and anatomical structures. Many segment shape descriptors (ratio variables, partial warp scores) had intermediate loadings on the first axis while shape characters of anatomical structures had low loadings. The highest loadings on the second principal component came from a

subset of the segment shape variables. Owing to the limited number of cases, species clusters could hardly be recognized.

A fourth ordination (not shown) including the location of the segment along the thallus axis and the number of sister and daughter segments made clear that some of the morphometric variables correlate with these properties. For example, segments further away from the base were smaller and their medullar siphons were narrower. Also, the number of daughter segments was positively correlated with the width of the mother segment.

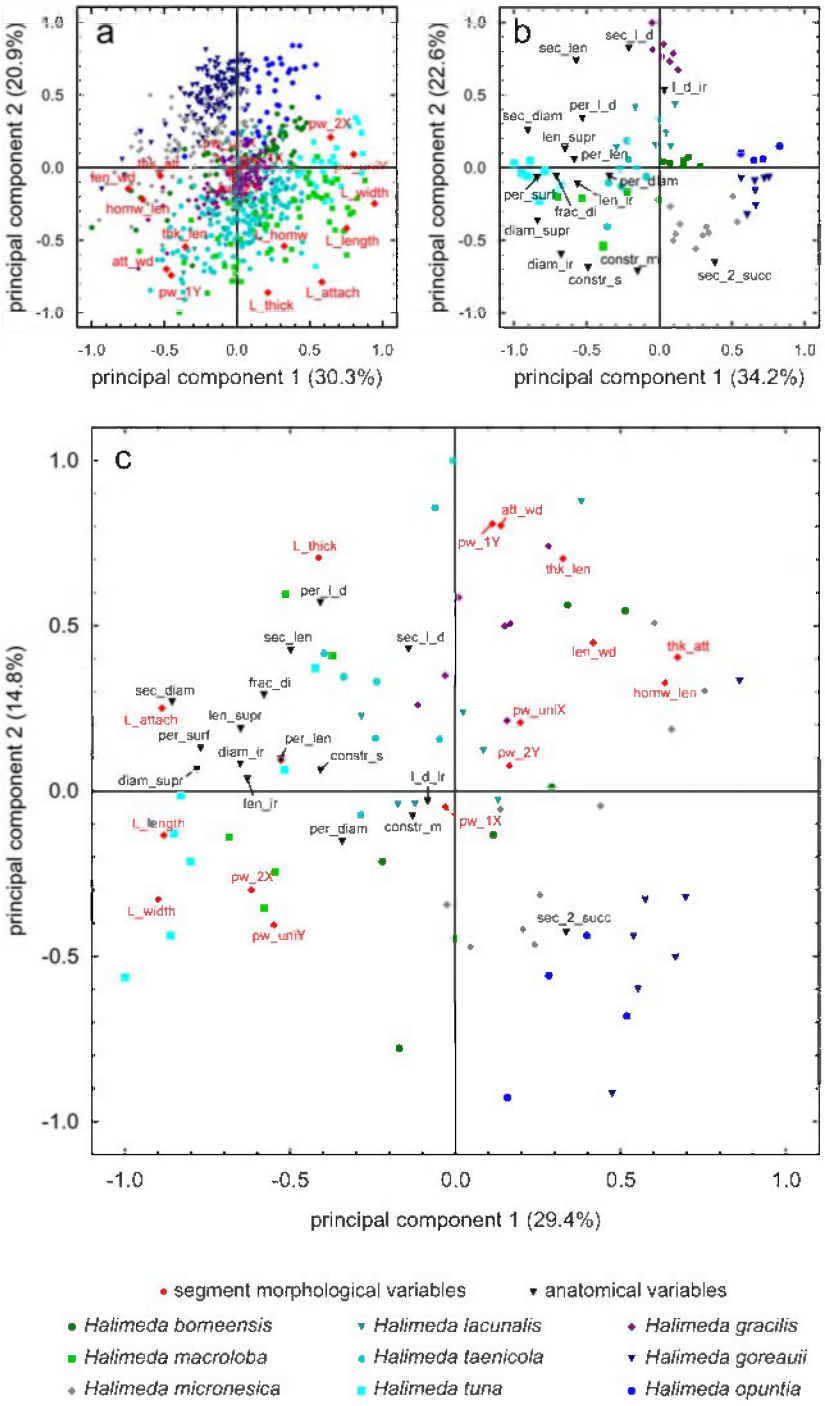

Fig. 1. Ordinations of morphometric data. a. PCA biplot of segment morphological data. b. PCA biplot of anatomical data. c. Biplot of the PCA based on segment morphological and anatomical data. Case coordinates were divided by the maximum absolute value to fit within the [-1,1] range.

Deviant segments

Fig. 2 shows representative examples of the patterns that segments' deviations follow along the thallus axis. Patterns tended to change according to the thallus habit of the species. For erect species, segment morphology was strongly deviant in the basal thallus region and less but variably deviant higher up the thallus. Sprawling species, on the other hand, showed no such pattern. With regards to anatomical data, no consistent patterns were observed. Nonetheless, the correlation between segment morphological deviation and anatomical deviation was significant (Fig. 3; Spearman rank test: $R = 0.3$, $p = 0.001$).

One-way ANOVA tests showed that Euclidean distances between segments and their specimen mean were significantly different in the different thallus parts, both for segment morphology ($F = 65.2$, $p < 0.001$) and for anatomy ($F = 4.28$, $p = 0.016$). The patterns however, differed between segment morphological and anatomical deviations. Deviations of segment morphology are significantly higher in the basal thallus region than higher up the thallus (Tukey HSD: $p < 0.001$) while there is no significant difference between the central and the apical thallus regions ($p = 0.889$). Anatomical deviations were high in the basal and apical thallus parts, and low in the central part. The only significant difference was between the deviations of basal and central parts (Tukey HSD, $p = 0.015$).

The apicality of a segment proved to have a significant effect on its morphological deviation ($F = 4.13$, $p = 0.042$) but not on its anatomical deviation ($F = 0.79$, $p = 0.37$). Calcification, on the other hand, seemed to influence the deviation of the anatomical and not of the segment morphological observations: the deviation of anatomical observations was significantly higher for non-calcified segments ($F = 3.98$, $p = 0.049$).

Frequency tables of seriously deviant segments (Table 2) supported the observation that segment morphology was much more deviant in the basal thallus region. The probability of encountering a seriously deviant segment in the basal-most quarter of the thallus is about 40% and the chi-square and log-likelihood-ratio tests showed that serious segment morphological deviation and thallus part were related (p-values < 0.001 for deviation of size, shape and general morphology). In general, the groups of apical and non-calcified segments did not turn out to contain more deviant segments than could be expected by chance alone.

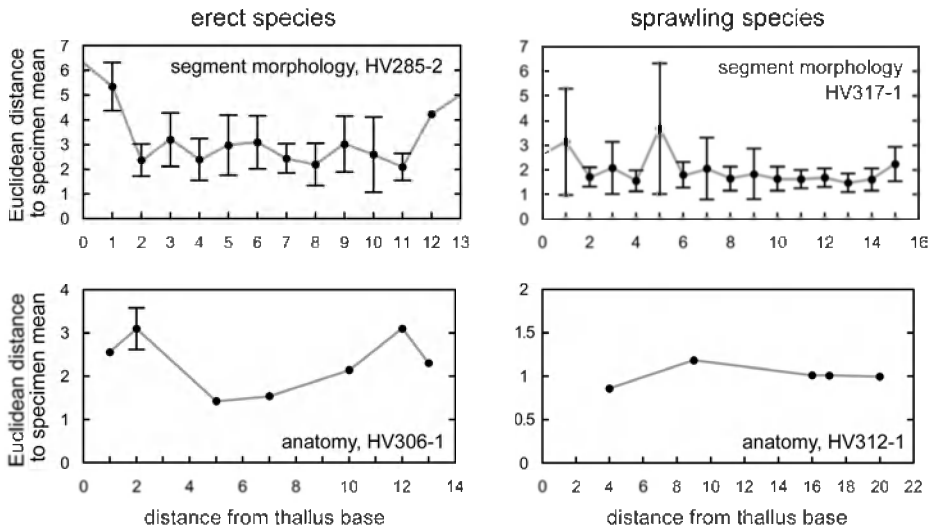

Fig. 2. Deviance of segments as a function of their distance from the thallus base. The graphs depict the course of the Euclidean distance between individual segments and the average segment in multivariate space as a function of the segments' location in the thallus. The upper graphs refer to segment morphological data; the lower graphs concern anatomical data. The graphs on the left hand side concern erect species (HV285-2, *H. taenicola* and HV306-1, *H. lacunalis*); those on the right hand side refer to sprawling species (HV312-1 and HV317-1, both *H. gracilis*). Deviances are given as the average ± 1 S.D.

Table 2. Frequency tables showing patterns of deviance. Observed frequencies of non-deviant and deviant segments are given in each first and second data column, respectively. Each third column gives the probability of deviance for the segment property in question. When larger than 0.25, this value is in boldface. Frequency tables are given for each of six variable groups (columns) and three segment characteristics (rows). The results of the chi-square and log-likelihood ratio tests for deviances from the expected frequencies are also listed: the chi-square and G-values are followed by the level of significance (*: 0.05 > p > 0.01; **: 0.01 > p > 0.001; ***: 0.001 > p). Subscripts c denote that Yates' correction was used.

		segment size			**segment shape**			**segment morphology**		
		no	yes		no	yes		no	yes	
thallus part	base	85	59	**0.41**	89	55	**0.38**	90	54	**0.38**
	center	763	47	0.06	758	52	0.06	755	55	0.07
	apex	361	31	0.08	362	30	0.08	364	28	0.07
		χ^2 = 169 (***)			χ^2 = 139 (***)			χ^2 = 132 (***)		
		G = 115 (***)			G = 96.1 (***)			G = 91.3 (***)		
apical	no	886	92	0.09	870	108	0.11	875	103	0.11
	yes	323	45	0.12	339	29	0.08	334	34	0.09
		χ^2 = 2.33			χ^2 = 2.93			χ^2 = 0.49		
		G = 2.25			G = 3.07			G = 0.50		
calcified	no	177	29	0.14	187	19	0.09	191	15	0.07
	yes	1032	108	0.09	1022	118	0.1	1018	122	0.11
		χ^2 = 4.05 (*)			χ^2 = 0.24			χ^2 = 2.23		
		G = 3.73			G = 0.25			G = 2.41		

		medulla			**cortex**			**anatomy**		
		no	yes		no	yes		no	yes	
thallus part	base	14	7	**0.33**	15	6	**0.29**	15	6	**0.29**
	center	55	3	0.05	53	5	0.09	55	3	0.05
	apex	21	3	0.13	22	2	0.08	20	4	0.17
		χ^2_c = 10 (**)			χ^2_c = 5.8			χ^2_c = 7.5 (**)		
		G_c = 7.7 (**)			G_c = 3.5			G_c = 5.6 (*)		
apical	no	78	8	0.09	74	12	0.14	78	8	0.09
	yes	12	5	**0.29**	16	1	0.06	12	5	**0.29**
		χ^2 = 5.2 (*)			χ^2_c = 0.27			χ^2 = 5.2 (*)		
		G = 4.3 (*)			G_c = 0.29			G = 4.3 (*)		
calcified	no	9	5	**0.36**	13	1	0.07	9	5	**0.36**
	yes	81	8	0.09	77	12	0.13	81	8	0.09
		χ^2 = 7.8 (**)			χ^2_c = 0.05			χ^2 = 7.8 (**)		
		G = 6.1 (*)			G_c = 0.06			G = 6.1 (*)		

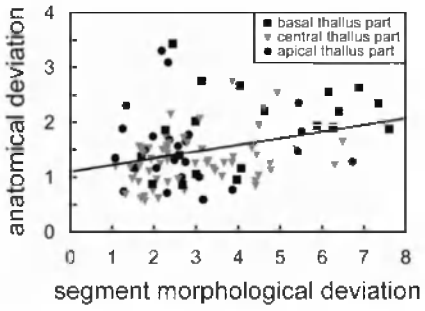

Fig. 3. (above) Scatterplot of deviation in segment morphological versus deviation in anatomical characters.

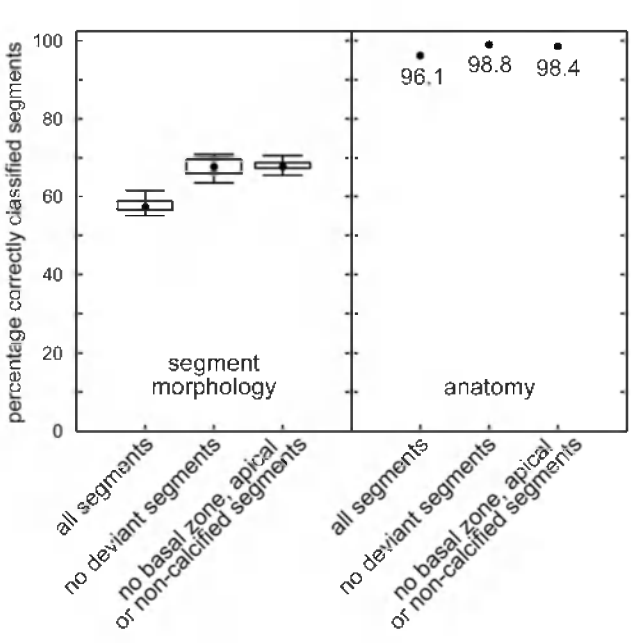

Fig. 4. (right) Adequacy of species group membership prediction of different groups of segments. The left-hand side of the graph depicts classification success of segment morphology-based DA models; the right-hand side is based on DA models built using anatomical variables. The segments that were included/excluded from the analyses are indicated along the horizontal axis. Boxes indicate the 25–75 percentile range and whiskers depict the non-outlier range.

Whereas the graphs for the anatomical data (Fig. 2, lower two graphs) did not show recurrent patterns and the ANOVAs left doubt for some characters, the contingency tables indicated that deviations of the observed frequencies from the expected frequencies were significant in the majority of cases. Significant deviation was observed for all the examined segment properties (thallus part, apicality and calcification). In all cases, the chi-square and log-likelihood ratio tests were significant for counts of segments seriously deviant in their medullar and general anatomical characters. When only cortical characters were examined, the observed frequencies of seriously deviant segments corresponded to the frequencies that could be expected by chance.

Influence of deviant segments on taxonomic power

Fig. 4 shows the classification success of individual segments in species groups, according to the six DA models built. Models incorporating all segments performed worst. For segment morphology, they achieved an average of 58% successful allocations. Both other models reached classification successes of about 10% higher. A one-way ANOVA showed that the differences were significant ($F = 178.15$, $p < 0.001$). A post-hoc comparison found significant differences between the model with all segments (model 1) and both other (2 & 3) models (Tukey HSD: $p < 0.001$ for both cases). The models that excluded all deviant segments (model 2) and BAN-segments (model 3) did not differ significantly.

Models based on anatomical variables yielded very good (> 95%) separation between species. The model built using all segments performed worse than both other models, which achieved very comparable membership predictions (96.1% versus 98.8% and 98.4%).

Discussion

Qualitative characters and measurements of a very limited number of structures have dominated *Halimeda* taxonomy for many years. Over the last few decades, however, it has become apparent that quite a few taxa are non-monophyletic, embodied considerable cryptic diversity, or are, perhaps as a consequence of regional bias, ill-defined (Noble, 1987; South, 1992; Dargent, 1997; Kooistra et al., 1999, 2002; Verbruggen & Kooistra, 2004). This and a parallel study (Verbruggen et al., 2005) aim to lay the foundation for a new approach towards taxonomy that encompasses molecular and morphometric information.

In the course of explorative analyses of our data, segments showing considerable morphometric deviation from the remainder of the segments in the specimen were detected. Deviations in both anatomical features and segment morphology were observed. The revelation that segments towards the base of the algal body showed larger deviation in erect species while they did not in sprawling species does not require much explanation. The basal segments of erect species are adapted for attachment to the substratum. Sprawling species, on the other hand, depend on secondary holdfasts for attachment. Their primary base is often difficult to track down or becomes lost altogether when the plants spread out and, with time and incidents, lose connection with their base. In our specimens of *H. gracilis* and *H. opuntia*, no primary holdfasts were present and the basal reference segment was arbitrarily chosen.

The observation that deviations at the base exceeded those of other thallus parts was confirmed statistically in subsequent analyses. It was also demonstrated that apical and non-calcified segments had a tendency towards aberrance. Although the latter had been previously indicated by the ANOVAs, the contingency tables provided conclusive evidence for the divergent proportions of seriously deviant segments in these segment types. Notwithstanding the fact that chi-square analyses prohibit drawing conclusions in terms of cause and consequence, in combination with the high probabilities of encountering seriously deviant segments in the non-calcified and apical segment classes and the results of the ANOVAs, little doubt remains about the anomaly of these segments. Here again, the explanation is obvious from the biology of *Halimeda* thalli. Branches grow one segment at a time (Hillis-Colinvaux et al., 1965, 1980; Drew & Abel, 1988; Hay et al., 1988). New segments develop at night (Hay et al.,

1988) and, during the following 2–3 days, grow to their full size and calcify (Hillis-Colinvaux et al., 1965, 1980; Hay et al., 1988). This probably explains why segment size was more often deviant in non-calcified segments. The number of segments with seriously deviant shape, on the other hand, did not appear to be related to the degree of calcification of the segment, indicating that segments take on a shape similar to that of adult segments before completion of the calcification process. This is also suggested in Figure 1b from Hay et al. (1988).

From an anatomical point of view, segment formation starts from uncorticated regions on the distal rim of the mother segment (Hillis-Colinvaux, 1980). From these regions, a tuft of filaments grows outwards. This tuft becomes increasingly organized and starts showing differentiation between medulla and cortex between day 1 and 2. Utricles attach to one another near the end of this period. After this, substantial growth of filaments and utricles still has to occur to attain the final segment size around day 2–3. This explains why the non-calcified segments in our study were often seriously deviant in anatomical characters. These non-calcified segments typically had attached utricles and had already taken the final segment form, but had not yet attained the final segment size. As a consequence, utricles and medullary filaments were smaller than those of adult segments.

The question remains: does the incorporation of deviant segments into a morphometric dataset hamper taxonomic studies based on this dataset? Using the discriminant analysis methods introduced in Verbruggen et al. (2005), the effect of exclusion of certain segment types on the taxonomic power of the morphometric data was verified. The statistical experiment was designed to allow three comparisons. Firstly, the effect of introducing deviant segments to the analysis was verified. Secondly, the effect of introducing BAN-segments was examined. Lastly, the taxonomic power of models with deviant segments was compared to that of models with BAN-segments.

The juxtaposition of the results with and without deviant segments leaves no doubt about the significant deterioration of discriminating power caused by the deviant segments (Fig. 4, left panel). For anatomical data, results cannot be compared statistically, but a rise of taxonomic power was observed when deviant segments were omitted (Fig. 4, right panel). Similarly, excluding BAN-segments yielded results comparable to analyses that excluded deviant segments. This result, in combination with the observation that deviant segments are primarily found in BAN-regions, suggests that BAN-segments are primarily responsible for the lowered taxonomic power in our analyses that included all segments.

In earlier taxonomic works, the use of mature segments from the central thallus region for anatomical investigation was proposed (Taylor, 1950; Hillis-Colinvaux, 1980), however without any rationale being given. In more recent literature it was shown that aberrant basal segments can actually aid taxonomy. Noble (1986) was the first to illustrate the difference in anatomy of segments from the base and center of thalli and used this information as supplementary evidence to erect *H. magnidisca*. Dragastan et al. (2002) investigated the anatomy of segments throughout the thalli of recent species and compared these to the anatomy of fossil segments. They provided convincing evidence that several fossil segments were mistakenly described as new species while they actually concerned aberrant (basal) segments of recent species.

Deviant segments from the basal thallus region have thus on the one hand generated substantial taxonomic confusion in the past, but on the other hand integration of their morphological properties has led to a firmer taxonomy. Our data clearly confirm the first statement: we demonstrated that basal segments blur group boundaries. Unfortunately, in its current form and extent, our dataset prohibits testing the second statement of increased taxonomic adeptness by incorporating information of basal segments as a set of additional characters.

The present study explored a combined molecular and morphometric approach towards *Halimeda* taxonomy. Our aim with this combined approach was to tackle taxonomic issues within complexes of closely related or morphologically similar species. With the present sampling and analysis methods,

deviant segments significantly lowered the taxonomic power of the data. Exclusion of all seriously deviant segments or only BAN-segments yielded nearly-identical results. Therefore, we suggest exclusion of BAN segments from future studies. However, if the present morphometric method fails in certain cases, the answer could lie in the incorporation of deviant segments. In this case, data from the basal segments must not be merged with that of segments from the central region but must be coded in separate variables. In other words, they must be treated as a supplementary source of data.

References

H.V. is indebted to the Bijzonder Onderzoeksfonds (Ghent University, grant 011D9101) and O.D.C. to the Fund for Scientific Research Flanders (grant 3G002496 and postdoctoral research grant). We thank Wiebe Kooistra for providing many of the specimens used in this study and Ellen Cocquyt for laboratory assistance and extensive fine-tuning of the molecular methods. H.V. acknowledges Claude Payri, Paino Vanai and the Environmental Service of Wallis and Futuna for facilitating fieldwork on Uvea Island. We thank two reviewers and the communicating editor for their valuable suggestions and improvements to the manuscript.

References

Bookstein F.L., 1989. Principal warps: thin-plate splines and the decomposition of deformations. *IEEE Transaction on Pattern Analysis and Machine Intelligence* 11: 567–585.

Bookstein F.L., 1991. *Morphometric tools for landmark data.* Cambridge, Cambridge University Press, 435 pp.

Dargent O., 1997. Etude systématique du genre *Halimeda* (Caulerpales, Bryopsidophycées), dans la zone de contact entre l'Océan Indien et l'Océan Pacifique. MSc thesis, Université Pierre et Marie Curie (Paris VI), Paris, France, 30 pp.

Dragastan O.N., Littler D.S. & Littler M.M., 2002. Recent vs. fossil *Halimeda* species of Angaur Island, Palau and adjacent western Pacific areas. *Acta Palaeontologica Romaniae. Special publication no. 1.* Cartea Universitara, University of Bucharest, Bucharest, Romania, 20 pp.

Drew E.A. & Abel K.M., 1988. Studies on *Halimeda.* II: Reproduction, particularly the seasonality of gametangia formation, in a number of species from the Great Barrier Reef Province. *Coral Reefs* 6: 207–218

Hay M.E., Paul V.J., Lewis S.M., Gustafson K., Tucker J. & Trindell R.N., 1988. Can tropical seaweeds reduce herbivory by growing at night? Diel patterns of growth, nitrogen content, herbivory, and chemical versus morphological defenses. *Oecologia* 75: 233–245

Hillis-Colinvaux L., Wilbur K.M. & Watabe N., 1965. Tropical marine algae: growth in laboratory culture. *Journal of Phycology* 1: 69–78.

Hillis-Colinvaux L., 1980. Ecology and taxonomy of *Halimeda*: primary producer of coral reefs. *Advances in Marine Biology* 17: 1–327.

Klecka W.R., 1980. *Discriminant analysis*. Sage, Beverly Hills, CA.

Kooistra W.H.C.F. & Verbruggen H., 2005. Genetic patterns in the calcified tropical seaweeds *Halimeda opuntia*, *H. distorta*, *H. hederacea* and *H. minima* (Bryopsidales, Chlorophyta) provide insights in species boundaries and inter-oceanic dispersal. *Journal of Phycology* 41: 177–187.

Kooistra W.H.C.F., Caldéron M. & Hillis L.W., 1999. Development of the extant diversity in *Halimeda* is linked to vicariant events. *Hydrobiologia* 398: 39–45.

Kooistra W.H.C.F., Coppejans E.G.G. & Payri C., 2002. Molecular systematics, historical ecology and phylogeography of *Halimeda* (Bryopsidales). *Molecular Phylogenetics and Evolution* 24: 121–138.

Kuhl F.P. & Giardina C.R., 1982. Elliptic Fourier features of a closed contour. *Computer Graphics and Image Processing* 18: 236–258.

Lachenbruch P.A., 1975. *Discriminant Analysis*. Hafner Press, New York.

Littler D.S. & Littler M.M., 2000. *Caribbean reef plants. An identification guide to the reef plants of the Caribbean, Bahamas, Florida and Gulf of Mexico.* OffShore Graphics, Washington, 542 p.

Littler D.S. & Littler M.M., 2003. *South Pacific reef plants. A divers' guide to the plant life of South Pacific coral reefs.* OffShore Graphics, Washington, 331 pp.

Noble J.M., 1986. *Halimeda magnidisca* (Caulerpales, Chlorophyta), a new species from the Great Barrier Reef, Australia. *Phycologia* 25: 331–339.

Noble J.M., 1987. A taxonomic study of the genus *Halimeda* Lamouroux (Chlorophyta, Caulerpales) from the Heron Island region of the southern Great Barrier Reef, Australia. MSc thesis, University of Melbourne, Melbourne, Australia. 200p.

Rohlf F.J. & Marcus L.M., 1993. A revolution in morphometrics. *Trends in Ecology and Evolution* 8: 129–132.

Saunders G.W. & Lehmkuhl K.V., 2003. Molecular phylogeny and the biodiversity of algae: a chronic cascade of cryptic taxa. *Book of Abstracts*. Third European Phycological Congress, Queen's University Belfast, p 38.

Siemer B.L., Stam W.T., Olsen J.L. & Pedersen P.M., 1998. Phylogenetic relationships of the brown algal orders Ectocarpales, Chordariales, Dictyosiphonales, and Tilopteridales (Phaeophyceae) based on RUBISCO large subunit and spacer sequences. *Journal of Phycology* 34: 1038–1048.

Slice D.E., 2000. Morpheus *et al.* Software for morphometric research. Beta version of 01/31/2000. Free for download from http://life.bio.sunysb.edu/morph/morpheus/

South G.R., 1992. Contributions to a catalogue of the Marine Algae of Fiji. 1. Halimeda (Chlorophyceae). *Marine Studies Program, volume 2*. Fiji, The University of the South Pacific, 16 pp.

Taylor W.R., 1950. *Plants of Bikini and other Northern Marshall Islands.* Ann Arbor, University of Michigan Press, 227 p.

Taylor W.R., 1960. *Marine algae of the eastern tropical and subtropical coasts of the Americas.* Ann Arbor, University of Michigan Press, 870 p.

van der Strate H.J., Boele-Bos S.A., Olsen J.L., van de Zande L. & Stam W.T., 2002. Phylogeographic studies in the tropical seaweed *Cladophoropsis membranacea* (Chlorophyta, Ulvophyceae) reveal a cryptic species complex. *Journal of Phycology* 38: 572–582.

Verbruggen H. & Kooistra W.H.C.F., 2004. Morphological characterization of lineages within the calcified tropical seaweed genus *Halimeda* (Bryopsidales, Chlorophyta). *European Journal of Phycology* 39: 213–228.

Verbruggen H., De Clerck O., Cocquyt E., Kooistra W.H.C.F. & Coppejans E., 2005. Morphometric taxonomy of siphonous green algae: a methodological study within the genus *Halimeda* (Bryopsidales). *Journal of Phycology* 41: 126–139.

Vroom P.S., Smith C.M. & Keeley S.C., 1998. Cladistics of the Bryopsidales: a preliminary analysis. *Journal of Phycology* 34: 351–360.

Zuccarello G.C. & West J.A., 2003. Multiple cryptic species: Molecular diversity and reproductive isolation in the *Bostrychia radicans/B. moritziana* complex (Rhodomelaceae, Rhodophyta) with focus on North American isolates. *Journal of Phycology* 39: 948–959.

Zuccarello G.C., Sandercock B. & West J.A., 2002. Diversity within red algal species: variation in world-wide samples of *Spyridia filamentosa* (Ceramiaceae) and *Murrayella periclados* (Rhodomelaceae) using DNA markers and breeding studies. *European Journal of Phycology* 37: 403–417.

Part 5

DNA barcoding and morphometrics pinpoint species boundaries

Molecular and morphometric data pinpoint species boundaries in *Halimeda* section *Rhipsalis*

Heroen Verbruggen, Olivier De Clerck, Wiebe H.C.F. Kooistra & Eric Coppejans

Journal of Phycology 41: in press (2005)

Abstract

Molecular systematic studies have changed the face of algal taxonomy. Particularly at the species level, molecular phylogenetic research has revealed the inaccuracy of morphology-based taxonomy: cryptic and pseudo-cryptic species were shown to exist within many morphologically conceived species. This study focused on section *Rhipsalis* of the green algal genus *Halimeda*. This section was known to contain cryptic diversity and to comprise species with overlapping morphological boundaries. In the present study, species diversity within the section and identity of individual specimens were assessed using ITS1–5.8S–ITS2 (nrDNA) and *rps*3 (cpDNA) sequence data. The sequences grouped in a number of clear-cut genotypic clusters that were considered species. The same specimens were subjected to morphometric analysis of external morphological and anatomical structures. Morphological differences between the genotypic cluster species were assessed using discriminant analysis. It was shown that significant morphological differences exist between genetically delineated species and that allocation of specimens to species on the basis of morphometric variables is nearly perfect. Anatomical characters yielded better results than external morphological characters. Two approaches were offered to allow future morphological identifications: a probabilistic approach based on classification functions of discriminant analyses, and the classical approach of an identification key.

Introduction

The last two decades have seen the incorporation of molecular phylogenetic methods in algal systematic research. Several studies have shown that morphological taxonomic insights did not correspond with the evolutionary history inferred from DNA sequences. This has been especially true for species-level studies, in which many cases of cryptic and pseudo-cryptic diversity were revealed (e.g. van der Strate et al. 2002, Zuccarello and West 2003, Gurgel et al. 2003, Cohen et al. 2004, De Clerck et al. 2005). Cryptic species are species that are morphologically indistinguishable whereas pseudo-cryptic entities are distinguishable morphologically once the appropriate characters are considered (Knowlton 1993). Such key-traits may not immediately catch the attention of the observer because they are often more subtle than trends in environmentally induced phenotypic plasticity shared among the entities. Morphological plasticity in its own right has also lead to erroneous taxonomy; several molecular phylogenetic studies have demonstrated that morphological oddities at the fringes of the plasticity spectrum have been described as new species (e.g. Zuccarello and West 2002, Yano et al. 2004, Kooistra and Verbruggen 2005).

Thalli of the tropical green algal genus *Halimeda* are composed of green, calcified segments (Lamouroux 1812, Hillis-Colinvaux 1980). Anatomically, the thalli consist of a single, branched, siphonous cell. The highly organized siphonous branches form the segments and string them together (Barton 1901, Hillis-Colinvaux 1980). *Halimeda* is a well-studied example of a genus in which species diver-

sity was underestimated by morphology-based taxonomy. First, all but one of the pantropical species were shown to consist of two unrelated species, one inhabiting the Caribbean and a second populating Indo-Pacific coasts (Kooistra et al. 2002). Second, a considerable number of additional cryptic species were found within both ocean basins (Verbruggen and Kooistra 2004, Verbruggen et al. submitted).

Systematists are now facing the challenge of distinguishing among species that have not been recognized by many generations of alpha-taxonomists. In an attempt to provide a tool for this purpose, Verbruggen et al. (2005a, b) applied a series of morphometric techniques to nine *Halimeda* species representing the five sections of the genus. The present study puts the morphometric techniques explored in Verbruggen et al. (2005a) into practice within *Halimeda* section *Rhipsalis*. In this section, medullar siphons that go through the nodes between segments fuse with their neighbors laterally, resulting in a meshwork of pores interconnecting the siphons at the height of the node (Kooistra et al. 2002, Verbruggen and Kooistra 2004). The section is further characterized by segment agglutination in the basal thallus region (Kooistra et al. 2002, Verbruggen and Kooistra 2004). Most species belonging to section *Rhipsalis* grow on sandy or muddy substrates of tropical lagoons and mangroves. Their holdfast is modified into a large bulbous structure to allow attachment in loose substratum. However, this holdfast type is not a defining trait for the section because bulbous holdfasts can be found, at times, in other sections (Verbruggen and Kooistra 2004) and one species in the section (*H. melanesica*, species authorities listed in Appendix 1) has lost the bulbous holdfast secondarily (Kooistra et al. 2002, Verbruggen and Kooistra 2004).

The section features several taxonomic problems. First, Noble (1987) noticed that the absence of nodal fusions, which sets *H. melanesica* apart from other species, was not constant within the species. She noted considerable blurring of the boundary between *H. melanesica* and *H. incrassata* because of this variability. Second, *H. incrassata* turned out to consist of two unrelated species, one in the Atlantic and one in the Indo-Pacific (Kooistra et al. 2002). The morphological boundaries between the entities remained a mystery. Third, current species boundaries contradict genetic patterns in the species pair *H. simulans–borneensis*. On a morphological basis, *H. borneensis* was thought to be restricted to SW Pacific waters. *Halimeda simulans* was reported from the Caribbean and several locations in the Indo-Pacific (Hillis-Colinvaux 1980). Verbruggen et al. (2005a) showed that Indo-Pacific specimens identified as *H. simulans* did not belong to the clade of Atlantic *H. simulans* but instead clustered with *H. borneensis*. Fourth, a similar situation occurs with the *H. monile–cylindracea* species pair. *Halimeda cylindracea* is an Indo-Pacific species, and Indo-Pacific specimens identified as *H. monile* belong to *H. cylindracea*. Fifth, the status of *H. stuposa*, which had never been questioned in traditional taxonomic research, was doubted by Kooistra et al. (2002) because the SSU sequence obtained from an isotype specimen was nearly identical to that of *H. borneensis*.

This study aims (1) to identify genotypic clusters in a set of ITS1–5.8S–ITS2 and *rps*3 sequences and to redefine species on the basis of these clusters, (2) to assess whether it is possible to distinguish between genotypic cluster species on the basis of morphometric variables, (3) to pinpoint species boundaries using morphometric variables, (4) to present a probabilistic approach toward species identification based on measurements of anatomical structures, and (5) to present a more classical identification method (i.e. a dichotomous key).

Materials and methods

Specimen collection, DNA sequencing and phylogenetic inference

Specimens were collected from natural populations throughout the species' ranges (Appendix 1). Part of the thallus was preserved in ethanol 95% or silica-gel for DNA extraction; the remainder of the specimen was preserved in liquid preservative (ethanol 95% or formalin 5%) for morphometric analyses. Specimens were identified using Hillis-Colinvaux (1980).

Extraction of total genomic DNA followed Kooistra et al. (2002), but for a few specimens, a standard cetyl trimethyl ammonium bromide (CTAB) procedure was used. The nuclear ribosomal ITS1–5.8S–ITS2 region and the plastid UCP7 region (*rps*19–*rps*3) were amplified according to Kooistra et al. (2002) and Provan et al. (2004), respectively. Sequences were determined with forward and reverse primers, using an ABI Prism 3100 automated sequencer (Applied Biosystems, Foster City, CA). Of the *rps*19–*rps*3 sequences, partial *rps*19 and the intergenic spacer were discarded, leaving only partial *rps*3 sequences. The *rps*3 sequences were aligned on the basis of their amino acid sequences using ClustalW 1.82 with default settings (European Bioinformatics Institute [EBI] server, www.ebi.ac.uk /clustalw). The ITS1–5.8S–ITS2 sequences were aligned using ClustalW 1.82 (EBI server, default settings). Sequences and alignments were submitted to Genbank (see Appendix 1 for accession numbers) and Treebase (preliminary accession number SN2128).

Both alignments were subjected to MP analysis in PAUP* 4.0b10 (Swofford 2003). Starting trees were obtained by random stepwise addition. A single tree was retained at each step. Branch swapping was achieved by tree bisection-reconnection. Gaps were treated as missing data. The number of rearrangements was limited to 100 million per addition-sequence replicate. The analysis performed 50 addition-sequence replicates and was carried out without outgroup (midpoint rooting). MP bootstrapping (1000 replicates) was performed using the same MP settings (Felsenstein 1985). Genotypic clusters in the DNA data were identified by eye from the obtained phylograms.

Morphometrics

Measurements and morphometric analyses were carried out as detailed in Verbruggen et al. (2005a), with a number of modifications. Per specimen, ten segments were photographed. These segments were picked at random, after exclusion of apical and non-calcified segments, and segments from the basal thallus zone, as recommended by Verbruggen et al. (2005b). From the aligned digital images, categorical shape variables were scored. Landmarks were placed on the images as described in Figure 2a of Verbruggen et al. (2005a) and served for landmark analysis and calculation of conventional measurements and ratio shape variables. In the light of the conclusions of Verbruggen et al. (2005a), elliptic Fourier analysis of segment outlines was omitted. Table 1 lists the segment variables and their abbreviations. Two data sets were constructed from the data: a first one with data of all segments (10 per specimen), and a second one with a single entry per specimen (median values of segments belonging to the specimen in question).

Measurements of anatomical structures were made according to Verbruggen et al. (2005a), with some slight modifications. Anatomical investigation was limited to a single segment from the central part of the thallus, following the recommendations of Verbruggen et al. (2005b). All anatomical observations were made with an Olympus BX51 microscope (Olympus Europe, Hamburg, Germany). The diameter of side branches of medullar siphons at their constriction was not measured. Peripheral utricles were drawn and digitized as described in Verbruggen et al. (2005a). Images were aligned to have the upper plane of utricles horizontal, and were overlain with a pattern of horizontal lines (Fig. 1A). The pattern consisted of five equidistant horizontal lines and was superimposed on the utricle in such a way that the upper line touched the top side of the utricle and the lower line went through the base of the utricle. Ten landmarks (see Fig. 1A) were digitized on the pictures using tpsDig 1.40 (Rohlf 2004). From the landmark files, several size and shape variables were calculated (Fig. 1B, C): utricle height and width, their ratio (formula 1), the relative width at 75, 50 and 25% of the utricle's height (formulas 2, 3 and 4). Table 2 lists the anatomical variables and their abbreviations. Ten replicate measurements per segment were made (e.g. measurements of ten random peripheral utricles within a single segment). Two data sets were created: a first one with data of all replicates (10 per specimen), and a second one with a single entry per specimen (median values of replicates). All data sets are available from the corresponding author upon request.

Table 1. Variables describing segment morphology.

categorical shape variables		
s01	form_seg	categorical segment form: reniform, ovate, elliptical, obovate, cuneate, rectangular
s02	seg_widt	categorical variable for relative segment width: narrow, medium, broad
s03	stalk	categorical variable describing the proximal stalk zone: absent, intermediate, present
s04	form_bas	categorical variable for the form of the segment base: auriculate to acute in five steps
s05	lobedne	categorical variable describing the segment's lobedness: absent, shallow, medium, deep
s06	numlobes	number of lobes: 1 to 6 (six meaning many)
conventional measurements		
s07	length	segment length (mm)
s08	width	segment width (mm)
s09	attach	width of attachment zone (mm)
s10	homw	height of maximal segment width (mm)
s11	thick	segment thickness (mm)
ratio shape variables		
s12	thk_len	relative segment thickness: thickness over length ratio
s13	thk_att	ratio of segment thickness over the width of the attachment zone
partial warp scores (landmark analysis)		
s14	pw_UniX	uniform shape change score X
s15	pw_UniY	uniform shape change score Y
s16	pw_1X	partial warp score 1X
s17	pw_1Y	partial warp score 1Y
s18	pw_2X	partial warp score 2X
s19	pw_2Y	partial warp score 2Y

Statistical analysis of morphometrics

Data exploration

Explorative data analysis included visual examination of univariate histograms. Measurement data were log-transformed for analyses requiring so (neperian logarithm; indicated with prefix L_ added to the variable name). Principal component analyses (PCA) were carried out to explore the multivariate data sets in more detail. All PCA were carried out in Statistica 6.0 (Statsoft, Tulsa, OK).

Initial discriminant analyses

The four data sets were subjected to discriminant analysis (DA) using the General Discriminant Analysis module of Statistica. Genotypic clusters found in the molecular phylogenies were used as a priori groups in DA. Classifications were carried out with equal prior probabilities and without cross-validation. All effects were entered at once.

DA of degenerate data sets

After initial DA, further DA were carried out on partial data sets, with the aim of singling out characters or character combinations that allow good separation between species. Structure coefficients of the canonical roots of previous DA were used as a guide for further DA: variables uncorrelated with major canonical roots were omitted. Furthermore, we closed in on specific species groups by including only those species in DA.

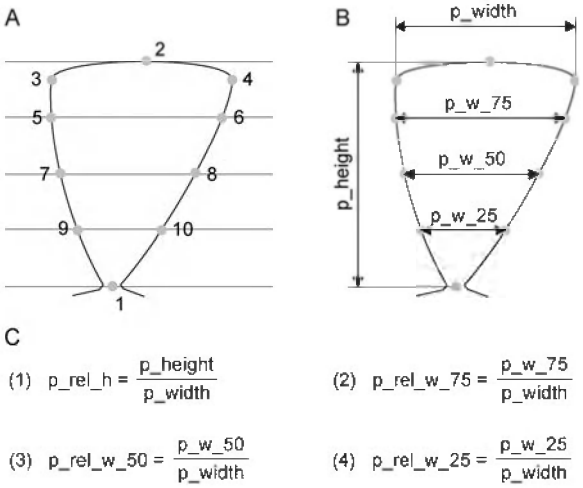

Fig. 1. Peripheral utricle measurements. Panel A shows how the utricles were overlain with a line pattern and the resulting ten digitized positions. Panel B illustrates the measurements calculated from the landmark files. Panel C shows the ratios calculated from the measurements.

Table 2. Variables describing anatomical structures.

medullar characters		
a01	diam_ir	distance between two subsequent ramifications (µm)
a02	constr_m	medullary siphon diameter (µm)
a03	len_ir	length over diameter ratio of the siphon segment: len_ir / dia_ir
a04	ir_rel_len	constriction of main branch diameter (µm)
a05	dichotomy	fraction dichotomous ramifications
a06	trichotomy	fraction trichotomous ramifications
a07	quadrichotomy	fraction quadrichotomous ramifications
nodal properties		
a08	node_act	distance from below node to supranodal ramification (µm)
a09	len_supr	thickness of the supranodal interramification (µm)
a10	diam_supr	actual pore size or node height (µm)
peripheral utricles		
a11	p_surf	surface diameter peripheral utricle (µm)
a12	p_height	height of peripheral utricle (µm)
a13	p_width	diameter of peripheral utricle (µm)
a14	p_rel_w_75	relative width of peripheral utricle at 3/4 of its height
a15	p_rel_w_50	relative width of peripheral utricle at 1/2 of its height
a16	p_rel_w_25	relative width of peripheral utricle at 1/4 of its height
a17	p_rel_h	relative height of utricle: p_height over p_width ratio
secondary utricles		
a18	s_height	height (µm) of the secondary utricle
a19	s_width	maximal diameter (µm) of the secondary utricle
a20	s_rel_h	relative height of secondary utricle: s_height over s_width ratio
a21	s_succ	number of peripheral utricles carried by the secondary utricle
tertiary utricles		
a22	t_height	height (µm) of the tertiary utricle
a23	t_width	maximal diameter (µm) of the tertiary utricle
a24	t_rel_h	relative height of tertiary utricle: t_height over t_width ratio
a25	t_succ	number of secondary utricles carried by the tertiary utricle

Results

Sequence data, genotypic clusters and identifications

Information on length, base composition, and variability of sequence data are listed in Table 3. Figures 2 and 3 depict the phylograms obtained by MP analysis of ITS1–5.8S–ITS2 and *rps*3 sequence data, respectively. The trees featured a number of genotypic clusters of closely related specimens separated from other such clusters by long branches with high bootstrap support. Specimens forming a genotypic cluster in the ITS–5.8S–ITS2 tree, also grouped in the *rps*3 tree and vice versa.

Species names were assigned to the genotypic clusters on the basis of correspondence with morphology-based identifications of specimens belonging to the clusters. In a few cases, genotypic clusters and morphological identifications did not match. Several specimens with a *H. simulans* morphology were recovered in the *H. borneensis* cluster, and the *H. incrassata* 1a genotypic cluster contained multiple specimens that stood midway between *H. incrassata* and *H. melanesica* morphologies.

There was a discrepancy in branch lenghts between the *H. monile–simulans–incrassata* 2 group and the remainder of the species in the *rps*3 tree, branches between species being much longer within the group in question. Furthermore, within-species sequence divergence was large within *H. monile* and *H. incrassata* 2.

Table 3. Length, variability and composition of DNA data.

	ITS1–5.8S–ITS2	*rps*3
sequence length	436–472	660–876
alignment length	485	1014
constant positions	338	422
variable positions	147	592
parsimony informative positions	116	497
T	19.1%	26.0%
C	29.3%	18.7%
A	20.8%	34.6%
G	30.8%	20.7%
indels	5.6%	26.6%

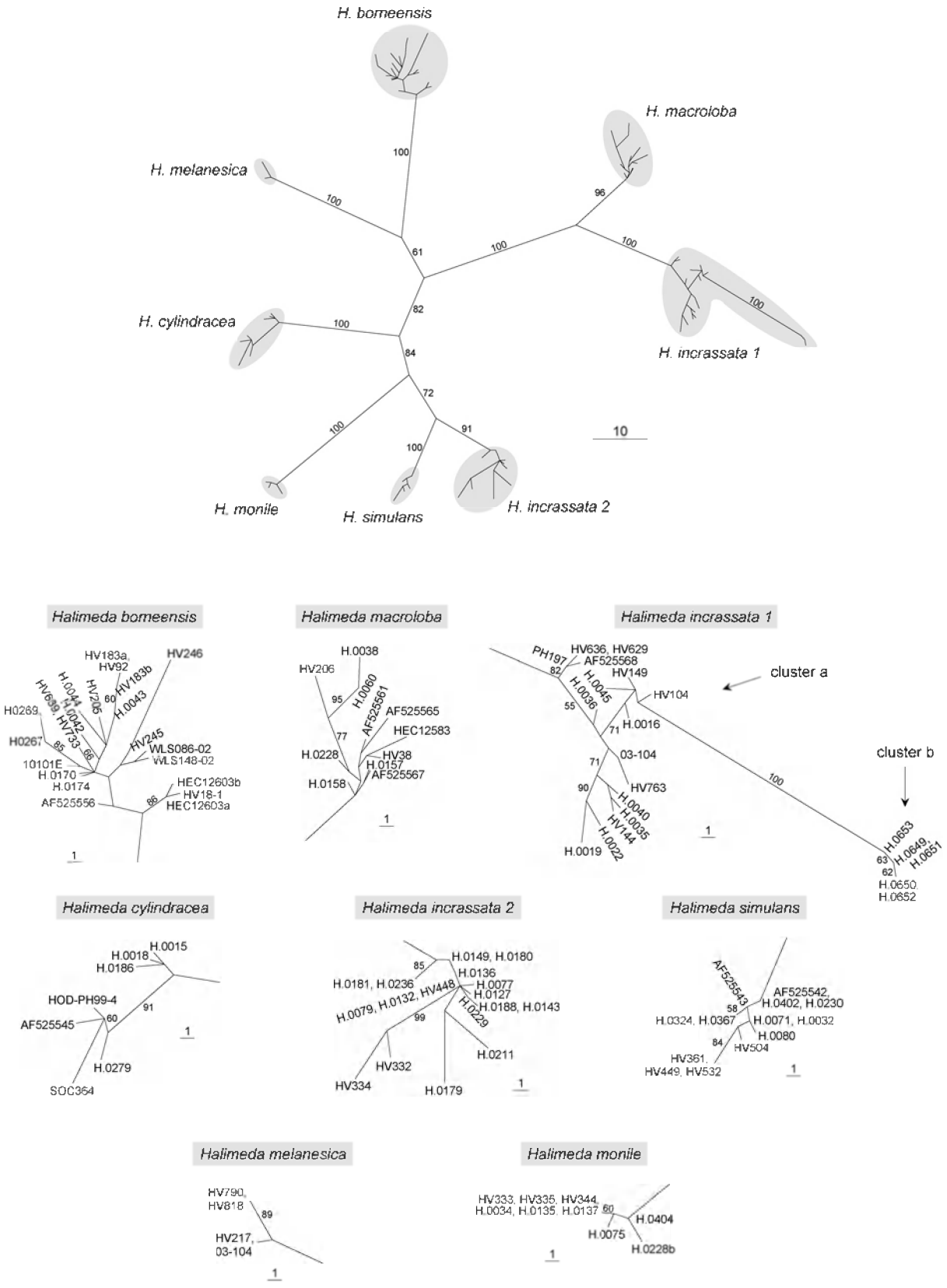

Fig. 2. Maximum Parsimony tree inferred from nuclear ribosomal ITS1–5.8S–ITS2 DNA sequences. One of 19 MP trees of 309 steps. Maximum Parsimony bootstrap values are indicated at branches.

These discrepancies were caused by codon indels.

Within the Indo-Pacific *H. incrassata* diversity (named *H. incrassata* 1 in Figs 2 and 3), two genotypic clusters were present. The first cluster (1a) represented the bulk of the specimens and occurs throughout the Indo-Pacific. The second cluster (1b) contained five specimens from Honolua Bay, Maui, Hawaii. In the ITS1–5.8S–ITS2 tree (Fig. 2), cluster 1b branched off from within cluster 1a, which was left paraphyletic. The branch leading towards cluster b was very long and obtained 100% bootstrap support. In the *rps*3 tree, clusters 1a and 1b were both monophyletic and received high bootstrap support. Cluster 1a was closest sister to *H. macroloba*; cluster 1b was sister to the *H. macroloba–incrassata* 1a clade. Clusters 1a and 1b were retained as distinct entities for further analyses.

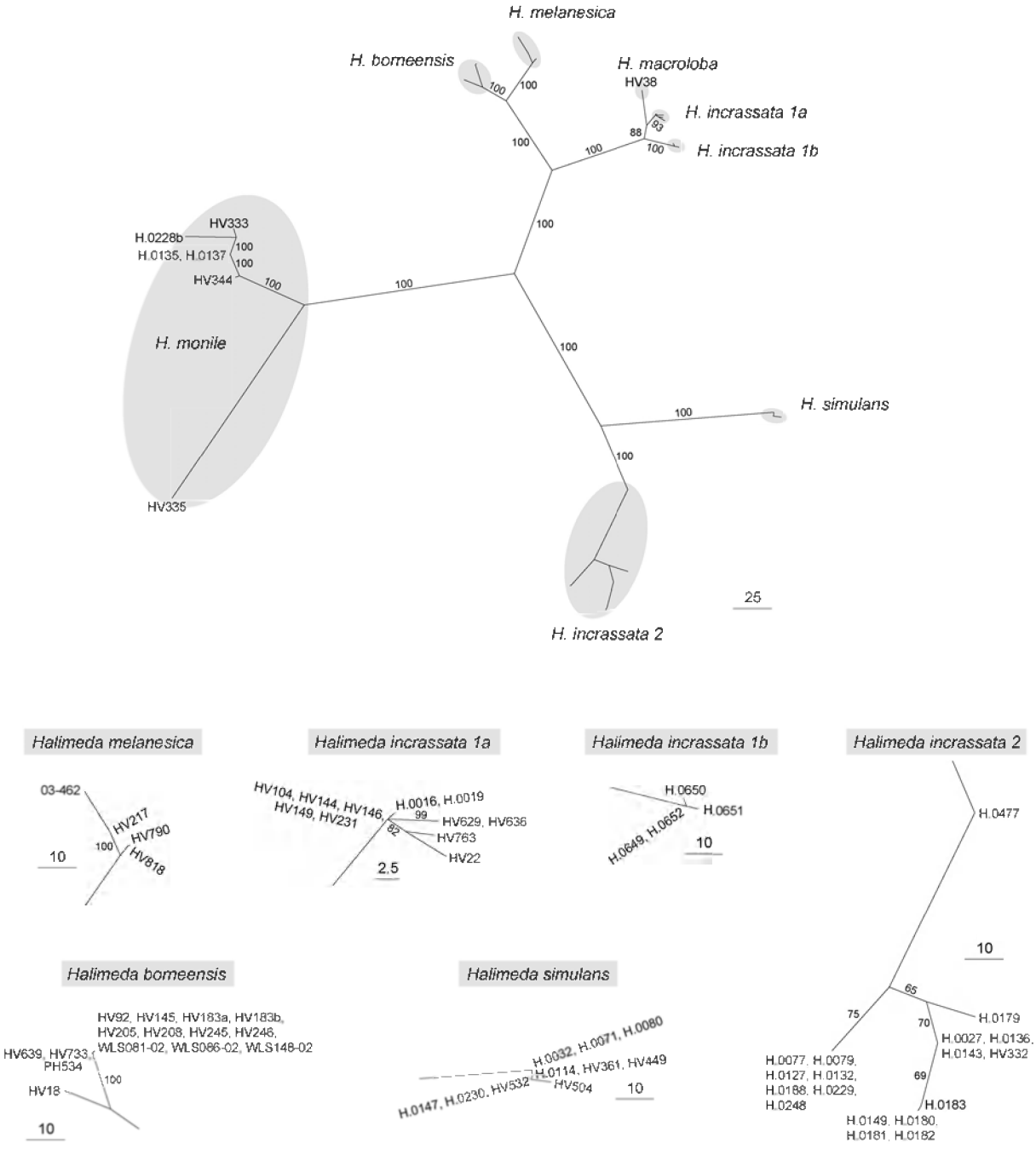

Fig. 3. Maximum Parsimony tree inferred from plastid *rps*3 DNA sequences. One of 49 MP trees of 1178 steps. Maximum Parsimony bootstrap values are indicated at branches.

We were unable to obtain *H. stuposa* specimens suitable for DNA analysis. Amplification of DNA from the specimen sequenced by Kooistra et al. (2002) failed on several attempts. As a consequence, this species was not represented in the trees. Nonetheless, *H. stuposa* was retained as a separate entity in further analyses.

Exploration of morphometric data

Segment morphological variables were scored from 90 specimens and anatomical variables from 86 specimens belonging to ten species (genotypic clusters). This resulted in data for 900 segments, 860 nodal and medullar structures, 860 peripheral utricles, 1030 secondary and 536 tertiary utricles, adding up to a total of 14312 anatomical measurements.

Figure 4 shows the biplots of PCA carried out on segment morphological and anatomical data sets (single entry per specimen). In the biplot of segment morphological data (panel A), certain genotypic clusters occupied non-overlapping regions (e.g. *H. monile* vs. *H. simulans* – encircled in figure). Most of the genotypic cluster species, however, showed partial or complete overlap in the first two dimensions of principal component space. All species involved in taxonomic problems (see introduction) showed mutual overlap except *H. stuposa*, the two specimens of which fell outside of the *H. borneensis* range. Species within the look-alike species pairs *H. simulans–borneensis* and *H. monile–cylindracea* showed considerable overlap. The three *H. incrassata* genotypic cluster species and *H. melanesica* occupied partially overlapping areas.

Principal component analysis of anatomical data resulted in the biplot shown in panel B (Fig. 4). Genotypic cluster species were far from randomly dispersed on the graph. The left hand side of the graph (second and third quadrant) contained *H. incrassata* 1a, *H. incrassata* 1b, *H. incrassata* 2 and *H. macroloba*. The first and fourth quadrant (right hand side of graph) contained the other species. Apart from this basic subdivision, most genotypic cluster species occupied overlapping regions in the biplot.

Initial discriminant analyses

The DA carried out on the complete sets of medians demonstrated differences between all species. Figure 5 depicts canonical biplots for segment morphological and anatomical data. The biplot of segment morphological data (panel A) did not show obvious species separation in the first two roots. The anatomical data, on the other hand, separated several species using only the first two canonical roots.

For the segment morphological data, all interspecific distances (squared Mahalanobis distances) were significantly different from zero, except for *H. simulans–borneensis* ($p = 0.2989$), *H. monile–cylindracea* ($p = 0.4036$) and *H. melanesica–incrassata* 1a ($p = 0.2729$). Classification tests based on segment morphology achieved between 58% and 100% success (average 74%), meaning that specimens belonging to a species were allocated to that species in 58% to 100% of the cases tested. The worst classification results were obtained for *H. borneensis*, which was often mistaken for *H. simulans* (4/17). *Halimeda incrassata* 2 was casually misclassified as *H. simulans* (2/23), *H. incrassata* 1a (2/23), or *H. borneensis* (2/23). *Halimeda incrassata* 1a also obtained relatively low classification success. Its specimens were occasionally allocated to various other species. Adding categorical shape variables increased classification success by about 10% (average 83%).

The anatomical data set achieved higher classification success (average 97%). For most species all specimens were correctly classified. Only *H. borneensis* and *H. monile* were mistaken for each other; one specimen was misclassified in each direction. All interspecific squared Mahalanobis distances were significantly different from zero at the 5% significance level.

When the original data (10 replicates per specimen) were used instead of the median values, there was considerably more overlap in the canonical biplots (not shown). Even for the anatomical data, no clear-cut clusters were obvious in the first two canonical dimensions. Nonetheless, classification success was only slightly less; for anatomical data it was rarely lower than 90%.

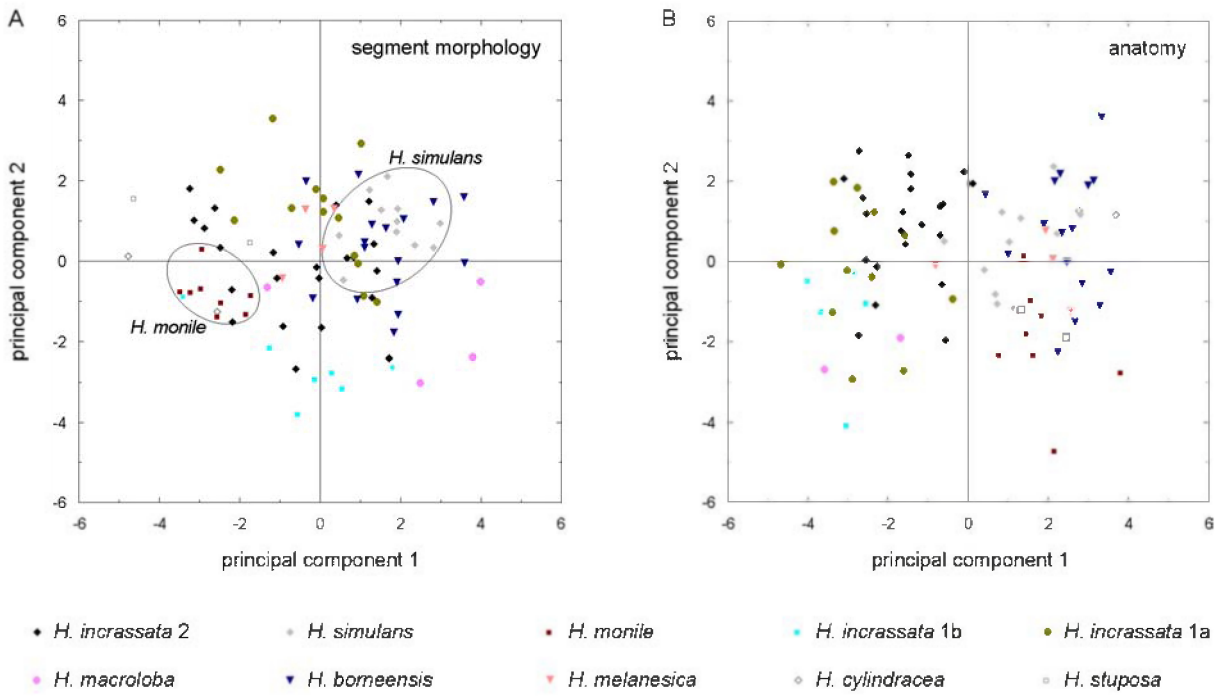

Fig. 4. Principal Component Analysis biplots of segment morphological (A) and anatomical (B) data (one entry per specimen). In panel A, the areas occupied by *H. monile* and *H. simulans* have been encircled. Variables included in the analysis were the log-transformed s07, s08, s11–s19 for segment morphology and the log-transformed a01–a05, a08–a20, a22–a24 for anatomy.

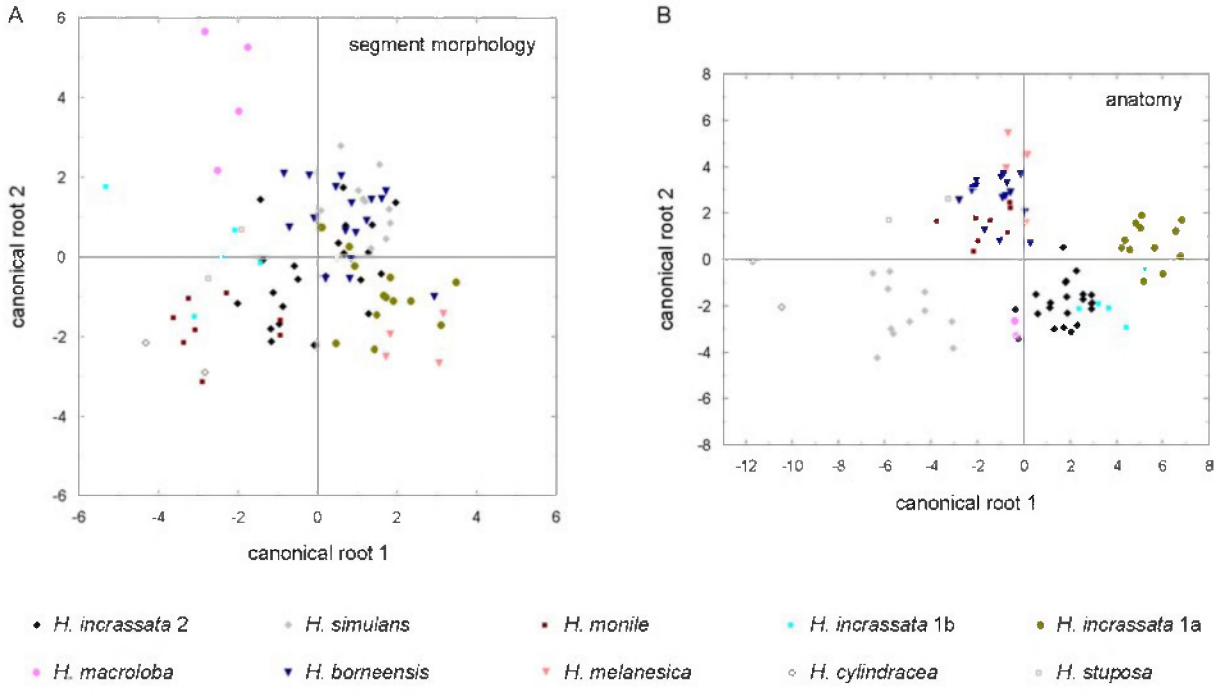

Fig. 5. Discrimination of ten *Halimeda* species based on segment morphology (A) and anatomy (B). The variables included in DA were s07, s11–s19 for segment morphology and a01–a05, a08–a12, a14–a20, a22–24 for anatomy.

Probabilistic identification approach

Table 4 presents the classification functions of anatomical variables for the ten studied species. These classification functions resulted from DA of the anatomical data set (median values; excluding tertiary utricles). The functions allowed 96% correct identifications. Misidentifications only occurred for the species *H. monile* and *H. borneensis* (87% correct allocations). All other species obtained 100% classification success.

Additional discriminant analyses

Further discriminant analyses, containing only subsets of characters and taxa, were carried out to single out characters with diagnostic value. These results are not presented in full because they are not of general interest. Below, we will expand on the distinction between the three *H. incrassata* entities as an example. Instead of reporting the results in full, they were interpreted and used to set up an identification key. This key, presented in Table 5, incorporates traditional and morphometric data and led to 100% correct identifications of the specimens incorporated in this study.

Table 4. Classification functions for anatomical variables. Specimens can be identified by filling in the values obtained for the different variables. The species that receives the highest score is the species to which the specimen belongs with the highest probability. Probability values can be calculated by dividing the scores for each species by the sum of all scores. *Halimeda favulosa* is not included; this species can be easily recognized by its exceptionally large peripheral utricles (see line 1 of identification key – Table 5).

species	score
H. incrassata 2	81.8 · L_diam_ir – 107.5 · L_constr_m + 146.9 · L_len_ir + 115.9 · L_node_act – 2.13 · L_len_supr + 207.9 · L_diam_supr + 385.8 · L_p_surf + 122.7 · L_p_height + 187.6 · L_p_width + 21.9 · L_p_rel_w_75 + 112.5 · L_p_rel_w_50 – 30.4 · L_p_rel_w_25 + 239.0 · L_p_rel_h – 103.2 · L_s_height + 323.1 · L_s_width – 3028
H. simulans	80.6 · L_diam_ir – 97.1 · L_constr_m + 142.2 · L_len_ir + 113.9 · L_node_act + 0.77 · L_len_supr + 219.9 · L_diam_supr + 333.7 · L_p_surf + 72.0 · L_p_height + 183.5 · L_p_width – 23.5 · L_p_rel_w_75 + 112.4 · L_p_rel_w_50 – 32.6 · L_p_rel_w_25 + 221.0 · L_p_rel_h – 91.4 · L_s_height + 313.2 · L_s_width – 2697
H. monile	66.8 · L_diam_ir – 102.6 · L_constr_m + 143.9 · L_len_ir + 121.2 · L_node_act + 7.09 · L_len_supr + 212.8 · L_diam_supr + 365.3 · L_p_surf + 89.2 · L_p_height + 203.8 · L_p_width + 2.23 · L_p_rel_w_75 + 107.8 · L_p_rel_w_50 – 17.6 · L_p_rel_w_25 + 255.9 · L_p_rel_h – 93.5 · L_s_height + 297.6 · L_s_width – 2843
H. incrassata 1b	72.9 · L_diam_ir – 104.4 · L_constr_m + 147.4 · L_len_ir + 123.8 · L_node_act + 4.87 · L_len_supr + 226.4 · L_diam_supr + 401.4 · L_p_surf + 108.0 · L_p_height + 225.6 · L_p_width + 7.46 · L_p_rel_w_75 + 110.9 · L_p_rel_w_50 – 3.01 · L_p_rel_w_25 + 252.3 · L_p_rel_h – 105.5 · L_s_height + 320.3 · L_s_width – 3279
H. incrassata 1a	62.8 · L_diam_ir – 110.9 · L_constr_m + 151.7 · L_len_ir + 107.0 · L_node_act + 2.47 · L_len_supr + 210.8 · L_diam_supr + 405.5 · L_p_surf + 181.7 · L_p_height + 169.1 · L_p_width + 80.6 · L_p_rel_w_75 + 112.9 · L_p_rel_w_50 – 46.3 · L_p_rel_w_25 + 224.9 · L_p_rel_h – 106.9 · L_s_height + 313.6 · L_s_width – 3179
H. macroloba	83.2 · L_diam_ir – 108.9 · L_constr_m + 151.8 · L_len_ir + 115.1 · L_node_act + 6.09 · L_len_supr + 213.9 · L_diam_supr + 384.3 · L_p_surf + 128.6 · L_p_height + 146.4 · L_p_width + 24.4 · L_p_rel_w_75 + 147.1 · L_p_rel_w_50 – 67.6 · L_p_rel_w_25 + 252.9 · L_p_rel_h – 88.0 · L_s_height + 317.6 · L_s_width – 3073
H. borneensis	60.9 · L_diam_ir – 105.9 · L_constr_m + 153.2 · L_len_ir + 109.5 · L_node_act + 2.42 · L_len_supr + 209.8 · L_diam_supr + 369.1 · L_p_surf + 100.2 · L_p_height + 202.8 · L_p_width + 24.2 · L_p_rel_w_75 + 114.1 · L_p_rel_w_50 – 10.4 · L_p_rel_w_25 + 249.2 · L_p_rel_h – 96.0 · L_s_height + 287.9 · L_s_width – 2777
H. melanesica	54.8 · L_diam_ir – 102.1 · L_constr_m + 140.4 · L_len_ir + 99.3 · L_node_act + 11.24 · L_len_supr + 211.7 · L_diam_supr + 368.8 · L_p_surf + 145.8 · L_p_height + 159.4 · L_p_width – 11.6 · L_p_rel_w_75 + 134.0 · L_p_rel_w_50 – 49.4 · L_p_rel_w_25 + 218.9 · L_p_rel_h – 90.9 · L_s_height + 289.5 · L_s_width – 2769
H. cylindracea	80.6 · L_diam_ir – 84.7 · L_constr_m + 132.8 · L_len_ir + 108.2 · L_node_act + 3.99 · L_len_supr + 222.9 · L_diam_supr + 289.6 · L_p_surf + 70.4 · L_p_height + 136.7 · L_p_width – 35.8 · L_p_rel_w_75 + 114.8 · L_p_rel_w_50 – 34.2 · L_p_rel_w_25 + 184.8 · L_p_rel_h – 77.2 · L_s_height + 302.3 · L_s_width – 2395
H. stuposa	76.8 · L_diam_ir – 104.8 · L_constr_m + 146.7 · L_len_ir + 103.2 · L_node_act – 3.52 · L_len_supr + 218.7 · L_diam_supr + 330.7 · L_p_surf + 91.8 · L_p_height + 174.3 · L_p_width – 95.0 · L_p_rel_w_75 + 140.4 · L_p_rel_w_50 – 54.7 · L_p_rel_w_25 + 251.6 · L_p_rel_h – 76.0 · L_s_height + 289.4 · L_s_width – 2656

Figure 6A depicts the canonical biplot of the DA carried out on segment morphological data of *H. incrassata* specimens. Entity 1b was distinct; entities 1a and 2 showed considerable overlap. Segment size (represented by L_length) was highly correlated with the principal root and allowed distinction between entity 1b and the other two entities (Fig. 6B). None of the individual segment morphological characters allowed unambiguous distinction between entities 1a and 2. The canonical biplot based on anatomical variables (Fig. 7A) showed perfect separation between all three *H. incrassata* entities. Entities 1a and 2 separated along the first root; entity 1b separated from the rest along the second root. Root 1 had the highest correlation with variables associated with peripheral utricles (L_p_height and L_p_surf). Nonetheless, neither of these characters allowed unambiguous separation between entities 1a and 2 (e.g. L_p_surf: Fig. 7B). The second root showed high correlation with characters associated with nodal anatomy (L_node_act, L_diam_supr and L_len_supr). Length of the supranodal siphon could be used to distinguish between en-

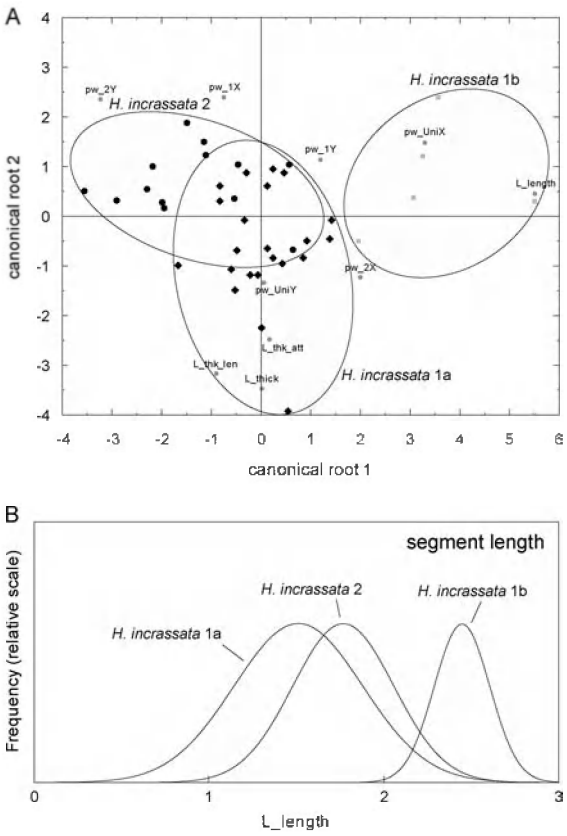

Fig. 6. Discrimination between *H. incrassata* entities using segment morphological variables. (A) Canonical biplot of DA with variables s7, s11–s19 (log-transformed when necessary). (B) Estimated distribution of viariable L_length for the three *H. incrassata* entities. All based on dataset of median values. Symbols as in Figures 5 and 6.

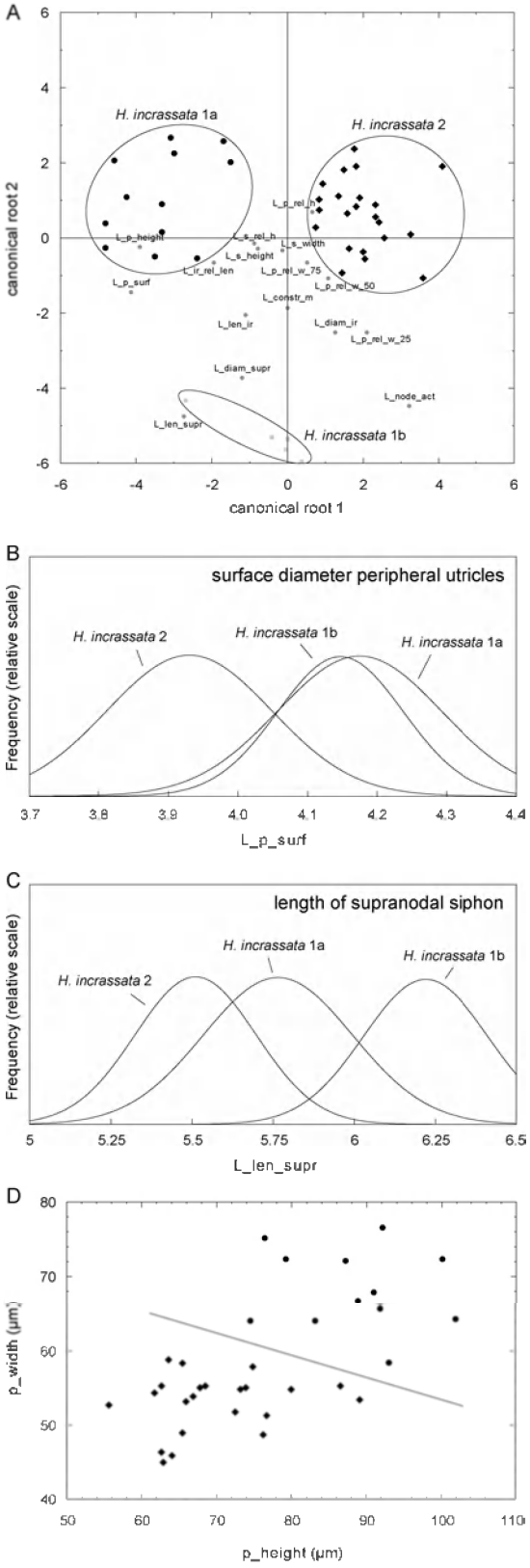

Fig. 7. Discrimination between *H. incrassata* entities using anatomical variables. (A) Canonical biplot of DA with (log-transformed) variables a1–a12, a14–a20. (B) Estimated distribution of variable L_p_surf for the three *H. incrassata* entities. (C) Estimated distribution of variable L_len_supr for the three entities. (D) *H. incrassata* 1a and 2 observations separate perfectly using two variables associated with peripheral utricles. All based on dataset of median values.

Table 5. Key to *Halimeda* species of section *Rhipsalis*.

The correctness of identifications based on this key is expected to decrease if segment selection and measurements do not follow the following guidelines. Juvenile specimens must be avoided. Ten segments must be chosen at random from the central region of the specimen (see Verbruggen et al. 2005b). All segment measurements must be expressed in mm, and the median values over the ten segments must be used in the key. One segment from the central region must be dissected according to Verbruggen et al. (2005a) and guidelines in this study. Anatomical measurements must be taken in tenfold (see Materials and Methods) and expressed in µm. The median values of these ten measurements must be used in the key. **If these directions are not strictly followed, the use of the presented key is fundamentally faulty.**

1 a	Segment surface rugose, appearing pitted. Peripheral utricles exceeding 110 µm in surface diameter and 170 µm in height ..... *H. favulosa*
1 b	Segment surface smooth to somewhat rugose, very rarely appearing pitted. Peripheral utricles smaller 2
2 a	Thallus with extensive (no less than 2 cm, often more than 4 cm high) basal zone made up of massive, stipitate, cylindrical to slightly flattened segments 3
2 b	Basal zone different 7
3 a	Cylindrical segments restricted to basal zone. Segments higher up the thallus flattened and broader than long. Peripheral utricles exceeding 40 µm in surface diameter and 45 µm in height 4
3 b	Majority of segments higher up the thallus also cylindrical, never broader than high. Peripheral utricles smaller ..... *H. cylindracea*
4 a	Supranodal siphons longer than 350 µm 5
4 b	Supranodal siphons shorter 6
5 a	Segment length exceeding 8.5 mm. Nodal fusions obvious; height of nodal fusions (including cell walls) exceeding 42 µm. Diameter of supranodal siphons exceeding 140 µm. Peripheral utricles exceeding 42% of their maximal width at 1/4th from their base. Subperipheral utricles markedly swollen, almost round ..... *H. incrassata* 1b
5 b	Segment length less than 8.5 mm. Nodal fusions not always obvious; height of nodal fusions not exceeding 42 µm. Diameter of supranodal siphons generally less than 140 µm. Peripheral utricles not generally reaching 42% of their maximal width at 1/4th from their base. Subperipheral utricles not markedly swollen, elongate ..... *H. incrassata* 1a
6 a	The result of [–3.4 · (width of peripheral utricles) + 283 µm] exceeds the height of the peripheral utricles. Nodal fusions always obvious; fusion height (including cell walls) exceeding 32 µm. Holdfast generally bulbous ..... *H. incrassata* 2
6 b	The result of the equation is less than the height of the peripheral utricles. Nodal fusions not always obvious; fusion height less than 38 µm. Holdfast generally matted ..... *H. incrassata* 1a
7 a	Segment width exceeding 12.5 mm ..... *H. macroloba*
7 b	Segment width smaller than 12.5 mm 8
8 a	Peripheral utricles exceeding 56 µm in width and 72 µm in height 6
8 b	Peripheral utricles smaller 9
9 a	Width of peripheral utricles exceeding the result of [–1.67 · (width of secondary utricles) + 124 µm] 10
9 b	Width of peripheral utricles smaller than the result of the equation 11
10 a	Nodal fusions obvious; height of nodal fusion (including cell walls) exceeding 30 µm. Length of supranodal siphon not exceeding 335 µm. Width of secondary utricles exceeding 42 µm ..... *H. incrassata* 2
10 b	Nodal fusions not always obvious; height of nodal fusion less than 30 µm. Length of supranodal siphon exceeding 335 µm. Width of secondary utricles smaller than 45 µm ..... *H. melanesica*

11 a Height over width ratio of peripheral utricles exceeding 1.6 12

11 b Height over width ratio of peripheral utricles not exceeding 1.6 13

12 a Length of supranodal siphons exceeding 300 µm. Height of nodal fusions (including cell walls) exceeding 45 µm. Width of peripheral utricles exceeding 30 µm ..... *H. monile*

12 b Supranodal siphons shorter than 300 µm. Height of nodal fusions less than 45 µm. Width of peripheral utricles less than 35 µm ..... *H. stuposa*

13 a Numerous cylindrical segments; longer than broad. Segment width smaller than the result of [10.83 · (segment thickness) – 15.33] ..... *H. monile*

13 b Segments rarely cylindrical; of variable shape, often about as broad as long or broader than long. Segment width bigger than the result of the equation 14

14 a Peripheral utricles exceeding 55 µm in height and 40 µm in width. Segment length over width ratio exceeding 0.9. Segment width less than 5.7 mm. Segment thickness less than 1 mm 15

14 b Peripheral utricles less than 55 µm in height, rarely exceeding 40 µm in width. Segment length over width ratio less than 0.9. Segment width exceeding 5.7 mm. Segment thickness exceeding 0.8 mm 16

15 a Attached to rocky substrate by means of a felty holdfast disc. Segment length over width ratio exceeding 0.9. Segment width less than 6 mm. Peripheral utricles reaching less than 45% of their maximal width at 1/4 of their height ..... *H. melanesica*

15 a Anchored in sand by means of a bulbous holdfast composed of rhizoids with attached grains of sand or anchored in silt by means of a long, slender tuft of rizoids. Segment length over width ratio usually less than 0.9. Segments generally broader than 6 mm. Peripheral utricles usually exceeding 45% of their maximal width at 1/4 of their height ..... *H. borneensis*

16 a Height of peripheral utricles exceeding the result of [3 · (diameter of medullar siphons) – 145] ..... *H. borneensis*

16 b Height of peripheral utricles smaller than the result of the equation ..... *H. simulans*

tity 1b and both other entities, but slight overlap of estimated distributions was present between 1a and 1b (Fig. 7C). Since no individual characters could distinguish between entities 1a and 2 unambiguously, combinations of characters were plotted. For example, in the plot of height versus width of peripheral utricles, no overlap was present between the species (Fig. 7D).

Discussion

Species delineation and DNA barcoding

On the basis of DNA sequence data, specimens could be classified into a number of clear-cut genotypic clusters. Whereas within-cluster genetic divergences are comparable among genotypic clusters in the ITS1–5.8S–ITS2 data, the discrepancy in sequence divergences of the *rps*3 data causes within-cluster genetic divergences to be much larger within the *H. monile–simulans–incrassata* 2 clade than those within the remainder of the section. This discrepancy is caused by the presence of codon indels within the *rps*3 gene in the *H. monile–simulans–incrassata* 2 clade. Irrespective of the discrepancy, genotypic clusters are concordant among the markers used.

Now that our set of sequences has been partitioned into clear-cut and named genotypic clusters, identification of new specimens on the basis of DNA barcodes is possible. The use of DNA barcoding as an identification technique is becoming increasingly popular. When using appropriate markers, it allows unambiguous identification, helps unmask look-alike species regardless of their life stage, and has the

potential to reveal the existence of species new to science (Besansky et al. 2003, Hebert et al. 2004a, b, Hogg & Hebert 2004).

Our aim, however, was not to replace traditional identification methods by DNA barcoding but rather to have DNA sequence data serve as a foundation on which to construct a new taxonomy, based on reliable, morphological differences between species.

Evolution of *H. incrassata* 1

It is beyond doubt that clusters a and b of *H. incrassata* 1 are distinct from one another. In the *rps*3 tree both are monophyletic. In the ITS1–5.8S–ITS2 tree, *H. incrassata* 1b branches off from within the *H. incrassata* 1a genotypic cluster and sits on a long branch with 100% bootstrap support.

In most cases, our genotypic cluster species are monophyletic and can also be regarded genealogical species (Baum & Donoghue 1995). Interfertility assays confirm that, at least for what the *H. monile–simulans–incrassata* 2 clade is concerned, the genotypic cluster, genealogical and biological species concepts correspond (K. E. Clifton, pers. comm.). The phylogenetic pattern within *H. incrassata* 1 hinders the equation of our genotypic cluster species with genealogical species. If *H. incrassata* 1b is to be considered a species, *H. incrassata* 1a is left non-monophyletic in the ITS1–5.8S–ITS2 tree and thus does not comply with the genealogical species definition (Baum & Donoghue 1995). However, two things must be noted in this context. First, several aspects of ITS sequence evolution and alignment may lead to suboptimal topologies (Alvarez and Wendel 2003). Especially the ClustalW alignment algorithm, which does not take structural features of ITS into account but was preferred to avoid subjectivity in alignments, may lead to suboptimal alignments (Gómez-Zurita et al. 2000, Denduangboripant and Cronk 2001). Second, only a single phylogenetic inference method was applied to the data (MP). It cannot be judged from our data that both clusters within *H. incrassata* 1 comply with the biological species concept. In any case, the problem is merely one of species definitions and does not hinder taxonomic inference from our morphometric data. Following the genotypic cluster species concept, *H. incrassata* 1a and 1b have been retained as different species in our analyses.

The topological discordance between the *rps*3 and ITS–5.8S–ITS2 trees is also of interest. The fact that *H. incrassata* 1b is recovered within *H. incrassata* 1a in one tree and as the closest sister of the *H. macroloba–incrassata* 1a clade in the other tree, could indicate reticulate speciation or incomplete lineage sorting (e.g. Avise 2000). Our data do not allow identification of the discordance's cause. Verbruggen et al. (submitted) found multiple topological discordances in *Halimeda* section *Halimeda* and we refer to their paper for a more elaborate discussion of putative reticulate evolution within the genus *Halimeda*.

Morphometrics

The identification problems listed in the introduction are clearly reflected in PCA. Species in which identification problems are present or within which cryptic diversity is contained, show partial to complete overlap in the biplots of all major principal components. This is particularly obvious in the anatomical biplot, where the data are polarized into two major species groups, each of which contains a set of taxonomic problems. Given that the biplots represent the most obvious differences in the data, and thus reflect the absence of obvious differences between problem species, one should not be surprised that the section under study has suffered from misidentifications and taxonomic conservatism in the past.

The initial discriminant analyses shed light on the nature of similarities and differences between species. In the canonical biplot based on segment morphological characters, problematic species pairs occupy overlapping areas. Clear-cut separation of a few species in the first and second dimension of the canonical biplot based on anatomy indicates that anatomical characters hold more conclusive differ-

ences. This is confirmed by the much higher classification success of DA based on anatomical characters.

Separation of species using the data set of median values is much more complete than with the data set of ten replicates per specimen, both for segment morphological and anatomical data. This is not surprising: by using medians, only the most representative values are retained and the edges of the variable distributions are considerably narrowed, accentuating interspecific differences and downplaying intra-individual morphological plasticity.

The conclusion of the explorative DA must be that morphological differences between species exist. From the significance of interspecific Mahalanobis distances and the success of classification tests, it can be concluded that these differences are highly significant. That DA points to significant differences between species does not imply that these differences correspond to those traditionally used in literature. It may even be that the differences are so mathematically complex that they cannot be translated into simple morphological clues for future identifications.

The issue of future identification of specimens has been approached in two ways. First, classification functions of DA offer a framework for probabilistic species identification. Second, interpretation of additional DA on increasingly trimmed down data sets leads to an identification key. Before discussing these identification methods in more detail, a few taxonomic issues that could escape notice in the mathematical approach will be stressed.

Taxonomic remarks

The principal character setting *H. melanesica* apart from species in section *Rhipsalis* is the absence of nodal fusions and the matted holdfast in the former (Valet 1966, Hillis-Colinvaux 1980). With the discovery of small nodal fusions in *H. melanesica*, Noble (1987) stressed the blurring of the boundary between *H. melanesica* and *H. incrassata*. The present study sheds more light on the identity of and distinction between *H. melanesica* and the different *H. incrassata* species. Whereas the species *H. incrassata* 1b and 2 contain specimens with large nodal fusions, the genotypic clusters given the denomination *H. melanesica* and *H. incrassata* 1a contain specimens without and with minute nodal pores. The genotypic clusters with specimens featuring small nodal pores were given their names on the basis of the presence of a matted holdfast in all specimens with a *H. melanesica* DNA barcode and the presence of a more extensive holdfast in certain specimens bearing a *H. incrassata* 1a barcode. The segment morphological characters used in this study do not allow unequivocal designation of specimens to *H. incrassata* 1a or *H. melanesica*, but the distinction can easily be made on the basis of anatomical measurements. The most obvious difference is the size of peripheral utricles. Medians of surface diameter and height do not exceed 50 µm and 67 µm respectively in *H. melanesica*. Peripheral utricles of our specimens of *H. incrassata* 1a are larger: no less than 57 µm in diameter and 74 µm in height. Post-hoc morphometric examination of the type specimen of *H. melanesica* (PC0021851, Muséum National d'Histoire Naturelle, Paris [PC]) confirms that the genotypic cluster given the *H. melanesica* denomination is indeed *H. melanesica*. Morphological distinction between the three *H. incrassata* genotypic cluster species is less straightforward. Especially clusters 1a and 2 are difficult to discern between using morphometric data. For details on the distinguishing characters, we refer to lines four to six of the identification key (Table 5).

Information on the origin of specimens can help in their identification. In our definition, *H. borneensis* seems to be restricted to the Indo-Pacific and *H. simulans* to the Atlantic. Even though certain specimens belonging to the *H. borneensis* genotypic cluster were identified as *H. simulans* on the basis of a previous monograph (Hillis-Colinvaux 1980), no specimens belonging to the *H. simulans* genotypic cluster were found in the Indo-Pacific. Based on this finding, it seems likely that all Indo-Pacific records of *H. simulans* are false and to be considered *H. borneensis*. Similarly, *H. incrassata* 1a and *H. cylindracea* are restricted to the Indo-Pacific while *H. incrassata* 2 and *H. monile* occur only in the

Atlantic. In the light of our results, reports of *H. monile* and *H. simulans* in Indo-Pacific waters should be considered erroneous until their identity is reconfirmed using DNA barcoding or the identification methods presented here. Despite the fact that geographic information seems very useful for identification of certain *Halimeda* species, it should be used with extreme caution because seaweeds are among the most prevalent invasive marine species (e.g. Jousson et al. 2000, Rueness and Rueness 2000, De Clerck et al. 2002). *Halimeda opuntia*, a profuse pantropical species, is believed to have invaded in the Caribbean during the last millennium (Kooistra and Verbruggen 2005).

Probabilistic identification approach

Identification of specimens comes down to allocating them to groups at the specific rank in a taxonomic framework. Inferring the species to which a specimen belongs is a matter of following identification rules prescribed by systematists. In biological taxonomy, it usually concerns morphological identification rules, and systematists tend to compact such rules into dichotomous identification keys that lead to unambiguous (absolute) allocation of specimens to species.

There are, however, alternative ways to approach identification. On the one hand, the kind of data can be altered (e.g. physiological properties, DNA barcodes). On the other hand, the identification rules can be probabilistic rather than absolute. This means that following the identification rules leads to probability values for each species considered. In essence, absolute identification is a mere variant of probabilistic identification with the probabilities for all but one species equal to 0, and the probability of one species equal to 1. Probabilistic methods are most often used if the characters used do not allow absolute identification or when large amounts of information have to be processed automatically (e.g. in clinical microbiology: Gyllenberg and Koski 2002, Kassama et al. 2002).

We provide a probabilistic method of specimen identification on the basis of anatomical measurements for species of *Halimeda* section *Rhipsalis* (Table 4). If measurements on new specimens are taken according to the methods described in this paper and Verbruggen et al. (2005a, b), the classification functions can be used to calculate scores for each of the ten species included in our morphometric analyses. The species obtaining the highest score is the taxon to which the specimen belongs with the highest probability.

ID key construction

For the construction of an identification key, further DA were carried out on trimmed down data sets. The identification key incorporates traditional as well as morphometric data and leads to 100% correct identifications for the specimens incorporated in this study.

The DA expose the importance of characters for species differentiation. Segment morphological characters do not usually allow for delineation of species or groups of species. This does not mean that segment characteristics do not contain any useful information, but that on the basis of segment data alone, one cannot make the distinction between all species. Anatomical data provide much better diagnostic characters, validating the results of Verbruggen et al. (2005a), and further stressing that the trend of increasing focus on anatomy for identification purposes continues. Anatomy is the key to discern between cryptic entities and look-alikes. Therefore, identification based on superficial comparison is firmly discouraged.

Not all anatomical characters are equally important for species recognition. Especially peripheral utricles yield taxonomically useful measurements, substantiating the attention paid to these measurements by former systematists. Nonetheless, certain measurements not or rarely used in previous taxonomic treatises prove useful in a number of cases. Examples are nodal fusion height (a08), the distance between the nodal fusion and the first ramification of the siphon above the node (a09), and diameter of medullar siphons (a01).

It is difficult to predict whether and how addition of specimens to our data set will influence the correctness of the identification key. We have strived for representative sets of specimens of the different species, not avoiding specimens in the grey zone between morpho-species. Certain species were included merely to sketch a more complete picture even though they can easily be recognized using classical characters (e.g. *H. macroloba*). On the other hand, certain species are underrepresented in our data because they are rare or highly geographically restricted (*H. melanesica*, *H. stuposa*). Whether or not the threshold values used in the identification keys will need updating when increasing numbers of specimens are added remains an open question.

Acknowledgements

We are appreciative to the Bijzonder Onderzoeksfonds (Ghent University, grant 011D9101), the Fund for Scientific Research Flanders (grant 3G002496 and postdoctoral fellowship to ODC) and the King Leopold III Fund for Nature Exploration and Conservation. We thank E. Cocquyt for her assistance with the molecular work. C. De maire and C. VanKerckhove are acknowledged for caring over the GENT herbarium collection and database and for assistance with administration. We thank K. Page, H. Spalding and P. Vroom for providing us with the Hawaiian *H. incrassata* specimens and L. de Senerpont-Domis and W. Prud'homme van Reine for a collection of Indonesian material. We thank K. Arano, M.A. Coffroth, P. Colinvaux, O. Dargent, G. De Smedt, F. Gurgel, O.A. Gussmann, I. Hendriks, L. Hillis, F. Leliaert, L. Liao, C. Payri, W. Prud'homme van Reine, M. van Veghel, B. Wysor, F. Zechman and G. Zuccarello for various collections. M. Wynne is acknowledged for sending the type material of *H. borneensis*. H.V. acknowledges Claude Payri, Paino Vanai and the Environmental Service of Wallis and Futuna for facilitating fieldwork on Uvea Island. H.V. further thanks T. and C. Leigh, D. Olandesca, R. Diaz and C. Galanza for their helping hand during expeditions. Two anonymous reviewers are acknowledged for their constructive remarks.

References

Alvarez, I. & Wendel, J.F. 2003. Ribosomal ITS sequences and plant phylogenetic inference. *Mol. Phylogen. Evol.* 29: 417–34.

Avise, J.C. 2000. *Phylogeography. The history and formation of species.* Harvard University Press, Cambridge, MA. 447 pp.

Barton, E. S. 1901. The genus *Halimeda*. *Monographs of the Siboga Expedition* 60: 32 pp. Leiden, The Netherlands.

Baum, D. A. & Donoghue, M. J. 1995. Choosing among alternative phylogenetic species concepts. *Syst. Bot.* 20: 560–73.

Besansky, N. J., Severson, D. W. & Ferdig, M. T. 2003. DNA barcoding of parasites and invertebrate disease vectors: what you don't know can hurt you. *Trends Parasitol.* 19: 545–6.

Cohen, S., Faugeron, S., Martinez, E. A., Correa, J. A., Viard, F., Destombe, C. & Valero, M. 2004. Molecular identification of two sibling species under the name *Gracilaria chilensis* (Rhodophyta, Gracilariales). *J. Phycol.* 40: 742–7.

De Clerck, O., Anderson, R. J., Bolton, J. J. & Robertson-Andersson, D. 2002. *Schimmelmannia elegans* (Gloiosiphoniaceae, Rhodophyta): South Africa's first introduced seaweed? *Phycologia* 41: 184–90.

De Clerck, O., Gavio, B., Fredericq, S. & Coppejans, E. 2005. Systematics of *Grateloupia filicina* (Halymeniaceae, Rhodophyta), based on *rbc*L sequence analyses and morphological evidence, including the reinstatement of *G. minima* and the description of *G. capensis* spec. nov. *J. Phycol.* 41: 391–410.

Denduangboripant, J. & Cronk, Q.C.B. 2001. Evolution and alignment of the hypervariable arm 1 of *Aeschynanthus* (Gesneriaceae) ITS2 nuclear ribosomal DNA. *Mol. Phylogen. Evol.* 20: 163–72.

Felsenstein, J. 1985. Confidence limits on phylogenies: an approach using the bootstrap. *Evolution* 39: 783–91.

Gómez-Zurita, J., Juan, C. & Petitpierre, E. 2000. Sequence, secondary structure and phylogenetic analyses of the ribosomal internal transcribed spacer 2 (ITS2) in the *Timarcha* leaf beetles (Coleoptera : Chrysomelidae). *Insect Mol. Biol.* 9: 591–604.

Gurgel, C. F. D., Liao, L. M., Fredericq, S. & Hommersand, M. H. 2003. Systematics of *Gracilariopsis* (Gracilariales, Rhodophyta) based on rbcL sequence analyses and morphological evidence. *J. Phycol.* 39: 154–71.

Gyllenberg, M. & Koski, T. 2002. Bayesian predictiveness, exchangeability and sufficientness in bacterial taxonomy. *Math. Biosci.* 177: 161–84.

Hebert, P. D. N., Penton, E. H., Burns, J. M., Janzen, D. H. & Hallwachs W. 2004a. Ten species in one: DNA barcoding reveals cryptic species in the neotropical skipper butterfly *Astraptes fulgerator*. *Proc. Natl. Acad. Sci. USA* 101: 14812–17.

Hebert, P. D. N., Stoeckle, M. Y., Zemlak, T. S. & Francis, C. M. 2004b. Identification of birds through DNA barcodes. *PLoS Biology* 2: e312.

Hogg, I.D. & Hebert, P. D. N. 2004. Biological identification of springtails (Hexapoda : Collembola) from the Canadian Arctic, using mitochondrial DNA barcodes. *Can. J. Zool.* 82: 749–54.

Hillis-Colinvaux, L. 1980. Ecology and taxonomy of *Halimeda*: primary producer of coral reefs. *Adv. Mar. Biol.* 17: 1–327.

Jousson, O., Pawlowski, J., Zaninetti, L., Zechman, F.W., Dini, F., Di Guiseppe, G., Woodfield, R., Millar, A. & Meinesz, A. 2000. Invasive alga reaches California. *Nature* 408: 157–8.

Kassama, Y., Rooney, P. J. & Goodacre, R. 2002. Fluorescent amplified fragment length polymorphism probabilistic database for identification of bacterial isolates from urinary tract infections. *J. Clin. Microbiol.* 40: 2795–800.

Kooistra, W. H. C. F., Coppejans, E. G. G. & Payri, C. 2002. Molecular systematics, historical ecology, and phylogeography of *Halimeda* (Bryopsidales). *Mol. Phylogen. Evol.* 24: 121–38.

Kooistra, W. H. C. F. & Verbruggen, H. 2005. Genetic patterns in the calcified tropical seaweeds *Halimeda opuntia*, *H. distorta*, *H. hederacea* and *H. minima* (Bryopsidales, Chlorophyta) provide insights in species boundaries and inter-oceanic dispersal. *J. Phycol.* 41: 177–187.

Knowlton, N. 1993. Sibling species in the sea. *Annu. Rev. Ecol. Syst.* 24: 189–216.

Lamouroux, J. V. F. 1812. Extrait d'un mémoire sur la classification de polypes coralligènes non entièrement pierreux. *Nouveau Bulletin Scientifique de la Société Philomathique* 3: 181–8.

Noble, J. M. 1987. A taxonomic study of the genus *Halimeda* Lamouroux (Chlorophyta, Caulerpales) from the Heron Island region of the southern Great Barrier Reef, Australia. Masters degree thesis, University of Melbourne, Melbourne, Australia, 200 pp.

Provan, J., Murphy, S. & Maggs, C. A. 2004. Universal plastid primers for Chlorophyta and Rhodophyta. *Eur. J. Phycol.* 39: 43–50.

Rohlf, F. J. 2004. tpsDig version 1.40. Department of Ecology and Evolution, State University of New York at Stony Brook. Available for download from http://life.bio.sunysb.edu/morph/.

Rueness, J. & Rueness, E. 2000. *Caulacanthus ustulatus* (Gigartinales, Rhodophyta) from Brittany (France) is an introduction from the Pacific Ocean. *Cryptogamie Algol.* 21: 355–63.

Swofford, D.L. 2003. PAUP*. Phylogenetic Analysis Using Parsimony (*and other methods). Version 4. Sinauer Associates, Sunderland, Massachusetts.

Valet, G. 1966. Sur une espèce rare et une nouvelle espèce d'*Halimeda* de Mélanésie. Revue Générale de Botanique 73: 680–5.

van der Strate, H. J., Boele-Bos, S. A., Olsen, J. L., van de Zande, L. & Stam, W. T. 2002. Phylogeographic studies in the tropical seaweed *Cladophoropsis membranacea* (Chlorophyta, Ulvophyceae) reveal a cryptic species complex. *J. Phycol.* 38: 572–82.

Verbruggen, H. De Clerck, O., Cocquyt, E., Kooistra, W. H. C. F. & Coppejans, E. 2005a. Morphometric taxonomy of siphonous green algae: a methodological study within the genus *Halimeda* (Bryopsidales). *J. Phycol.* 41: 126–139.

Verbruggen, H., De Clerck, O. & Coppejans, E. 2005b. Deviant segments hamper a morphometric approach towards *Halimeda* taxonomy. *Crypt. Algol.* 26: accepted.

Verbruggen, H., De Clerck, O., Schils, T., Kooistra, W. H. C. F. & Coppejans, E. Evolution and phylogeography of the *Halimeda cuneata/discoidea/tuna* cryptic species complex. submitted.

Verbruggen, H. & Kooistra, W. H. C. F. 2004. Morphological characterization of lineages within the calcified tropical seaweed genus *Halimeda* (Bryopsidales, Chlorophyta). *Eur. J. Phycol.* 39: 213–28.

Yano, T., Kamiya, M., Arai, S. & Kawai, H. 2004. Morphological homoplasy in Japanese *Plocamium* species (Plocamiales, Rhodophyta) inferred from the Rubisco spacer sequence and intracellular acidity. *Phycologia* 43: 383–93.

Zuccarello, G. C. & West, J. A. 2002. Phylogeography of the *Bostrychia calliptera-B. pinnata* complex (Rhodomelaceae, Rhodophyta) and divergence rates based on nuclear, mitochondrial and plastid DNA markers. *Phycologia* 41: 49–60.

Zuccarello, G. C. & West, J. A. 2003. Multiple cryptic species: Molecular diversity and reproductive isolation in the *Bostrychia radicans/B. moritziana* complex (Rhodomelaceae, Rhodophyta) with focus on North American isolates. *J Phycol.* 39: 948–59.

Appendix 1. Specimen list.

Specimen numbers correspond to their accession numbers in the Ghent University Herbarium (GENT), unless other herbarium acronyms are indicated in brackets (L = NHN Leiden, MICH = University of Michigan Herbarium). The last four columns represent the Genbank accession numbers of ITS and *rps*3 sequences, and inclusion in segment morphological and anatomical morphometric databases. Species authorities of all species cited in the text are *H. borneensis* W.R. Taylor, *H. cylindracea* Decaisne, *H. incrassata* (J. Ellis) J.V. Lamouroux, *H. macroloba* Decaisne, *H. melanesica* Valet, *H. monile* (J. Ellis & Solander) J.V. Lamouroux, *H. simulans* M.A. Howe, *H. stuposa* W.R. Taylor.

species	specimen	geographical origin	ITS	*rps*3	segment	anatomy
H. borneensis	10101E	Maisel Islands, Indonesia	AF525558			
	cc38608 (MICH)	Borneo, Indonesia **(holotype)**			+	
	H.0042	Moorea, French Polynesia	AF525552			
	H.0043	Moorea, French Polynesia	AF525553			
	H.0044	Moorea, French Polynesia	AF525554			
	H.0170	Pangasinan, The Philippines	AF525557			
	H.0174	Pangasinan, The Philippines	AF525555			
	H.0267	New Caledonia	AF525550			
	H.0269	New Caledonia	AF525551			
	HEC12603a	Chwaka, Zanzibar, Tanzania	AF407239			
	HEC12603b	Chwaka, Zanzibar, Tanzania	AF525559			
	HV18-1	Chwaka, Zanzibar, Tanzania	AY786512	AY835514	+	+
	HV23c	Chwaka, Zanzibar, Tanzania			+	+
	HV92	Moorea, French Polynesia	AY835458	AY835515	+	+
	HV145	Moorea, French Polynesia		AY835516	+	+
	HV183a	Arue, Tahiti, French Polynesia	AY835459	AY835517	+	+
	HV183b	Arue, Tahiti, French Polynesia	AY786513	AY835518	+	+
	HV205	Faaa, Tahiti, French Polynesia	AY835460	AY835519	+	+
	HV208	Faaa, Tahiti, French Polynesia		AY835520	+	+
	HV245	Maraa, Tahiti, French Polynesia	AY835461	AY835521	+	+
	HV246	Maraa, Tahiti, French Polynesia	AY835462	AY835522	+	+
	HV639	Olango, The Philippines	AY835463	AY835523	+	+
	HV733	Uson, The Philippines	AY835464	AY835524	+	+
	PH534	Zamboanga, The Philippines		AY835525	+	+
	WLS081-02	Wallis Island (Pacific Ocean)		AY835526	+	+
	WLS086-02	Wallis Island (Pacific Ocean)	AY835465	AY835527	+	+
	WLS148-02	Wallis Island (Pacific Ocean)	AY835466	AY835528	+	+
		Zamboanga, The Philippines	AF525556			
H. cylindracea	H.0015	Great Barrier Reef, Australia	AF525549		+	+
	H.0018	Great Barrier Reef, Australia	AF525548			
	H.0186	Great Barrier Reef, Australia	AF416388			
	H.0279	New Caledonia	AF407236			
	HOD-PH99-4	Bantayan, The Philippines	AY835467		+	+
	SOC364	Socotra (Yemen)	AF525546			
		Great Barrier Reef, Australia	AF525545			
H. incrassata 1a	03-104 (L)	Panjang, Indonesia	AY835468		+	+
	H.0016	Great Barrier Reef, Australia	AY835469	AY835529	+	+
	H.0019	Great Barrier Reef, Australia	AF525572	AY835530	+	+
	H.0022	Great Barrier Reef, Australia	AF525571			
	H.0035	Tahiti, French Polynesia	AF407242			
	H.0036	Tahiti, French Polynesia	AF525569			
	H.0040	Rangiroa, French Polynesia	AF525570			
	H.0045	Rangiroa, French Polynesia	AF525573			
	HV22	Chwaka, Zanzibar, Tanzania		AY835531	+	+
	HV104	Moorea, French Polynesia	AY835470	AY835532	+	+
	HV144	Moorea, French Polynesia	AY835471	AY835533	+	+
	HV146	Moorea, French Polynesia		AY835534	+	+
	HV149	Moorea, French Polynesia	AY835472	AY835535	+	+
	HV231	Maraa, Tahiti, French Polynesia		AY835536	+	+
	HV629	Olango, The Philippines	AY835473	AY835537	+	+
	HV636	Olango, The Philippines	AY835474	AY835538	+	+
	HV763	Tangat, The Philippines	AY835475	AY835539	+	+
	PH197	Mactan, The Philippines	AF407241		+	
		Mactan, The Philippines	AF525568			
H. incrassata 1b	H.0649	Honolua Bay, Maui, Hawaii, USA	AY835476	AY835540	+	+
	H.0650	Honolua Bay, Maui, Hawaii, USA	AY835477	AY835541	+	+
	H.0651	Honolua Bay, Maui, Hawaii, USA	AY835478	AY835542	+	+
	H.0652	Honolua Bay, Maui, Hawaii, USA	AY835479	AY835543	+	+
	H.0653	Honolua Bay, Maui, Hawaii, USA	AY835480		+	+
H. incrassata 2	H.0027	Galeta, Panama		AY835544	+	+
	H.0077	Bocas del Toro, Panama	AY835481	AY835545	+	+
	H.0079	Bocas del Toro, Panama	AY835482	AY835546	+	+

	H.0127	Bocas del Toro, Panama	AY835483	AY835547	+	+
	H.0132	San Andres, Panama	AY835484	AY835548	+	+
	H.0136	St. Martin, Netherlands Antilles	AY835485	AY835549	+	+
	H.0143	Isla Grande, Panama	AY835486	AY835550	+	+
	H.0145	Florida, USA			+	+
	H.0146	Florida, USA			+	+
	H.0149	Florida, USA	AY835487	AY835551	+	+
	H.0179	Lee Stocking, Bahamas	AF407233	AY835552	+	+
	H.0180	Florida, USA	AY835488	AY835553	+	+
	H.0181	Florida, USA	AF525537	AY835554	+	+
	H.0182	Florida, USA		AY835555	+	+
	H.0183	Florida, USA	AF525538	AY835556	+	+
	H.0188	Bocas del Toro, Panama	AY835489	AY835557	+	+
	H.0211	San Blas, Panama	AF525539			
	H.0229	Puerto Morelos, Mexico	AY835490	AY835558	+	+
	H.0236	Texas, USA	AF525540			
	H.0248	San Blas, Panama		AY835559	+	+
	H.0477	Bocas del Toro, Panama		AY835560	+	+
	HV332	St. Ann's Bay, Jamaica	AY835491	AY835561	+	+
	HV334	St. Ann's Bay, Jamaica	AY835492		+	+
	HV448	Discovery Bay, Jamaica	AY835493		+	+
H. macroloba	H.0038	Tahiti, French Polynesia	AF525563			
	H.0060	Viti Levu, Fiji	AF525564			
	H.0157	Pangasinan, The Philippines	AF525560			
	H.0158	Pangasinan, The Philippines	AF525566			
	H.0228	Exmouth, W Australia	AF525562			
	HEC12583	Zanzibar, Tanzania	AF407240			
	HV5	Matemwe, Zanzibar, Tanzania			+	
	HV17	Chwaka, Zanzibar, Tanzania			+	
	HV38	Nungwi, Zanzibar, Tanzania	AY786514	AY835562	+	+
	HV206	Faaa, Tahiti, French Polynesia	AY786515		+	+
		Zanzibar, Tanzania	AF525561			
		Zamboanga, The Philippines	AF525565			
		Great Barrier Reef, Australia	AF525567			
H. melanesica	03-462 (L)	Maratua, Indonesia	AY835494	AY835563	+	+
	HV217	Afaahiti, Tahiti, French Polynesia	AY835495	AY835564	+	+
	HV790	Bulusan, Luzon, The Philippines	AY835496	AY835565	+	+
	HV818	Dancalan, Luzon, The Philippines	AY835497	AY835566	+	+
H. monile	H.0034	Galeta, Panama	AY835498		+	+
	H.0075	Bocas del Toro, Panama	AY835499		+	+
	H.0135	San Andres, Panama	AY835500	AY835567	+	+
	H.0137	St. Martin, Netherlands Antilles	AY835501	AY835568	+	+
	H.0228b	Puerto Morelos, Mexico	AF407234	AY835569	+	+
	H.0404	Isla Grande, Panama	AY835502			
	HV333	St. Ann's Bay, Jamaica	AY835503	AY835570	+	+
	HV335	St. Ann's Bay, Jamaica	AY835504	AY835571	+	+
	HV344	Drax Hall, Ocho Rios, Jamaica	AY835505	AY835572	+	+
H. simulans	H.0032	Galeta, Panama	AY835506	AY835573	+	+
	H.0071	Bocas del Toro, Panama	AY835507	AY835574	+	+
	H.0080	Bocas del Toro, Panama	AY835508	AY835575	+	+
	H.0114	Portobelo, Panama		AY835576	+	+
	H.0147	Florida, USA		AY835577	+	+
	H.0230	Puerto Morelos, Mexico	AF525541	AY835578	+	+
	H.0324	San Blas, Panama	AF525544			
	H.0367	Escudo de Veraguas, Panama	AF407235			
	H.0402	Isla Grande, Panama	AY835509			
	HOD-MAR01-43	Martinique, French Antilles			+	+
	HV361	Drax Hall, Ocho Rios, Jamaica	AY835510	AY835579	+	+
	HV449	Discovery Bay, Jamaica	AY835511	AY835580	+	+
	HV504	Ocho Rios, Jamaica	AY835512	AY835581	+	+
	HV532	Blue Lagoon, Portland, Jamaica	AY835513	AY835582	+	+
		Isla Providencia, Colombia	AF525542			
		Galeta, Panama	AF525543			
H. stuposa	L.0238148 (L)	Rongelap, Marshall Islands **(isotype)**			+	+
	L.0238149 (L)	Eniwetok, Marshall Islands **(isotype)**			+	+

Phylogeny and taxonomy of *Halimeda incrassata*, including the description of *H. kanaloana* and *H. heteromorpha* spp. nov. [1]

Heroen Verbruggen, Olivier De Clerck, Antoine D.R. N'Yeurt, Heather Spalding & Peter S. Vroom

Manuscript submitted

Abstract

The tropical green algal genus *Halimeda* Lamouroux is one of the best studied examples of cryptic diversity within the algae. Former molecular and morphometric studies revealed that within section *Rhipsalis* of the genus, *Halimeda incrassata* (Ellis) Lamouroux embodied three pseudo-cryptic entities and that the morphological boundaries between *H. incrassata* and *H. melanesica* Valet were ill defined. In this paper, *H. incrassata* is retaxonomized: two of the pseudo-cryptic entities are described as *H. kanaloana* Vroom and *H. heteromorpha* N'Yeurt and *H. incrassata* is redescribed to include a sole, monophyletic entity. Likeness and disparity among the three pseudo-cryptic species and *H. melanesica* are discussed. Monophyly of *H. heteromorpha*, which was questioned in a former study, is reinterpreted using sets of 32 ITS1–ITS2 and 21 plastid *rps*3 sequences and multiple alignment and inference methods. The phylogenetic structure of section *Rhipsalis* is inferred from nuclear 18S–ITS1–5.8S–ITS2 and concatenated plastid sequences (*tuf*A & *rpl*5–*rps*8–*inf*A) and interpreted in terms of biogeographic hypotheses.

Introduction

Marine macroalgae of the chlorophyte genus *Halimeda* abound throughout the tropics and can be easily recognized by their green, calcified segments. The genus is an ecologically important reef alga throughout the tropical Indo-Pacific and Caribbean Sea, being a prominent primary producer (e.g. Littler et al., 1988), source of food and habitat (e.g. Rossier & Kulbicki, 2000; Chittaro, 2004) and carbonate sand producer (e.g. Drew, 1983; Freile et al., 1995; Payri, 1995).

Halimeda is presently subdivided into five sections characterized by ecological and morphological properties (Kooistra et al., 2002; Verbruggen & Kooistra, 2004). Within speciose sections, taxonomic problems are obvious. Boundaries between certain species are ambiguously defined (Verbruggen et al., 2005c), and several cases of cryptic diversity are known (Kooistra et al., 2002; Verbruggen et al., 2005c, submitted). To address these problems, DNA barcoding and morphometric analyses are being used to repartition the genus into species that are genetically and morphologically distinct (Kooistra & Verbruggen, 2005; Verbruggen et al., 2005c, submitted).

Section *Rhipsalis* of the genus, which is characterized by pores interconnecting medullar siphons at nodes and segment agglutination in the basal thallus region (Verbruggen & Kooistra, 2004), presently contains 11 tropical species, 4 of which are restricted to the Atlantic Ocean, and 7 of which are Indo-Pacific (Verbruggen et al., 2005c). Even though most species range throughout the Caribbean or Indo-Pacific, certain species have very small distribution ranges. For instance, *H. stuposa* and *H. favulosa*

[1] This chapter is not to be considered as printed matter in the sense of ICBN (St. Louis code) article 29.

seem to be endemic to the Marshall Islands and the Bahamas, respectively (species authorities listed in Table 1).

Section *Rhipsalis* was recently studied using molecular and morphometric techniques (Verbruggen et al., 2005c). The combination of both approaches allowed redelimitation of formerly ill-defined species within the *H. borneensis–simulans* and *H. cylindracea–monile* morphological groups. Additionally, *H. incrassata* was shown to consist of three cryptic entities that were initially recognized by deviant DNA sequences (Kooistra et al., 2002; Verbruggen et al., 2005c) and subsequently characterized using morphometric techniques (Verbruggen et al., 2005c). Noble (1987) noted a blurring of the species boundary between *H. melanesica* and *H. incrassata* because the absence of nodal fusions, a feature diagnostic to *H. melanesica*, is not constant within the species. The study by Verbruggen et al. (2005c) corroborates this blurring but shows that *H. melanesica* and *H. incrassata* are genetically distinct and that morphological characters other than nodal fusion patterns allow distinction between the entities.

Another point of interest from the paper by Verbruggen et al. (2005c) is the putative paraphyly of *H. incrassata* 1a, one of the cryptic species within *H. incrassata*. This entity, regarded a genotypic cluster species by Verbruggen et al. (2005c) and described below as *H. heteromorpha*, was monophyletic in a maximum parsimony (MP) phylogram inferred from *rps*3 sequences (Verbruggen et al., 2005c). However, in the MP phylogram inferred from ITS1–5.8S–ITS2 sequences, *H. incrassata* 1b (described below as *H. kanaloana*) branched off from within *H. incrassata* 1a, leaving the latter paraphyletic (Verbruggen et al. 2005c).

Table 1. Full species names and authorities of all species, varieties and forms cited in the text, sorted in alphabetical order. Most information was extracted from AlgaeBase (Guiry & Nic Dhonncha, 2004).

Flabellia petiolata (Turra) Nizamuddin
Halimeda bikinensis W.R. Taylor
Halimeda borneensis W.R. Taylor
Halimeda brevicaulis Kützing
Halimeda cylindracea Decaisne
Halimeda discoidea Decaisne
Halimeda distorta (Yamada) Hillis-Colinvaux
Halimeda favulosa M.A. Howe
Halimeda goreauii W.R. Taylor
Halimeda gracilis Harvey ex J.G. Agardh
Halimeda heteromorpha N'Yeurt
Halimeda incrassata (J. Ellis) J.V. Lamouroux
Halimeda incrassata f. *ovata* E.S. Barton
Halimeda incrassata var. *ovata* J.G. Agardh
Halimeda incrassata f. *rotunda* E.S. Barton
Halimeda incrassata f. *tripartita* E.S. Barton
Halimeda kanaloana Vroom
Halimeda macroloba Decaisne
Halimeda melanesica Valet
Halimeda micronesica Yamada
Halimeda minima (W.R. Taylor) Colinvaux
Halimeda monile (J. Ellis & Solander) J.V. Lamouroux
Halimeda opuntia (Linnaeus) J.V. Lamouroux
Halimeda polydactylis J.G. Agardh
Halimeda simulans M.A. Howe
Halimeda stuposa W.R. Taylor
Halimeda tridens (Ellis & Solander) J.V. Lamouroux
Halimeda triloba Decaisne
Halimeda tuna (J. Ellis & Solander) J.V. Lamouroux
Penicillus capitatus Lamarck
Udotea flabellum (J. Ellis & Solander) M.A. Howe

The goal of this paper is to retaxonomize *Halimeda incrassata* through careful description of the three pseudo-cryptic entities within the species (named *H. incrassata*, *H. kalanoana* and *H. heteromorpha*), stressing their morphological similarities and dissimilarities, distribution range and ecology. *Halimeda melanesica* is redescribed and included in the comparisons. Additionally, we aim to investigate the monophyly of *H. incrassata* 1a (*H. heteromorpha*) in more detail by inferring the evolutionary relationships between large sets of sequences of *H. macroloba*, *H. heteromorpha* and *H. kanaloana* using multiple inference methods and alternative sequence alignments. Finally, we aim explore the evolutionary and biogeographic history of *Halimeda* section *Rhipsalis* by phylogenetic inference using plastid and nuclear DNA sequence data.

Materials and methods

Taxa from section *Rhipsalis* were collected throughout most of their distribution ranges. Specimens were preserved partly in 95% ethanol or silica-gel for molecular analyses, partly in wet preservative (95% ethanol or 5% formalin) for anatomical observations.

Observations and measurements of vegetative and reproductive structures followed Verbruggen et al. (2005a, c) and Vroom & Smith (2003), respectively. Specimens were identified using the key of Ver-

bruggen et al. (2005c). Geographic origins and herbarium accession numbers of examined specimens are listed in Appendix 1. Extraction of DNA followed Kooistra et al. (2002).

Table 2. Accession numbers of DNA sequences used in phylogenetic analyses. Specimen numbers correspond to accession numbers in the Ghent University Herbarium (GENT).

species	specimen	SSU–ITS	*tuf*A	*rpl*5–*rps*8–*inf*A
H. borneensis	HV183b	AY786513	...submit...	...submit...
H. cylindracea	SOC364	AF525546	...submit...	...submit...
H. heteromorpha	HV146		...submit...	...submit...
	PH197	AF407241		
H. incrassata	H.0179	AF407233	...submit...	...submit...
H. kanaloana	H.0649	AY835476	...submit...	...submit...
H. macroloba	HV38	AY786514	...submit...	...submit...
H. melanesica	HV790	AY835496	...submit...	...submit...
H. monile	H.0034		...submit...	...submit...
	H.0228	AF407234		
H. simulans	HV449	AY835511	...submit...	...submit...
H. micronesica	WLS420-02	AY786518	...submit...	...submit...
H. gracilis	HV317	AY786526	...submit...	AY826384
H. discoidea	SOC299	AF407254		
H. opuntia	H.0262	AF525639		
F. petiolata	H.0495	AF416390		
P. capitatus	H.0349	AF416404		
U. flabellum	H.0415	AF407270		

For the examination of evolutionary relationships within section *Rhipsalis*, three DNA sequence sets were created. Part of the plastid *tuf*A gene was amplified according to Famà et al. (2002) and the plastid *rpl*5–*rps*8–*inf*A region according to Provan et al. (2004). Part of the nuclear ribosomal cistron (18S [SSU] from ca. position 500, ITS1, 5.8S, ITS2, and ca. 50 bases into 28S [LSU]) was amplified according to Kooistra et al. (2002). Amplified products were sequenced with an ABI Prism 3100 automated sequencer (Applied Biosystems, Foster City, CA) and submitted to Genbank (Table 2). For the plastid regions, *H. gracilis* and *H. micronesica* were sequenced as outgroups (Table 2). Sequences from the nuclear 18S–ITS1–5.8S–ITS2 region of ingroup taxa, as well as *H. discoidea*, *H. micronesica*, *H. gracilis* and *H. opuntia* as close outgroup taxa and *Udotea flabellum*, *Penicillus capitatus*, and *Flabellia petiolata* as far outgroup taxa were downloaded from GenBank (accession numbers listed in Table 2). Partial *tuf*A and *rpl*5–*rps*8–*inf*A sequences were aligned according to a blueprint created by ClustalW 1.82 alignment of their amino acid sequences as described in Verbruggen et al. (submitted). The ClustalW alignment was performed through the European Bioinformatics Institute (EBI) server, using default settings. The *tuf*A and *rpl*5–*rps*8–*inf*A sequence data sets were concatenated before analysis. The 18S–ITS1–5.8S–ITS2 sequences were aligned by eye, starting from the alignment of Verbruggen & Kooistra (2004). All alignments used in this study are available from the first author upon request.

Nuclear and plastid DNA data sets were subjected to maximum likelihood (ML) analysis in PAUP* 4.0b10 (Swofford 2003), using the nucleotide substitution model selected by Modeltest 3.5 (Posada & Crandall, 1998). Starting trees were obtained by stepwise random sequence addition. A single tree was retained at each step. Branch swapping was achieved by tree bisection-reconnection (TBR). The number of rearrangements was limited to 1000 per addition-sequence replicate. The analysis performed 25 addition-sequence replicates. ML bootstrapping (100 replicates) was performed with the same settings. MP bootstrapping (100 replicates) was performed with 100 addition-sequence replicates per bootstrap replicate, a limitation of the number of rearrangement per addition-sequence replicate of 100 million and gaps treated as missing data. Alternative topologies were tested against the obtained phylograms using the Shimodaira–Hasegawa (SH) test (Shimodaira & Hasegawa, 1999; Goldman et al., 2000) implemented in PAUP* 4.0b10, with resampling-estimated log-likelihood (RELL) optimization and 1000 bootstrap replicates.

For the reinvestigation of monophyly of *H. heteromorpha*, two batches of sequences were downloaded from Genbank (see results for accession numbers). The first batch of sequences consists of 32 18S–ITS1–5.8S–ITS2–28S sequences of *H. macroloba* (11 sequences), *H. heteromorpha* (= *H. incrassata* 1a; 16 sequences), and *H. kanaloana* (= *H. incrassata* 1b; 5 sequences). Two alignments were created

from this batch of sequences: (1) the ClustalW alignment used in Verbruggen et al. (2005), and (2) a manual alignment in which ambiguously aligned sequence blocks were coded in gap matrix (see results). Partial 18S, 5.8S and partial 28S were removed from both alignments because they were virtually invariant. The two alignments were subjected to three inference methods (ML, maximum parsimony [MP] and Bayesian Inference [BI]). ML analysis was carried out in PAUP* 4.0b10, using the nucleotide substitution model selected by MrModeltest 2.0 (Nylander, 2004). Options for ML analysis were: starting trees by stepwise random sequence addition, retaining a single tree at each step, TBR branch swapping, maximum 1000 rearrangements per addition-sequence replicate, 50 addition-sequence replicates. ML bootstrapping (100 replicates) was carried out with 5 addition-sequence replicates per bootstrap replicate. MP analysis was carried out in PAUP* 4.0b10, with the following options: starting trees by stepwise random sequence addition, retaining multiple trees at each step, TBR branch swapping, maximum 10^8 rearrangements per addition-sequence replicate, 100 addition-sequence replicates, with gaps treated as fifth base. MP bootstrapping (100 replicates) was carried out with the same settings. Bayesian inference was performed in MrBayes 3.0B4 (Ronquist & Huelsenbeck, 2003), using the nucleotide substitution model selected by MrModeltest 2.0. Analyses were run with four Markov chains for 10^6 generations, with a tree saved every 100th generation. The first 1000 trees were discarded as burn-in. The 11 *H. macroloba* sequences were used as outgroup for ML and MP analysis, the *H. macroloba* sequence AF525562 for BI.

The second batch of sequences downloaded for the reinvestigation of *H. heteromorpha* monophyly was one of 21 plastid *rps*3 sequences of *H. incrassata* 2, *H. monile*, *H. simulans*, *H. melanesica*, *H. borneensis*, *H. macroloba* (1 sequence of each), *H. heteromorpha* (= *H. incrassata* 1a; 11 sequences) and *H. kanaloana* (= *H. incrassata* 1b; 4 sequences). These protein-coding sequences were aligned on the basis of a blueprint created by ClustalW alignment of their amino acid sequences (ClustalW 1.82 at the EBI server: www.ebi.ac.uk/clustalw/, with standard settings) as in Verbruggen et al. (2005c). ML, MP and BI analyses were carried out as detailed above for the ITS1–ITS2 sequence alignments. Sequences AY835573 (*H. simulans*), AY835552 (*H. incrassata* 2), AY835572 (*H. monile*), AY835514 (*H. borneensis*) and AY835565 (*H. melanesica*) were used as outgroup for ML and MP analysis, the *H. incrassata* 2 sequence AY835552 for BI.

Results

Molecular phylogenies of section *Rhipsalis*

Sequences from the nuclear ribosomal DNA cistron that were used for inference of a molecular phylogeny of section *Rhipsalis* ranged from within the 18S gene (ca. position 500), through the ITS1–5.8S–ITS2 region, and ca. 50 bases into the 28S gene, adding up to sequence lengths of 1724–1755 base pairs for ingroup species. The relatively conserved 18S, 5.8S and 28S sequences could be readily aligned with very few gap introductions. Within both ITS regions, variable parts alternated with more conserved parts. Alignment of the more variable parts required introduction of gaps. The alignment totalled to 1840 positions, of which 247 were parsimony informative. Modeltest selected a Tamura and Nei (1993) substitution model with substitution rates following a gamma distribution (shape = 0.5151) and proportion of invariable sites equal to 0.5824.

Partial *tuf*A sequences were all of equal length (859 base pairs), and the alignment contained no indels. Sequences of the *rpl*5–*rps*8–*inf*A region ranged widely in length (686–808 base pairs) due to large length differences in the *rps*8–*inf*A spacer, which was excluded from analyses (cf. Verbruggen et al., submitted). Coding regions were almost constant in length and aligned readily. Two codon gaps had to be introduced for alignment of the ingroup sequences. Inclusion of outgroup sequences required introductions of several more codon gaps. Base substitutions in the *tuf*A and *rpl*5–*rps*8–*inf*A sequences occurred mainly at third codon positions. The concatenated alignment counted 1557 positions of which 132 were parsimony informative. Modeltest selected a Tamura and Nei (1993) substitution model with

substitution rates following a gamma distribution (shape = 0.5713) and proportion of invariable sites equal to 0.4758.

Phylograms inferred from nuclear ribosomal and concatenated plastid DNA sequences are presented in Figs 1 and 2, respectively. *Halimeda heteromorpha* and *H. kanaloana*, two new species that will be described below, correspond to haplotype groups *H. incrassata* 1a and *H. incrassata* 1b of Verbruggen et al. (2005c), respectively.

The nuclear phylogram (Fig. 1) contained two major lineages. The first clade contained the three Atlantic species; the second comprised all Indo-Pacific species. Within the Indo-Pacific clade, a very well-supported subgroup containing all Indo-Pacific species except *H. cylindracea* was present. This subgroup contained a polytomy of *H. melanesica*, *H. borneensis*, and the *H. macroloba–heteromorpha–kanaloana* lineage. The *H. heteromorpha–kanaloana* cluster received relatively high bootstrap support.

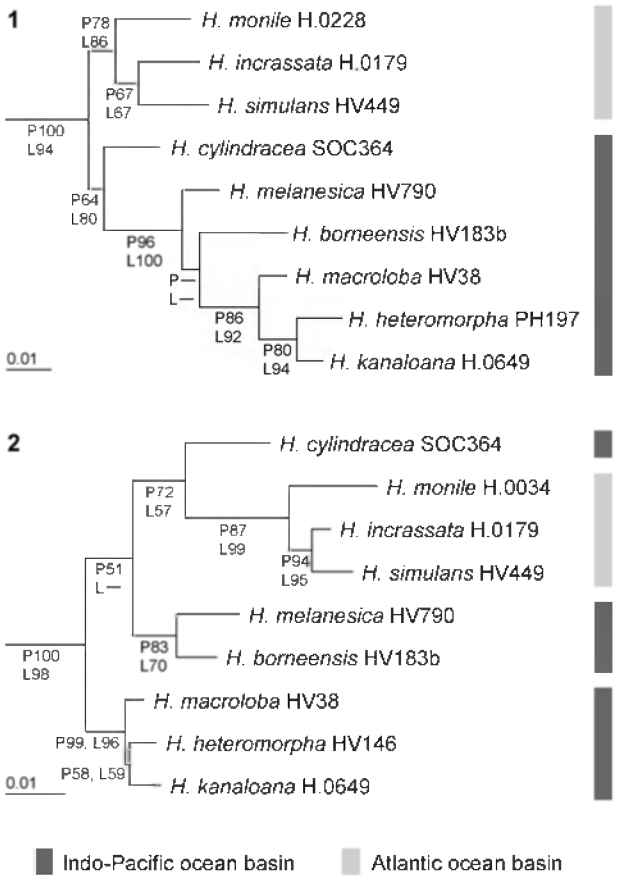

Figs 1-2. Phylograms inferred by maximum likelihood analysis. **Fig. 1.** Phylogram inferred from SSU–ITS1–5.8S–ITS2 sequence data (–ln L = 6779.4578). **Fig. 2.** Phylogram inferred from concatenated plastid sequence data (–ln L = 4454.7443). Outgroups were pruned from the trees. Maximum parsimony (P) and maximum likelihood (L) bootstrap values are indicated at branches. Scale bars represent 0.01 substitutions per site. Grey bars along the right hand side indicate the geographic origin of species.

In the phylogram inferred from plastid sequences (Fig. 2), the section split up in three major groups. The first group, which united *H. cylindracea* with the Atlantic species *H. monile*, *H. incrassata* and *H. simulans*, received mediocre bootstrap support. Within this clade, the three Atlantic species formed a monophyletic group with high bootstrap support. The second cluster within the plastid phylogeny grouped *H. melanesica* and *H. borneensis*. The third major lineage consisted of *H. macroloba*, *H. heteromorpha* and *H. kanaloana*. In contrast with the nuclear tree, the *H. heteromorpha–kanaloana* cluster received low bootstrap support.

The nuclear and plastid phylograms did not entirely correspond. Although they agreed on the *H. monile–incrassata–simulans* and *H. macroloba–heteromorpha–kanaloana* species clusters, affinities among these clusters and the other species were incongruent. *Halimeda melanesica* and *H. borneensis*, which formed a monophyletic group with unclear affinities in the plastid tree, formed a basal grade of a well-supported clade that also contained the *H. macroloba–heteromorpha–kanaloana* cluster in the nrDNA clade. The species *H. cylindracea*, which took a basal position in the Indo-Pacific clade of the nrDNA tree, was recovered at the base of a clade which otherwise existed of Atlantic species in the plastid phylogram. Monophyly of an Indo-Pacific species cluster, which is suggested by the nrDNA tree, is not supported by the plastid phylogram.

However, enforcement of a monophyletic Indo-Pacific species cluster did not result in a significantly worse plastid DNA topology (SH test, length difference = 0.81482, p = 0.421). The ML tree obtained under this enforcement was nearly identical to the nrDNA topology of Fig. 1 with the exception that the *H. melanesica–borneensis* cluster remained monophyletic, as the sister group of the *H. macro-*

loba–heteromorpha–kanaloana clade. Enforcement of the exact topology of the nrDNA tree (Fig. 1) did not produce a significantly worse plastid DNA topology (SH test, length difference = 12.88158, p = 0.054).

Three alternative topologies were tested against the original nrDNA topology, using SH tests on the nrDNA data. The ML topology in which *H. cylindracea* was sister to the Atlantic species trio was not significantly worse (length difference = 2.38519, p = 0.333). Introduction of a monophyletic *H. melanesica–borneensis* group was also not significantly worse (length difference = 0.49487, p = 0.441). Finally, the cpDNA topology of Fig. 2 was tested against the nrDNA sequence data. The SH test was significant (length difference = 26.58934, p = 0.010), meaning that, in the light of the nrDNA data, the cpDNA topology is worse than the original nrDNA phylogram.

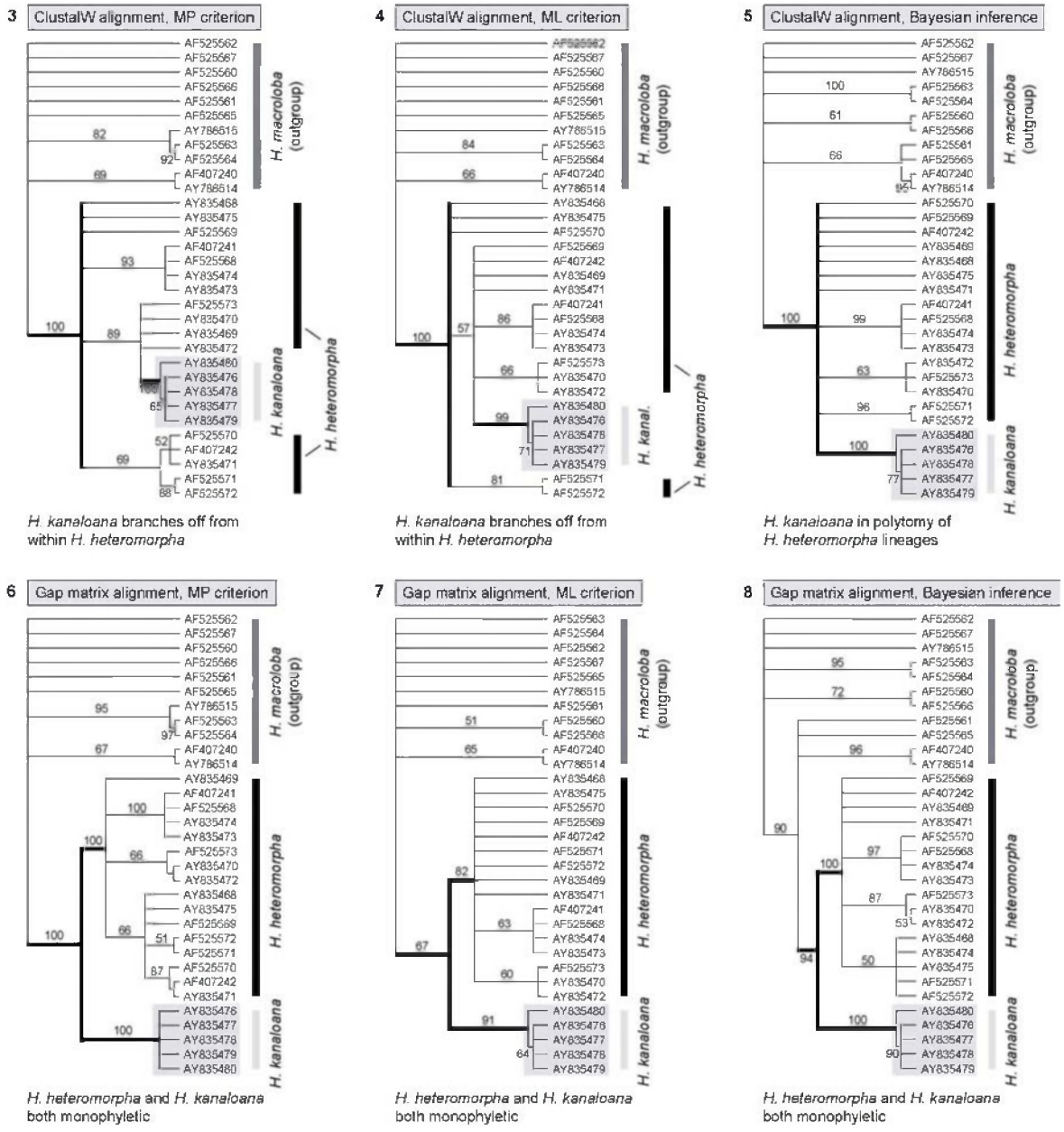

Figs 3–8. Fifty percent majority rule consensus trees resulting from: **Fig. 3.** MP bootstrap analysis of the ClustalW alignment of the ITS1–ITS2 data. **Fig. 4.** ML bootstrap analysis of the ClustalW alignment of the ITS1–ITS2 data. **Fig. 5.** Bayesian analysis of the ClustalW alignment of the ITS1–ITS2 data. **Fig. 6.** MP bootstrap analysis of the gap matrix alignment of the ITS1–ITS2 data. **Fig. 7.** ML bootstrap analysis of the gap matrix alignment of the ITS1–ITS2 data. **Fig. 8.** Bayesian analysis of the gap matrix alignment of the ITS1–ITS2 data. Clade support is given as bootstrap proportions (ML and MP trees) and posterior probabilities (BI trees). Bold lines indicate the roots of *H. heteromorpha* and *H. kanaloana*.

Monophyly or paraphyly of *H. heteromorpha*

After the ClustalW alignment of 18S–ITS1–5.8S–ITS2–28S sequences used by Verbruggen et al. (2005c) had been stripped of 18S, 5.8S, 28S and all taxa except *H. macroloba*, *H. incrassata* 1a (= *H. heteromorpha*) and *H. incrassata* 1b (= *H. kanaloana*), the alignment counted 240 positions. ITS1 sequences ranged from 78 to 89 bases in length; for ITS2 this was 141–146 bases. MrModeltest selected a symmetrical model of base substitution (Zharkihk, 1994) with gamma shape parameter 0.3256 for this ClustalW ITS1–ITS2 alignment. The gap matrix alignment differed from the ClustalW alignment in that individual bases and sequence blocks showing ambiguous alignment between species were separated and individual gaps or blocks of gaps were inserted in the species where this base or sequence block was not present. The alignment totalled 266 positions, 26 more than the ClustalW alignment. MrModeltest selected a Kimura 80 base substitution model (Kimura, 1980) with gamma shape parameter 0.2916 for this gap matrix alignment.

Figures 3 through 8 depict the 50% majority rule consensus trees of ML bootstrap, MP bootstrap, and BI analyses of the ClustalW and gap matrix alignments of the ITS1–ITS2 sequence data. All trees showed strong support of the clade containing *H. heteromorpha* and *H. kanaloana* sequences. The trees also agreed on the monophyly of *H. kanaloana*. The position of *H. kanaloana* in relation to *H. heteromorpha*, however, differed between trees. In the MP and ML bootstrap consensus trees inferred from the ClustalW alignment (Figs 3, 4), *H. kanaloana* branched off from within *H. heteromorpha*, leaving the latter paraphyletic. In the BI tree inferred from the ClustalW alignment (Fig. 5), the *H. kanaloana* clade sat in a polytomy with all *H. heteromorpha* lineages, also suggesting non-monophyly of the latter. In all trees based on the gap matrix alignment, the clade containing *H. heteromorpha* and *H. kanaloana*, and the individual species *H. kanaloana* and *H. heteromorpha* were monophyletic with high support.

The alignment of *rps*3 sequences consisted of 909 positions, with individual sequences ranging from 672–828 bases in length. MrModeltest selected a general time reversible model with substitution rates following a gamma distribution (shape parameter 0.2721). Figures 9 through 11 show the 50% majority rule consensus trees of ML bootstrap, MP bootstrap, and BI analyses of the plastid *rps*3 sequence data. *Halimeda kanaloana* and *H. heteromorpha* were both monophyletic, irrespective of the inference method used. Contrary to the nuclear ribosomal tree (Fig. 1), *H. kanaloana* and *H. heteromorpha*, did not cluster together in the *rps*3 trees. In the MP tree (Fig. 9), *H. heteromorpha* showed a sister relationship with *H. macroloba*. In the ML and BI trees (Figs 10, 11), the *H. heteromorpha*, *H. macroloba* and *H. kanaloana* clades sprouted from a single trichotomy.

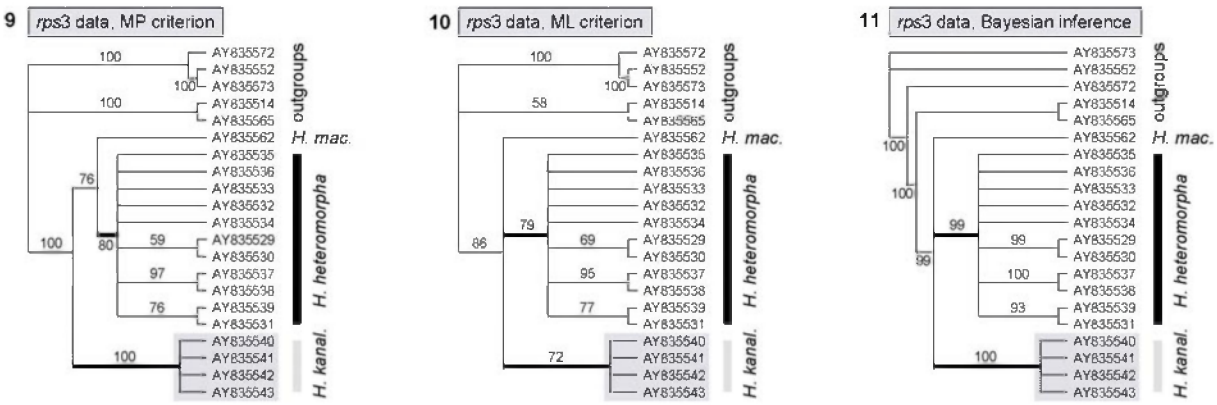

Figs 9–11. Fifty percent majority rule consensus trees resulting from: Fig. 9. MP bootstrap analysis of the *rps*3 alignment. **Fig. 10.** ML bootstrap analysis of the *rps*3 alignment. **Fig. 11.** Bayesian analysis of the *rps*3 alignment. Clade support is given as bootstrap proportions (ML and MP trees) and posterior probabilities (BI trees). Bold lines indicate the roots of *H. heteromorpha* and *H. kanaloana*.

Descriptions

In what follows, two new species of *Halimeda* are described and two other species are redescribed into single, evolutionarily meaningful entities. The species and their allies are illustrated in Figs 12–70. Ecological data have been incorporated in the species descriptions to report and illustrate adaptive morphological variability. The dimensions of structures reported in the descriptions were taken from the data sets of Verbruggen et al. (2005c). They represent the upper and lower boundaries of median values of 10 replicate measurements per specimen (see Verbruggen et al., 2005a, c) from non-apical, calcified segments from the central and upper parts of the thallus (Verbruggen et al., 2005b). Herbarium acronyms stand for Bishop Museum, Honolulu, Hawai`i, USA (BISH); Ghent University Herbarium, Ghent, Belgium (GENT); National Herbarium of the Netherlands, Leiden University branch, Leiden, The Netherlands (L); Muséum National d'Histoire Naturelle, Paris, France (PC).

Halimeda kanaloana Vroom, sp. nov.

Figs 12, 13, 39, 40, 49, 50, 61, 62, 69–70.

Diagnosis: *Halimeda kanaloana* Vroom a speciebus affinibus differt haptero magno bulboso in arenis specimen adfigente, parte thalli basali e segmentis magnis cylindricis vel paulo complanatis constante, segmentis magnis trilobis obovoideis vel cuneatis in partibus thalli centralibus distalibusque (longitudine mediana 9–14 mm, latitudine 6–11 mm, crassitie 1.5–2.9 mm), siphonibus medullaribus ad segmentorum nodos in unum conjungentibus, poris manifestis ad segmentorum nodos connectentibus siphones adjacentes (altitudine pororum mediana 47–69 µm parietibus cellularum inclusis), stratis utriculorum 4–5, utriculis peripheralibus magnis (diametro mediano 56–73 µm, altitudine 69–98 µm) attingentibus 42% suae maximae latitudinis ad quartem partem altitudinis suae et a superficie visis angulis rotundatis semper carentibus, et utriculis subperipheralibus valde inflatis.

Halimeda kanaloana Vroom differs from related species through the combination of a large bulbous holdfast anchoring the specimen in sand, a basal thallus region of massive cylindrical to slightly flattened segments, large obovoid to cuneate trilobed segments in the central and distal thallus regions (median length 9–14 mm, width 6–11 mm, thickness 1.5–2.9 mm), medullar siphons fusing into a single unit at segment nodes, obvious pores connecting neighbouring siphons at segment nodes (median pore height including cell walls 47–69 µm), 4–5 utricle layers, large peripheral utricles (median diameter 56–73 µm, height 69–98 µm) that reach 42% of their maximal width at one fourth of their height and that never have rounded corners in surface view, and markedly inflated subperipheral utricles.

Holotype: From the personal collection of Heather Spalding HS-2004-172, slated for eventual deposition at the Bishop Musuem, Honolulu, Hawai`i, USA (BISH). Collected at Keyhole, Mau`i, Hawai`i, U.S.A. Growing in a monospecific meadow at a depth of 56 m. Collected on 6 September 2004, during dive 565 of the submersible Pisces V.

Paratypes: H.0649 through H.0658 (GENT), Honolua Bay, Mau`i, Hawai`i, USA. HS-2004-162, HS-2004-171, HS-2004-173 through HS-2004-178 from Keyhole, Mau`i, Hawai`i, USA. HS-2004-157, HS-2004-159, HS-2004-161 from Kaho`olawe, Hawai`i, USA.

Etymology: The epithet *kanaloana* means belonging to Kanaloa, the Hawai`ian god of the ocean.

Description: *Halimeda kanaloana* forms extensive meadows in sandy environments. Occasional individuals are found as shallow as 1–2 m, with dense stands beginning at 15 m and ending abruptly around 85m. Within the meadows, plants are evenly spaced, suggesting competition for resources. Specimens are anchored in sand by means of a gritty, bulbous anchoring holdfast up to 8 cm in length (Figs 12, 13), within which the rhizoids tightly cling to sand. Very rarely, specimens were found attached to rock.

The heavily calcified stipe is sparsely branched and, in older specimens, overgrown by sponges, encrusting coralline algae, and filamentous algal epiphytes (Figs 12, 13). The basal thallus region consists mainly of squat cylindrical segments with some bilobed and laterally fused segments that produce additional branches (Figs 12, 13). Most branching occurs mid-frond, just above the basal region (Figs 12, 13). In the central region, axes often contain long series of less heavily calcified, trilobed segments, several of which produce branches (Figs 12, 13). Young segments located toward branch apices are lightly calcified and often become crumbly in herbarium presses.

Median lengths and widths of centrally located segments range from 9 to 14 mm and 6 to 11 mm, respectively, with median length over width ratios ranging from 1.02 to 1.48 and median thickness ranging from 1.5 to 2.9 mm. The great majority of segments from the central and apical thallus parts are obovate–cuneate (88%), meaning that they are broadest at or near their tip rather than at or near their base. The segment base is always acute. About one third of the segments are obovate and unlobed. The remaining segments are shallowly to deeply lobed. Of the lobed segments, the majority are trilobed (56%) or bilobed (29%). The lobed segments usually produce a branch from each lobe. On trilobed segments where only two branches form, the third lobe is often reduced in size.

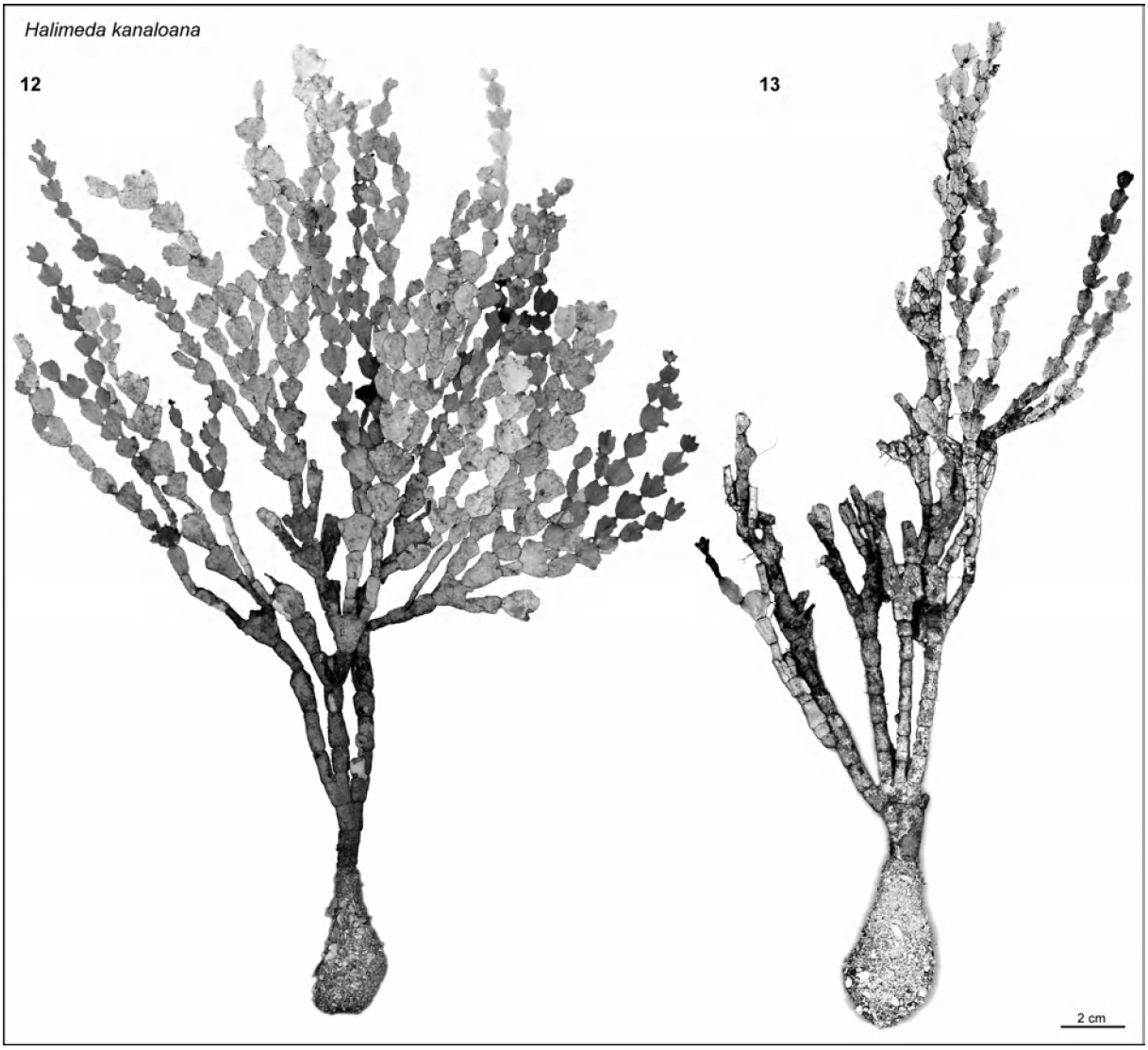

Figs 12–13. *Halimeda kanaloana* thalli. **Fig. 12.** Specimen HS-2004-172 (holotype) from Mau`i, Hawaii. **Fig. 13.** Specimen HS-2004-161 from Mau`i, Hawaii. Both specimens are slated for deposition at the Bishop Museum (BISH).

Medullar siphons adhere into a single unit at segment nodes and individual siphons cannot be isolated from this unit without sectioning it. Dissected nodes feature a marked belt of thickened cell wall material (Figs 39, 40). This adhesion belt, whose median height ranges from 47 to 69 μm, is perforated by numerous large pores (Fig. 40). Median distance from the base of nodes to the first medullary ramification of the segment (supranodal siphon length) ranges from 391 to 614 μm; its median diameter ranges from 148 to 170 μm. Medullar siphons ramify in trichotomies, rarely in dichotomies (Fig. 39). Median medullar siphon diameters range from 123 to 161 μm, with median length over width ratios ranging from 7.8 to 10.6.

The cortex consists of 4 to 5 utricle layers (Fig. 49). Peripheral utricles adhere to one another at their distal end, remaining firmly attached after decalcification. In surface view, peripheral utricles are arranged in a non-uniform pattern of polygons (Fig. 50) and never exhibit rounding of corners. Median peripheral utricle diameters and heights range from 56 to 73 μm and 69 to 98 μm, respectively, with median height over diameter ratios ranging from 1.08 to 1.51. Subperipheral utricles exhibit markedly inflated morphologies (Fig. 49). Median secondary utricle diameters and heights range from 51 to 58 μm and 67 to 99 μm, respectively, with median height over diameter ratios ranging from 1.29 to 1.78.

Compared to segments from higher up the thallus, segments composing the stipe have rigid, thick-walled, elongate utricles (Fig. 62). The thicker cell walls are obvious in surface view (Fig. 61). Siphon fusion at nodes in the lower thallus regions is the same as in more apically situated nodes of the thallus.

Halimeda kanaloana is holocarpic with reproductive individuals found in low numbers during many months of the year. Transparent gametophores are 2.7 to 3.4 mm long and 50 to 90 μm wide and are produced from medullary siphons that are pushed through tiers of utricles before emerging from the cortex. Although reproductive structures form on all surfaces of bleached segments, they are often concentrated on terminal edges (Fig. 69). Gametophores usually exhibit 1 or 2 dichotomies about halfway along their length separating the terminal, deeply pigmented gametangia into 2 to 3 distinct clusters (Fig. 70). Eight to 25 gametangia commonly occur on each gametophore with diameters ranging from 100 to 320 μm. The gametophore branches dichotomously several additional times among each gametangial cluster. Each cluster contains a conspicuous discharge papilla.
Distribution: *Halimeda kanaloana* forms extensive meadows between the islands of Mau`i, Kaho`olawe, Lana`i and Moloka`i in the main Hawai`ian islands (Abbott & Huisman, 2004, as *H. incrassata*). Specimens attributed to *H. incrassata* from the Ryukyu Islands, Japan (Tsuda & Kamura, 1991) most likely also represent *H. kanaloana*. A distribution map is presented in Fig. 71.

***Halimeda heteromorpha* N'Yeurt, sp. nov.**

Figs 14–26, 41–43, 51–54, 63, 64.

Diagnosis: *Halimeda heteromorpha* N'Yeurt a speciebus affinibus differt haptero implexo in saxis specimen adfigente, siphonibus medullaribus ad segmentorum nodos in unum conjungentibus, poris ad segmentorum nodos connectentibus segmenta adjacentia omnino nullis vel parvis (altitudine pororum mediana 25–36 μm parietibus cellularum inclusis), stratis utriculorum 2–3, utriculis peripheralibus magnis (diametro mediano 57–79 μm, altitudine 74–102 μm) non vulgo attingentibus 42% suae maximae latitudinis ad quartem partem altitudinis suae et a superficie visis angulis rotundatis semper carentibus, et utriculis subperipheralibus non manifeste inflatis.

Halimeda heteromorpha N'Yeurt differs from related species through the combination of a matted holdfast attaching the specimen to rock, medullar siphons adhering into a single unit at segment nodes, total absence of pores connecting neighbouring segments at segment nodes or smallish nodal pores (median pore height including cell walls 25–36 μm), 2–3 utricle layers, large peripheral utricles (median diameter 57–79 μm, height 74–102 μm) that do not generally reach 42% of their maximal width

at one fourth of their height and that never have rounded corners in surface view and subperipheral utricles that are not markedly inflated.

Holotype: HV149 (GENT). Collected between Papetoai and motu Tiahura, Moorea, French Polynesia. Growing at the base of a coral boulder on the landward side of the barrier reef, close to the reef crest.

Paratypes: HV22, HEC12238 (GENT), Chwaka Bay, Zanzibar, Tanzania. HEC11946, HEC12065 (GENT), Matemwe, Zanzibar, Tanzania. HV104, HV144, HV146 (GENT), Moorea, French Polynesia. UPF097 (UPF), Marquesas, French Polynesia. UPF097, 2808, 2809, 2815, 2823 (UPF), Tahiti, French Polynesia. UPF2803, 2810, 2814 (UPF), Moorea, French Polynesia. HV629, HV636, PH245 (GENT), Olango, Philippines. HV763 (GENT), Tangat, Philippines. L.0399613 (L), Panjang Island, Berau Archipelago, Indonesia.

Etymology: The epithet *heteromorpha* refers to the variable external morphology of the species.

Description: *Halimeda heteromorpha* is characterized by highly variable ecology and morphology. It occurs in a broad spectrum of relatively shallow water habitats. Specimens are attached to rocky substrate by means of a rhizoidal mat of variable shape and consistency. In specimens that are directly attached to rock, the holdfast consists of a firm, dense mat of rhizoids (Figs 16, 19, 21). In specimens that grow on sand- or silt-covered rock, the holdfast zone is more flaccid (Figs 14, 15).

Specimens attached to rocky substrates in lagoon habitats have several branches arising from the lowermost few segments (Figs 14, 16, 18). Segments are broader than long or about as broad as long (Fig. 25). Segment size diminishes from the base to the apices. Specimens that grow from within crevices in rock or coral boulders have a long, stipitate base composed of elongate, relatively thick segments (Fig. 17). Segments from the upper thallus are small, broader than long or about as broad as long (Fig. 26). Specimens from extremely sheltered bays and mangrove channels are large and densely ramified close to their base (Fig. 15), although the resulting axes are sparsely branched (Fig. 15). Specimens collected from shallow, surge-affected reef habitats consist of relatively large, round segments and feature more or less homogeneous branching throughout the thallus (Fig. 19). Specimens collected from sheltered fore-reef slopes exhibit relatively large, trilobed segments with homogeneous branching throughout the thallus (Fig. 21). Finally, specimens collected from small crevices in rock boulders on reef flats that are exposed to vigorous tidal currents and moderate wave action exhibit diminutive thalli with relatively small segments (Fig. 20). Segment merger in the basal thallus zone is relatively rare, occurring only in the forms represented in Figs 17 and 19.

Median lengths and widths of centrally located segments range from 2.3 to 8.2 mm and 2.4 to 9.1 mm, respectively, with median length over width ratios ranging from 0.66 to 1.16 and median thickness ranging from 0.6 to 1.4 mm. Segments from specimens located in exposed habitats (Figs 19, 22), extremely sheltered bays (Figs 15, 24) and sheltered fore-reef slopes (Figs 21, 23) are situated at the high end of these spectra. The surface of segments from the central and upper thallus parts are rough, often ruffled, especially in the small, upper segments of the forms depicted in Figs 17, 18, 25 and 26. Segments are moderately to poorly calcified and somewhat pliable, although specimens from surge-affected sites (Fig. 19) and the fore-reef slope (Fig. 21) have more strongly calcified segments with relatively pliable nodes. Segment shape is extremely variable among, and to a lesser extent within, ecotypes. In specimens from surge-affected sites, segments are more or less discoid (Figs 19, 22). In populations from fore-reef slopes, segments are markedly trilobed (Fig. 23). Finally, in specimens from lagoon habitats, the majority of segments are ovate–obovate (70%), with 32% of segments unlobed and 58% shallowly trilobed.

Medullar siphons adhere closely at nodes, showing an adhesion band in dissected nodes (Figs 41–43). Pores between parallel siphons are small (Fig. 42) or absent (Fig. 43). Median adhesion belt heights range from 25 to 36 μm. Median supranodal siphon lengths and diameters range from 242 to 535 μm and from 100 to 166 μm, respectively. Medullar siphons ramify in trichotomies, rarely in dichotomies

(Fig. 41). Median medullar siphon diameters range from 89 to 129 µm, with median length over width ratios ranging from 7.05 to 11.7.

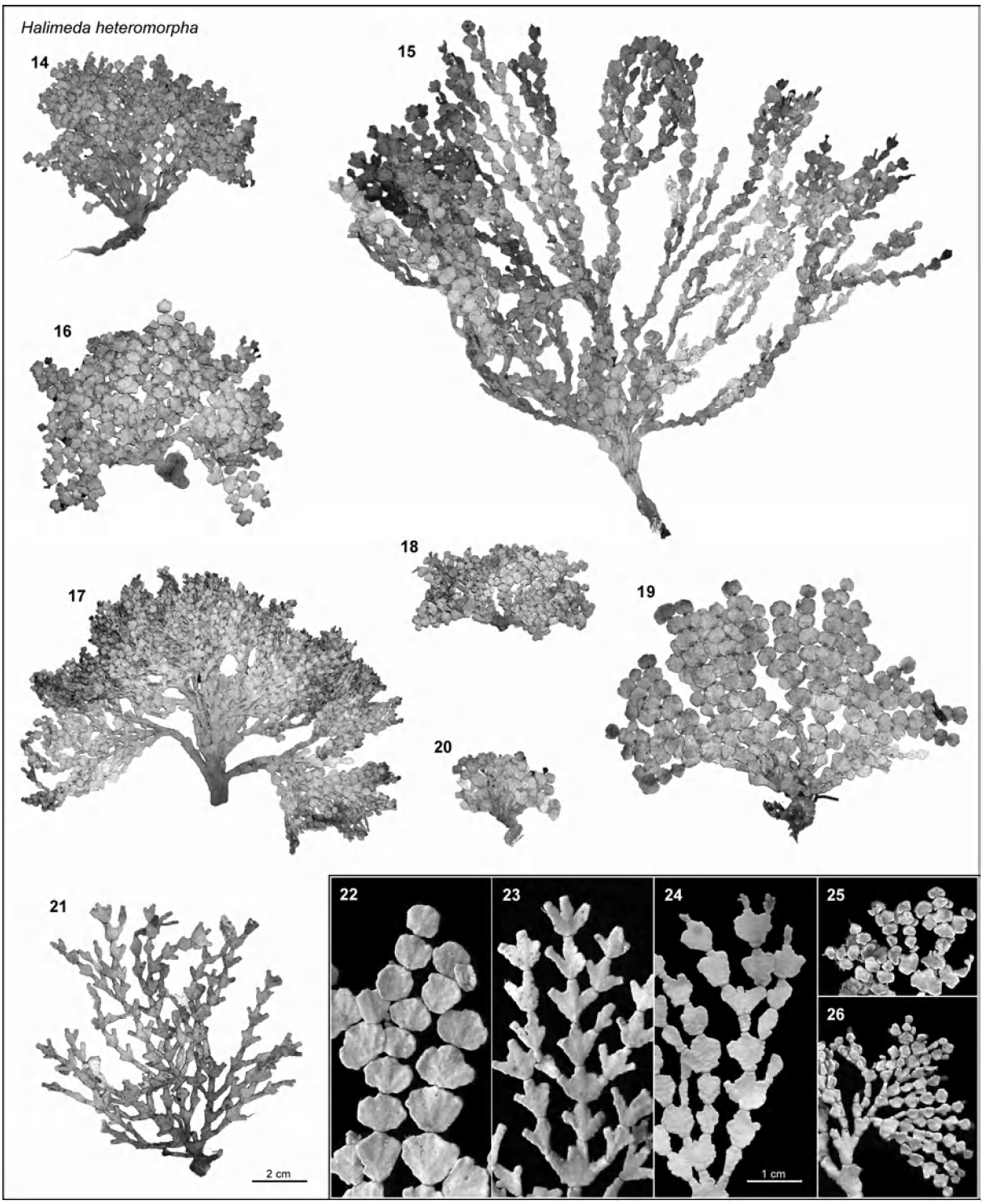

Figs 14–26. *Halimeda heteromorpha* thalli. **Fig. 14.** Specimen HV231 from French Polynesia. **Fig. 15.** Specimen HV22 from Zanzibar. **Fig. 16.** Specimen HV144 from French Polynesia. **Fig. 17.** Specimen HV146 from French Polynesia. **Fig. 18.** Specimen HV104 from French Polynesia. **Fig. 19.** Specimen HV629 from The Philippines. **Fig. 20.** Specimen HV636 from The Philippines. **Fig. 21.** Specimen HV763 from The Philippines. **Fig. 22.** Specimen HV629 from The Philippines. **Fig. 23.** Specimen HV763 from The Philippines. **Fig. 24.** Specimen HV22 from Zanzibar. **Fig. 25.** Specimen HV104 from French Polynesia. **Fig. 26.** Specimen HV146 from French Polynesia. Scale is uniform among thallus pictures (Figs 14–21) and among insets of segment morphology details (Figs 22–26). All specimens from the Ghent University Herbarium (GENT).

The cortex consists of 2 to 3 utricle layers (Figs 51, 53). Peripheral utricles adhere to one another at their distal end, remaining attached after decalcification. Median peripheral utricle diameters and heights range from 57 to 79 µm and 74 to 102 µm, respectively, width median height over diameter ratios ranging from 0.98 to 1.66. In surface view, peripheral utricles appear as a non-uniform pattern of polygons, without rounding in the corners (Figs 52, 54). Subperipheral utricles are not markedly inflated (Figs 51, 53). Median secondary utricle diameters and heights range from 42 to 66 µm and 54 to 111 µm, respectively, with median height over diameter ratios ranging from 1.09–2.05.

Cortex of thick, basal segments (observed in stipitate segments of the specimen depicted in Fig. 17) consists of a couple more utricle layers than the upper segments (Fig. 64). In comparison to segments from central and apical thallus parts (cf. Figs 51, 53), utricles of stipitate segments are more rigid, thick-walled and elongate. The thicker cell walls are especially visible in surface view (Fig. 63). Siphon fusion at nodes is highly similar in all thallus regions.

Distribution: *Halimeda heteromorpha* occurs throughout the tropical parts of the Indo-Pacific ocean basin. A compilation of distribution data from personal identifications of specimens from the GENT, L, and UPF herbaria and convincing literature reports (e.g. Barton 1901 as *H. incrassata* f. *ovata*, Noble 1987 as *H. melanesica*) is mapped in Fig. 71.

***Halimeda incrassata* (J. Ellis) J.V. Lamouroux**

Figs. 27–31, 44, 45, 55, 56, 65, 66.

Holotype: The type specimen of *H. incrassata* has been lost (Barton, 1901; Hillis-Colinvaux, 1980).

Lectotype: The illustrations of Ellis (1767), which have been reproduced in Hillis-Colinvaux (1980: p. 20), are hereby designated as the lectotype.

Description: *Halimeda incrassata* thalli are anchored in sandy substrates by means of a 2–5 cm long, bulbous holdfast that consists of a network of rhizoidal siphons adhering to sand particles. The species inhabits a spectrum of sandy-bottom habitats, including lagoons, seagrass beds, mangroves, and sand patches on outer reef slopes.

Thalli generally feature a sparsely branched, basal zone of thick, rigid segments (Figs 27–31). In this basal region, neighbouring segments occasionally fuse (Fig. 28) and are often covered with a thick layer of epiphytes, particularly encrusting corallines (Figs 27, 29, 30). Major branches typically arise in the lower half of the thallus with more apically situated segments featuring flattened morphologies. Specimens collected from sheltered, low-light environments near the edge of mangrove swamps (Fig. 28) differ from average specimens by having large, fan-like bases composed of fused segments, from which many long branches arise.

Median lengths and widths of centrally located segments range from 3.4 to 9.7 mm and 2.8 to 9.6 mm, respectively, with median length over width ratios ranging from 0.69 to 1.43, and median thickness ranging from 0.9 to 2.0 mm. The majority of segments are obovate–cuneate (79%), being broadest at or near their tip rather than at or near their base. The base is most often acute (61% of segments). Segments are unlobed (42%) or shallowly lobed (36%) with the majority of lobed segments trilobed (72%). Although all specimens feature both trilobed and unlobed segments, one type of segment morphology is dominant in the majority of cases.

Medullar siphons adhere into a single bundle at nodes and individual siphons cannot be separated from the bundle. Dissected nodes feature an obvious adhesion belt. Many large pores connect neighbouring siphons (Figs 44, 45). Median adhesion belt heights range from 33 to 53 µm. Median supranodal siphon lengths and diameters range from 163 to 327 µm and 95 to 150 µm, respectively. Medullar siphons ramify in trichotomies, rarely in dichotomies (Fig. 44). Median medullar siphon diameters range from 85 to 153 µm, with median length over width ratios ranging from 5.6 to 11.4.

The cortex consists of 2 to 3 utricle layers (Fig. 55). Peripheral utricles adhere to one another at their distal end, remaining attached after decalcification. Median peripheral utricle diameters and heights range from 43 to 63 µm and 55 to 90 µm, respectively, with median height over diameter ratios ranging from 1.09 to 1.63. In surface view, peripheral utricles appear as an irregular pattern of polygons with slight rounding in corners (Fig. 56). Subperipheral utricles are not markedly inflated (Fig. 55). Median secondary utricle diameters and heights range from 42 to 67 µm and 52 to 128 µm, respectively, with median height over diameter ratios ranging from 1.04 to 2.48.

Thick, basal segments exhibit more utricle layers than segments higher up the thallus (Fig. 66). Basal, stipitate segments have more rigid, thick-walled and elongated utricles than segments from the central thallus region (cf. Fig. 55). A preparation of the segment surface shows the thicker cell walls best (Fig. 65). Siphon fusion at nodes in the lower thallus region is like that higher up the thallus.

Distribution: *Halimeda incrassata* occurs in the tropical western Atlantic Ocean and has recently been found at Madeira, an isolated subtropical eastern Atlantic island (specimens H.0668 & H.0669, GENT). A distribution map is given in Fig. 71.

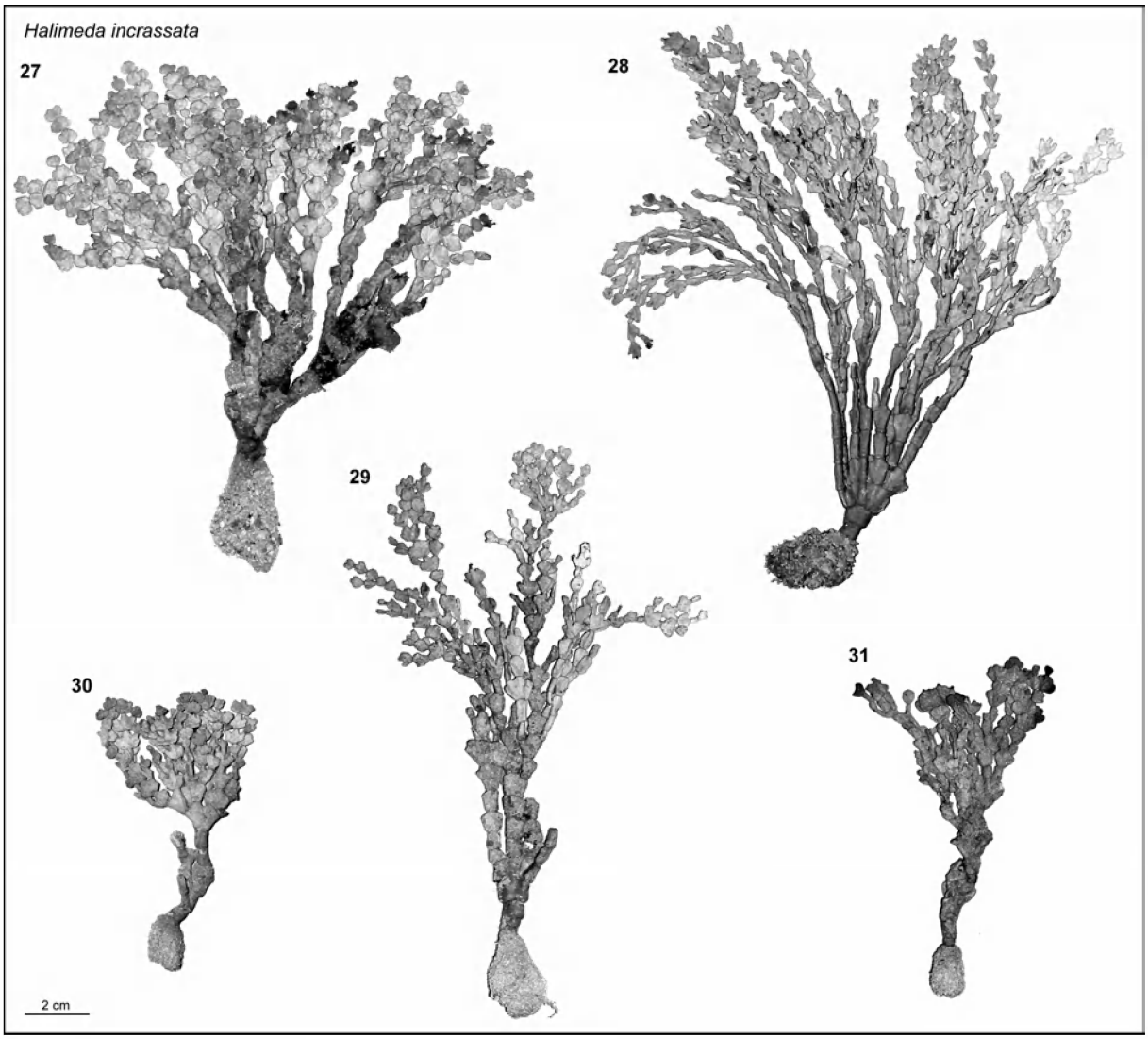

Figs 27–31. *Halimeda incrassata* thalli. **Fig. 27.** Specimen HOD-MAR01-42 from Martinique. **Fig. 28.** Specimen H.0667 from Panama. **Fig. 29.** Specimen HV978 from Jamaica. **Fig. 30.** Specimen H.0666 from Panama. **Fig. 31.** Specimen HV899 from Jamaica. All specimens from the Ghent University Herbarium (GENT).

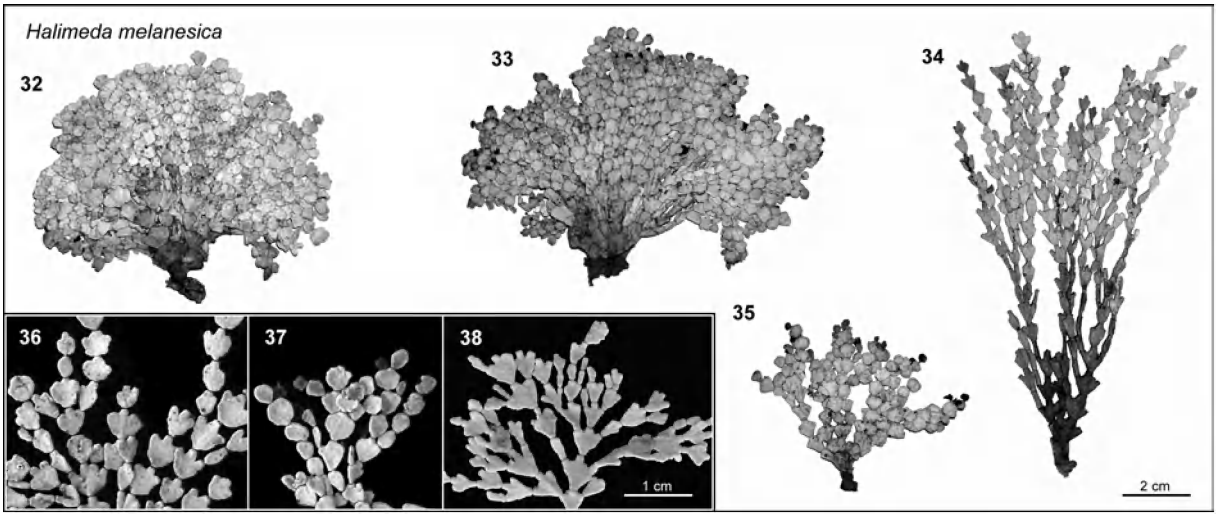

Figs 32–38. *Halimeda melanesica* thalli. **Fig. 32.** Specimen HV818 from The Philippines. **Fig. 33.** Specimen HV217 from French Polynesia. **Fig. 34.** Specimen HV790 from The Philippines. **Fig. 35.** Specimen HV217 from French Polynesia. **Fig 36.** Specimen HV790 from The Philippines. **Fig 37.** Specimen HV217 from French Polynesia. **Fig. 38.** Specimen L.0399626 from Indonesia. All specimens from the Ghent University Herbarium (GENT) except L.0399626 from NHN-Leiden (L).

Halimeda melanesica Valet

Figs 32–38, 46–48, 57, 58, 67, 68.

Holotype: PC0021851 (PC), Lifou Island, Loyalty Islands, New Caledonia.

Description: *Halimeda melanesica* attaches to rocky substrate by means of a firm, dense mat of rhizoids (Figs 32–35) and appears to be restricted to surge-affected habitats. Individuals are known to occur from wave-affected infralittoral fringe-zones to deeper-water habitats characterized by strong swells.

Two thallus morphologies can be distinguished within the diversity of this species. The first morphology consists of a densely branched, compact thallus inhabiting shallow, wave-affected sites (Figs 32, 33, 35). The second is composed of a laxly branched thallus from deeper, surge-affected sites (Fig. 34). The densely branched form exhibits a basal zone of relatively large segments that often take the form of or merge into a flabellate structure from which many branches arise (Figs 32, 33). Segments get smaller towards the apices. The laxly branched form features a firm basal zone of large, rigid segments. The upper part of the thallus is more flexible and is composed of smaller, thinner segments.

Median lengths and widths of centrally located segments range from 3.8 to 5.5 mm and 4.0 to 5.4 mm, respectively, with median length over width ratios ranging from 0.93 to 1.07, and median thickness ranging from 0.7 to 0.9 mm. Specimens of the laxly branched form contain segment morphologies toward the high end of the length and width spectra, while specimens of the densely branched form contain segments towards the low end. The surface of segments from central and upper thallus parts is generally smooth, never ruffled, sometimes shiny. Most segments are obovate–cuneate (95% – Figs 36, 38). Elliptical and ovate segments are restricted to specimens from shallow, wave-affected sites (Fig. 37). The base is usually acute (97% – Figs 36, 38). The majority of segments are lobed (87% – Figs 36–38), and, although deep and medium lobes occur (both 23%), most lobes are shallow (54%). When lobed, segments are usually trilobed (97% – Figs 36–38).

Medullar siphons adhere closely at nodes, showing an adhesion band in dissected nodes (Figs 46–48). Pores between parallel siphons are small (Fig. 47) or absent (Fig. 48). Median adhesion belt height ranges from 25 to 30 μm. Median supranodal siphon lengths and diameters range from 356 to 525 μm and 97 to 140 μm, respectively. Medullar siphons ramify in trichotomies, rarely in dichotomies (Fig.

46). Median medullar siphon diameters range from 79 to 108 µm, with median length over width ratios ranging from 7.27 to 10.8.

The cortex consists of 3 utricle layers (Fig. 57). Peripheral utricles adhere to one another at their distal end, remaining attached after decalcification. Median peripheral utricle diameters and heights range from 40–50 µm and 40–53 µm, respectively, with median height over diameter ratios ranging from 1.17–1.44. In surface view, peripheral utricles appear as a non-uniform pattern of polygons without rounding in corners (Fig. 58). Subperipheral utricles are relatively slender (Fig. 57). Median secondary

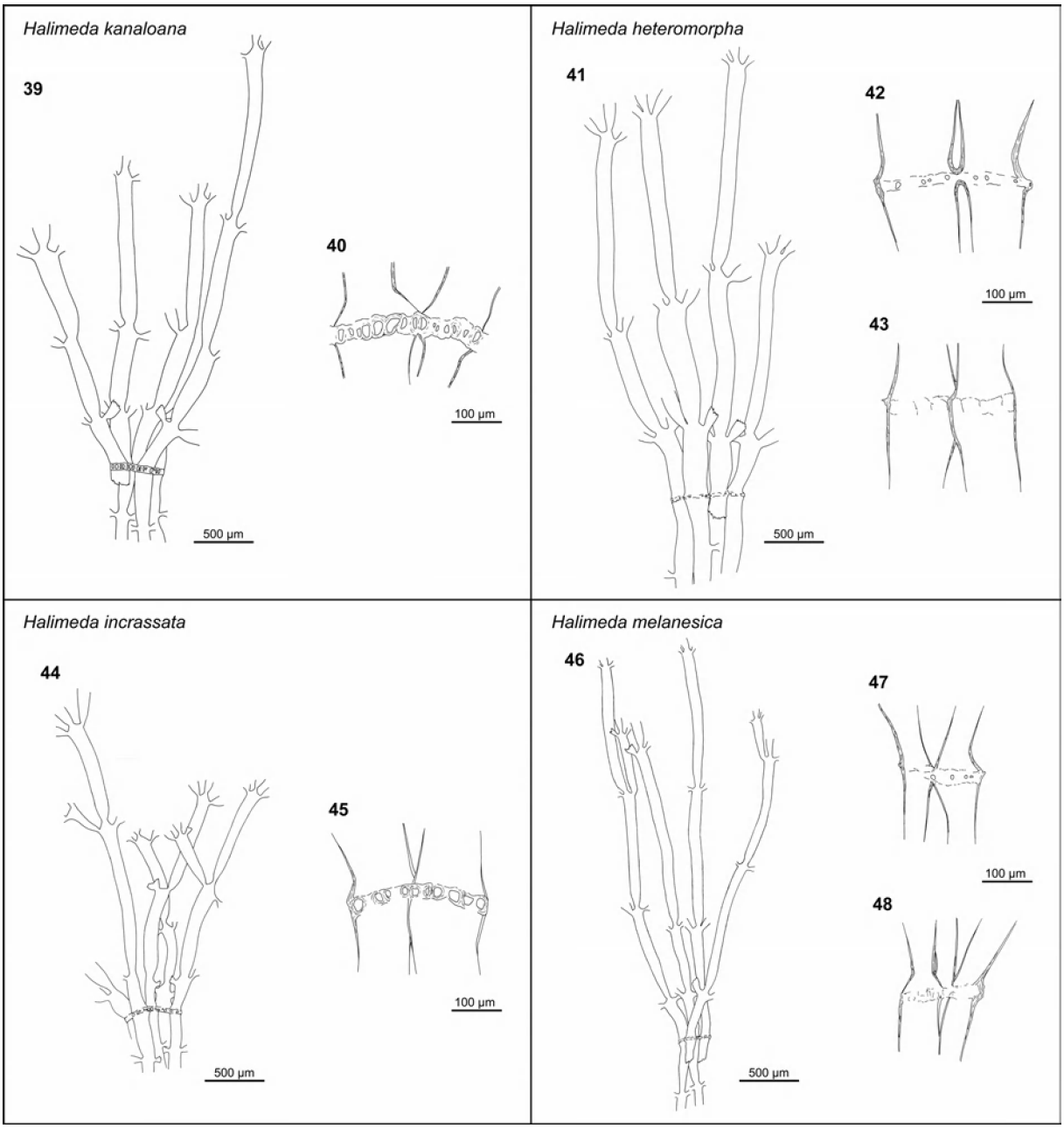

Figs 39–48. Medullar and nodal features. **Figs 39–40.** *H. kanaloana* specimen H.0649. **Fig. 39.** Medulla. **Fig. 40.** Detail of nodal siphon fusion. **Figs 41–43.** *H. heteromorpha*. **Fig. 41.** Medulla of specimen HV629. **Fig. 42.** Detail of nodal siphon fusion in specimen HV629. **Fig. 43.** Detail of nodal siphon adhesion in specimen HV636. **Figs 44–45.** *H. incrassata* specimen HV448. **Fig. 44.** Medulla. **Fig. 45.** Detail of nodal siphon fusion. **Figs 46–48.** *H. melanesica*. **Fig. 46.** Medulla of specimen HV818. **Fig. 47.** Detail of nodal siphon fusion in specimen HV818. **Fig. 48.** Detail of nodal fusion in specimen HV217. All specimens from the Ghent University Herbarium (GENT).

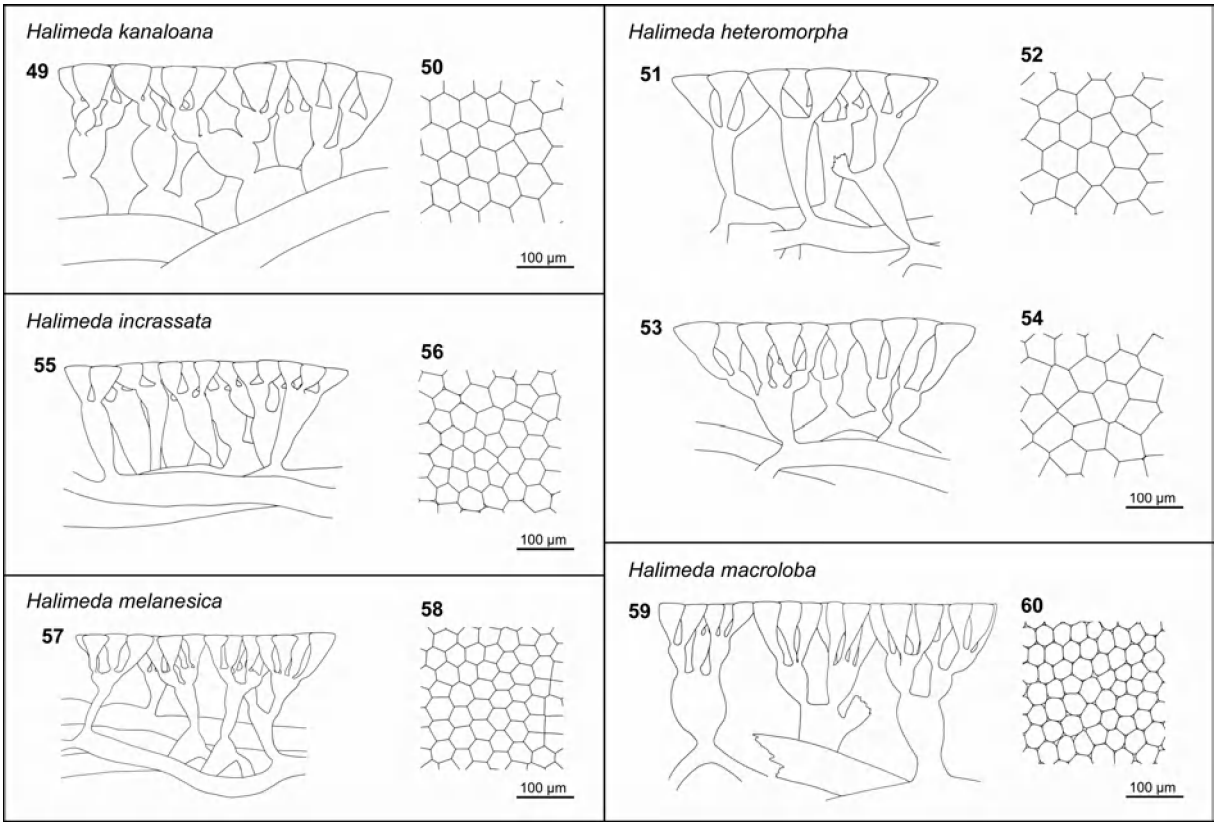

Figs 49–60. Cortical features in cross-sectional and surface preparations. **Figs 49–50.** *H. kanaloana* specimen H.0649. **Fig. 49.** Cross-sectional view. **Fig. 50.** Surface view. **Figs 51–54.** *H. heteromorpha.* **Figs 51–52.** Specimen HV22. **Fig. 51.** Cross-sectional view. **Fig. 52.** Surface view. **Figs 53–54.** Specimen HV763. **Fig. 53.** Cross-sectional view. **Fig. 54.** Surface view. **Figs 55–56.** *H. incrassata* specimen HV332. **Fig. 55.** Cross-sectional view. **Fig. 56.** Surface view. **Figs 57–58.** *H. melanesica* specimen HV818. **Fig. 57.** Cross-sectional view. **Fig. 58.** Surface view. **Figs 59–60.** *H. macroloba* specimen HV206. **Fig. 59.** Cross-sectional view. **Fig. 60.** Surface view. All specimens from the Ghent University Herbarium (GENT).

utricle diameters and heights range from 32–45 µm and 49–92 µm, respectively, with height over diameter ratios ranging from 0.93–1.06.

The cortex of thick, basal segments consists of 3–4 utricle layers (Fig. 68). Subperipheral utricles of the basal segments are larger and more swollen than higher up the thallus (cf. Fig. 57). The utricles are also more rigid and thick walled. Peripheral utricles are similar in shape and size at the base and higher up the thallus, except that they have thicker cell walls (most obvious in surface view – Fig. 67). Siphon fusion at nodes in the lower thallus region is no different from that higher up the thallus.

Distribution: *Halimeda melanesica* occurs throughout the tropical parts of the Indo-Pacific ocean basin. A distribution map compiled as described for *H. heteromorpha* is shown in Fig. 71.

Discussion

Phylogeny and biogeography

The phylograms in Figs 1 and 2 represent the evolutionary history of the nrDNA and plastid DNA of the group under scrutiny. *Halimeda favulosa* and *H. stuposa*, two members of section *Rhipsalis* of which we were unable to obtain specimens suitable for DNA analysis, are not represented in the trees. Kooistra et al. (2002) showed that the SSU nrDNA sequence of *H. stuposa* had clear affinities with that of *H. borneensis*, to the degree that *H. stuposa* was considered to be a stunted form of *H. borneensis*. *Halimeda favulosa*, a rare species endemic to the Bahamas (Taylor, 1960, Hillis-Colinvaux, 1980), is expected to be related to the remaining Atlantic species *H. monile*, *H. simulans* and *H. incrassata*.

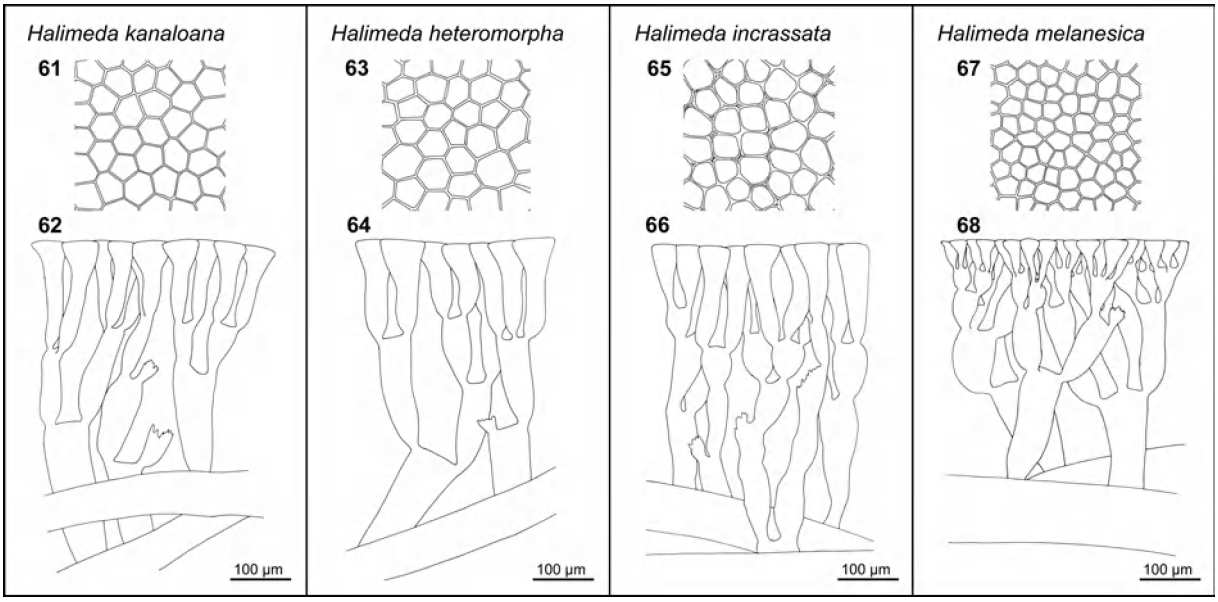

Figs 61–68. Cortical features of basal segments in cross-sectional and surface preparations. **Figs 61–62.** *H. kanaloana* specimen H.0653. **Fig. 61.** Surface view. **Fig. 62.** Cross-sectional view. **Figs 63–64.** *H. heteromorpha* specimen HV146. **Fig. 63.** Surface view. **Fig. 64.** Cross-sectional view. **Figs 65–66.** *H. incrassata* specimen HV448. **Fig. 65.** Surface view. **Fig. 66.** Cross-sectional view. **Figs 67–68.** *H. melanesica*. **Fig. 67.** Surface view of specimen HV818. **Fig. 68.** Cross-sectional view of specimen HV790. All specimens from the Ghent University Herbarium (GENT).

Shimodaira-Hasegawa tests, likelihood-based tests commonly used to check whether alternative topologies are significantly worse than the obtained topology for a given sequence alignment (Goldman et al., 2000), show that many of the disagreements between the nrDNA and cpDNA phylograms are minor.

The clear-cut separation of Atlantic and Indo-Pacific species in the nrDNA phylogram suggests separate diversification of section *Rhipsalis* in both ocean basins. Even though the cpDNA phylogram did not show a basal split into Atlantic and Indo-Pacific species, a SH test pointed out that the introduction of such a split did not result in a significantly worse tree. Past research has demonstrated all five sections of *Halimeda* to feature a basal or near-basal separation of Indo-Pacific and Atlantic species (Kooistra et al., 2002; Verbruggen & Kooistra, 2004; Verbruggen et al. submitted). This denotes that, after an initial divergence of the genus (i.e. section formation), a vicariance event allowed independent diversification of each of the sections in the Caribbean Sea and Indo-Pacific ocean basin (Kooistra et al., 1999, 2002). This pattern is common in marine taxa of Tethyan origin, from parrotfishes (Streelman et al., 2002) to mangrove trees (Ellison et al., 1999). In *Halimeda*, the vicariance event involved has been hypothesized to be the closure of the Tethyan Seaway in the Middle East in the Miocene (Kooistra et al., 1999) and the rise of the Central American Isthmus in the Pliocene (Kooistra et al., 1999, 2002).

In section *Rhipsalis*, the position of *H. cylindracea* deserves additional attention in this biogeographic context. This species was recovered as the closest sister to Atlantic *Rhipsalis* species in the cpDNA phylogram (Fig.

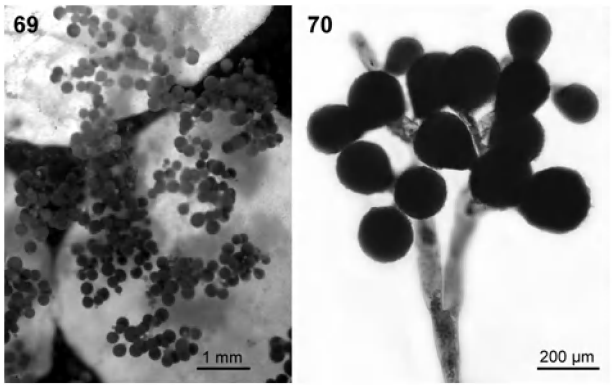

Figs 69–70. Fertile *H. kanaloana*, specimen HS 2004-162 from the personal herbarium of Heather Spalding, slated for deposition at the Bishop Musuem. **Fig. 69.** Placement of gametangia along margins and on surface of segments. **Fig. 70.** detail of gametophore.

2) and occurs at the base of the Indo-Pacific clade in the nrDNA phylogram (Fig. 1). Yet, enforcing the position suggested by the other data set did not result in significantly worse topologies. This suggests that the species diverged very early in the evolutionary history of the section, before the vicariance event that caused the separation of sequence diversity.

Evolution of the *H. heteromorpha–kanaloana–macroloba* species cluster

Both the plastid and nuclear phylograms (Figs 1, 2) exhibit a sister relationship between *H. kanaloana* and *H. heteromorpha*. Nonetheless, this cluster receives mediocre bootstrap support from the cpDNA data set. The consensus trees from Figs 3–11, which include multiple specimens per species, shed more light on the evolution of the *H. heteromorpha–kanaloana–macroloba* species cluster. In the plastid *rps*3 trees (Figs 9–11), *H. heteromorpha* and *H. kanaloana* are both monophyletic and the relationship between these species and *H. macroloba* is not satisfactorily resolved. The 18S–ITS1–5.8S–ITS2 data set leaves no doubt about the sister relationship between *H. heteromorpha* and *H. kanaloana* (Fig. 1). However, by examination of a larger set of ITS1–ITS2 sequences of the *H. macroloba–heteromorpha–kanaloana* species group, this sister relationship can be questioned (Figs 3–8; Verbruggen et al., 2005c). Alternative alignments favour paraphyly (Figs 3–5) or monophyly (Figs 6–8) of *H. heteromorpha*, with *H. kanaloana* branching off from within *H. heteromorpha* (Figs 3, 4) or sitting in a polytomy of *H. heteromorpha* lineages (Fig. 5). These topological discrepancies point out the sensitivity of phylogenetic inference methods to differences in the alignment. Alignment difficulties are often encountered in ITS data due to the occurrence of indels, especially in parts not showing secondary structure constancy (Alvarez & Wendel, 2003). The study by Verbruggen et al. (2005c) aimed to delineate species on the basis of DNA sequence data, and, so as not to introduce subjectivity in the data, an automated alignment method was preferred over a manual one. The gap matrix alignment used in this study is more conservative than the ClustalW alignment used by Verbruggen et al. (2005c) because sites or regions where the alignment of sequences between species was ambiguous were separated into sequence blocks. As a consequence, non-homology of characters (bases) at the same alignment position was precluded. Our results (Figs 3–11) suggest that the ClustalW algorithm with standard settings may not yield the most appropriate alignment for inference of phylogenetic relationships among species because the more conservative gap matrix alignment of ITS1–ITS2 data and the *rps*3 data both suggest monophyly of *H. heteromorpha* and *H. kanaloana*.

In the Pacific Ocean, *H. heteromorpha* occurs only in the archipelagos of the southern hemisphere whereas *H. kanaloana* is limited to the northern hemisphere (Hawaii and probably the Ryukyu islands, Fig. 71). In the most plausible topologies of the *H. heteromorpha–kanaloana–macroloba* species

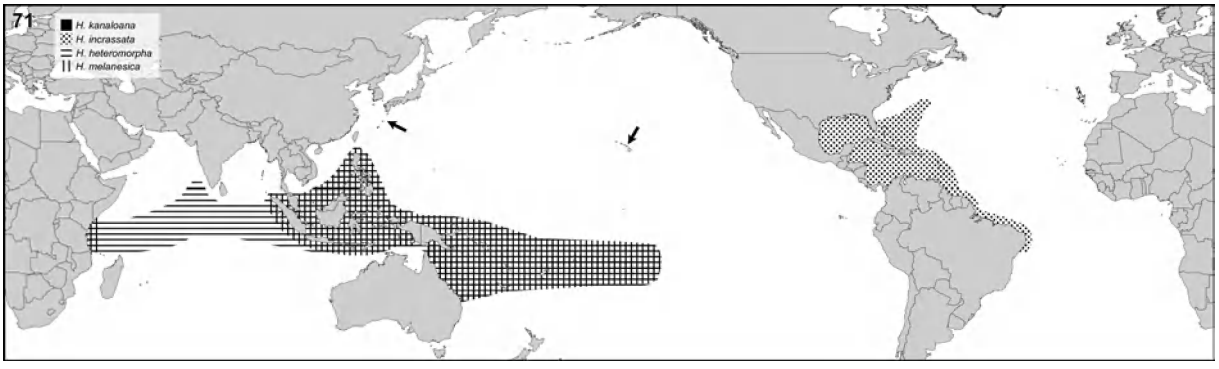

Fig. 71. Distribution maps of *H. heteromorpha*, *H. incrassata*, *H. kanaloana* and *H. melanesica*. Note that *H. incrassata* s.l. and *H. melanesica* have been reported for several more Indo-Pacific localities. Given the taxonomic confusion, we included only localities from which we have studied materials and localities of which identifications in the literature were supported by illustrations and/or utricle measurements. Distribution ranges given here are uncertain for what SE Asia, Madagascar and India-Sri Lanka are concerned. For the SE Asian region, however, large collections (GENT and L herbaria) from Indonesia, The Philippines and Papua New Guinea were examined.

group (the ones based on the longest sequence alignments: Figs 1, 2), *H. macroloba* branches off first, leaving *H. heteromorpha* and *H. kanaloana* as closest relatives. There are several examples of sibling species that have non-overlapping ranges in the north and south Pacific (Palumbi, 1997; Bernardi et al., 2001; Bay et al., 2004). Such distributions could have originated by cross-equatorial jump dispersal (Rotondo et al., 1981). Considering the inhibition of cross-equatorial dispersal by the equatorial counter current (Tomczak & Godfrey, 2003), limited gene flow can be expected between putative founder populations in northern and southern Pacific populations, leading to morpho-ecological and DNA sequence divergence.

Species boundaries

Perception and accurate delineation of species is one of the major issues currently facing algal systematists. Molecular phylogenetic techniques have provided a new perspective on algal diversity and have revealed ill-defined species boundaries in all major marine algal groups (e.g. van der Strate et al.,2002; Zuccarello & West, 2003; Gurgel et al., 2003; Cohen et al., 2004; Yano et al., 2004; De Clerck et al., 2005; Kooistra & Verbruggen, 2005). Determining diagnostic differences requires sequencing numerous specimens and delving into formerly disregarded morphological variability. In *Halimeda* section *Rhipsalis*, DNA sequencing and morphometric methods have acted in synergy to pinpoint species differences (Verbruggen et al., 2005c). The morphological distinction among some of the species described above was already suggested by Verbruggen et al. (2005c). This study explores those differences in more detail and compares diagnostic features for each species with other species where confusion could arise. It must be stressed that cited dimensions refer to median values of ten replicate measurements taken as described in Verbruggen et al. (2005a, c). This approach narrows the range of the listed values, particularly because median values are not heavily impacted by outliers. As a consequence of the narrower measurement ranges, species overlap is small or disappears entirely, and boundaries between species are better definable. The advantage of using the median range instead of the actual range of measurements makes identification more straightforward and unambiguous. We encourage the use of medians from a series of replicate measurements as a standard in *Halimeda* taxonomy and identification.

The most obvious difference between the species described above is the presence or absence of a bulbous holdfast. Whereas *H. kanaloana* and *H. incrassata* are anchored in sand by means of a massive bulb composed of rhizoids and sand, *H. melanesica* and *H. heteromorpha* are attached to rocky substrates by a felty mat of rhizoids. However, relying on this character to distinguish between these species pairs is not without danger. Collections may lack holdfasts, rendering the character useless, or holdfasts may vary in shape and structure depending on environmental regimes (Verbruggen & Kooistra, 2004). For instance, *H. heteromorpha* can exhibit a more elaborate holdfast when growing on silt- or sand- covered rock (Figs 14, 15), and *H. melanesica* is known to occasionally form bulbous holdfasts (e.g. HEC5671, GENT).

The species *H. incrassata* and *H. kanaloana* both have massive, bulbous holdfasts and both feature many large pores at nodes. However, there are several diagnostic features that clearly separate them. First, subperipheral utricles of *H. kanaloana* are markedly inflated while those of *H. incrassata* are not. Second, the median distance between the base of the nodal fusions and the first siphon ramification above the node exceeds 350 µm in *H. kanaloana* whereas it is shorter in *H. incrassata*. Third, peripheral utricles of *H. incrassata* tend to be smaller than those of *H. kanaloana*. The median diameter of peripheral utricles of *H. incrassata* ranges from 43 to 63 µm; for *H. kanaloana* this range is 56 to 73 µm. Additionally, *H. incrassata* exhibits slight rounding of peripheral utricles whereas *H. kanaloana* consistently exhibits angular corners (observed in surface view). From an ecological point of view, *H. incrassata* favours shallow sites (seagrass beds, mangroves, shallower parts of reef slopes) whereas *H. kanaloana* is known from deeper sand and rubble flats (15 to >100 m deep) where it often forms quasi monospecific stands. Finally, *H. incrassata* and *H. kanaloana* have non-overlapping dis-

tribution ranges, the former being restricted to the Atlantic and the second known only from the North Pacific Ocean.

Halimeda incrassata and *H. heteromorpha* differ in a number of obvious characters. First, *H. incrassata* is anchored in sand by means of a large, sand-encrusted bulbous holdfast whereas *H. heteromorpha* is attached to rock or sand- or silt-covered rock by a much smaller, felty holdfast. Second, *H. incrassata* features a relatively high nodal adhesion belt (median height 33–53 µm) with many obvious, large pores while *H. heteromorpha* exhibits a narrower adhesion belt (median height 25–36 µm) with diminutive pores. Less conclusive differences include the length of the supranodal siphon (163–327 µm in *H. incrassata* vs. 242–535 µm in *H. heteromorpha*) and the diameter of peripheral utricles, which tends to be smaller in *H. incrassata* (median range 43–63 µm) than in *H. heteromorpha* (median range 57–79 µm). Ecological differences between both species are obvious. Whereas *H. incrassata* grows on sand (mostly in seagrass beds and mangroves), *H. heteromorpha* grows on rocky substrates in a variety of habitats. Finally, *H. incrassata* is a strictly Atlantic species whereas *H. heteromorpha* is restricted to the Indo-Pacific basin.

The species *H. heteromorpha* and *H. kanaloana* are close relatives within a well-supported clade that also contains *H. macroloba* (see above). *Halimeda heteromorpha* stands apart from both other species in having a felty, non-bulbous holdfast and reduced nodal fusions (median adhesion belt height 25–36 µm vs. 47–69 µm in *H. kanaloana*). Peripheral utricles of *H. heteromorpha* and *H. kanaloana* are almost identical in size, but those of *H. kanaloana* tend to broaden more closely to their base. More specifically, utricles of *H. kanaloana* exceed 42% of their maximal width at 1/4th from their base, whereas this is rarely the case in *H. heteromorpha*. Subperipheral utricles in *H. kanaloana* are markedly inflated whereas those of *H. heteromorpha* are not. In this respect, *H. kanaloana* has more affinity to *H. macroloba* (Figs 59, 60). Reproductively, *H. macroloba* and *H. kanaloana* both produce gametophores from internal medullary siphons; however, gametophores (a feature hypothesized to be of phylogenetic importance in Vroom & Smith [2003]) in *H. kanaloana* are longer and thicker than in *H. macroloba*. From an ecological and geographic perspective, *H. heteromorpha*, *H. kanaloana* and *H. macroloba* also differ. Whereas *H. macroloba* is a sand-growing species restricted to shallow, lagoon habitats, *H. kanaloana* is a sand-dwelling species that occurs most commonly in deep-water habitats. *Halimeda heteromorpha* is a rock-grower from relatively shallow sites. Our observations indicate that reproduction in *H. macroloba* and *H. kanaloana* occurs almost continuously, with small fractions of populations being fertile during many months of the year (see also Merten, 1971). No fertile *H. heteromorpha* occurred among our collections, indicating that the species differs from *H. macroloba* and *H. kanaloana* in this respect. *Halimeda heteromorpha* has a distribution range covering the tropics of the Indian Ocean and the South Pacific. This range does not seem to overlap with that of *H. kanaloana*, which is so far only known from Hawai`i and the Ryukyu Islands (i.e. northern Pacific Ocean). *Halimeda macroloba* ranges throughout the Indo-Pacific (Hillis-Colinvaux, 1980), including the Ryukyu Islands (Tsuda & Kamura, 1991) and Hawai`i (Abbott & Huisman, 2004).

Halimeda heteromorpha and *H. melanesica* stand apart from the remainder of the section by their reduced nodal fusion pattern and their epilithic habit with a matted holdfast. Furthermore, their segment morphology can be extremely similar. First, the trilobed segments of *H. melanesica* specimens from surge-affected sites (Fig. 34) can be very similar to those of *H. heteromorpha* from fore-reef slopes (Fig. 23). Second, segments of the wave-affected form of *H. melanesica* (Fig. 37) show a striking resemblance to those of lagoon forms of *H. heteromorpha* (Figs 25, 26). Nonetheless, there are a few morphological characters that allow identification. First, peripheral utricles are smaller in *H. melanesica* (median diameter 40–50 µm, height 40–53 µm vs. 57–79 µm and 74–102 µm in *H. heteromorpha*). Second, the subperipheral utricles are markedly thinner (more slender) in *H. melanesica*. The median diameter of secondary utricles ranges from 42 to 66 µm in *H. heteromorpha* while the range

for *H. melanesica* is 32–45 µm. The height of the secondary utricles does not differ significantly between both species, which makes that secondary utricles of *H. melanesica* appear as more slender.

Some ecotypes of *H. heteromorpha* could be confused with more distantly related species. For example, specimens exhibiting round segments (Figs 19, 22) are similar to *H. tuna* and *H. discoidea* from section *Halimeda* and *H. bikinensis*, whose relationships to current sections are unclear (Verbruggen & Kooistra, 2004). However, anatomical characters allow unequivocal distinction between the discoid *H. heteromorpha* morphology and the other species. The most evident character to examine in this context is nodal fusion pattern. Whereas in *H. heteromorpha* all medullar siphons adhere into a single unit that may be interconnected by small pores, nodal siphons show complete fusion in pairs or triplets in all section *Halimeda* species and in *H. bikinensis* (Verbruggen & Kooistra, 2004). Trilobed specimens of *H. heteromorpha* (Figs 21, 23) bear superficial resemblance to trilobed specimens of *H. minima*, *H. goreauii* or *H. distorta* from section *Opuntia* (cf. Kooistra & Verbruggen, 2005); however, fusion of nodal siphons into a single unit clearly differentiates *H. heteromorpha* from these species. Species in section *Opuntia* feature incomplete fusion in pairs, triplets or small groups (Verbruggen & Kooistra, 2004)

The use of basal, stipitate segments in species delineation remains enigmatic. Both Noble (1986) and Dragastan et al. (2002) considered these segments useful for diagnostic purposes. However, Verbruggen et al. (2005b) showed that inclusion of basal segments in morphometric data sets impaired the accuracy of automated identification. Despite this revelation, it was argued that the anatomy of basal segments may be useful when coded as a separate set of variables. Regarded in such a manner, information contained in basal segments would benefit species identification without interfering with diagnostic characters from more apically situated segments. Nodal fusion in segments from the four focal species of this study typically did not differ between basal and more apical segments. However, in all species, the appearance and size of peripheral and subperipheral utricles differed between basal segments and segments located higher up the thallus. In the four species studied, utricles of basal segments were more rigid, thick-walled and elongate than in segments from the central thallus region. Whether this is a result of segment function (thallus support) or segment age (basal segments are older) cannot be concluded. Although none of the three *H. incrassata* entities could be recognized on the basis of basal segment anatomy alone, differences in size and rounding of peripheral utricles observed in normal segments appeared to be present in basal segments, too. We have not attempted morphometric analysis of basal segments.

Nomenclature and taxonomy

The synonyms *H. tridens* and *H. brevicaulis* were both originally described from Atlantic collections, and even though the name *H. tridens* was subsequently applied to Indo-Pacific material (e.g. Taylor, 1950), our molecular analysis reveals that neither of these species names is appropriate for Pacific specimens. *Halimeda polydactylis*, a species of Pacific origin, was regarded as a synonym of *H. incrassata* by Barton (1901). However, specimens referred to as *H. polydactylis* have been synonymized with *H. cylindracea* (Hillis 1959). The species *H. triloba*, described by Decaisne (1842), was depicted in Kützing (1857) as a mixture of specimens with affinities to *H. opuntia* and *H. incrassata*. According to Barton (1901), Decaisne's type material belongs to *H. opuntia*, of which *H. triloba* is considered a synonym. As a consequence, *H. triloba* should not interfere with nomenclature of *H. incrassata*-like species.

Halimeda heteromorpha is an amalgam of different forms, several of which had been described before as forms or varieties under *H. incrassata*. A first variety, *H. incrassata* var. *ovata* (= *H. incrassata* f. *ovata*) conforms to our specimens from lagoon habitats (Figs 14, 16–18). Furthermore, *H. incrassata* f. *tripartita* may conform to our specimens from the sheltered fore-reef slope (Figs 21, 23) and *H. incrassata* f. *rotunda* probably conforms to our specimens from surge-affected sites (Figs 19, 22).

Even though we have not studied the specimens on which Barton (1901) based her descriptions, her illustrations are fairly conclusive. Instead of raising one of the forms to the specific rank, we have chosen the new epithet *H. heteromorpha*. This choice is appropriate because the names of the forms give a strong suggestion towards shape characteristics that are not diagnostic for *H. heteromorpha* as a whole. Furthermore, various forms of the species have been a source of confusion. For example, *H. incrassata* f. *ovata* has been applied to specimens belonging to *H. borneensis* (Payri & Meinesz, 1985; Payri et al., 2000). We decided not to keep or present any kind of subdivision of the species into forms because of a lack of molecular support and the existence of several intermediate morphologies in the collections studied (e.g. Fig. 24 as intermediate between Figs 22 and 23).

Specimens of *H. heteromorpha* have often been mistaken for *H. melanesica* because of the similar holdfast type and nodal fusion pattern (e.g. Noble, 1987; Dargent, 1997; Verbruggen & Kooistra, 2004). Literature reports of *H. melanesica* should therefore be scrutinised. Valet, who described *H. melanesica*, did not compare it to specimens belonging to the *H. incrassata* group (Valet, 1966).

Cryptic and pseudo-cryptic diversity

Cryptic species, sometimes referred to as sibling species, are defined as species that are impossible to distinguish based on morphological characters (Knowlton, 1993; Sáez & Lozano, 2005). Pseudo-cryptic species are species that are readily distinguished morphologically once the appropriate characters are considered. Although there can be many clues to discover (pseudo-)cryptic diversity, the most common one is DNA sequence analysis, as has been the case in *H. incrassata* and many other marine algal species (e.g. van der Strate et al., 2002; Cohen et al., 2004; De Clerck et al., 2005).

Whether a discovery of hidden diversity should be categorised as cryptic or pseudo-cryptic is subjective and depends on how much effort is spent looking for morphological differences (Sáez et al., 2003). This is well exemplified by *H. incrassata*. Kooistra et al. (2002) disclosed two discrete entities within this species on the basis of nuclear ribosomal DNA sequence data. A third entity was added by Verbruggen et al. (2005c) on the basis of nuclear ITS and plastid *rps*3 sequences. Although initially regarded cryptic species, morphometric analyses revealed several morphological differences between the species (Verbruggen et al., 2005c; this study).

It is not unthinkable that additional pseudo-cryptic entities will be discovered within the *H. incrassata* complex. For example, Indo-Pacific *H. incrassata* specimens depicted by Tseng (1984) and South (1992) do not appear to belong to *H. kanaloana* or *H. heteromorpha* on a morphological basis. The same is true for an entity from Papua New Guinea encountered in the Ghent University Herbarium (Coppejans et al., 2001). Because we did not have access to specimens appropriately preserved for DNA analysis, it cannot be concluded whether the entities in question represent extra pseudo-cryptic entities or additional morphologies within the species *H. heteromorpha* or *H. kanaloana*.

Acknowledgements

HV is indebted to BOF (Ghent University, grant 011D9101), FWO-Flanders (project 3G002496 and travel grant) and the King Leopold III Fund for Nature Exploration and Conservation. ODC thanks FWO-Flanders for a postdoctoral fellowship grant. Funding for PSV and for translation of species diagnoses was provided through the NOAA Fisheries Office of Habitat Conservation as part of the NOAA Coral Reef Conservation Program. AN is grateful for funding from the Territory of French Polynesia and the University of French Polynesia which contributed to this study. HV acknowledges Eric Coppejans and Wiebe Kooistra for providing facilities, discussions about *Halimeda* taxonomy and evolution, and for providing large collections of specimens. We further thank Olivier De Clerck for commenting on our manuscript. HV thanks Ellen Cocquyt, Cathy De maire and Christelle VanKerckhove for assistance in the laboratory, preparation of herbarium specimens, and help with paperwork. We thank Ed Drew for sending photographs of *Halimeda* collections from the Great Barrier

Reef, Mike Wynne and Stuart Lindsay of the University of Michigan Herbarium for sending photographs of *Halimeda* collections from the Marshall Islands, and Bruno de Reviers and Edith Bury of the Muséum National d'Histoire Naturelle (Paris) for giving us access to the holotype specimen of *H. melanesica*. Latin translations of species diagnoses were provided by Mark Garland (http://www.botanicallatin.org). We thank Paul Colinvaux, Olivier Dargent, Lisette de Sénerpont-Domis, Roxie Diaz, Cristine Galanza, Llewellya Hillis, Manfred Kaufmann, Tom & Courtney Leigh, Frederik Leliaert, Lawrence Liao, Kimberly Page, Deborah Olandesca, Claude Payri, Willem Prud'homme van Reine, Heather Spalding and Peter Wirtz for specimen collection. Collection of the deep-water specimens of *H. kanaloana* has been made possible through funds from NOAA Ocean Exploration #NA04OAR4600100 and NOAA Hawaii Undersea Research Laboratory Award #NA16RU1333.

References

Abbott, I.A. & Huisman, J.M. (2004). *Marine green and brown algae of the Hawaiian Islands.* Bishop Museum Press, Honolulu, Hawaii. 259 pp.

Alvarez, I., Wendel, J.F., (2003). Ribosomal ITS sequences and plant phylogenetic inference. *Mol. Phylogen. Evol.*, **29**: 417–434.

Barton, E.S. (1901). The genus *Halimeda*. *Siboga Expedition Monograph* 60. Brill, Leiden, The Netherlands. 32 pp.

Bay, L.K., Choat, J.H., van Herwerden, L. & Robertson, D.R. (2004). High genetic diversities and complex genetic structure in an Indo-Pacific tropical reef fish (*Chlorurus sordidus*): evidence of an unstable evolutionary past? *Mar. Biol.*, **144**: 757–767.

Bernardi, G., Holbrook, S.J., Schmitt, R.J. (2001). Gene flow at three spatial scales in a coral reef fish, the three-spot dascyllus, *Dascyllus trimaculatus*. *Mar. Biol.*, **38**: 457–465.

Cohen, S., Faugeron, S., Martinez, E.A., Correa, J.A., Viard, F., Destombe, C. & Valero, M. (2004). Molecular identification of two sibling species under the name *Gracilaria chilensis* (Rhodophyta, Gracilariales). *J. Phycol.*, **40**: 742–747.

Chittaro, P.M. (2004). Fish-habitat associations across multiple spatial scales. Coral Reefs, 23: 235–244.

Coppejans, E., Leliaert, F., Dargent, O. & De Clerck, O. (2001). The green algae (Chlorophyta) of the north coast of Papua New Guinea. *Cryptogamie Algologie*, **22**: 375–443.

Dargent, O. (1997). Etude systématique du genre *Halimeda* (Caulerpales, Bryopsidophycées), dans la zone de contact entre l'Océan Indien et l'Océan Pacifique. *Masters degree thesis,, Université Pierre et Marie Curie (Paris VI)*. Paris, France. 30 pp.

Decaisne, M.J. (1842). Mémoires sur les Corallines ou Polypiers calcifères. *Annales des Sciences Naturelles, Botanique* Ser. 2, **18**: 96–128.

De Clerck, O., Gavio, B., Fredericq, S. & Coppejans, E. (2005). Systematics of *Grateloupia filicina* (Halymeniaceae, Rhodophyta), based on *rbc*L sequence analyses and morphological evidence, including the reinstatement of *G. minima* and the description of *G. capensis* spec. nov. *J. Phycol.*, **41**: in press.

Dragastan, O.N., Littler, D.S. & Littler, M.M. (2002). Recent vs. fossil *Halimeda* species of Angaur Island, Palau and adjacent western Pacific areas. *Acta Palaeontologica Romaniae. Special publication no. 1.* Cartea Universitara, University of Bucharest. Bucharest, Romania. 20 pp.

Drew, E.A. (1983). *Halimeda* biomass, growth rates and sediment generation on reefs in the central Great Barrier Reef province. *Coral Reefs*, **2**: 101–110.

Ellis, J. (1767). Extract of a letter from John Ellis, Esq. F.R.S. to Dr. Linnaeus, of Upsal F.R.S., on the animal nature of the genus of zoophytes called *Corallina*. *Philosophical Transactions* **57**, 404–427.

Ellison, A.M., Farnsworth, E.J. & Merkt, R.E. (1999). Origins of mangrove ecosystems and the mangrove biodiversity anomaly. *Global Ecol. Biogeogr.*, **8**: 95–115.

Famà, P., Wysor, B., Kooistra, W.H.C.F. & Zuccarello, G.C. (2002). Molecular phylogeny of the genus *Caulerpa* (Caulerpales, Chlorophyta) inferred from chloroplast *tuf*A gene. *J. Phycol.*, **38**: 1040–1050.

Freile, D., Milliman, J.D. & Hillis, L. (1995). Leeward bank margin *Halimeda* meadows and draperies and their sedimentary importance on the western Great Bahama bank slope. *Coral Reefs*, **14**: 27–33.

Goldman, N., Anderson, J.P. & Rodrigo, A.G. (2000). Likelihood-based tests of topologies in phylogenetics. *Syst. Biol.*, 49: 652– 670.

Guiry, M.D. & Nic Dhonncha, E. (2004). AlgaeBase version 2.1. World-wide electronic publication, National University of Ireland, Galway. http://www.algaebase.org; searched on 30 December 2004.

Gurgel, C.F.D., Liao, L.M., Fredericq, S. & Hommersand, M.H. (2003). Systematics of *Gracilariopsis* (Gracilariales, Rhodophyta) based on *rbc*L sequence analyses and morphological evidence. *J. Phycol.*, **39**: 154–171.

Hillis, L. (1959). A revision of the genus *Halimeda* (order Siphonales). *Publications of the Institute of Marine Science*, **6**: 321–403.

Hillis-Colinvaux, L. (1980). Ecology and taxonomy of *Halimeda*: primary producer of coral reefs. *Adv. Mar. Biol.*, **17**: 1–327.

Kimura, M. (1980). A simple method for estimating evolutionary rate of base substitutions through comparative studies of nucleotide sequences. *J. Mol. Evol.*, **16**: 111–120.

Kooistra, W.H.C.F., Caldéron, M. & Hillis, L.W. (1999). Development of the extant diversity in *Halimeda* is linked to vicariant events. *Hydrobiologia*, **398**: 39–45.

Kooistra, W.H.C.F., Coppejans, E.G.G. & Payri, C. (2002). Molecular systematics, historical ecology and phylogeography of *Halimeda* (Bryopsidales). *Mol. Phylogen. Evol.*, **24**: 121–138.

Kooistra, W.H.C.F. & Verbruggen, H. (2005). Genetic patterns in the calcified tropical seaweeds *Halimeda opuntia*, *H. distorta*, *H. hederacea* and *H. minima* (Bryopsidales, Chlorophyta) provide insights in species boundaries and inter-oceanic dispersal. *J. Phycol.*, **41**: 177–187.

Knowlton, N. (1993). Sibling species in the sea. *Annu. Rev. Ecol. Syst.*, **24**: 189–216.

Kützing, F.T. (1857). *Tabulae phycologicae.* Vol. 7. Nordhausen, Germany. 40 pp.

Littler, M.M., Littler, D.S. & Lapointe, B.E. (1988). A comparison of nutrient- and light-limited photosynthesis in psammophytic versus epilithic forms of *Halimeda* (Caulerpales, Halimedaceae) from the Bahamas. *Coral Reefs*, **6**: 219–225.

Merten, S.M.J. (1971). Ecological observations of *Halimeda macroloba* Decaisne (Chlorophyta) on Guam. *Micronesica*, **7**: 27–44.

Noble, J.M. (1986). *Halimeda magnidisca* (Caulerpales, Chlorophyta), a new species from the Great Barrier Reef, Australia. *Phycologia*, **25**: 331–339.

Noble, J.M. (1987). A taxonomic study of the genus *Halimeda* Lamouroux (Chlorophyta, Caulerpales) from the Heron Island region of the southern Great Barrier Reef, Australia. *Masters degree thesis, University of Melbourne.* Melbourne, Australia. 200 pp.

Nylander, J.A.A. (2004) MrModeltest v2.0. Department of Systematic Zoology, Uppsala University, Sweden.

Palumbi, S.R. (1997) Molecular biogeography of the Pacific. *Coral Reefs*, **16** (suppl.): 47–52.

Payri C.E. (1995) Carbonate production of some calcifying algae in a French-Polynesia coral-reef. *Bull. Soc. Géol. France*, **166**: 77–84.

Payri, C.E. & Meinesz, A. (1985). Taxonomy and distribution of the genus *Halimeda* (Chlorophyta, Caulerpales) in French Polynesia. *Proc. 5th Int. Coral Reef Congr.*, **6**: 641–648.

Payri, C., N'Yeurt, A.D.R. & Orempuller, J. (2000). *Algae of French Polynesia.* Au Vent des Iles, Tahiti, French Polynesia. 320 pp.

Posada, D. & Crandall, K.A. (1998). Modeltest: testing the model of DNA substitution. *Bioinformatics*, **14**: 817–818.

Provan, J., Murphy, S. & Maggs, C.A. (2004). Universal plastid primers for Chlorophyta and Rhodophyta. *Eur. J Phycol.*, **39**: 43–50.

Ronquist, F. & Huelsenbeck, J.P. (2003) MrBayes 3: Bayesian phylogenetic inference under mixed models. *Bioinformatics*, **19**: 1572–1574.

Rossier, O. & Kulbicki, M. (2000). A comparison of fish assemblages from two types of algal beds and coral reefs in the south-west lagoon of New Caledonia. Cybium, 24: 3–26.

Rotondo, G.M., Springer, V.G., Scott, G.A.J. & Schlanger, S.O. (1981) Plate movement and island integration - a possible mechanism in the formation of endemic biotas, with special reference to the Hawaiian Islands. *Systematic Zoology*, **30**: 12–21.

Sáez, A.G. & Lozano, E. (2005) Body doubles. *Nature*, **433**: 111.

Sáez, A.G., Probert, I., Geisen, M., Quinn, P., Young, J.R. & Medlin, L.K. (2003) Pseudo-cryptic speciation in coccolithophores. *Proc. Nat. Acad. Sci. U.S.A.*, 100: 7163–7168.

Shimodaira, H. & Hasegawa, M. (1999). Multiple comparisons of log-likelihoods with applications to phylogenetic inference. *Mol. Biol. Evol.*, **16**: 1114–1116.

South, G.R. (1992). *Contributions to a catalogue of the Marine Algae of Fiji.* 1. *Halimeda* (Chlorophyceae). Marine studies program technical report. University of the South Pacific, Suva, Fiji. 16 pp.

Streelman, J.T., Alfaro, M., Westneat, M.W., Bellwood, D.R. & Karl, S.A. (2002). Evolutionary history of the parrotfishes: Biogeography, ecomorphology, and comparative diversity. *Evolution*, **56**: 961–971.

Swofford, D.L. (2003). PAUP*. Phylogenetic Analysis Using Parsimony (*and other methods). Version 4. Sinauer Associates, Sunderland, Massachusetts.

Tamura, K. & Nei M. (1993). Estimation of the number of nucleotide substitutions in the control region of mitochondrial DNA in humans and chimpanzees. *Mol. Biol. Evol.*, **10**: 512–526.

Taylor, W.R. (1950). *Plants of Bikini and other northern Marshall Islands. Algae: Chlorophyceae.* Univ. of Michigan Press, Ann Arbor, MI. 218 pp.

Taylor, W.R. (1960). *Marine algae of the eastern tropical and subtropical coasts of the Americas.* Univ. of Michigan Press, Ann Arbor, MI. 870 pp.

Tomc zak, M. & Godfrey, J.S. (2003). *Regional Oceanography: an introduction*, 2nd edition. Daya Publishing House, Delhi, India. 390 pp.

Tseng, C.K. (1984). *Common Seaweeds of China.* Science Press, Beijing, China. 316 pp.

Tsuda, R.T. & Kamura, S. (1991). Floristics and geographic distribution of *Halimeda* (Chlorophyta) in the Ryukyu Islands. *Jap. J. Phycol.*, **39**: 57–76.

Valet, G. (1966). Sur une espèce rare et une nouvelle espèce d'*Halimeda* de Mélanésie. *Revue Générale de Botanique*, **73**: 680–685.

van der Strate, H.J., Boele-Bos, S.A., Olsen, J.L., van de Zande, L. & Stam, W.T. (2002). Phylogeographic studies in the tropical seaweed *Cladophoropsis membranacea* (Chlorophyta, Ulvophyceae) reveal a cryptic species complex. *J Phycol.*, **38**: 572–582.

Verbruggen, H. & Kooistra, W.H.C.F. (2004). Morphological characterization of lineages within the calcified tropical seaweed genus *Halimeda* (Bryopsidales, Chlorophyta). *Eur. J Phycol.*, **39**: 213–228.

Verbruggen, H., De Clerck, O., Cocquyt, E., Kooistra, W.H.C.F. & Coppejans, E. (2005a). Morphometric taxonomy of siphonous green algae: a methodological study within the genus *Halimeda* (Bryopsidales). *J. Phycol.*, **41**: 126–139.

Verbruggen, H., De Clerck, O. & Coppejans, E. (2005b). Deviant segments hamper a morphometric approach towards *Halimeda* taxonomy. *Cryptogam. Algol.*, **26**: in press.

Verbruggen, H., De Clerck, O., Kooistra, W.H.C.F. & Coppejans, E. (2005c). Molecular and morphometric data pinpoint species boundaries in *Halimeda* section *Rhipsalis* (Bryopsidales, Chlorophyta). *J. Phycol.*, **41**: in press.

Verbruggen, H., De Clerck, O., Schils, T., Kooistra, W.H.C.F. & Coppejans, E. (submitted). Evolution and phylogeography of the *Halimeda cuneata/discoidea/tuna* cryptic species complex (Bryopsidales, Chlorophyta).

Vroom, P.S. & Smith, C.M. (2003). Reproductive features of Hawaiian *Halimeda velasquezii* (Bryopsidales, Chlorophyta), and an evolutionary assessment of reproductive characters in *Halimeda*. *Cryptogam. Algol.*, **24**: 355–370.

Yano, T., Kamiya, M., Arai, S. & Kawai, H. (2004). Morphological homoplasy in Japanese *Plocamium* species (Plocamiales, Rhodophyta) inferred from the Rubisco spacer sequence and intracellular acidity. *Phycologia*, **43**: 383–93.

Zharkikh, A. (1994). Estimation of evolutionary distances between nucleotide sequences. *J. Mol. Evol.*, **39**: 315–329.

Zuccarello, G.C. & West, J.A. (2003). Multiple cryptic species: Molecular diversity and reproductive isolation in the *Bostrychia radicans/B. moritziana* complex (Rhodomelaceae, Rhodophyta) with focus on North American isolates. *J. Phycol.*, **39**: 948–959.

Appendix 1. List of studied specimens and their geographical origin.

All specimens are in the Ghent University Herbarium (GENT) unless otherwise indicated (between brackets after the specimen number; HS is short for the personal herbarium of Heather Spalding – these specimens will be deposited in the Bishop Museum).

Halimeda heteromorpha

HEC12238	Chwaka, Zanzibar	Tanzania
HOD-TZ97-435	Chwaka, Zanzibar	Tanzania
HV22	Chwaka, Zanzibar	Tanzania
HEC11946	Matemwe, Zanzibar	Tanzania
HEC12065	Matemwe, Zanzibar	Tanzania
HIMS0020	La Digue	Seychelles
SEY313	La Digue	Seychelles
SEY314	La Digue	Seychelles
SEY326	La Digue	Seychelles
SEY112	Praslin	Seychelles
HEC6140	Bi Ya Doo	Maldives
HEC12568	Magala Furi	Maldives
L.0399613 (L)	Panjang, Berau	Indonesia
Snellius-II-10506	Sumba	Indonesia
HV629	Olango	Philippines
HV636	Olango	Philippines
HEC12271	Olango	Philippines
PH245	Olango	Philippines
HV763	Tangat	Philippines
PH194	Mactan	Philippines
PH197	Mactan	Philippines
HOD-PH99-109	Sanga Sanga	Philippines
HOD-PH99-117	Sanga Sanga	Philippines
HOD-PH99-128	Sanga Sanga	Philippines
C&PvR13144	Madang	Papua New Guinea
C&PvR13284	Madang	Papua New Guinea
C&PvR13322	Madang	Papua New Guinea
C&PvR13398	Madang	Papua New Guinea
C&PvR13492	Madang	Papua New Guinea
C&PvR13613	Madang	Papua New Guinea
C&PvR13703	Madang	Papua New Guinea
C&PvR13860	Madang	Papua New Guinea
HEC4514	Madang	Papua New Guinea
HEC7537	Madang	Papua New Guinea
HEC7551	Madang	Papua New Guinea
HEC7589	Madang	Papua New Guinea
H.0016	Great Barrier Reef	Australia
H.0019	Great Barrier Reef	Australia
H.0022	Great Barrier Reef	Australia
H.0064	Marquesas Islands	French Polynesia
H.0065	Marquesas Islands	French Polynesia
UPF097 (UPF)	Marquesas Islands	French Polynesia
HV104	Moorea	French Polynesia
HV144	Moorea	French Polynesia
HV146	Moorea	French Polynesia
HV149	Moorea	French Polynesia
H.0035	Tahiti	French Polynesia
H.0036	Tahiti	French Polynesia
HV231	Tahiti	French Polynesia
UPF097 (UPF)	Tahiti	French Polynesia
UPF2808 (UPF)	Tahiti	French Polynesia
UPF2809 (UPF)	Tahiti	French Polynesia
UPF2815 (UPF)	Tahiti	French Polynesia
UPF2823 (UPF)	Tahiti	French Polynesia
H.0040	Rangiroa	French Polynesia
H.0045	Rangiroa	French Polynesia

Halimeda incrassata		
H.0136	St. Martin	Netherlands Antilles
H.0179	Lee Stocking	Bahamas
H.0145	Florida	U.S.A.
H.0146	Florida	U.S.A.
H.0149	Florida	U.S.A.
H.0180	Florida	U.S.A.
H.0181	Florida	U.S.A.
H.0182	Florida	U.S.A.
H.0183	Florida	U.S.A.
HV978	Florida Keys	U.S.A.
H.0236	Texas	U.S.A.
HV448	Discovery Bay	Jamaica
HV899	Priory	Jamaica
HV332	St. Ann's Bay	Jamaica
HV334	St. Ann's Bay	Jamaica
H.0229	Puerto Morelos	Mexico
H.0077	Bocas del Toro	Panama
H.0079	Bocas del Toro	Panama
H.0127	Bocas del Toro	Panama
H.0188	Bocas del Toro	Panama
H.0477	Bocas del Toro	Panama
H.0027	Galeta	Panama
H.0143	Isla Grande	Panama
H.0667	Long Key	Panama
H.0132	San Andres	Panama
H.0211	San Blas	Panama
H.0248	San Blas	Panama
H.0666	San Blas	Panama
Halimeda kanaloana		
HS-2004-157 (HS)	Kaho`olawe	Hawai`i (U.S.A.)
HS-2004-159 (HS)	Kaho`olawe	Hawai`i (U.S.A.)
HS-2004-161 (HS)	Kaho`olawe	Hawai`i (U.S.A.)
HS-2004-162 (HS)	Keyhole, Mau`i	Hawai`i (U.S.A.)
HS-2004-171 (HS)	Keyhole, Mau`i	Hawai`i (U.S.A.)
HS-2004-172 (HS)	Keyhole, Mau`i	Hawai`i (U.S.A.)
HS-2004-173 (HS)	Keyhole, Mau`i	Hawai`i (U.S.A.)
HS-2004-174 (HS)	Keyhole, Mau`i	Hawai`i (U.S.A.)
HS-2004-175 (HS)	Keyhole, Mau`i	Hawai`i (U.S.A.)
HS-2004-176 (HS)	Keyhole, Mau`i	Hawai`i (U.S.A.)
HS-2004-177 (HS)	Keyhole, Mau`i	Hawai`i (U.S.A.)
HS-2004-178 (HS)	Keyhole, Mau`i	Hawai`i (U.S.A.)
H.0649	Honolua Bay, Mau`i	Hawai`i (U.S.A.)
H.0650	Honolua Bay, Mau`i	Hawai`i (U.S.A.)
H.0651	Honolua Bay, Mau`i	Hawai`i (U.S.A.)
H.0652	Honolua Bay, Mau`i	Hawai`i (U.S.A.)
H.0653	Honolua Bay, Mau`i	Hawai`i (U.S.A.)
H.0654	Honolua Bay, Mau`i	Hawai`i (U.S.A.)
H.0655	Honolua Bay, Mau`i	Hawai`i (U.S.A.)
H.0656	Honolua Bay, Mau`i	Hawai`i (U.S.A.)
H.0657	Honolua Bay, Mau`i	Hawai`i (U.S.A.)
H.0658	Honolua Bay, Mau`i	Hawai`i (U.S.A.)
SUVA6705 (SUVA)	Sorol, Yap	Micronesia
Halimeda melanesica		
HEC8243	Diani, Kenya	Kenya
HEC5564	Mombasa	Kenya
HEC5671	Mombasa	Kenya
HEC5860	Mombasa	Kenya
HEC7216	Mombasa	Kenya
HEC6814	Tiwi	Kenya
HEC6816	Tiwi	Kenya
HEC8386	Tiwi	Kenya
Berau-03-462 (L)	Maratua, Berau	Indonesia
Snellius-II-11254	Taka Bone Rate	Indonesia
Snellius-II-11312	Taka Bone Rate	Indonesia
Snellius-II-11180	Tukang Besi	Indonesia
HV818	Dancalan, Luzon	Philippines

PH318	Dancalan, Luzon	Philippines
HV790	Dapdap, Luzon	Philippines
HEC12322	Dapdap, Luzon	Philippines
PH278	Dapdap, Luzon	Philippines
PH401	Zamboanga	Philippines
PH402	Zamboanga	Philippines
PH456	Zamboanga	Philippines
PH495	Zamboanga	Philippines
PH521	Zamboanga	Philippines
PH522	Zamboanga	Philippines
HOD-PH99-42	Zamboanga	Philippines
HOD-PH99-48	Zamboanga	Philippines
HOD-PH99-54	Zamboanga	Philippines
HOD-PH99-111	Sanga Sanga	Philippines
C&PvR13761	Madang	Papua New Guinea
HEC6547	Madang	Papua New Guinea
HEC7849b	Madang	Papua New Guinea
PC0021851 (PC)	Lifou	New Caledonia
H.0665	Seashell Cove	Fiji
HV217	Afaahiti, Tahiti	French Polynesia
UPF094 (UPF)	Afaahiti, Tahiti	French Polynesia
UPF2804 (UPF)	Afaahiti, Tahiti	French Polynesia
UPF2811 (UPF)	Afaahiti, Tahiti	French Polynesia
UPF2812 (UPF)	Afaahiti, Tahiti	French Polynesia
UPF2813 (UPF)	Afaahiti, Tahiti	French Polynesia
UPF2821 (UPF)	Afaahiti, Tahiti	French Polynesia
UPF2832 (UPF)	Afaahiti, Tahiti	French Polynesia
H.0061	Marquesas Islands	French Polynesia
UPF095 (UPF)	Marquesas Islands	French Polynesia

Part 6

Summary and prospects for *Halimeda* evolutionary studies

Summary

Heroen Verbruggen

Molecular tools have revolutionized the field of algal systematics. Of the higher-level taxonomy from the eighties and before, ever less remains standing (e.g. chlorophytes: Lopez-Bautista & Chapman 2003; phaeophytes: Draisma et al. 2001, Rousseau et al. 2001, Kawai & Sasaki 2004; rhodophytes: Freshwater et al. 1994, Choi et al. 2000, Saunders & Hommersand 2004). Even down to the genus- and species-level, application of molecular methods has wiped out long-standing taxonomies (e.g. Siemer et al. 1998, Kooistra 2002, van der Strate et al. 2002, Zuccarello et al. 2002, Zuccarello & West 2003).

Throughout the course of Kooistra's work (Hillis et al. 1998, Kooistra et al. 1999, 2002) and the research presented here, the green algal genus *Halimeda* has become one of the prime examples of green algal genera in which species and section boundaries have been thoroughly upset by the application of molecular phylogenetics.

Sectional subdivision

Molecular phylogenetic assessments uncovered five principal monophyletic lineages within the genus *Halimeda* (Kooistra et al. 2002). Verbruggen & Kooistra (2004 – Chapter 5) defined these lineages morphologically. Morphological data was gathered from specimens used in the molecular analyses as well as from collections having a similar morphology and originating from the same geographical region. Starting from the lineages and their morphological synapomorphies, five natural sections within *Halimeda* were defined and illustrated. All or most medullary siphons traversing the nodes between segments fuse into a single unit in specimens of lineage 1 (section *Rhipsalis*), and segments at the thallus base fuse with one another. Medullary siphons of specimens in lineage 2 (section *Micronesicae*) traverse the node without fusing. Medullary siphons of specimens in lineage 3 (section *Halimeda*) divide frequently below the nodes and become entangled among one another. The segments of specimens in this lineage possess a continuous uncorticated band along the distal perimeter instead of three or more pits as encountered in segments of specimens in all other lineages. Members of lineage 4 (section *Pseudo-opuntia*) possess club-shaped subperipheral utricles. Medullary siphons of specimens in lineage 5 (section *Opuntia*) fuse over only a short distance at the nodes and retain their identity. Apart from these synapomorphies, the lineages can be delimited further by a characteristic combination of symplesiomorphies and homoplasies. In addition, the morphology of *H. bikinensis* was examined. This species was not included in the molecular analyses and has an ambiguous position in the sectional system, showing characters of sections *Halimeda* and *Pseudo-opuntia*.

Phylogenetics and biogeography

Kooistra & Verbruggen (2005 – Chapter 6) used molecular tools to study species limits, evolution and phylogeography in *Halimeda* section *Opuntia*. This section includes sprawling and pendant thalli composed of strongly calcified segments. Within this section, identification of Atlantic material is straightforward, but Indo-Pacific material is often difficult to key out. This is particularly true for specimens resembling *H. opuntia*, *H. distorta*, and *H. hederacea*; many specimens do not fit any type or are morphologically intermediate. The goals of Kooistra & Verbruggen (2005) were to define morphologically and genetically distinct groups among such specimens and to assess phylogeographic

patterns within these groups. Specimens were collected throughout the geographical and morphological range. Sequences of *H. minima* and *H. gracilis* were included as outgroups. Two morphological groups were discerned within the ingroup; the first fit *H. opuntia*, whereas most specimens in the second group, referred to as the *distorta–hederacea* complex, did not fit any species description unambiguously. The latter were subdivided into two subgroups corresponding more or less to *H. hederacea* and *H. distorta*, yet intermediates between these morphs existed. A phylogeny inferred from partial nuclear rDNA sequences showed one lineage with *H. opuntia* and a second one containing the *distorta–hederacea* complex, thus corroborating the two major morphological groups. The *distorta–hederacea* complex contained two clades that showed only partial correspondence with the morphological subgroups. Therefore, *H. hederacea* was synonymized with *H. distorta*. Phylogeographic structure within *H. opuntia* indicated that this species dispersed from the Indo-Pacific into the Atlantic. Fossil records of the species also show occurrence at Pacific sites throughout the last 10^5 years and a sudden appearance in the Caribbean and Bahamas during the last millennium.

Verbruggen et al. (submitted-1 – Chapter 7) reported that nuclear ribosomal and plastid DNA sequences of specimens belonging to *Halimeda* section *Halimeda* revealed many more genetically delineable species than those recognized by classical taxonomy. Discordances between cladograms inferred from nuclear and plastid DNA sequences suggested that reticulate evolution has been involved in speciation within the clade. Nonetheless, the data did not allow ruling out incomplete lineage sorting as causal factor of the discordances. The fact that several pseudo-cryptic species are restricted to the margins of the generic distribution range was interpreted as an indication that gene flow at distributional extremities is low enough to allow genetic differentiation and speciation. In a clade of *H. cuneata* sibling species from widely separated subtropical localities in the Indian Ocean, the South African sibling branched off first, leaving the Arabian and West Australian species as closest relatives. It was hypothesized that geographic isolation of the siblings may have taken place following Pleistocene or Pliocene periods of climatic cooling during which subtropical species occupied larger distribution ranges. A more basal separation of Atlantic, Indo-Pacific, and Mediterranean species was interpreted as an indication for vicariance. The alternative events that could have caused this vicariance were discussed.

Morphometric tools for Halimeda taxonomy

Species-level taxonomy of Bryopsidalean genera is often based on quantifiable morphological characters. Yet there are relatively few examples of statistically founded morphometric studies within this group of siphonous algae and macroalgae in general. Molecular phylogenetic studies have revealed cases of cryptic diversity in several Bryopsidalean genera and call for new approaches toward taxonomy. Verbruggen et al. (2005a, b – Chapters 8 and 9) presented a combined molecular and morphometric approach toward *Halimeda* taxonomy using a selection of specimens representing the five natural lineages within the genus. A phylogeny was inferred from partial nuclear rDNA sequences (3' end of small subunit, internal transcribed spacer region 1, 5.8S, internal transcribed spacer region 2, and 5' end of large subunit). Segment size and shape descriptors were acquired using different techniques, including landmark analysis and elliptic Fourier analysis. A broad range of anatomical structures was measured. Taxonomic utility of the different methods and characters was assessed using predictive discriminant analysis. Molecular data were used to delimit species groups. Segment morphological characters proved fairly good predictors for species membership, but anatomical variables yielded the best results. Segments aberrant in morphology and/or anatomy were primarily apical and non-calcified segments, and segments from the basal part of the algal body. Comparison of discriminant analyses that included and excluded deviant segments demonstrated the negative influence of such segments on the taxonomic power of the data. Omitting non-calcified and apical segments and segments from the basal thallus region yielded the same results as the exclusion of all deviant segments, irrespective of their location in the algal body. Therefore, the use of apical and non-calcified

segments, and segment from the basal thallus region in future morphometric taxonomic work was advised against. It was argued that statistically founded morphometric studies can probably help elucidate taxonomic issues within other Bryopsidalean genera as well.

DNA barcoding and morphometrics pinpoint species boundaries

Molecular techniques have revealed cryptic species within many morphologically conceived algal species. This raised the question whether such species are truly cryptic or whether they are morphologically recognizable and thus result from overconservative taxonomy. Verbruggen et al. (2005c – Chapter 10) addressed this issue within *Halimeda* section *Rhipsalis*. This section was known to contain cryptic diversity and to comprise species with overlapping morphological boundaries. In the study of Verbruggen et al. (2005c), species diversity within the section and identity of individual specimens were assessed using ITS1–5.8S–ITS2 (nrDNA) and *rps*3 (cpDNA) sequence data. The sequences grouped in a number of clear-cut genotypic clusters that were considered species. The same specimens were then subjected to morphometric analysis of external morphological and anatomical structures. Morphological differences between the genotypic cluster species were assessed using discriminant analyses. It was shown that significant morphological differences exist between genetically delineated species and that allocation of specimens to species on the basis of morphometric variables is nearly perfect. Anatomical characters yielded better results than external morphological characters. Two approaches were offered to allow future morphological identifications: a probabilistic approach based on classification functions of discriminant analyses, and the classical approach of an identification key.

In a subsequent study (Verbruggen et al. submitted-2 – Chapter 11), the phylogenetic structure of section *Rhipsalis* was inferred from nuclear 18S–ITS1–5.8S–ITS2 and concatenated plastid sequences (*tuf*A & *rpl*5–*rps*8–*inf*A) and the species *H. incrassata* was retaxonomized. Two pseudo-cryptic entities within this species were described as *H. kanaloana* Vroom and *H. heteromorpha* N'Yeurt. The original species *H. incrassata* was redescribed to include a sole, monophyletic entity. Likeness and disparity among the three pseudo-cryptic species and *H. melanesica* were discussed.

References

Choi H.G., Kraft G.T. & Saunders G.W. (2000) Nuclear small-subunit rDNA sequences from *Ballia* spp. (Rhodophyta): proposal of the Balliales ord. nov., Balliaceaea fam. nov., *Ballia nana* sp. nov. and *Inkyulee* gen. nov. (Ceramiales). *Phycologia* **39**: 272–287.

Draisma S.G.A., Prud'homme van Reine W.F., Stam W.T. & Olsen J.L. (2001) A reassessment of phylogenetic relationships within the phaeophyceae based on RUBISCO large subunit and ribosomal DNA sequences. *Journal of Phycology* **37**: 586–603.

Freshwater D.W., Fredericq S., Butler B.S., Hommersand M.H. & Chase M.W. (1994) A gene phylogeny of the red algae (Rhodophyta) based on plastid *rbc*L. *Proceedings of the National Academy of Sciences of the U.S.A.* **91**: 7281–7285.

Hillis L.W., Engman J.A. & Kooistra W.H.C.F. (1998) Morphological and molecular phylogenies of *Halimeda* (Chlorophyta, Bryopsidales) identify three evolutionary lineages. *Journal of Phycology* **34**: 669–681.

Hillis-Colinvaux L. (1980) Ecology and taxonomy of *Halimeda*: primary producer of coral reefs. *Advances in Marine Biology* **17**: 1–327.

Kawai H. & Sasaki H. (2004) Morphology, life history, and molecular phylogeny of *Stschapovia flagellaris* (Tilopteridales, Phaeophyceae) and the erection of the Stschapoviaceae fam. nov. *Journal of Phycology* **40**: 1156–1169.

Kooistra W.H.C.F. (2002) Molecular phylogenies of Udoteaceae (Bryopsidales, Chlorophyta) reveal nonmonophyly for *Udotea*, *Penicillus* and *Chlorodesmis*. *Phycologia* **41**: 453–462.

Kooistra W.H.C.F., Caldéron M. & Hillis L.W. (1999) Development of the extant diversity in *Halimeda* is linked to vicariant events. *Hydrobiologia* **398**: 39–45.

Kooistra W.H.C.F., Coppejans E.G.G. & Payri C. (2002) Molecular systematics, historical ecology, and phylogeography of *Halimeda* (Bryopsidales). *Molecular Phylogenetics and Evolution* **24**: 121–138.

Kooistra W.H.C.F. & Verbruggen H. (2005) Genetic patterns in the calcified tropical seaweeds *Halimeda opuntia*, *H. distorta*, *H. hederacea* and *H. minima* (Bryopsidales, Chlorophyta) provide insights in species boundaries and inter-oceanic dispersal. *Journal of Phycology* **41**: 177–187.

Lopez-Bautista J.M. & Chapman R.L. (2003) Phylogenetic affinities of the Trentepohliales inferred from small-subunit rDNA. *International Journal of Systematic and Evolutionary Microbiology* **53**: 2099–2106.

Rousseau F., Burrowes R., Peters A.F., Kuhlenkamp R. & de Reviers B. (2001) A comprehensive phylogeny of the Phaeophyceae based on nrDNA sequences resolves the earliest divergences. *Comptes Rendus de l'Académie des Sciences de Paris – Life sciences* **324**: 305–319.

Saunders G.W. & Hommersand M.H. (2004) Assessing red algal supraordinal diversity and taxonomy in the context of contemporary systematic data. *American Journal of Botany* **91**: 1494–1507.

Siemer B.L., Stam W.T., Olsen J.L. & Pedersen P.M. (1998) Phylogenetic relationships of the brown algal orders Ectocarpales, Chordariales, Dictyosiphonales, and Tilopteridales (Phaeophyceae) based on RUBISCO large subunit and spacer sequences. *Journal of Phycology* **34**: 1038–1048.

van der Strate H.J., Boele-Bos S.A., Olsen J.L., van de Zande L. & Stam W.T. (2002) Phylogeographic studies in the tropical seaweed *Cladophoropsis membranacea* (Chlorophyta, Ulvophyceae) reveal a cryptic species complex. *Journal of Phycology* **38**: 572–582.

Verbruggen H., De Clerck O., Cocquyt E., Kooistra W.H.C.F. & Coppejans E. (2005a) Morphometric taxonomy of siphonous green algae: a methodological study within the genus *Halimeda* (Bryopsidales). *Journal of Phycology* **41**: 126–139.

Verbruggen H., De Clerck O. & Coppejans E. (2005b) Deviant segments hamper a morphometric approach towards *Halimeda* taxonomy. *Cryptogamie Algologie* **26**: accepted.

Verbruggen H., De Clerck O., Kooistra W.H.C.F. & Coppejans E. (2005c) Molecular and morphometric data pinpoint species boundaries in *Halimeda* section *Rhipsalis* (Bryopsidales, Chlorophyta). *Journal of Phycology* **41**: in press.

Verbruggen H., De Clerck O., Schils T., Kooistra W.H.C.F. & Coppejans E. (submitted-1) Evolution and phylogeography of the *Halimeda cuneata/discoidea/tuna* cryptic species complex.

Verbruggen H. & Kooistra W.H.C.F. (2004) Morphological characterization of lineages within the calcified tropical seaweed genus *Halimeda* (Bryopsidales, Chlorophyta). *European Journal of Phycology* **39**: 213–228.

Verbruggen H., De Clerck O., N'Yeurt A., Spalding H. & Vroom P.S. (submitted-2) Phylogeny and taxonomy of *Halimeda incrassata*, including the description of *H. kanaloana* and *H. heteromorpha* spp. nov. (Bryopsidales, Chlorophyta).

Zuccarello G.C., Sandercock B. & West J.A. (2002) Diversity within red algal species: variation in world-wide samples of *Spyridia filamentosa* (Ceramiaceae) and *Murrayella periclados* (Rhodomelaceae) using DNA markers and breeding studies. *European Journal of Phycology* **37**: 403–417.

Zuccarello G.C. & West J.A. (2003) Multiple cryptic species: Molecular diversity and reproductive isolation in the *Bostrychia radicans/B. moritziana* complex (Rhodomelaceae, Rhodophyta) with focus on North American isolates. *Journal of Phycology* **39**: 948–959.

Prospects for *Halimeda* evolutionary studies

Heroen Verbruggen

Despite the fact that this study has yielded certain insights about morphological and molecular evolution of *Halimeda* and that these insights have resulted in a few taxonomic decisions, several questions remain unanswered and the obtained results point out a number of topics that deserve additional study.

Taxonomic issues

Section *Halimeda*

The most obvious issue that has not been addressed is the morphological taxonomy of section *Halimeda*. Kooistra et al. (2002) and Verbruggen et al. (submitted-1) showed that this section contains about double the number of genealogical species than those currently recognized by classical, morphology-based taxonomy. The question whether or not the different genealogical species can be diagnosed with morphological characters has remained unanswered. The most evident approach to answer this question is to conduct a morphometric study of vegetative structures, combined with a more traditional taxonomic study (cf. Verbruggen et al. 2005, submitted-2). Preliminary results indicate that the seven cryptic species within *H. cuneata* show small differences in external morphology. Molecular and morphological differences and similarities among the *H. cuneata* entities must be examined using a larger sample size, including specimens from Madagascar and SE Australia, from where *H. cuneata* has been reported (Pichon 1978, Millar & Kraft 1994) but from where no specimens were studied in Verbruggen et al. (submitted-1). Furthermore, *H. cuneata* features two morphologies in SW Australia (John Huisman personal communication), an issue that most definitely deserves additional taxonomic attention. A number of morphological differences between *H. tuna* 1 and 2 (numbered after Verbruggen et al. submitted-1) have been described in the literature (Hillis 1959, Hillis-Colinvaux 1980) but need to be reexamined within a more elaborate set of species (e.g. *H. cuneata* f. *undulata*, *H. gigas*, *H. lacunalis*, *H. magnidisca*, *H. xishaensis*) because Hillis-Colinvaux' perception of *H. tuna* does not stroke with insights from molecular data and because several of the species mentioned above were not recognized by Hillis-Colinvaux (1980) or had not yet been described at the time of Hillis-Colinvaux' monograph. *Halimeda discoidea* 2 and 3 show a few obvious external and anatomical differences and they also stand apart ecologically. The differences between *H. discoidea* 1 and 2 are much less obvious, but Kooistra et al. (2002) reported that peripheral utricles of these species differ in the extent of lateral attachment. These differences need to be reinvestigated with inclusion of *H. cuneata* f. *digitata*, which is genetically indistinguishable from *H. discoidea* 1 (Verbruggen et al. submitted-1). Within section *Halimeda*, additional attention must be paid to the distinction between *H. gigas* and *H. magnidisca*. Noble (1986) distinguished the latter from the former on the basis of smaller peripheral utricles, attachment in sandy substrate with a large, bulbous holdfast and the presence of a stipe-like structure consisting of a series of cylindrical segments. The specimens that were considered to be *H. magnidisca* in Kooistra et al. (2002) and Verbruggen et al. (submitted-1) form an intermediate between both species. They feature a minute bulbous holdfast, utricles of intermediate size and a much less pronounced stipe region. Whether these specimens belong to *H. gigas*, *H. magnidisca* or a yet undescribed species needs to be examined using DNA sequencing and morphological examination of *H. gigas* and *H. magnidisca* from their type localities. A last species with uncertain affinities is *H.*

xishaensis. This species, which was described from the Xisha Islands (China) by Dong & Tseng (1980), strongly resembles certain specimens belonging to *H. discoidea* 1.

Halimeda incrassata complex

A second evident taxonomic issue is the *H. incrassata* complex. Despite the taxonomic revision of Verbruggen et al. (submitted-2), the affinities of a number of illustrations from the literature and specimens from the Ghent University Herbarium remain unclear. Whether these specimens belong to *H. incrassata*, *H. kaneloa*, *H. heteromorpha*, or one or more yet undescribed species remains to be seen. The availability of material suited for analysis of DNA and anatomical structures is a crucial problem in this context.

Halimeda minima group

A third species group within which taxonomic uncertainty is present is *H. minima–howensis–velasquezii*. The species *H. minima* shows much morphological variability and molecular phylogenetic studies of 18S–ITS1–5.8S–ITS2 sequences show that the species comprises two (possibly three) clear-cut and widely distributed clades, suggesting that multiple reproductively isolated populations may exist within this morphological species (Kooistra et al. 2002, Verbruggen & Kooistra 2004, Kooistra & Verbruggen 2005). In the studies mentioned above, too few specimens were studied in order to obtain a complete image of the species. In my opinion (which is solely based on casual morphological observations), many Indo-Pacific specimens belonging to *H. minima* were reported as *H. copiosa* (e.g. Noble 1987, Coppejans et al. 2000). The principal cause of this confusion may be that well-developed specimens from outer reef slopes strongly resemble the Atlantic species *H. copiosa* as described by Goreau & Graham (1967). This issue should be addressed with molecular analyses and a more thorough, quantitative morphological investigation. The species *H. howensis*, described from the highly isolated and most southern coral reef in the world (Lord Howe Island), shows clear morphological affinities with *H. copiosa* (in my opinion *H. minima*) from the Great Barrier Reef but is much smaller (Kraft 2000). Whether this species is indeed distinct or represents a small morphology of *H. minima* may be determined by incorporation of *H. howensis* in a molecular–morphological systematic study. The species *H. velasquezii*, which has been reported throughout the Indo-Pacific basin (e.g. Taylor 1962, Valet 1966, Vroom & Smith 2003), strongly resembles *H. minima*. Analysis of DNA sequences of this species (unpublished results) point out that this morphological species comprises two genealogical species, of which one shows affinities with *H. renschii* (the sister species of *H. minima*) and the other with *H. distorta* (sensu Kooistra & Verbruggen 2005). Thorough morphological and molecular studies of an extensive set of specimens are necessary to get more insight in the taxonomy of the *H. minima–howensis–velasquezii* morphological complex. Because some *H. minima* specimens can take on a morphology resembling that of *H. goreauii*, this species should also be included in such a study.

Halimeda distorta–hederacea complex

The *H. distorta–hederacea* complex also deserves additional attention. The 18S–ITS1–5.8S–ITS sequences of Kooistra & Verbruggen (2005) demonstrated that this group existed of a basal, paraphyletic group of specimens of which most had a *H. hederacea* morphology and a derived, monophyletic group of specimens with a *H. distorta* morphology. On the basis of these results and the existence of specimens with intermediate morphologies, the distinction between both species could not be maintained and they were merged in the species *H. distorta*. Furthermore, the study of Kooistra & Verbruggen (2005) clarified the distinction between *H. opuntia* and *H. distorta*. However, the study of Kooistra & Verbruggen (2005) has two flaws. First, anatomical observations were not made. Second, only one molecular marker was used and since the study of Verbruggen en Kooistra (2005), it has become clear that different molecular markers sometimes sketch a different picture of evolutionary relationships (Verbruggen et al. 2005, submitted-1). Therefore, it is advisable that the *H. distorta–*

hederacea is investigated more thoroughly, using anatomical–morphometric techniques and additional molecular markers.

Halimeda gracilis

Unpublished ITS1–5.8S–ITS2 sequence data reveal three genotypic clusters within *H. gracilis*, two of which occur in the Indo-Pacific basin and the other occurs in the Caribbean. Furthermore, the species exhibits much morphological variability. A revision of this species with the aim to check whether this morphological variability corresponds to the genotypic clusters, is therefore recommended.

Halimeda bikinensis

A last taxonomic uncertainty concerns *H. bikinensis*. Verbruggen & Kooistra (2004) elaborately discussed the morphology and possible affinities of this species with sections *Halimeda* and *Pseudo-opuntia*. Extraction of DNA from the type material failed and the position of the species within the genus has remained unresolved. To clarify this issue, DNA sequences of recent collections of this species could be determined. However, to my knowledge, no such collections are available.

Intraspecific morphological variation

Several authors state that *Halimeda* species show morphological differences according to the habitat they inhabit (e.g. Gilmartin 1960, Hillis-Colinvaux 1980, Vroom et al. 2003). However, so far no detailed study of the environmental, geographic and genetic components of intraspecific morphological variability has been carried out. From the most comprehensive study so far, which focused on the tropical species *H. heteromorpha*, morphology seemed strongly correlated with habitat characteristics derived from field notes (Verbruggen et al. submitted-2). Morphological and genetic similarity of specimens belonging to this species are not significantly correlated (unpublished results). However, the morphological variation does seem to have a geographic component (unpublished results), even though this may be a consequence of incomplete sampling of certain regions and the absence of certain types of habitats in some regions. Solid evidence of environmentally induced morphological variability can only be furnished through transplantation and common garden experiments. Another approach exists of large-scale sampling of specimens from different regions and careful measuring and noting of all kinds of environmental factors that may influence morphology. Ecological factors that may have an impact on morphology are depth (Gilmartin 1960), light intensity (Hillis-Colinvaux 1980), nutrient content and chemical composition of the water column (Smith et al. 2004), intensity and type of water movement (e.g. wave action, surge, unidirectional current; Kaandorp 1999), grazing pressure and epiphyte density. Integrated statistical analysis of a morphometric dataset, DNA sequence data, and the collected environmental data could offer much insight in the relationships among these data (e.g. Thorpe et al. 1996, Sanders et al. 2004) but does not allow inferring cause and consequence.

Marine speciation mechanisms

Reticulate speciation

The use of molecular tools in systematic studies of *Halimeda* has brought several questions concerning marine speciation mechanisms into prominence. One of the most important aspects in this context is the possibility of reticulate speciation (Verbruggen et al. submitted-1). Despite the fact that reticulate speciation is a very important speciation mechanism in streptophytes (e.g. Otto & Whitton 2000, Denboh et al. 2003, Linder & Rieseberg 2004) and corals (e.g. van Oppen et al. 2001, 2002, 2004), this speciation mechanism has hardly been studied in marine green algae. Except for the indications of reticulate speciation in *Halimeda*, which were based on discordances between plastid and nuclear phylogenies, conflicting phylogenetic information has been shown to exist between regions within the nrDNA cistron of *Caulerpa* (Caulerpaceae, Bryopsidales; Durand et al. 2002), a far sister of

Halimeda. Endoreduplication, the doubling of the nuclear genome without subsequent nuclear division, is common in green algae (e.g. Kapraun 1993, Kapraun 1994, Kapraun & Buratti 1998) and is known to occur in *Halimeda* (Kapraun 1994). Endoreduplication increases the chances of successful bivalent pairing of chromosomes and meiosis of hybrid nuclei and, as a consequence, is beneficial to hybrid speciation. Molecular techniques allow studying hybrid speciation in more detail. Especially single-copy nuclear markers, quantitative genetics, and genome evolution offer perspectives (Hegarty & Hiscock 2005).

Reproductive isolation

A second theme that deserves more attention in the study of evolution, speciation and taxonomy of *Halimeda* is the biological species concept. Sexual reproduction within the genus occurs by simultaneous release of micro- and macrogametes into the water column. The phenology of many species is predictable and certain species release their gametes in different time frames during the same morning (Drew & Abel 1988, Clifton 1997, Clifton & Clifton 1999). For most species, however, the phenology and gamete release timeframes are unknown. Furthermore, it is unclear whether species have the same phenology throughout their distribution ranges. The only thoroughly studied regions are the Great Barrier Reef (Drew & Abel 1988) and the Caribbean coast of Panama (Clifton 1997; Clifton & Clifton 1999) but these regions don't share any species except *H. opuntia*. Drew & Abel (1988) found that the reproductive season at the Great Barrier Reef did not always correspond with the sporadic records of reproduction in other regions. The fact that within one region different species are fertile on the same morning (cf. Clifton 1997, Clifton & Clifton 1999), makes interfertility studies relatively easy. On the other hand, the reproductive seasonality also has its disadvantages for interfertility research. For example, if an experiment has to be repeated, it may take months for the species to become reproductive again. The stimuli of sexual reproduction are unknown and, as a consequence, the process cannot be induced when desired. Even though I am in favor of a thorough assessment of reproductive compatibility to aid species delineation, this way of working and the biological species concept in itself are imperfect as well. For example, interfertility tests among strictly allopatric species are very hard to interpret in the framework of species delineation because sexual contact is impossible because of the geographic separation. Kenneth Clifton already performed hybridization experiments with the closely related, sympatric species *H. incrassata*, *H. monile* and *H. simulans* (personal communication). These three species are not interfertile, meaning that the morphological, biological and genealogical species concepts are applicable to these species (Verbruggen et al. 2005, submitted-2).

Geographic speciation modes

The geographic modes of speciation have been a central theme in evolutionary theory for a long time. Benthic and sedentary marine organisms mainly depend upon ocean surface currents for their dispersal. Such currents are capable of carrying propagules over long distances (e.g. Scheltema 1968). On a timescale of hundreds to a few thousand years, the position and direction of surface currents are more or less constant, causing certain regions to be in contact and other regions to be isolated on this timescale. As a consequence, ocean currents provide connectivity between certain populations and isolation of other populations. Whereas connectivity promotes genetic homogenization of species over a large area and consequently slows down speciation, isolation allows divergence of geographically isolated populations and promotes speciation. By changes in the surface current patterns on the timescale of tens of thousands of years, divergent populations will regain contact and, if the populations are still reproductively compatible, the species will be rehomogenized. This phenomenon is better known as surface circulation vicariance (Veron 1995). Next to barriers induced by currents, there are also more substantive barriers that influence population differentiation and speciation, such as the temporary separation of the Indian and Pacific Oceans as a consequence of the emergence of the Indonesian Archipelago and the Torres Strait during ice ages (e.g. McMillan & Palumbi 1995, Benzie et al.

2002). A glacial land barrier at Bab-el-Mandeb (Sheppard et al. 1992) could, in a similar way, be responsible for the high endemism of the Red Sea (e.g. Klausewitz 1989). On the other hand, several examples of sympatric marine speciation are known (e.g. Hellberg 1998, Darling et al. 2000).

Verbruggen et al. (submitted-1) suggest that examples of each of the major geographic speciation modes are present in *Halimeda* section *Halimeda*. Particularly the fact that latitudinally separated populations of *H. discoidea* along the East African coast differ more strongly genetically than populations that are longitudinally separated over a much greater distance is very intriguing. In the light of this finding, it would be interesting to include *H. discoidea* samples from other subtropical areas in the study and check whether the observed pattern occurs in other regions or is specific to the NW Indian Ocean. Concerning the pattern observed in the NW Indian Ocean, it was proposed that seasonal upwelling of cold water along the southern coast of the Arabian peninsula, from which *H. discoidea* is absent, could contribute to the genetic isolation of populations from the warmer waters of the tropical Indian Ocean, the Gulf of Oman, and possibly also the Red Sea. The genetic pattern found for *H. discoidea* is probably not unique. Many reef associated organisms have isolated populations in the warmer waters of the Gulf of Oman, the Red Sea and the northern coast of Socotra. Whether the phylogeographic patterns of these species accord with those of *H. discoidea* is most probably a function of their temperature tolerance and dispersive features. The reproductive season may also be of importance because the currents through the Arabian Sea change direction during the SW and NE monsoon seasons. A more detailed phylodemographic study of the species *H. discoidea* and other warm water species in the region is a necessity to confirm and understand this interesting form of peripatric divergence and speciation.

Halimeda seems to offer perspectives for the study of geographic speciation modes in the Caribbean Sea as well. From a biogeographic point of view, the Caribbean Sea is very homogeneous. Nonetheless, there are two *Halimeda* species with a interesting, small distribution range. The first species, *H. favulosa*, belongs to section *Rhipsalis* and is endemic to the Bahamas. The second species, *H. lacrimosa*, belongs to section *Pseudo-opuntia* and occurs in the Bahamas, the Florida Keys and one location in northern Cuba. It thus seems that two *Halimeda* species originated in the northern periphery of the Caribbean basin. An interesting aspect about these putative speciation events in the Bahamas is that, complementary to molecular data, information from the fossil record can be integrated in a study. Limestone cores that go back in time to before the presumed origination of the species in question have already been drilled in the tropical Bahama banks (e.g. McNeill et al. 1998). Furthermore, both *H. lacrimosa* and *H. favulosa* have conspicuous segment morphological and anatomical features that make their recognition in limestone cores easy. A potential timeframe for the origination of both species is the Pleistocene, when the edges of the Bahama platform got steeper and the currents along the platform intensified, thus isolating the Bahamas from the Caribbean and Florida (Ginsburg 2001).

References

Benzie J.A.H., Ballment E., Forbes A.T., Demetriades N.T., Sugama K. & Haryanti Moria S. (2002) Mitochondrial DNA variation in Indo-Pacific populations of the giant tiger prawn, *Penaeus monodon*. *Molecular Ecology* **11**: 2553–2569.

Clifton K.E. (1997) Mass spawning by green algae on coral reefs. *Science* **275**: 1116–1118.

Clifton K.E. & Clifton L.M. (1999) The phenology of sexual reproduction by green algae (Bryopsidales) on Caribbean coral reefs. *Journal of Phycology* **35**: 24–34.

Cole K.M. (1990) Chromosomes. In: Cole K.M. & Sheat R.G. *Biology of the red algae*. Cambridge University Press, Cambridge. pp. 71–101.

Coppejans E., Leliaert F. & De Clerck O. (2000) Annotated list of new records of marine macroalgae for Kenya and Tanzania, since Isaac's and Jaasund's publications. *Biologisch Jaarboek Dodonaea* **67**: 31–93.

Darling K.F., Wade C.M., Stewart I.A., Kroon D., Dingle R. & Leigh Brown A. (2000) Molecular evidence for genetic mixing of Arctic and Antarctic subpolar populations of planktonic foraminifers. *Nature* **405**: 43–48.

Denboh T., Ichimura T., Hendrayanti D. & Coleman A.W. (2003) *Closterium moniliferum–ehrenbergii* (Charophyceae, chlorophyta) species complex viewed from the 1506 group I intron and ITS2 of nuclear rDNA. *Journal of Phycology* **39**: 960–977.

Dong M. & Tseng C.K. (1980) Studies on some marine green algae from the Xisha Islands, Guandong Province, China. II. *Studia Marina Sinica* **17**: 1–10.

Drew E.A. & Abel K.M. (1988) Studies on *Halimeda*. II: reproduction, particularly the seasonality of gametangia formation, in a number of species from the Great Barrier Reef Province. *Coral Reefs* **6**: 207–218.

Durand C., Manuel M., Boudouresque C.F., Meinesz A., Verlaque M. & Le Parco Y. (2002) Molecular data suggest a hybrid origin for the invasive *Caulerpa racemosa* (Caulerpales, Chlorophyta) in the Mediterranean Sea. *Journal of Evolutionary Biology* **15**: 122–133.

Gilmartin M. (1960) The ecological distribution of the deep water algae of Eniwetok. *Ecology* **41**: 210–221.

Ginsburg R.N. (2001) *Subsurface geology of a prograding carbonate platform margin, Great Bahama Bank: results of the Bahamas drilling project.* SEPM Special Publication 70, Tulsa, OK.

Goreau T.F. & Graham E.A. (1967) A new species of *Halimeda* from Jamaica. *Bulletin of Marine Science* **17**: 432– 441.

Hellberg M.E. (1998) Sympatric sea shells along the sea's shore: the geography of speciation in the marine gastropod *Tegula*. *Evolution* **52**: 1311–1324.

Hegarty M.J. & Hiscock S.J. (2005) Hybrid speciation in plants: new insights from molecular studies. *New Phytologist* **165**: 411–423.

Hillis L. (1959) A revision of the genus *Halimeda* (order Siphonales). *Publications of the Institute of Marine Science* **6**: 321–403.

Hillis-Colinvaux L. (1980) Ecology and taxonomy of *Halimeda*: primary producer of coral reefs. *Advances in Marine Biology* **17**: 1–327.

Kaandorp J.A. (1999) Morphological analysis of growth forms of branching marine sessile organisms along environmental gradients. *Marine Biology* **134**: 295–306.

Kapraun D.F. (1993) Karyology of marine green algae. *Phycologia* **32**: 1–21.

Kapraun D.F. (1994) Cytophotometric estimation of nuclear DNA contents in thirteen species of the Caulerpales (Chlorophyta). *Cryptogamic Botany* **4**: 410–418.

Kapraun D.F. & Buratti J.R. (1998) Evolution of genome size in the Dasycladales (Chlorophyta) as determined by DAPI cytophotometry. *Phycologia* **37**: 176–183.

Klausewitz W. (1989) Evolutionary history and zoogeography of the Red Sea ichthyofauna. *Fauna of Saudi Arabia* **10**: 310–337.

Kooistra W.H.C.F., Coppejans E.G.G. & Payri C. (2002) Molecular systematics, historical ecology, and phylogeography of *Halimeda* (Bryopsidales). *Molecular Phylogenetics and Evolution* **24**: 121–138.

Kooistra W.H.C.F. & Verbruggen H. (2005) Genetic patterns in the calcified tropical seaweeds *Halimeda opuntia*, *H. distorta*, *H. hederacea* and *H. minima* (Bryopsidales, Chlorophyta) provide insights in species boundaries and inter-oceanic dispersal. *Journal of Phycology* **41**: 177–187.

Kraft G.T. (2000) Marine and estuarine benthic algae (Chlorophyta) of Lord Howe Island, Southwestern Pacific. *Australian Systematic Botany* **13**: 509–648.

Linder C.R. & Rieseberg L.H. (2004) Reconstructing patterns of reticulate evolution in plants *American Journal of Botany* **91**: 1700–1708.

McMillan W.O. & Palumbi S.R. (1995) Concordant evolutionary patterns among Indo-West Pacific butterflyfishes. *Proceedings of the Royal Society of London Series B - Biological Sciences* **260**: 229–236.

McNeill D.F., Grammer G.M. & Williams S.C. (1998) A 5 my chronology of carbonate platform margin aggradation, southwestern Little Bahama Bank, Bahamas. *Journal of Sedimentary Research* **68**: 603–614.

Millar A.J.K. & Kraft G.T. (1994) Catalogue of marine benthic green algae (Chlorophyta) of New South Wales, including Lord Howe Island, South-western Pacific. *Australian Systematic Botany* **7**, 419–453.

Noble J.M. (1986) *Halimeda magnidisca* (Caulerpales, Chlorophyta), a new species from the Great Barrier Reef, Australia. *Phycologia* **25**: 331–339.

Noble J.M. (1987) *A taxonomic study of the genus Halimeda Lamouroux (Chlorophyta, Caulerpales) from the Heron Island region of the southern Great Barrier Reef, Australia.* Masters degree thesis, University of Melbourne, Melbourne, Australia.

Otto S.P. & Whitton J. (2000) Polyploid incidence and evolution. *Annual Review of Genetics* **34**: 401–437.

Pichon M. (1978) Recherches sur les peuplements à dominance d'anthozoaires dans les récifs coralliens de Tuléar (Madagascar). *Atoll Research Bulletin* **222**, 1–447.

Sanders K.L., Malhotra A. & Thorpe R.S. (2004) Ecological diversification in a group of Indomalayan pitvipers (*Trimeresurus*): convergence in taxonomically important traits has implications for species identification. *Journal of Evolutionary Biology* **17**: 721–731.

Scheltema R.S. (1968) Dispersal of larvae by equatorial ocean currents and its importance to the zoogeography of shoal-water tropical species. *Nature* **217**: 1159–1162.

Sheppard C., Price A. & Roberts C. (1992) *Marine ecology of the Arabian region. Patterns and processes in extreme tropical environments*. Academic Press.

Smith J.E., Smith C.M., Vroom P.S., Beach K.L. & Miller S. (2004) Nutrient and growth dynamics of *Halimeda tuna* on Conch Reef, Florida Keys: Possible influence of internal tides on nutrient status and physiology. *Limnology and Oceanography* **49**: 1923–1936.

Taylor W.R. (1962) Two undescribed species of *Halimeda*. *Bulletin of the Torrey Botanical Club* **89**: 172–177.

Thorpe R.S., Black H. & Malhotra A. (1996) Matrix correspondence tests on the DNA phylogeny of the Tenerife lacertid elucidate both historical causes and morphological adaptation. *Systematic Biology* **45**: 335–343.

Valet G. (1966) Sur une espèce rare et une nouvelle espèce d'*Halimeda* de Mélanésie. *Revue Générale de Botanique* **73**: 680–685.

van Oppen M.J.H., Koolmees E.M. & Veron J.E.N. (2004) Patterns of evolution in the scleractinian coral genus *Montipora* (Acroporidae). *Marine Biology* **144**: 9–18.

van Oppen M.J.H., McDonald B.J., Willis B. & Miller D.J. (2001) The evolutionary history of the coral genus *Acropora* (Scleractinia, Cnidaria) based on a mitochondrial and a nuclear marker: Reticulation, incomplete lineage sorting, or morphological convergence? *Molecular Biology and Evolution* **18**: 1315–1329.

van Oppen M.J.H., Willis B.L., van Rheede T. & Miller D.J. (2002) Spawning times, reproductive compatibilities and genetic structuring in the *Acropora aspera* group: evidence for natural hybridization and semi-permeable species boundaries in corals. *Molecular Ecology* **11**: 1363–1376.

Verbruggen H., De Clerck O., Kooistra W.H.C.F. & Coppejans E. (2005) Molecular and morphometric data pinpoint species boundaries in *Halimeda* section *Rhipsalis* (Bryopsidales, Chlorophyta). *Journal of Phycology* **41**: in press.

Verbruggen H., De Clerck O., Schils T., Kooistra W.H.C.F. & Coppejans E. (submitted-1) Evolution and phylogeography of the *Halimeda cuneata/discoidea/tuna* cryptic species complex.

Verbruggen H. & Kooistra W.H.C.F. (2004) Morphological characterization of lineages within the calcified tropical seaweed genus *Halimeda* (Bryopsidales, Chlorophyta). *European Journal of Phycology* **39**: 213–228.

Verbruggen H., De Clerck O., N'Yeurt A., Spalding H. & Vroom P.S. (submitted-2) Phylogeny and taxonomy of *Halimeda incrassata*, including the description of *H. kaneloa* and *H. heteromorpha* spp. nov. (Bryopsidales, Chlorophyta).

Veron J.E.N. (1995) *Corals in space and time: the biogeography and evolution of the Scleractinia.* University of New South Wales Press, Sydney.

Vroom P.S. & Smith C.M. (2003) Reproductive features of Hawaiian *Halimeda velasquezii* (Bryopsidales, Chlorophyta), and an evolutionary assessment of reproductive characters in *Halimeda*. *Cryptogamie Algologie* **24**: 355–370.

Vroom P.S., Smith C.M., Coyer J.A., Walters L.J., Hunter C.L., Beach K.S. & Smith J.E. (2003) Field biology of *Halimeda tuna* (Bryopsidales, Chlorophyta) across a depth gradient: comparative growth, survivorship, recruitment, and reproduction. *Hydrobiologia* **501**: 149–166.

Samenvatting

Heroen Verbruggen

Moleculaire technieken hebben een revolutie teweeggebracht in de systematische algologie. Van de taxonomie op hoger niveau van de jaren tachtig en daarvoor blijft steeds minder overeind (bv. groenwieren: Lopez-Bautista & Chapman 2003; bruinwieren: Draisma et al. 2001, Rousseau et al. 2001, Kawai & Sasaki 2004; roodwieren: Freshwater et al. 1994, Choi et al. 2000, Saunders & Hommersand 2004). Ook op het niveau van genera en soorten hebben moleculaire studies gevestigde taxonomieën van de kaart geveegd (bv. Siemer et al. 1998, Kooistra 2002, van der Strate et al. 2002, Zuccarello et al. 2002, Zuccarello & West 2003).

Door het onderzoek van Kooistra (Hillis et al. 1998, Kooistra et al. 1999, 2002) en het hier voorgestelde werk, is het genus *Halimeda* één van de best bestudeerde voorbeelden geworden van groenwiergenera waarin soorts- en sectiegrenzen grondig werden herzien met behulp van moleculair fylogenetisch onderzoek.

Sectionele indeling

Moleculaire fylogenetische studies brachten vijf grote monofyletische groepen aan het licht binnen het genus *Halimeda* (Kooistra et al. 2002). Verbruggen & Kooistra (2004 – Hoofdstuk 5) definieerden deze groepen op morfologische basis. De gegevens hiervoor werden vergaard van specimens gebruikt in de moleculaire analyses en collecties met een gelijkaardige morfologie die uit dezelfde geografische regio kwamen. Vertrekkende van die groepen en hun morfologische synapomorfieën, werden vijf natuurlijke secties gedefinieerd en geïllustreerd. In groep 1 (sectie *Rhipsalis*) versmelten alle of de meeste medullaire sifons die door de knoop tussen opeenvolgende segmenten gaan tot een eenheid en versmelten segmenten nabij de basis van de thallus met elkaar. In specimens behorende tot de tweede groep (sectie *Micronesicae*) overbruggen medullaire sifons de knoop tussen segmenten zonder te versmelten. In de derde groep (sectie *Halimeda*), vertakken de medullaire sifons frequent onder de knoop en raken ze onderling verstrengeld. De segmenten van soorten in deze groep bezitten een continue ongecorticeerde band langsheen hun distale rand in plaats van drie of meerdere kuiltjes zoals dit het geval is in alle andere groepen. Leden van groep 4 (sectie *Pseudo-opuntia*) bezitten clavate subperifere utriculi. Medullaire sifons van specimens in groep 5 (sectie *Opuntia*) versmelten over korte afstand aan de knopen en behouden hun identiteit. Naast deze synapomorfieën kunnen de groepen ook gekarakteriseerd worden door kenmerkende combinaties van symplesiomorfieën en homoplasieën. Bovendien werd de morfologie van *H. bikinensis* onderzocht. Deze soort was niet opgenomen in de moleculaire analyses en heeft, door het bezit van kenmerken van secties *Halimeda* en *Pseudo-opuntia*, een onduidelijke positie in het sectionele systeem.

Fylogenetische en biogeografische studies

Kooistra & Verbruggen (2005 – Hoofdstuk 6) gebruikten moleculaire technieken om soortslimieten, evolutie en fylogeografie van *Halimeda* sectie *Opuntia* te bestuderen. Deze sectie bevat sterk verkalkte thalli die zich uitspreiden over het substraat of neerhangen van wanden. Binnen deze sectie is identificatie van Atlantisch materiaal eenvoudig maar Indo-Pacifisch materiaal is vaak moeilijk op naam te brengen, in het bijzonder specimens die lijken op *H. opuntia*, *H. distorta*, en *H. hederacea*. Veel specimens stemmen niet overeen met een type of zijn morfologisch intermediair. De doelstellingen van

Kooistra & Verbruggen (2005) waren om binnen zulke specimens morfologisch en genetisch verschillende groepen af te bakenen en om fylogeografische patronen binnen die groepen te achterhalen. Een breed gamma specimens werd verzameld van verschillende geografische locaties. Sequenties van *H. minima* en *H. gracilis* werden gebruikt als uitgroep. Twee morfologische groepen werden onderscheiden binnen de ingroep; de eerste groep stemde overeen met *H. opuntia* en de tweede groep bevatte specimens die in de meeste gevallen met geen enkele beschrijving perfect overeenstemden. De tweede groep werd het *H. distorta–hederacea* complex genoemd en werd onderverdeeld in twee subgroepen die min of meer overeenstemden met *H. distorta* en *H. hederacea*. Intermediairen tussen de *H. distorta* en *H. hederacea* morfologieën waren aanwezig. Een fylogenie afgeleid uit partiële nucleaire rDNA sequenties vertoonde één tak met *H. opuntia* en een tweede met het *H. distorta–hederacea* complex, wat dus de twee morfologische hoofdgroepen ondersteunt. Het *H. distorta–hederacea* complex bevatte twee groepen sequenties die slechts gedeeltelijk overeenstemden met de morfologische subgroepen. Daarom werd *H. hederacea* verenigd met *H. distorta*. De fylogeografische structuur van *H. opuntia* toonde aan dat deze soort zich van de Pacifische naar de Atlantische Oceaan heeft verbreid. Fossiele gegevens ondersteunen dit: terwijl de soort al minstens 10^5 jaar voorkomt op Pacifische locaties komt ze nog maar sinds het laatste millennium voor in de Caraïben en de Bahamas.

Verbruggen et al. (ingediend-1 – Hoofdstuk 7) rapporteerden dat nucleaire ribosomale en chloroplast DNA sequenties van specimens uit *Halimeda* sectie *Halimeda* veel meer genetisch afgelijnde soorten bevat dan er in de traditionele taxonomie werden erkend. Tegenstrijdigheden tussen cladogrammen afgeleid uit nucleaire en chloroplast DNA sequenties wezen erop dat reticulate speciatie kon zijn opgetreden binnen de sectie. Toch kon op basis van de gegevens niet worden uitgesloten dat *incomplete lineage sorting* aan de basis lag van de tegenstrijdigheden. Het feit dat verschillende pseudo-cryptische soorten een nauw areaal hebben aan de rand van het verspreidingsgebied van het genus werd geïnterpreteerd als een aanwijzing dat genmigratie aan de rand van het generisch verspreidingsgebied laag genoeg is om genetische differentiatie en speciatie toe te laten. In een tak met *H. cuneata* cryptische soorten van ver gescheiden subtropische locaties in de Indische Oceaan, was de Zuid-Afrikaanse soort basaal en waren de Arabische en West-Australische soorten nauwste verwanten. De hypothese dat geografische isolatie van de cryptische soorten gebeurde na periodes van wereldwijde afkoeling gedurende het Pleistoceen of Plioceen werd geformuleerd. Een meer basale opdeling van Atlantische, Indo-Pacifische en Mediterrane soorten werd geïnterpreteerd als een indicatie voor vicariantie. De verschillende paleogebeurtenissen die deze vicariantie zouden kunnen hebben veroorzaakt werden besproken.

Morfometrische technieken voor Halimeda *taxonomie*

Taxonomie op soortsniveau is binnen genera van de Bryopsidales vaak gebaseerd op kwantificeerbare morfologische kenmerken. Nochtans zijn er relatief weinig voorbeelden van statistisch onderbouwde studies binnen deze groep sifonale algen en macrowieren in het algemeen. Moleculaire fylogenetische studies hebben cryptische diversiteit aangetoond in verschillende genera van de Bryopsidales en vragen om nieuwe taxonomische benaderingen. Verbruggen et al. (2005a, b – Hoofdstukken 8 en 9) stelden een gecombineerde moleculaire en morfometrische benadering van *Halimeda* taxonomie voor. Er werd gebruik gemaakt van een selectie specimens uit de vijf natuurlijke groepen van het genus. Er werd een fylogenie afgeleid uit gedeeltelijke nucleaire rDNA sequenties (3' einde van SSU, ITS 1, 5.8S, ITS2 en 5' einde van LSU). De grootte en vorm van segmenten werden gecodeerd in variabelen met behulp van verschillende technieken, waaronder *landmark* analyse en elliptische Fourier analyse. Een breed gamma anatomische structuren werd opgemeten. De taxonomische bruikbaarheid van de verschillende methoden en kenmerken werd bepaald met behulp van predictieve discriminant analyse. De moleculaire gegevens werden gebruikt om soorten af te bakenen. Segmentmorfologische kenmerken waren redelijk goede schatters voor de soort waartoe specimens behoren, maar anatomische kenmerken boekten de beste resultaten.

Segmenten afwijkend in externe morfologische en/of anatomische kenmerken waren in de eerste plaats apicale en onverkalkte segmenten en segmenten van het onderste deel van de thallus. Vergelijking van discriminant analyses met en zonder afwijkende segmenten wees op de negatieve invloed van zulke segmenten op de taxonomische kracht van de gegevens. Het weglaten van onverkalkte en apicale segmenten en segmenten uit het onderste deel van de thallus bracht gelijkaardige resultaten voort als het weglaten van alle afwijkende segmenten zonder rekening te houden met hun locatie in de thallus. Daarom werd het afgeraden apicale en onverkalkte segmenten, en segmenten van het onderste deel van de thallus te gebruiken in toekomstige taxonomische studies. Er werd geargumenteerd dat statistisch onderbouwde studies waarschijnlijk ook kunnen bijdragen aan het opklaren van taxonomische problemen binnen andere genera van de Bryopsidales.

DNA barcodes en morfometrie lokaliseren soortsgrenzen

Moleculaire technieken hebben cryptische soorten aan het licht gebracht binnen verschillende morfologische wiersoorten. Dit resulteerde in de vraag of zulke soorten werkelijk cryptisch zijn of dat wel degelijk morfologisch herkenbaar zijn en dus resulteren uit conservatieve taxonomische praktijken. Verbruggen et al. (2005c – Hoofdstuk 10) bestudeerden deze vraagstelling binnen *Halimeda* sectie *Rhipsalis*. Van deze sectie was geweten dat ze cryptische diversiteit bevatte en dat de soortsgrenzen tussen sommige soorten overlapten. In de studie van Verbruggen et al. (2005c) werden soortsdiversiteit binnen de sectie en de identiteit van individuele specimens bepaald met behulp van ITS1–5.8S–ITS2 (nrDNA) en *rps*3 (cpDNA) sequentiegegevens. De sequenties groepeerden in een aantal duidelijk gescheiden genotypische groepen die als soorten werden beschouwd. De externe morfologie en anatomie van dezelfde specimens werden daarna onderzocht met behulp van de methoden beschreven in Verbruggen et al. (2005a, b – Hoofdstukken 8 en 9). Morfologische verschillen werden vastgesteld met behulp van discriminant analyse. Zo werd aangetoond dat er significante morfologische verschillen bestaan tussen de genotypische soorten en dat toewijzing van specimens aan soorten op basis van morfometrische variabelen nagenoeg perfect is. Anatomische kenmerken leidden tot betere resultaten dan externe morfologische kenmerken. Twee benaderingen voor toekomstige morfologische identificaties werden voorgesteld: een probabilistische benadering gebaseerd op klassificatiefuncties van discriminant analyses en de klassieke benadering van een identificatiesleutel.

In een daaropvolgende studie (Verbruggen et al. ingediend-2 – Hoofdstuk 11) werd de fylogenetische structuur van sectie *Rhipsalis* afgeleid uit nucleaire 18S–ITS1–5.8S–ITS2 en samengevoegde chloroplast sequenties (*tuf*A & *rpl*5–*rps*8–*inf*A) en werd de taxonomie van de soort *H. incrassata* herzien. Twee pseudo-cryptische entiteiten werden beschreven als *H. kanaloana* Vroom en *H. heteromorpha* N'Yeurt. De originele soort *H. incrassata* werd herbeschreven zodat ze nog slechts één, monofyletische entiteit bevat. Gelijkenis en verschil tussen de drie pseudo-cryptische soorten en *H. melanesica* werden besproken.

Referenties

Choi H.G., Kraft G.T. & Saunders G.W. (2000) Nuclear small-subunit rDNA sequences from *Ballia* spp. (Rhodophyta): proposal of the Balliales ord. nov., Balliaceae fam. nov., *Ballia nana* sp. nov. and *Inkyulee* gen. nov. (Ceramiales). *Phycologia* **39**: 272–287.

Draisma S.G.A., Prud'homme van Reine W.F., Stam W.T. & Olsen J.L. (2001) A reassessment of phylogenetic relationships within the phaeophyceae based on RUBISCO large subunit and ribosomal DNA sequences. *Journal of Phycology* **37**: 586–603.

Freshwater D.W., Fredericq S., Butler B.S., Hommersand M.H. & Chase M.W. (1994) A gene phylogeny of the red algae (Rhodophyta) based on plastid *rbc*L. *Proceedings of the National Academy of Sciences of the U.S.A.* **91**: 7281–7285.

Hillis L.W., Engman J.A. & Kooistra W.H.C.F. (1998) Morphological and molecular phylogenies of *Halimeda* (Chlorophyta, Bryopsidales) identify three evolutionary lineages. *Journal of Phycology* **34**: 669–681.

Kawai H. & Sasaki H. (2004) Morphology, life history, and molecular phylogeny of *Stschapovia flagellaris* (Tilopteridales, Phaeophyceae) and the erection of the Stschapoviaceae fam. nov. *Journal of Phycology* **40**: 1156–1169.

Kooistra W.H.C.F. (2002) Molecular phylogenies of Udoteaceae (Bryopsidales, Chlorophyta) reveal nonmonophyly for *Udotea*, *Penicillus* and *Chlorodesmis*. *Phycologia* **41**: 453–462.

Kooistra W.H.C.F., Caldéron M. & Hillis L.W. (1999) Development of the extant diversity in *Halimeda* is linked to vicariant events. *Hydrobiologia* **398**: 39–45.

Kooistra W.H.C.F., Coppejans E.G.G. & Payri C. (2002) Molecular systematics, historical ecology, and phylogeography of *Halimeda* (Bryopsidales). *Molecular Phylogenetics and Evolution* **24**: 121–138.

Kooistra W.H.C.F. & Verbruggen H. (2005) Genetic patterns in the calcified tropical seaweeds *Halimeda opuntia*, *H. distorta*, *H. hederacea* and *H. minima* (Bryopsidales, Chlorophyta) provide insights in species boundaries and inter-oceanic dispersal. *Journal of Phycology* **41**: 177–187.

Lopez-Bautista J.M. & Chapman R.L. (2003) Phylogenetic affinities of the Trentepohliales inferred from small-subunit rDNA. *International Journal of Systematic and Evolutionary Microbiology* **53**: 2099–2106.

Rousseau F., Burrowes R., Peters A.F., Kuhlenkamp R. & de Reviers B. (2001) A comprehensive phylogeny of the Phaeophyceae based on nrDNA sequences resolves the earliest divergences. *Comptes Rendus de l'Académie des Sciences de Paris – Life sciences* **324**: 305–319.

Saunders G.W. & Hommersand M.H. (2004) Assessing red algal supraordinal diversity and taxonomy in the context of contemporary systematic data. *American Journal of Botany* **91**: 1494–1507.

Siemer B.L., Stam W.T., Olsen J.L. & Pedersen P.M. (1998) Phylogenetic relationships of the brown algal orders Ectocarpales, Chordariales, Dictyosiphonales, and Tilopteridales (Phaeophyceae) based on RUBISCO large subunit and spacer sequences. *Journal of Phycology* **34**: 1038–1048.

van der Strate H.J., Boele-Bos S.A., Olsen J.L., van de Zande L. & Stam W.T. (2002) Phylogeographic studies in the tropical seaweed *Cladophoropsis membranacea* (Chlorophyta, Ulvophyceae) reveal a cryptic species complex. *Journal of Phycology* **38**: 572–582.

Verbruggen H., De Clerck O., Cocquyt E., Kooistra W.H.C.F. & Coppejans E. (2005a) Morphometric taxonomy of siphonous green algae: a methodological study within the genus *Halimeda* (Bryopsidales). *Journal of Phycology* **41**: 126–139.

Verbruggen H., De Clerck O. & Coppejans E. (2005b) Deviant segments hamper a morphometric approach towards *Halimeda* taxonomy. *Cryptogamie Algologie* **26**: aanvaard.

Verbruggen H., De Clerck O., Kooistra W.H.C.F. & Coppejans E. (2005c) Molecular and morphometric data pinpoint species boundaries in *Halimeda* section *Rhipsalis* (Bryopsidales, Chlorophyta). *Journal of Phycology* **41**: in druk.

Verbruggen H., De Clerck O., Schils T., Kooistra W.H.C.F. & Coppejans E. (aanvaard-1) Evolution and phylogeography of the *Halimeda cuneata/discoidea/tuna* cryptic species complex.

Verbruggen H. & Kooistra W.H.C.F. (2004) Morphological characterization of lineages within the calcified tropical seaweed genus *Halimeda* (Bryopsidales, Chlorophyta). *European Journal of Phycology* **39**: 213–228.

Verbruggen H., De Clerck O., N'Yeurt A., Spalding H. & Vroom P.S. (aanvaard-2) Phylogeny and taxonomy of *Halimeda incrassata*, including the description of *H. kanaloana* and *H. heteromorpha* spp. nov. (Bryopsidales, Chlorophyta).

Zuccarello G.C., Sandercock B. & West J.A. (2002) Diversity within red algal species: variation in world-wide samples of *Spyridia filamentosa* (Ceramiaceae) and *Murrayella periclados* (Rhodomelaceae) using DNA markers and breeding studies. *European Journal of Phycology* **37**: 403–417.

Zuccarello G.C. & West J.A. (2003) Multiple cryptic species: Molecular diversity and reproductive isolation in the *Bostrychia radicans/B. moritziana* complex (Rhodomelaceae, Rhodophyta) with focus on North American isolates. *Journal of Phycology* **39**: 948–959.

Vooruitzichten voor evolutionaire studies van *Halimeda*

Heroen Verbruggen

Ondanks het feit dat deze studie bepaalde inzichten heeft opgeleverd over de morfologische en moleculaire evolutie van *Halimeda* en dat hieruit reeds een aantal taxonomische beslissingen zijn voortgevloeid, blijven er enerzijds een aantal vragen onbeantwoord en werden er anderzijds tal van onderwerpen aangeraakt die om verdere studie vragen.

Taxonomische vraagstellingen

Sectie *Halimeda*

De meest voor de hand liggende kwestie waaraan geen aandacht werd besteed is de morfologische taxonomie van sectie *Halimeda*. Kooistra et al. (2002) en Verbruggen et al. (ingediend-1) toonden aan dat deze sectie ongeveer dubbel zoveel genealogische soorten bevat dan momenteel omschreven door de klassieke, op morfologie en anatomie gebaseerde taxonomie. Het is dus zeer de vraag of deze soorten ook op basis van morfologische kenmerken van elkaar onderscheiden kunnen worden. De meest evidente aanpak om deze vraag te beantwoorden is een morfometrische studie uit te voeren van vegetatieve structuren, gecombineerd met een meer traditioneel taxonomische studie (cf. Verbruggen et al. 2005, ingediend-2). Voorlopige resultaten wijzen uit dat de zeven cryptische *H. cuneata* soorten kleine uiterlijke verschillen vertonen. Moleculaire en morfologische verschillen en gelijkenissen tussen de *H. cuneata*-entiteiten moeten echter worden onderzocht aan de hand van een groter aantal specimens, eveneens afkomstig van Madagascar en ZO Australië, gebieden waarvan *H. cuneata* is vermeld in de literatuur (Pichon 1978, Millar & Kraft 1994), maar waarvan geen specimens werden bestudeerd in Verbruggen et al. (ingediend-1). Bovendien vertoont *H. cuneata* twee morfologieën in ZW Australië (John Huisman persoonlijke mededeling), een kwestie die zeker bijkomende taxonomische aandacht verdient. Een aantal morfologische verschillen tussen *H. tuna* 1 en 2 (nummering naar Verbruggen et al. ingediend-1) werden reeds in de literatuur beschreven (Hillis 1959, Hillis-Colinvaux 1980) maar moeten worden herbekeken in een meer omvattend geheel van soorten (bv. *H. cuneata* f. *undulata*, *H. gigas*, *H. lacunalis*, *H. magnidisca*, *H. xishaensis*) omdat Hillis-Colinvaux' opvatting over *H. tuna* niet overeenstemt met inzichten uit moleculaire gegevens. Bovendien worden verschillende van de bovengenoemde soorten niet erkend door Hillis-Colinvaux (1980) of waren zij nog niet beschreven ten tijde van haar monografie. *Halimeda discoidea* 2 en 3 vertonen enkele duidelijke externe en anatomische verschillen en ook de ecologische kenmerken van deze soorten zijn erg verschillend. De verschillen tussen *H. discoidea* 1 en 2 lijken veel minder evident, al werd door Kooistra et al. (2002) vermeld dat de perifere utriculi van deze soorten zijdelingse aanhechting vertonen over verschillende lengtes. Deze verschillen moeten worden herbekeken met inbegrip van *H. cuneata* f. *digitata*, die genetisch niet te onderscheiden is van *H. discoidea* 1 (Verbruggen et al. ingediend-1). Binnen sectie *Halimeda* is ook bijkomende aandacht nodig voor het onderscheid tussen *H. gigas* en *H. magnidisca*. De laatstgenoemde soort werd door Noble (1986) onderscheiden van de eerstgenoemde door kleinere perifere utriculi, vasthechting in zanderig substraat door een grote, bolvormige vasthechtingsstructuur en de aanwezigheid van een soort stipes bestaande uit een reeks cilindrische segmenten. De specimens die in Kooistra et al. (2002) en Verbruggen et al. (ingediend-1) werden beschouwd als *H. magnidisca* vormen een intermediair tussen beide soorten: ze bezitten een zeer kleine bolvormige vasthechtingsstructuur, utriculi van intermediaire grootte en een veel minder uitgesproken

steelzone. Of deze specimens behoren tot *H. gigas*, *H. magnidisca*, of tot een tot nog toe onbeschreven soort zal moeten worden onderzocht aan de hand van DNA sequentiebepaling en morfologische studie van *H. gigas* en *H. magnidisca* uit de gebieden waarvan ze oorspronkelijk werden beschreven. Een laatste soort met onduidelijke affiniteiten is *H. xishaensis*. Zij werd beschreven van de Xisha eilanden (China) door Dong & Tseng (1980) en lijkt heel sterk op bepaalde *H. discoidea* 1 specimens.

Halimeda incrassata complex

Een tweede evident taxonomisch probleem is het *H. incrassata* complex. Ondanks de taxonomische revisie van Verbruggen et al. (ingediend-2) blijven de affiniteiten van een aantal illustraties uit de literatuur en specimens uit het herbarium van de Universiteit Gent onduidelijk. Of deze specimens behoren tot *H. incrassata*, *H. kaneloa*, *H. heteromorpha*, of één of meer nog onbeschreven soorten zal moeten blijken. De beschikbaarheid van materiaal geschikt voor DNA analyse en studie van anatomische structuren is hier een cruciaal probleem.

Halimeda minima groep

Een derde groep soorten waarbinnen nog taxonomische onzekerheid bestaat is *H. minima–howensis–velasquezii–renschii*. De soort *H. minima* vertoont erg veel morfologische variabiliteit en moleculair fylogenetische studies op basis van 18S–ITS1–5.8S–ITS2 sequenties tonen aan dat ze bestaat uit twee (mogelijk drie) welomlijnde en wijd verspreide clades. Dit suggereert dat er misschien meerdere reproductief gescheiden populaties vervat zitten binnen deze morfologische soort (Kooistra et al. 2002, Verbruggen & Kooistra 2004, Kooistra & Verbruggen 2005). In de bovengenoemde studies werden echter te weinig specimens bestudeerd om een volledig beeld te verkrijgen van deze soort. Naar mijn (enkel door morfologie onderbouwde) mening werden in de Indische en Pacifische Oceanen veel specimens behorende tot *H. minima* gerapporteerd als *H. copiosa* (bv. Noble 1987, Coppejans et al. 2000). De meest waarschijnlijke oorzaak van deze verwarring is dat groot uitgegroeide specimens van rifhellingen heel erg lijken op de Atlantische soort *H. copiosa* zoals deze werd beschreven door Goreau & Graham (1967). Deze mogelijke verwarring zou moeten onderzocht worden aan de hand van moleculaire analyses en een grondiger, kwantitatief morfologisch onderzoek. De soort *H. howensis*, beschreven van het erg geïsoleerde en meest zuidelijk gelegen koraalrif ter wereld (Lord Howe Island), vertoont duidelijke morfologische affiniteiten met *H. copiosa* (naar mijn mening *H. minima*) van het Groot Barrièrerif maar is veel kleiner (Kraft 2000). Of deze soort inderdaad een aparte soort is of dat ze een kleine vorm van de soort *H. minima* voorstelt kan vastgesteld worden door integratie van *H. howensis* in een moleculair–morfologisch systematische studie. Ook de soort *H. velasquezii*, die werd gerapporteerd doorheen het grootste deel van het Indo-Pacifisch bassin (bv. Taylor 1962, Valet 1966, Vroom & Smith 2003), lijkt erg veel op *H. minima*. Analyse van DNA sequenties van (ongepubliceerde resultaten) wijzen erop dat deze morfologische soort bestaat uit twee genealogische entiteiten, waarvan de ene affiniteiten vertoont met *H. renschii* (de zustersoort van *H. minima*) en de andere met *H. distorta* (sensu Kooistra & Verbruggen 2005). Grondige morfologische en moleculaire studies van een uitgebreide collectie specimens is noodzakelijk om meer inzicht te krijgen in de taxonomie van het *H. minima–howensis–velasquezii* morfologisch complex. Aangezien sommige *H. minima* specimens soms een *H. goreauii*-achtige morfologie aannemen, is het aangewezen ook deze soort te betrekken in zulke studie.

Halimeda distorta–hederacea complex

Ook het *H. distorta–hederacea* complex verdient nog bijkomende aandacht. Kooistra & Verbruggen (2005) toonden aan de hand van 18S–ITS1–5.8S–ITS2 sequenties aan dat deze groep bestaat uit een basale, parafyletische groep van specimens die hoofdzakelijk een *H. hederacea* morfologie hebben en een afgeleide, monofyletische groep enkel bestaande uit specimens met een *H. distorta* morfologie. Op basis van deze resultaten en het voorkomen van specimens met intermediaire morfologieën kon het

onderscheid tussen beide soorten niet worden gehandhaafd en werden ze ondergebracht in één soort *H. distorta*. Bovendien bracht de studie van Kooistra & Verbruggen (2005) duidelijkheid over het morfologisch onderscheid tussen *H. opuntia* en *H. distorta*. Kooistra & Verbruggen (2005) maakten echter geen gebruik van anatomische waarnemingen om hun conclusies te verifiëren. Bovendien is sinds de studie van Verbruggen en Kooistra (2005) gebleken dat verschillende moleculaire merkers soms een ander beeld geven van evolutionaire verwantschappen (Verbruggen et al. 2005, ingediend-1). Daarom is het wenselijk het *H. distorta–hederacea* complex grondiger te bestuderen met anatomisch–morfometrische technieken en bijkomende moleculaire merkers.

Halimeda gracilis

Ongepubliceerde ITS1–5.8S–ITS2 sequenties tonen aan dat er binnen *H. gracilis* drie haplotype groepen te onderscheiden zijn, waarvan er twee voorkomen in het Indo-Pacifisch bassin en één in de Caraïben. Bovendien vertoont deze soort erg veel morfologische variabiliteit. Een revisie van dit taxon, waarbij wordt onderzocht of deze morfologische variatie zich differentieert volgens de genotypische groepen, is dan ook wenselijk.

Halimeda bikinensis

Een laatste taxonomische onduidelijkheid betreft *H. bikinensis*. Verbruggen & Kooistra (2004) bespraken uitgebreid de morfologie van deze soort en mogelijke affiniteiten met secties *Halimeda* en *Pseudo-opuntia*. DNA extractie uit het typemateriaal bleek onmogelijk en de positie van deze soort binnen het genus bleef dus onopgelost. Om in deze kwestie helderheid te scheppen zouden DNA sequenties bepaald moeten worden van recente collecties.

Intraspecifieke morfologische variatie

Verschillende auteurs vermelden dat *Halimeda* soorten morfologische verschillen vertonen afhankelijk van de habitat waarin ze groeien (bv. Gilmartin 1960, Hillis-Colinvaux 1980, Vroom et al. 2003). Er gebeurde echter nog nooit een uitvoerige studie van de ecologische, geografische en genetische componenten van intraspecifieke morfologische variabiliteit. Uit de meest omvattende taxonomische studie tot dusver, van de tropische soort *H. heteromorpha*, bleek dat morfologie sterk gecorreleerd was met habitatkenmerken afgeleid uit veldnotities (Verbruggen et al. ingediend-2). Morfologische en genetische gelijkenis tussen specimens van deze soort vertonen nauwelijks verband (ongepubliceerde resultaten). Er lijkt wel een geografische component te bestaan in de morfologische variatie (ongepubliceerde resultaten), al kan dit te wijten zijn aan onvolledige sampling van sommige gebieden en afwezigheid van bepaalde habitats in sommige regio's. Sluitend bewijs van ecologisch geïnduceerde morfologische variabiliteit kan enkel geleverd worden aan de hand van transplantatie- en "common garden" experimenten. Een andere aanpak bestaat uit het grootschalig inzamelen van specimens uit verschillende regio's, en het zorgvuldig opmeten en noteren van allerlei ecologische factoren die mogelijk belang kunnen hebben op de morfologie. Dit zijn: diepte (Gilmartin 1960), lichtintensiteit (Hillis-Colinvaux 1980), nutriëntengehalte en chemische samenstelling van de waterkolom (Smith et al. 2004), intensiteit en type van waterbewegingen (bv. golfslag, deining, éénrichtingsstroming; Kaandorp 1999), begrazingsdruk en epifytendensiteit. Geïntegreerde statistische analyse van een morfometrische gegevensbank van de verzamelde specimens, DNA sequentiegegevens, en de verzamelde ecologische factoren kan erg veel inzicht bieden in de verbanden tussen deze gegevens (bv. Thorpe et al. 1996, Sanders et al. 2004) maar laat geen oorzaak–gevolg conclusies toe.

Mariene speciatiemechanismen

Reticulate speciatie

Het gebruik van moleculaire benaderingen in systematische studies van *Halimeda* heeft verschillende vraagstellingen in verband met mariene speciatiemechanismen op de voorgrond gebracht. Eén van de belangrijkste aspecten in deze context is de mogelijkheid van reticulate speciatie (Verbruggen et al. ingediend-1). Ondanks het feit dat reticulate speciatie een zeer belangrijk soortsvormingsproces is bij streptofyten (bv. Otto & Whitton 2000, Denboh et al. 2003, Linder & Rieseberg 2004) en koralen (bv. van Oppen et al. 2001, 2002, 2004) is dit speciatiemechanisme nog nauwelijks bestudeerd bij mariene groenwieren. Behalve de aanwijzingen voor reticulate speciatie in *Halimeda* op basis van incongruenties tussen chloroplast en nucleaire fylogenieën werden er ook fylogenetische tegenstrijdigheden gevonden tussen regio's binnen het nrDNA cistron van *Caulerpa* (Caulerpaceae, Bryopsidales; Durand et al. 2002), een ver zustergenus van *Halimeda*. Endoreduplicatie, de verdubbeling van het nucleaire genoom zonder daaropvolgende kerndeling, is algemeen in groenwieren (bv. Kapraun 1993, 1994, Kapraun & Buratti 1998) en is ook gekend bij *Halimeda* (Kapraun 1994). Endoreduplicatie verhoogt de kans op succesvolle bivalente paring van chromosomen en meiose in hybride kernen en is bijgevolg bevorderlijk voor hybride speciatie. Moleculaire technieken laten toe hybride speciatie grondiger te bestuderen. In het bijzonder nucleaire merkers waarvan slechts één kopie voorkomt in het genoom, kwantitatief genetische methoden, en de studie van genoomevolutie bieden perspectieven (Hegarty & Hiscock 2005).

Reproductieve scheiding

Een tweede thema dat meer aandacht verdient binnen studies over evolutie, speciatie en taxonomie van *Halimeda* is het concept van de biologische soort. Seksuele reproductie binnen het genus gebeurt door gelijktijdige lozing van micro- en macrogameten in de waterkolom. Voor veel soorten lijkt de fenologie erg voorspelbaar en bepaalde soorten laten hun gameten vrij in verschillende tijdsvensters gedurende dezelfde ochtend (Drew & Abel 1988, Clifton 1997, Clifton & Clifton 1999). Voor de meeste soorten zijn de fenologie en de tijdsvensters van gameetlozing echter onbekend. Bovendien is het niet duidelijk of soorten in verschillende delen van hun areaal er dezelfde fenologie op nahouden. De enige grondig bestudeerde regio's zijn het Groot Barrièrerif (Drew & Abel 1988) en de Caraïbische kust van Panama (Clifton 1997; Clifton & Clifton 1999) maar deze regio's hebben behalve *H. opuntia* geen gemeenschappelijke soorten. Drew & Abel (1988) stelden vast dat het reproductief seizoen ter hoogte van het Groot Barrièrerif niet voor alle soorten overeenstemt met sporadische waarnemingen van reproductie in andere gebieden. Het feit dat binnen één gebied verschillende soorten op dezelfde ochtend fertiel zijn (cf. Clifton 1997, Clifton & Clifton 1999) maakt interfertiliteitsstudies relatief gemakkelijk. Anderzijds heeft reproductieve seizoenaliteit ook zijn nadelen voor interfertiliteitsonderzoek. Immers, indien een experiment moet worden herhaald, duurt het maanden vooraleer de soorten opnieuw reproductief worden. De stimuli van seksuele reproductie zijn onbekend en het proces kan dan ook niet naar believen geïnduceerd worden. Hoewel ik voorstander ben van een grondige vaststelling van reproductieve compatibiliteit voor soortsafbakening, is ook het biologisch soortsconcept niet volmaakt. Zo zijn bijvoorbeeld interfertiliteitstesten tussen strikt allopatrische soorten moeilijk te interpreteren in het kader van soortsbegrenzing omdat onderling seksueel contact is uitgesloten door de geografische scheiding. Kenneth Clifton voerde reeds kruisingsexperimenten uit met de nauwverwante, sympatrische soorten *H. incrassata*, *H. monile* en *H. simulans* (persoonlijke mededeling). Deze drie soorten zijn niet interfertiel, wat betekent dat het morfologisch, biologisch en genealogisch soortsconcept van toepassing is op deze soorten (Verbruggen et al. 2005, ingediend-2).

Geografische speciatiemodi

De geografische modi van speciatie vormen reeds lang een centraal thema in de evolutieleer. Benthische en sedentaire mariene organismen zijn voor hun verbreiding vooral aangewezen op oceaanstromingen. Zulke oppervlaktestromingen zijn in staat propagules te transporteren over lange afstanden (bv. Scheltema 1968). Op een tijdschaal van honderden tot een paar duizenden jaren zijn de positie en richting van oppervlaktestromingen min of meer constant, waardoor op deze tijdschaal bepaalde gebieden in constant contact staan met elkaar en bepaalde gebieden worden geïsoleerd. Bijgevolg zorgen oceaanstromingen enerzijds voor genetische verbondenheid tussen bepaalde populaties en genetische isolatie van andere populaties. Het eerstgenoemde zorgt voor genetische homogenizatie van soorten over een groot gebied en remt bijgevolg soortsvorming af terwijl het laatstgenoemde divergentie van geografisch gescheiden populaties toelaat en speciatie in de hand werkt. Door veranderingen in oppervlaktestromingen op een tijdschaal van tienduizenden jaren zullen divergente populaties terug in contact komen en zal, indien er geen reproductieve isolatie is opgetreden, de soort terug gehomogeniseerd worden. Dit fenomeen is gekend onder de naam oppervlaktestromingsvicariantie (Veron 1995). Er bestaan echter ook mariene barrières van meer materiële aard die een invloed hebben op populatiedifferentiatie en speciatie, zoals bijvoorbeeld de tijdelijke scheiding van de Indische en Pacifische Oceanen tijdens ijstijden ten gevolge van landbruggen ter hoogte van de Indonesische archipel en het nauw van Torres (bv. McMillan & Palumbi 1995, Benzie et al. 2002). Een glaciale landbrug ter hoogte van Bab-el-Mandeb (Sheppard et al. 1992) kan op een gelijkaardige manier verantwoordelijk zijn voor het hoge endemisme van de Rode Zee (bv. Klausewitz 1989). Anderzijds bestaan er tal van voorbeelden van sympatrische mariene speciatie (bv. Hellberg 1998, Darling et al. 2000).

Verbruggen et al. (ingediend-1) suggereren dat voor elk van de belangrijkste geografische modi, voorbeelden aanwezig zijn in *Halimeda* sectie *Halimeda*. In het bijzonder het feit dat latitudinaal gescheiden populaties van *H. discoidea* langsheen de Oost-Afrikaanse kust veel sterker genetisch verschillen dan populaties die longitudinaal gescheiden zijn over veel grotere afstand is erg intrigerend. Het zou in het licht van deze vaststelling interessant zijn om ook stalen van *H. discoidea* uit andere subtropische gebieden in de studie te betrekken en na te gaan of het bekomen patroon algemeen geldt of specifiek is voor de NW Indische Oceaan. Voor wat betreft het waargenomen patroon in de NW Indische Oceaan werd geopperd dat seizoenale opwelling van koud water langs de zuidkust van het Arabisch schiereiland, waar *H. discoidea* afwezig is, zou kunnen bijdragen aan de genetische isolatie van populaties in de warmere wateren van de tropische Indische Oceaan, de Golf van Oman en mogelijk ook de Rode Zee. Het patroon dat werd gevonden voor *H. discoidea* is waarschijnlijk niet uniek. Veel rifgeassocieerde organismen hebben geïsoleerde populaties in de warmere wateren van de Golf van Oman, de Rode Zee en de noordkust van Socotra. Of de fylogeografische patronen van deze soorten in de regio al dan niet gelijklopen met die van *H. discoidea* is waarschijnlijk een functie van hun temperatuurstolerantie en dispersiekenmerken. Ook het reproductieseizoen kan van belang zijn aangezien de stromingen doorheen de Arabische Zee tegengesteld zijn tijdens de ZW en NO moessonseizoenen. Een uitgebreidere fylodemografische studie van de soort *H. discoidea* en andere warmwatersoorten in de regio is noodzakelijk om deze interessante vorm van peripatrische speciatie te bevestigen en te begrijpen.

Ook in de Caraïben lijkt het genus *Halimeda* perspectieven te bieden voor de studie van geografische speciatiemodi in mariene ecosystemen. De Caraïbische Zee is vanuit biogeografisch standpunt heel homogeen. Er zijn echter twee *Halimeda* soorten met een erg interessant, nauw verspreidingsgebied. De eerste soort, *H. favulosa*, behoort tot sectie *Rhipsalis* en is endemisch voor de Bahamas. De tweede soort, *H. lacrimosa*, behoort tot sectie *Pseudo-opuntia* en komt voor in de Bahamas, de Florida Keys en één locatie in noordelijk Cuba. Het lijkt er dus op dat in de noordelijke periferie van het Caraïbisch bassin twee soorten *Halimeda* zijn ontstaan. Het interessante aspect aan deze speciatiegebeurtenissen in de Bahamas is dat complementair aan een moleculaire benadering ook fossiele gegevens kunnen

worden geïntegreerd. Op de tropische banken van de Bahamas werden reeds boorkernen genomen die teruggaan in de tijd tot vóór het verwachte ontstaan van de soorten in kwestie (bv. McNeill et al. 1998). Bovendien vertonen zowel *H. lacrimosa* als *H. favulosa* afwijkende segmentkenmerken en anatomische aspecten, wat hun herkenning in boorkernen erg gemakkelijk maakt. Een potentieel tijdskader voor het ontstaan van beide soorten is het Pleistoceen, toen de randen van het Bahama platform steiler werden en de stromingen langsheen het platform intensifieerden, waardoor de Bahamas sterker geïsoleerd waren van de Caraïben en Florida (Ginsburg 2001).

Referenties

Benzie J.A.H., Ballment E., Forbes A.T., Demetriades N.T., Sugama K. & Haryanti Moria S. (2002) Mitochondrial DNA variation in Indo-Pacific populations of the giant tiger prawn, *Penaeus monodon*. *Molecular Ecology* **11**: 2553–2569.

Clifton K.E. (1997) Mass spawning by green algae on coral reefs. *Science* **275**: 1116–1118.

Clifton K.E. & Clifton L.M. (1999) The phenology of sexual reproduction by green algae (Bryopsidales) on Caribbean coral reefs. *Journal of Phycology* **35**: 24–34.

Coppejans E., Leliaert F. & De Clerck O. (2000) Annotated list of new records of marine macroalgae for Kenya and Tanzania, since Isaac's and Jaasund's publications. *Biologisch Jaarboek Dodonaea* **67**: 31–93.

Darling K.F., Wade C.M., Stewart I.A., Kroon D., Dingle R. & Leigh Brown A. (2000) Molecular evidence for genetic mixing of Arctic and Antarctic subpolar populations of planktonic foraminifers. *Nature* **405**: 43–48.

Denboh T., Ichimura T., Hendrayanti D. & Coleman A.W. (2003) *Closterium moniliferum–ehrenbergii* (Charophyceae, chlorophyta) species complex viewed from the 1506 group I intron and ITS2 of nuclear rDNA. *Journal of Phycology* **39**: 960–977.

Dong M. & Tseng C.K. (1980) Studies on some marine green algae from the Xisha Islands, Guandong Province, China. II. *Studia Marina Sinica* **17**: 1–10.

Drew E.A. & Abel K.M. (1988) Studies on *Halimeda*. II: reproduction, particularly the seasonality of gametangia formation, in a number of species from the Great Barrier Reef Province. *Coral Reefs* **6**: 207–218.

Durand C., Manuel M., Boudouresque C.F., Meinesz A., Verlaque M. & Le Parco Y. (2002) Molecular data suggest a hybrid origin for the invasive *Caulerpa racemosa* (Caulerpales, Chlorophyta) in the Mediterranean Sea. *Journal of Evolutionary Biology* **15**: 122–133.

Gilmartin M. (1960) The ecological distribution of the deep water algae of Eniwetok. *Ecology* **41**: 210–221.

Ginsburg R.N. (2001) *Subsurface geology of a prograding carbonate platform margin, Great Bahama Bank: results of the Bahamas drilling project.* SEPM Special Publication 70, Tulsa, OK.

Goreau T.F. & Graham E.A. (1967) A new species of *Halimeda* from Jamaica. *Bulletin of Marine Science* **17**: 432– 441.

Hellberg M.E. (1998) Sympatric sea shells along the sea's shore: the geography of speciation in the marine gastropod *Tegula*. *Evolution* **52**: 1311–1324.

Hegarty M.J. & Hiscock S.J. (2005) Hybrid speciation in plants: new insights from molecular studies. *New Phytologist* **165**: 411–423.

Hillis L. (1959) A revision of the genus *Halimeda* (order Siphonales). *Publications of the Institute of Marine Science* **6**: 321–403.

Hillis-Colinvaux L. (1980) Ecology and taxonomy of *Halimeda*: primary producer of coral reefs. *Advances in Marine Biology* **17**: 1–327.

Kaandorp J.A. (1999) Morphological analysis of growth forms of branching marine sessile organisms along environmental gradients. *Marine Biology* **134**: 295–306.

Kapraun D.F. (1993) Karyology of marine green algae. *Phycologia* **32**: 1–21.

Kapraun D.F. (1994) Cytophotometric estimation of nuclear DNA contents in thirteen species of the Caulerpales (Chlorophyta). *Cryptogamic Botany* **4**: 410–418.

Kapraun D.F. & Buratti J.R. (1998) Evolution of genome size in the Dasycladales (Chlorophyta) as determined by DAPI cytophotometry. *Phycologia* **37**: 176–183.

Klausewitz W. (1989) Evolutionary history and zoogeography of the Red Sea ichthyofauna. *Fauna of Saudi Arabia* **10**: 310–337.

Kooistra W.H.C.F., Coppejans E.G.G. & Payri C. (2002) Molecular systematics, historical ecology, and phylogeography of *Halimeda* (Bryopsidales). *Molecular Phylogenetics and Evolution* **24**: 121–138.

Kooistra W.H.C.F. & Verbruggen H. (2005) Genetic patterns in the calcified tropical seaweeds *Halimeda opuntia*, *H. distorta*, *H. hederacea* and *H. minima* (Bryopsidales, Chlorophyta) provide insights in species boundaries and inter-oceanic dispersal. *Journal of Phycology* **41**: 177–187.

Kraft G.T. (2000) Marine and estuarine benthic algae (Chlorophyta) of Lord Howe Island, South-western Pacific. *Australian Systematic Botany* **13**: 509–648.

Linder C.R. & Rieseberg L.H. (2004) Reconstructing patterns of reticulate evolution in plants *American Journal of Botany* **91**: 1700–1708.

McMillan W.O. & Palumbi S.R. (1995) Concordant evolutionary patterns among Indo-West Pacific butterflyfishes. *Proceedings of the Royal Society of London Series B - Biological Sciences* **260**: 229–236.

McNeill D.F., Grammer G.M. & Williams S.C. (1998) A 5 my chronology of carbonate platform margin aggradation, southwestern Little Bahama Bank, Bahamas. *Journal of Sedimentary Research* **68**: 603–614.

Millar A.J.K. & Kraft G.T. (1994) Catalogue of marine benthic green algae (Chlorophyta) of New South Wales, including Lord Howe Island, South-western Pacific. *Australian Systematic Botany* **7**, 419–453.

Noble J.M. (1986) *Halimeda magnidisca* (Caulerpales, Chlorophyta), a new species from the Great Barrier Reef, Australia. *Phycologia* **25**: 331–339.

Noble J.M. (1987) *A taxonomic study of the genus Halimeda Lamouroux (Chlorophyta, Caulerpales) from the Heron Island region of the southern Great Barrier Reef, Australia.* Masters degree thesis, University of Melbourne, Melbourne, Australia.

Otto S.P. & Whitton J. (2000) Polyploid incidence and evolution. *Annual Review of Genetics* **34**: 401–437.

Pichon M. (1978) Recherches sur les peuplements à dominance d'anthozoaires dans les récifs coralliens de Tuléar (Madagascar). *Atoll Research Bulletin* **222**, 1–447.

Sanders K.L., Malhotra A. & Thorpe R.S. (2004) Ecological diversification in a group of Indomalayan pitvipers (*Trimeresurus*): convergence in taxonomically important traits has implications for species identification. *Journal of Evolutionary Biology* **17**: 721–731.

Scheltema R.S. (1968) Dispersal of larvae by equatorial ocean currents and its importance to the zoogeography of shoal-water tropical species. *Nature* **217**: 1159–1162.

Sheppard C., Price A. & Roberts C. (1992) *Marine ecology of the Arabian region. Patterns and processes in extreme tropical environments*. Academic Press.

Smith J.E., Smith C.M., Vroom P.S., Beach K.L. & Miller S. (2004) Nutrient and growth dynamics of *Halimeda tuna* on Conch Reef, Florida Keys: Possible influence of internal tides on nutrient status and physiology. *Limnology and Oceanography* **49**: 1923–1936.

Taylor W.R. (1962) Two undescribed species of *Halimeda*. *Bulletin of the Torrey Botanical Club* **89**: 172–177.

Thorpe R.S., Black H. & Malhotra A. (1996) Matrix correspondence tests on the DNA phylogeny of the Tenerife lacertid elucidate both historical causes and morphological adaptation. *Systematic Biology* **45**: 335–343.

Valet G. (1966) Sur une espèce rare et une nouvelle espèce d'*Halimeda* de Mélanésie. *Revue Générale de Botanique* **73**: 680–685.

van Oppen M.J.H., Koolmees E.M. & Veron J.E.N. (2004) Patterns of evolution in the scleractinian coral genus *Montipora* (Acroporidae). *Marine Biology* **144**: 9–18.

van Oppen M.J.H., McDonald B.J., Willis B. & Miller D.J. (2001) The evolutionary history of the coral genus *Acropora* (Scleractinia, Cnidaria) based on a mitochondrial and a nuclear marker: Reticulation, incomplete lineage sorting, or morphological convergence? *Molecular Biology and Evolution* **18**: 1315–1329.

van Oppen M.J.H., Willis B.L., van Rheede T. & Miller D.J. (2002) Spawning times, reproductive compatibilities and genetic structuring in the *Acropora aspera* group: evidence for natural hybridization and semi-permeable species boundaries in corals. *Molecular Ecology* **11**: 1363–1376.

Verbruggen H., De Clerck O., Kooistra W.H.C.F. & Coppejans E. (2005) Molecular and morphometric data pinpoint species boundaries in *Halimeda* section *Rhipsalis* (Bryopsidales, Chlorophyta). *Journal of Phycology* **41**: in druk.

Verbruggen H., De Clerck O., Schils T., Kooistra W.H.C.F. & Coppejans E. (ingediend-1) Evolution and phylogeography of the *Halimeda cuneata/discoidea/tuna* cryptic species complex.

Verbruggen H. & Kooistra W.H.C.F. (2004) Morphological characterization of lineages within the calcified tropical seaweed genus *Halimeda* (Bryopsidales, Chlorophyta). *European Journal of Phycology* **39**: 213–228.

Verbruggen, H., De Clerck O., N'Yeurt, A., Spalding H. & Vroom, P.S. (ingediend-2) Phylogeny and taxonomy of *Halimeda incrassata*, including the description of *H. kaneloa* and *H. heteromorpha* spp. nov. (Bryopsidales, Chlorophyta).

Veron J.E.N. (1995) *Corals in space and time: the biogeography and evolution of the Scleractinia.* University of New South Wales Press, Sydney.

Vroom P.S. & Smith C.M. (2003) Reproductive features of Hawaiian *Halimeda velasquezii* (Bryopsidales, Chlorophyta), and an evolutionary assessment of reproductive characters in *Halimeda*. *Cryptogamie Algologie* **24**: 355–370.

Vroom P.S., Smith C.M., Coyer J.A., Walters L.J., Hunter C.L., Beach K.S. & Smith J.E. (2003) Field biology of *Halimeda tuna* (Bryopsidales, Chlorophyta) across a depth gradient: comparative growth, survivorship, recruitment, and reproduction. *Hydrobiologia* **501**: 149–166.

Personal contribution

The introduction (Chapters 1 through 3) was written by me and reviewed by Olivier De Clerck and Eric Coppejans.

The concept and a first draft of Chapter 5 came from Wiebe Kooistra, who also carried out the phylogenetic analyses. I performed a morphological investigation of the five lineages, using specimens from the phylogenetic study and additional collections in the Ghent University herbarium (GENT), and the University of Michigan herbarium (MICH). Starting from the initial draft, the paper was rewritten and reviewed several times by both authors, largely during my visit to the Stazione Zoologica 'Anton Dohrn' in Naples in January 2003.

Chapter 6 was conceived by Wiebe Kooistra. The majority of DNA sequences were produced by Kooistra; a minority was generated by the Ghent University research group. Wiebe Kooistra carried out all phylogenetic analyses. My contribution to the paper was the investigation and illustration of the external morphology of the sequenced specimens and additional collections in GENT.

The scientific design, data gathering and statistical analysis of Chapter 7 were by me. Most DNA analyses (from extraction up until sequencing) were carried out by Ellen Cocquyt under my coordination. The paper was written by me and thoroughly reviewed by the co-authors.

Chapters 8 and 9 were conceptualized and written by me. I gathered and analyzed the morphometric data and coordinated the molecular work, which was carried out by Ellen Cocquyt (DNA extraction up until sequencing). The paper presented in Chapter 8 was significantly modified from the first version by Olivier De Clerck and Wiebe Kooistra. Both other co-authors reviewed the paper.

The concept, gathering of morphometric data and all analyses for Chapter 10 were by me. Ellen Cocquyt took care of the molecular lab work. The co-authors reviewed the manuscript.

The concept, illustrations and data analysis of Chapter 11 were by me. The description of *H. kanaloana* was written by Peter Vroom and me. The description of *H. heteromorpha* was authored by Antoine N'Yeurt and me. Heather Spalding provided specimens of and ecological information about *H. kanaloana*. The paper was written by me and reviewed by all co-authors.

The summary and perspectives (Chapters 12 through 15) were written by me and reviewed by Olivier De Clerck and Eric Coppejans.